THE HONG KONG
POLYTECHNIC UNIVERSITY
香港理工大學
Pao Yue-kong Library
包玉剛圖書館

Copyright Undertaking

This thesis is protected by copyright, with all rights reserved.

By reading and using the thesis, the reader understands and agrees to the following terms:

1. The reader will abide by the rules and legal ordinances governing copyright regarding the use of the thesis.
2. The reader will use the thesis for the purpose of research or private study only and not for distribution or further reproduction or any other purpose.
3. The reader agrees to indemnify and hold the University harmless from and against any loss, damage, cost, liability or expenses arising from copyright infringement or unauthorized usage.

If you have reasons to believe that any materials in this thesis are deemed not suitable to be distributed in this form, or a copyright owner having difficulty with the material being included in our database, please contact lbsys@polyu.edu.hk providing details. The Library will look into your claim and consider taking remedial action upon receipt of the written requests.

Pao Yue-kong Library, The Hong Kong Polytechnic University, Hung Hom, Kowloon, Hong Kong

http://www.lib.polyu.edu.hk

VIBRATION-BASED CONDITION ASSESSMENTS OF CABLES IN CABLE-SUPPORTED BRIDGES

by

Gang ZHENG

B.Eng., M. Phil.

A Thesis for the Degree of Doctor of Philosophy

Department of Civil and Structural Engineering

The Hong Kong Polytechnic University, Hong Kong

September 2002

Pao Yue-kong Library
PolyU • Hong Kong

To my wife, Yan-zhuo Chen

DECLARATION

I hereby declare that this thesis entitled "Vibration-Based Condition Assessments of Cables in Cable-Supported Bridges" has not been, either in whole or in part, previously submitted for a degree in this or any other institution, and the work presented in this thesis is original unless otherwise acknowledged in the text.

SIGNED

_____

Gang ZHENG

ACKNOWLEDGMENTS

I am greatly indebted to my supervisor, Professor J. M. Ko, for his excellent guidance, advice and sincere encouragement during my study and preparation of the thesis. I also would like to give my special thanks to my co-supervisor, Dr. Y. Q. Ni, for his high responsibility, persistent support and helpful advice throughout the course of my PhD project. I also wish to express deeply gratitude to my co-supervisor, Prof. X. Xu. His insight into and rich experience in finite element analysis have benefited me much in the research.

Special thanks are given to my research colleague, Mr. S. Zhan, for his great help in experimental works. He helped me in making a plan for field vibration tests of cables in the Dongting Lake Bridge. Gratitude is also due to Prof. Z. Q. Chen, and his group members, for their cooperation with me on the field tests in Yueyang. Sincere appreciation goes to Prof. B. F. Spencer, Dr. G. Q. Yang and Mr. Y. Gao for their help during my stay in the University of Notre Dame as a visiting scholar. I am also grateful to Prof. D. S. Lin, Dr. D. Q. Cao, Dr. Z. G. Sun, Prof. W. J. Lou, Dr. J. Y. Wang, Dr. Z. G. Ying, Dr. Y. Chen, Dr. K. Q. Fan, Mr. X. T. Zhou, Mr. Y. F. Duan and Miss H. Li for their helpful discussion with me about my research.

I gratefully acknowledge the financial support from The Hong Kong Polytechnic University through a HKPU scholarship in the past three years. Especially, the University provided me opportunity to attend several international conferences, which benefit me much both in the research and communication with worldwide colleagues.

Finally, I wish to thank all my family members for their understanding and support consistently throughout the work.

ABSTRACT

The study presented in this thesis concerns linear and nonlinear vibration analyses and condition assessments of cables in cable-supported bridges.

The linear vibration of large-diameter sagged structural cables is first investigated in this thesis. A three-node curved isoparametric finite element is formulated for dynamic analysis of bridge stay cables by regarding the cable as a combination of an 'ideal cable element' and a fictitious curved beam element in the variational sense. The three-dimensional finite element formulation is suited for both suspended and inclined cables and allows for the consideration of cable flexural rigidity, sag-extensibility, spatial variability of dynamic tension, boundary conditions, lumped masses and intermediate spring and/or intermediate dampers. A case study is eventually provided to compare the measured and computed frequencies of cables in a real bridge. The results show that ignoring bending stiffness gives rise to relative errors of 30% in predicting the natural frequencies of the 19th mode. Another case study reveals stiffness effects of attached dampers on the cable frequencies. The proposed finite element formulation provides a good base line model for accurate identification of cable tension force and other parameters based on measurement of multimode frequencies. Parametric studies are conducted to evaluate the relationship between the modal properties and cable parameters lying in a wide range covering most of the cables in existing cable-supported bridges, and the effect of cable bending stiffness and sag on natural frequencies.

The study is then extended to nonlinear oscillation of cables. A hybrid finite element/incremental harmonic balance method is developed for analysis of nonlinear periodically forced vibration of inclined cables with arbitrary sag. The proposed

method is an accurate algorithm in the sense that it accommodates multi-harmonic components and no mode-based model reduction is made in the solution process. Both the frequency- and amplitude-controlled algorithms are formulated and are alternatively implemented to obtain complete frequency-response curves including both stable and unstable solutions. The proposed method is also capable of analyzing both super- and sub- harmonic resonances and internal resonances. Case study of applying the proposed method to nonlinear dynamic behaviour analysis of the Tsing Ma Bridge cables is demonstrated. The analysis results show that the side-span free cables of the bridge display distinctly different nonlinear characteristics in the construction and final stages. The super-harmonic and internal resonance characteristics of a viscously damped cable with nearly commensurable natural frequencies are investigated. A suspended cable paradigm under internal resonance condition is studied to demonstrate the capability of the proposed method in analyzing modal coupling and internal resonances. Nonlinear response and modal interaction characteristics of the cable at different frequency regions are identified from analysis of response profiles and harmonic component features. The super-harmonic and internal resonance responses are respectively characterized based on the harmonic distribution. Under an in-plane harmonic excitation, the two-to-one internal resonance between the in-plane and out-of-plane modes and the super-harmonic resonance around the second symmetric in-plane mode are revealed. Strong nonlinear interaction among different modes in the parameter space ranging from primary resonance to super-harmonic resonance is observed. Spatial-temporal response profiles and numerical harmonic components at different parameter ranges are presented to highlight the plentiful nonlinear response behaviours of the cable.

Finally, parameter estimation of structural cables is investigated by employing both local and global optimization tools. As an analytical method, the local optimization tools are used to investigate the effects of selection of parameter and weight on the estimation of parameters. Both single- and multiple-parameter estimation procedures are studied. It is noticed in the numerical simulation that single-parameter estimation procedures cannot eliminate the trend in errors between the measured and analytical frequencies. Hence, no prominent procedures or parameters are found. The best estimation is given the multiple-parameter estimation procedures. Methods for cable tension identification are also discussed. Two global optimization tools, i.e the exhaust search and the genetic algorithm (GA) are adopted to discuss further problems in cable parameter estimation. Simulation studies are conducted to show the characteristics of the cost function surfaces under different conditions and to obtain the statistical properties of the cable parameters through the Monte Carlo method. Field vibration data from three real bridges are used to evaluate the condition of corresponding cables. The effects of quantity of modal frequencies and the noise levels on the solution uniqueness and distributions of multiple solutions are investigated. The correlation between the errors of different parameters is obtained through calculating the correlation coefficients.

LIST OF PUBLICATIONS

Y. Q. Ni, J. M. Ko and G. Zheng. (1999). "Free and forced vibration of large-diameter sagged cables taking into account bending stiffness", *Proceedings of the Second International Conference on Advances in Steel Structures*. Chan S. L. and Teng J. G. (eds.), Elesvier, Vol. **1**, 513-520.

J. M. Ko, G. Zheng and Y. Q. Ni. (2000). "Periodically forced vibration of nonlinear stay cables", *Proceedings of International Conference on Advanced Problems in Vibration Theory and Applications*. Zhang J. H. and Zhang X. N. (eds.), Science Press, 437-443.

G. Zheng, J. M. Ko and Y. Q. Ni. (2000). "Internal resonance of nonlinear cables with nearly commensurable natural frequencies", *Advances in Structural Dynamics*, Ko J. M. and Xu Y. L. (eds.), Elsevier, 1231-1238.

J. M. Ko, Y. Chen, G. Zheng and Y. Q. Ni. (2000). "Experimental study on vibration mitigation of a stay cable using nonlinear hysteretic dampers", *Advances in Structural Dynamics*, Ko J. M. and Xu Y. L. (eds.), Elsevier, 1325-1332.

G. Zheng, J. M. Ko and Y. Q. Ni. (2001). "Multimode-based evaluation of cable tension force in cable-supported bridges", *Smart Structures and Materials 2001: Smart Systems for Bridges, Structures, and Highways*, Liu S.C and Pines D. J (eds.), SPIE Vol. **4330**, 511-522.

Y. Q. Ni, Y. Chen, J. M. Ko and G. Zheng. (2002). "Optimal voltage/current input to ER/MR dampers for multi-switch control of stay cable vibration", *Proceedings of the Third World Conference on Structural Control*, 7-11 April 2002, Como, Italy.

J. M. Ko, G. Zheng, Z. Q. Chen and Y. Q. Ni. (2002). "Field vibration tests of bridge stay cables incorporated with magnetorheological (MR) dampers", *Smart Structures and Materials 2002: Smart Systems for Bridges, Structures, and Highways,* Liu S.C and Pines D. J (eds.), SPIE Vol. **4696**, 30-40.

Y. Q. Ni, G. Zheng and J. M. Ko. (2002). "Dynamic monitoring of bridge cables for condition assessment", *Proceedings of the 2nd International Conference on Advances in Structural Engineering and Mechanics*, (in CD format), C.-K. Choi and W.C. Schnobrich (eds.), Techno-Press, 21-23 August 2002, Daejeon, Korea.

G. Zheng, J. M. Ko and Y. Q. Ni. (2002). "Super-harmonic and internal resonances of a suspended cable with nearly commensurable natural frequencies", *Nonlinear Dynamics*, **30**(1), 55-70, 2002.

Y. Q. Ni, J. M. Ko and G. Zheng. (2002). "Dynamic analysis of large-diameter sagged cables taking into account flexural rigidity", *Journal of Sound and Vibration*, **257**(2), 301-319, 2002.

G. Zheng, Y. Q. Ni, H. Li and Y. F. Duan. (2002). "Parameter optimization of multi-TMDs for wind-induced vibration suppression of tall buildings", To appear in *Proceedings of The International Conference on Advances in Building Technology*, 4-6 December 2002, Hong Kong.

Y. Q. Ni, G. Zheng and J. M. Ko. (2002). "Nonlinear periodically forced vibration of stay cables", Accepted to *Journal of Vibration and Acoustics*, ASME.

G. Zheng, Y. Q. Ni, J. M. Ko and X. Xu. (2002). "Tension-dependent internal damping of a cable model", *Proceedings of the International Conference on Experimental and Computational Mechanics in Engineering*, 24-27 August 2002, Dunhuang, China.

LIST OF FIGURE CAPTIONS

LIST OF TABLE CAPTIONS

CONTENTS

CHAPTER 1

INTRODUCTION

1.1 MOTIVATION

Advances in modern construction technology have resulted in the increasing application of large-diameter and long-span structural cables in cable-supported bridges. As a result of carrying both road and rail traffic, the Tsing Ma Bridge in Hong Kong, a suspension bridge with a main span of 1377 m, has the most heavily loaded cables in the world. The main cable section of the bridge is approximately 1.1 m in diameter after compacting. The Akashi Kaikyo Bridge in Japan, which is the world 's longest suspension bridge with a main span of 1991 m, also has a main cable section of approximately 1.1 m diameter. The effect of bending stiffness in these large-diameter bridge cables is not negligible. With the Tatara Bridge being a landmark, the construction of cable-stayed bridges is now entering a new era, with main spans reaching 1000 m. The Stonecutters Bridge, currently under design in Hong Kong, is a cable-stayed bridge with a main span of 1018 m. The Tatara Bridge with an 890 m main span, is the longest existing cable-stayed bridge in the world, and its longest stay cables are approximately 460 m in length. A recent design trend for this bridge type is the multi-span cable-stayed bridge with three or more towers. A critical problem of multi-span cable-stayed bridges is the stabilization of the central tower(s), which has

resulted in increasing application of extremely long stabilizing cables. For example, the three-tower Ting Kau Bridge in Hong Kong utilizes eight longitudinal stabilizing cables of 465 m for strengthening the slender central tower. These long stay cables exhibit considerably large sags, and consequently, the effect of sag–extensibility on the cable static and dynamic characteristics is noticeable.

During the construction and service life of a cable-supported bridge, it is extremely important to accurately define the cable forces, whose changes from degradation or other factors affect internal force distribution in the deck and towers and influence bridge alignment. As a result, considerable attention is focused on understanding the dynamic response of stay cables in cable-supported bridges to evaluate the as-built tension or possible damage, validate the wind-tunnel models of the stay cables developed from design drawings and update the numerical models. Local cable vibration is usually considered separately from the motion of the whole bridge.

The existing cable theory was developed based on the assumption that the cable is perfectly flexible so that it is only capable of developing uniform normal stress over the cross-sectional area. This means that there is no bending resistance. For large diameter bridge cables, however, the bending resistance is not negligible. In order to accurately evaluate the dynamics of this kind of cable, a new analysis methodology for cables accounting for bending stiffness should be developed.

Evaluation of tension forces in bridge cables by measuring modal properties is

a fast and convenient non-destructive technique. This technique is at present implemented by the use of free-vibration theory of straight string. Following this theory, the natural frequencies of a cable are only dependent on the tension force, and are independent of cable cross-sectional area and bending moment. As a result, the tension force can be estimated from the measured fundamental natural frequency by using an explicit expression. Nevertheless, it has been reported that cable tension estimation using this method alone may deviate dramatically from the actual value when the cable parameters are not accurate enough. Evidently, this theoretical background cannot provide an accurate estimation of the tension forces for large diameter cables, sag and complex boundary conditions. For these kinds of cables, the tension forces can be accurately evaluated from measured modal data only when the bending stiffness, sag-extensibility and support constraints are accounted for. However, when there are several parameters to be determined, a nonlinear parametric identification procedure should be used for this purpose.

The condition of cables is crucial to the serviceability of cable-supported bridges. The tension forces in stay cables are an excellent indicator of overall structural health for cable-stayed bridges. When the tension forces of all cables are measured over time, a picture of how the load is redistributed in the stay cables can be drawn. Furthermore, the internal force redistribution in the deck and towers can be evaluated with the aid of the entire bridge finite element model. Wire corrosion and fatigue fracture of stay cables has occurred in a number of cable-stayed bridges. Cable deterioration has two modes: loss of metallic cross-sectional area producing external

and internal abrasion and corrosion, and localized faults such as broken wires, kinks, etc. Using the linear string theory, the reduction in cable cross-sectional area is unidentifiable from the measured modal data. Following the approach proposed in this thesis, however, it is possible to using the dynamic approach to identify the cable damage appearing as reduction in cross-sectional area, which consequently reduces the cable flexural rigidity.

1.2 OBJECTIVES

This thesis is devoted to studying the forward and inverse dynamics of bridge cables with large diameter, sag and complex boundary conditions. The main objectives of this research are:

(1) To develop a dynamic analysis methodology for stay cables accounting for flexural rigidity, torsional stiffness, sag effect, geometric nonlinearity and different boundary conditions.

The variational principle and finite element formulation will be established for arbitrary cables with various geometrical, material and mechanical properties. The nonlinear response analysis will be completed by the combined use of the finite element (FE) procedure and the incremental harmonic balance (IHB) technique. The corresponding finite element program will be developed and provide a tool for accurate evaluation of natural frequencies, mode shapes and dynamic response of structural cables.

With the program developed, non-dimensional analysis and sensitivity computation will be performed for the modal parameters of structural cables used in cable-supported bridges. Owing to the flexibility of the finite element method, the proposed method can deal with complex situations such as any discrete dampers or tie cables connected to stay cables. The proposed method also has a potential use for analyzing large-amplitude oscillation such as parametrically excited oscillation and internal resonance reported to happen on stay cable in cable-supported bridges.

(2) To develop a vibration-based identification procedure to evaluate cable tension and other geometric and material parameters.

Cables are different from other members in civil engineering structures due to their high flexibility. In fact, cables are the most flexible members even in a flexible structure like a cable-supported bridge and are characterized with very low fundamental frequencies. Cables can, therefore, be excited in oscillation with relatively higher order modes, which is of great importance for system identification, under either ambient or artificial excitation.

Since the bending stiffness is taken into account in the FE model of the cable, it is possible to use higher order modal information for the system identification of cable parameters. The use of multi-mode frequencies makes it possible to establish a multi-parameter identification approach and makes the identified results more reliable. System parameters to be considered in this study include the material properties, geometrical properties and boundary conditions.

Both the gradient optimization algorithm and the genetic algorithm (GA) will be introduced to identify cable parameters. The gradient optimization algorithm is efficient when an initial guess on cable parameters is close to the real parameters, as in the circumstances of newly constructed bridges. However, when considering old bridges, an initial guess near the real cable parameters may not be available, and the genetic algorithm is a preferable one. This method is expected to match the need for an accurate technique in cable condition assessment for cable-supported bridges, as has become greatly imperative when the conventional method failed to find out actual cable tension forces through field tests.

(3) To apply the aforementioned methodology for cable parameter identification in both numerical simulation and real application.

Numerical simulations are deployed to show the characteristics of the cost function surfaces and to obtain the statistical properties and relationships of, and between, cable parameters. Field tests are carried out to collect the cable vibration data. The modal frequencies of the cable will be extracted from the collected vibration signals and be used for identifying the cable parameters. Case studies are carried out for cables of average size, cables with an extremely large diameter, and cables with an extremely long length. The cables from the Dongting Lake Bridge, Changsha, China, and both the Tsing Ma Bridge and Ting Kau Bridge in Hong Kong, China, will be investigated.

(4) To study some advanced problems in cable vibration.

As the geometric nonlinearity of a cable will, of course, affect the cable vibration and consequently influence the results of identification using the above methods, which are based on the linear dynamics, the nonlinear vibration of cables under different configurations will be studied to understand the effects of nonlinearity on the dynamic response. The super-harmonic, sub-harmonic and internal resonances, which are believed to be possible candidate mechanisms for the wind-rain-induced vibration in cable-stayed bridges, will also be investigated.

1.3 ORIGINALITIES

Original aspects of the present study include the following:

(1) A general model for the dynamic analysis of large-diameter sagged cables is developed. This model is capable of taking into account initial cable tension, flexural rigidity, accurate cable profile (sag effects and inclination), cable extensibility, intermediate, accurate dynamic cable tension, dampers and supports and different boundary conditions and is parameter-identification-oriented. To the author's knowledge, a model that can deal with all the above important points was not yet available before this study. For example, Mehrabi and Tabatabai (1998) derived a unified finite difference formulation for free vibration of cables but subject to the following assumptions: (*i*) the cable dynamic tension keep constant along the cable length, which was originally suggested by Irvine (1981); (*ii*) the cable has supports at the same level; (*iii*) the axial, transverse in-plane and out-of-plane vibration modes are

uncoupled. The model by Henghold and Russell (1976) considered the geometric nonlinearity but did not account for the effects of flexural rigidity. This model is a general one in the sense that it was not restricted to an element type with specified node number. However, as the contribution of static cable tension is not explicitly expressed, this model could not be directly used for cable parameter identification.

(2) The present study develops a combined incremental harmonic balance (IHB) and finite element method for cable nonlinear oscillation analysis. This method can provide accurate temporal and spatial description for the steady-state oscillation of cables under periodic excitation whereas existing models in literature, based on the perturbation method, have to use a model with only very limited degrees of freedom (one to, up to date, four), which greatly restricts real application.

(3) The present study proposes a new identification method of using multi-mode frequencies for accurate estimation of cable parameters. Existing methods for vibration-based cable tension use only one frequency as input. The use of multiple-frequencies can greatly improve the accuracy and reliability of identified cable parameters.

(4) Both local and global optimization tools are used in this study to identify cable parameters. The global optimization method may avoid being captured by a local optimal solution. When a cable with little knowledge of its original values or design parameters is under study, a global optimization tool is the only option for obtaining a good solution.

(5) The present study investigates the effects of uncertainty in measurement on the accuracy of cable parameter estimation.

1.4 THESIS LAYOUT

The contents of this thesis are divided into eight Chapters.

Chapter One introduces the motivation for the present research and makes clear the objectives to be pursued in this PhD project.

Chapter Two contains a literature review, which covers five relatively independent subjects. These subjects include cable vibration in cable-supported bridges, cable tension measurements, dynamics of sagged cables, local and global optimization tools, and, vibration-based model updating procedures, with reasonable overlaps amongst them. Cable dynamics of cable-stayed bridges is reviewed in order to learn what kinds of cable vibration may exist in practical sagged structural cables. A survey of measurement methods for cable tension estimation used in modern cable-stayed bridges is then carried out and the problems encountered from previous research on this topic is discussed. Both linear and nonlinear dynamic theories of sagged cables are then reviewed to provide a theoretical background for further study on linear and nonlinear vibrations of cables. The finite element (FE) methods for cable structures are then briefly reviewed for the purpose of selecting or creating an element suitable for cable vibration analysis. Both local and global optimization methods are surveyed in order to select the most suitable one for the problem concerned. The

existing frequency-based model updating procedures are then investigated to make perceptions about state-of-art technology and find out clues for the parameter identification of stay cables.

Chapter Three introduces a combined model developed for three-dimensional free and forced linear vibration of sagged cables with large diameter and provides numerical examples to validate the model. With the developed finite element formulation, parametric studies are conducted to evaluate the relationship between the modal properties and cable parameters lying in a wide range covering most of the cables in existing cable-supported bridges. A case study is provided to compare the measured and calculated frequencies of the main cables of the Tsing Ma Bridge.

Chapter Four explores the nonlinear behaviour of structural cables under different configurations, corresponding to different construction stages in the erection of cable-supported bridges. The incremental harmonic balance (IHB) method and the nonlinear finite element method are combined together to solve the nonlinear vibration problem of the cables.

Chapter Five discusses an important phenomenon, the internal resonance, in nonlinear vibration of stay cables. Both super-harmonic and internal resonances of a suspended cable are investigated. The evolution within between the two kinds of resonances is clearly revealed, as may be the potential mechanism of the wind-rain-induced vibration occurring on stay cables in cable-stayed bridges.

Chapter Six describes the parameter estimation of structural cables based on frequency measurements. After defining the cost function constructed with the errors between the measured and calculated frequencies, the cable parameters are identified with a gradient-based optimization method. Both single- and multiple-mode based procedures are used to identify the cable tension. The method is also capable of making a multiple-parameter-estimation, in which all important cable parameters are identified simultaneously with the estimation of the cable tension.

Chapter Seven extends the investigation completed in Chapter Six. In this Chapter, the genetic algorithm (GA), as a global optimization method, is used to make multiple-parameter estimation. The genetic algorithm eschews the unrealistic requirement that a 'smart' guess on the initial solution, based on a local optimization algorithm, which is generally gradient-based, starts. The characteristics of the cost function surfaces and the statistical properties of identified cable parameters are investigated by the combined use of the Monte Carlo method and the genetic algorithm.

Chapter Eight summarizes the main conclusions obtained in this thesis from both the study of linear and nonlinear analysis of the cable vibration, and both the local and global parameter identification of the cables.

CHAPTER 2

LITERATURE REVIEW

2.1 CABLE VIBRATION IN CABLE-SUPPORTED BRIDGES

Structural cables are one of the most important members in cable-supported bridges. However, due to their extremely low internal damping and great flexibility, cables are susceptible to large amplitude vibrations under various types of excitations, such as wind-induced, wind-and-rain-induced, parametric-excited vibrations and coupled vibration with other structural components. In fact, different types of cable vibration have been reported to occur on cable-supported bridges worldwide. In this section, the wind-induced, wind-and-rain-induced and parametric-excited vibrations of cables are reviewed.

2.1.1 WIND-INDUCED VIBRATION

Cable vibrations can be excited by dynamic wind forces acting on the cable. Such forces are caused by turbulence in the on-coming airflow (buffeting), vortex shedding in the wake behind the cable, self-induction (galloping), fluid-elastic interaction between neighboring cables (wake galloping) (Post-Tensioning Institute, 2000).

Forces due to buffeting or vortex shedding do not originate from the cable motion, and therefore will not lead to aeroelastic instability but only to vibrations of limited amplitude. These vibrations can occur at any wind speed. On the other hand, the flow forces acting on the cable during self-excited vibrations are a function of the motion the cable itself. The aeroelastic instability leads to large amplitude vibration. These kinds of vibration start in a sudden fashion when the wind speed exceeds a certain critical value (critical wind speed) (Post-Tensioning Institute, 2000).

Wake galloping usually occurs in multiple parallel stay cables used in long-span cable-stayed bridges and induces the in-plane vibration of stay cables in the vertical direction (Matsumoto et al. 1989; Miyata 1991; Ohashi 1991; Wardlaw 1991). During wake galloping, stay cables are excited by the windstream induced from windward stay cables and the vibration usually occurs at the first mode. This kind of vibration is reported to occur in numerous bridges worldwide including the Longs Creek, the Papineau, the New Brunswick and the Fredericton Bridges in Canada; the Hitsuishijima, the Tempozan, the Yobuko, the Yokohama Bay, the Meiko Nishi and the Rokko Bridges in Japan; the Brotonne Bridge in France; the Köhlbrand Bridge in Germany; and the Sunshine Skyway Bridge in the United States (Yu 1997).

Wake galloping is affected by wind speed, wind direction and distance between the centers of two parallel cables and can be suppressed when the damping capacity is great enough. Wake galloping occurs when the wind direction is between 0° to 45° from the transverse direction of the bridge axis. When the distance between two cables is more than five times the cable diameter, wake galloping becomes very weak. The reported vibration amplitude of cables in cable-stayed bridges due to wake galloping varies from 0.2m to 0.5m peak to peak response. A logarithmic decrement

of 0.05 (or modal damping ratio of 0.8%) or more is believed to be large enough to suppress wake galloping (Miyata 1991; Narita and Yokoyama 1991). The response amplitude of cables in vortex shedding is relatively smaller than that in other types of vibrations whereas the frequencies are relatively high.

Vortex shedding is caused by alternative vortexes behind a cable and excites a cable when the frequencies of the cable and vortexes are equal (Woo et al. 1983; Ohashi 1991). As far as the vortex-shedding phenomenon is concerned, it is well known that it produces aerodynamic forces that originate in the wake behind the structure and mainly act in the across-wind direction. The type of excitation on circular cylinders is sensitive to the mass damping parameter, $\xi m/\rho B^2$, where ξ is the critical damping ratio, m is mass per unit cable length, ρ is the air density and B is the width of the cylinder. Beyond $\xi m/\rho B^2 \approx 5$ no motion will occur (Wardlaw 1991). Bridges with reported vortex shedding vibrations include the Higashi-Kobe Bridge in Japan and the Wheeling Bridge in the United States.

2.1.2 WIND-RAIN-INDUCED VIBRATION

The so-called wind-rain-induced vibration (sometimes also referred to as rain-induced vibration) refers to a special kind of cable vibration that occurs only on rainy days with slight or moderate wind but ceases to occur under similar wind excitation in dry conditions (Narita and Yokoyama 1991). Stay cables vibrate wildly in the cable plane along the vertical direction when wind-rain-induced vibration occurs. The maximum amplitude was reported to reach 0.6 m peak to peak response in violent vibrations at the Aratsu Bridge (Yoshimura 1992).

Wind tunnel tests (Ohshima 1987; Hikami and Shiraishi 1986) indicate that for different cable vibration modes this kind of vibration occurs in the same wind

speed range. Based on the wind tunnel tests, it is believed that the water rivulets formed on the upper or lower cable surface, which produce a periodic change of cable cross section, may be the cause of the unstable cable oscillation.

Wind-rain-induced vibration is often observed in stay cables with a smooth surface and a diameter between 120 mm to 200 mm when the bridge is located in flat and open land. Increased vibration has been observed to occur when the cable inclination coincides with wind direction and the wind direction has an angle of 30° to 80° to the cable plane (Miyata 1991). Compared with other kinds of cable vibration, relatively low frequency resonance is excited under the special wind-rain condition. Wind-rain-vibration is believed to be suppressed by a logarithmic decrement of 0.02 (or modal damping ratio of 0.32%) or above (Narita and Yokoyama 1991).

The first observation of wind-rain-induced vibration was made at the Meiko Nishi Bridge in Japan in 1984 (Hikami 1986). Similar observations have been reported from the Aratsu, the Hitsuishi Jima, the Iwaguro Jima, and the Tenpozan bridges in Japan (Narita and Yokoyama 1991; Yoshimura 1992); the Brotonne Bridge in France; the Köhlbrand Bridge in Germany; the Sunshine Skyway Bridge in the United States; and the Dongting Lake Bridge in China.

2.1.3 PARAMETRIC EXCITATION

In some cases, the large amplitude cable vibration observed cannot be explained as a result of aerodynamic instability but is believed to be excited by the motion of the bridge tower and/or the bridge deck (Yoshimura et al. 1989). When the cable is excited harmonically by the anchorage, the cable tension, and consequently

the cable stiffness will change periodically. There is then a possibility of parametrically excited oscillation.

In long-span cable-stayed bridges, significant vibration of the bridge deck and towers, on which stay cables are anchored, may occur (Persoon 1981). However, when parametric excitation occurs, even a small amplitude of anchorage (at the bridge tower or the bridge deck) leads to great steady-state cable response when the frequency of the anchorage motion is close to one or two times the stay cable natural frequencies (Takahashi 1991; Fujino et al. 1993a, 1993b; Pinto Da Costa et al. 1996). For example, the cables at the Wandre Bridge in France have been found to vibrate with a large amplitude of 0.3 m peak to peak response and beating phenomenon has been observed. However, there was no rain during the vibration and the wind did not reach critical speeds. An extreme example was given by Lilien and Pinto Da Costa (1994), in which a 10 cm excitation induced by girders and/or the mast leads to a large amplitude (15 m) oscillation of an inclined 440 m stay cable. Damping increases the excitation amplitude required for the onset of parametric excitation. However, if the instability does initiate, damping has a negligible role on the limitation of the resulting large oscillations (Pinto et al. 1996; Lilien 1994).

2.2 CABLE TENSION MEASUREMENTS

2.2.1 VIBRATION-BASED METHODS

2.2.1.1 Basic equation

Based on the string equation, cable tension can be expressed as a function of the cable length, L, the cable mass per unit length, m, and the fundamental frequency, f, as follows:

$$H = 4L^2 f^2 m \tag{2.1}$$

It should be noted that when the cable is inclined, H represents the horizontal component of the cable tension. The cable tension, T, will be a function of H and the inclination angle, α, i.e.

$$T = H/\cos\alpha = 4L^2 f^2 m/\cos\alpha \tag{2.2}$$

The above equations can only be applied if the seven lowest frequencies, measured with a 0.5% accuracy, lie in a straight line (Robert et al. 1991; Casas 1994) as shown in **Figure 2.1**. By using these equations, the cable tension can be readily calculated once the fundamental frequency is measured. If not the fundamental frequency, f, but the frequency, f_n, of another mode, n, is obtained, Equation (2.1) is revised as:

$$H = 4mL^2 \frac{f_n^2}{n^2} \tag{2.3}$$

Due to their simplicity, these equations have been widely used by engineers and researchers (Takahashi et al. 1983; Okamura 1986; Qiu et al. 1990; Shi and Zhang 1992; Kroneberger-Stanton and Hartsough 1992; Casas 1994; Chen and Yu 1995; Brönnimaan et al. 1998; Institute of Bridge Engineering 1998; Russell and Lardner

1998; Wang et al. 1999; Brownjohn et al. 1999; Cunha and Castano 1999; Cunha et al. 2001).

The method for the determination of cable tension in cable-stayed bridges has several other versions beside the basic one using Equation (2.1). The first variant is formulated in Equation (2.3). Sometimes, it is difficult to determine the mode order of measured frequencies on site and the cable tension can be determined by the averaged frequency interval, Δf, between a serial of equally spaced frequencies, i.e.

$$H = 4L^2(\Delta f)^2 m \tag{2.4}$$

When the cable is relative large in diameter, the bending stiffness of the cable needs to be considered. When the cable ends are pinned, the cable tension is expressed as (Shi and Zhang 1992; Lin 1997):

$$H = \frac{4mL^2 f_n^2}{n^2} - \frac{n^2\pi^2 EI}{L^2} \tag{2.5}$$

To consider different boundary conditions, the cable tension is obtained as (Qiu et al. 1990):

$$H = \beta f^2 \tag{2.6}$$

in which β is the calibration coefficient which should be determined on site. Taking β as $4L^2m$, Equation (2.6) is identical to Equation (2.1). However, β may change with cable tension. When the bending stiffness is to be considered for different construction stages of a stay cable, the tension can be determined as follows:

When the cable is tensioned to 50% of the designed value:

$$H = \beta f^2 - \frac{40EI}{L^2} \tag{2.7}$$

When the cable is tensioned to 100% of the designed value:

$$H = \beta f^2 - \frac{10EI}{L^2} \tag{2.8}$$

It should be noticed that the above equation is an approximation of Equation (2.5) while taking β as $4L^2m$.

2.2.1.2 Measurements in practice

Experiments were carried out to investigate methods for cable tension determination under different conditions. By comparing the measured natural frequencies with the theoretical predictions, the tension of a scale model of a guy wire for a 411 m tall radio navigation tower was determined experimentally with an accuracy of 3% by Russell and Lardner (1998). Their experiments found that when the first 10 natural frequencies of the cable were measured at a number of different tension levels they differed from the theoretical values by an average of 0.7%.

Unfortunately, field tests on cable tension determination are found to be difficult and not accurate enough in some cases. Difficulties may arise in the application of vibration measurements in the cables of cable-stayed bridges to obtain actual forces, as mentioned by Casas (1994). In particular, the influence of extensibility of very long cables in obtaining an accurate solution of frequency of vibration was shown in one example in the tests by Casas. Other problems were related to the difficulty of obtaining experimental vibration records in short cables with a sufficient time length to derive the natural frequencies of vibration with desired accuracy.

According to Casas, the vibration method itself was not accurate enough to derive the real forces in cables when the cables were extremely short, or long, or had

complex anchoring devices. He developed a method combining the force values derived from vibration measurements with other experimental techniques (strain gauges, pressure in tensioning jacks) that could define the real forces in the cables with sufficient accuracy and reliability to determine if the cable forces are within permissible boundaries defined during the design stage. The least-square minimization procedure was used to minimize global measurement errors and enable an accurate definition of forces in stay cables. The error in cable tension measurements between the results of the combined method and the jack measurement is 0~8%, with high reliability considering effects of various uncertain factors.

Generally, it is difficult to determine cable tension forces with high precision in field tests. Three techniques for cable tension measurement, by using a tensioning jack, strain gauges and the frequency-based method, respectively, were employed in a project of cable replacements of a cable-supported bridge (Wang 1997). In this project, the frequency-based technique was found to be more convenient with higher precision, which was finally confined to be within 5% of the design values and said to be the best one of several tests the measurement team ever carried out. Xu et al. (1997) found out the frequency differences between the numerically simulated and field test results were about 7% for the 5th in-plane mode of a free cable of a suspension bridge. When this frequency is used for cable tension determination, the relative error becomes larger than 10%. More recently, a full-scale test on a 100 m span curved cable-stayed bridge obtained even worse results and the cable tension forces were determined through the vibration method with an error up to 51% over the actual tension (Brownjohn et al. 1999).

Yen et al. (1997) compiled a comprehensive database of cable parameters from at least 14 cable-stayed bridges. The results of the statistical analysis showed that the sag to span length ratios were always less than 2%, and for 95% of the cables, it was less than 1.5%. The results also indicated that 95% of sag-extensibility factors (refer to Chapter 3 for details) were less than about 1.35, while 100% were less than 3.0. The difference between the sag-extensibility factors calculated with and without taking into account the contribution of grout and cover pipe was noticeable in the results. They also carried out field measurements to verify a finite differential method for solving the cable vibration equation taking into account cable bending stiffness. The cable-stayed Weirton-Steubenville Bridge in West Virginia, USA, was selected to conduct the field measurements with the existing load cells installed in the bridge to verify accuracy.

A modified approach for cable tension evaluation using the measured frequency was used during the construction of the 2nd Wuhan Yangtse River Bridge. The following steps were adopted (Institute of Bridge Engineering 1998):

(1) Calculate a basic value for the cable tension force, T_0, from formulation, $T = 4mL^2f^2$, based on measured fundamental natural frequency, f, the cable length, L, and mass per unit cable length, m. It should be noticed that at this step the cable bending stiffness is not considered.

(2) Estimate the cable tension force T from a trial-and-error method by comparing the first several measured and calculated frequencies from a finite element model considering the cable bending stiffness.

The frequency was measured with a relative error less than 1%. When the estimated cable tension is compared with the design ones listed in Table 2.1, the maximum

absolute error is 12.7% for cable WR9. Thirty percent of the measured cable tension forces deviated over 5% from the design ones.

2.2.2 HYDRAULIC PRESSURE METER

Cable tension can be measured by a hydraulic pressure meter in conjunction with a hydraulic jack, which is used in tensioning the cable (Wang 1997). **Figure 2.2** shows a hydraulic jack used to apply final tension to cable stays. The multi-strand, 430t-capacity hydraulic jack was used to apply final tension to cable stays in Ogawa Bridge (Kajima Corporation 1995).

Figure 2.3 shows a stay cable at its anchorage. The cable can be easily installed on site by means of a hydraulic tensioning jack and nut. **Figure 2.4** shows the anchorage of a stay cable under construction.

The hydraulic pressure meter is suitable for measuring cable tension in the construction stage but is generally not acceptable for tension measurements of in-service cables as the movement and installation of a hydraulic jack, especially those with high capacity, is particularly inconvenient.

2.2.3 TENSION/COMPRESSION LOAD CELL

Cable tension can also be conveniently measured by using tension/compress load cells with a compatible strain meter connected. However, the cost for a load cell is expensive and related to its working range. For example, load cell Type LC1011 (Omegadyne Inc. 2001) is priced at US$6,200, or HK$50,000, with a capability of 9.0 MN. **Figure 2.5** and **Figure 2.6** show two types of load cells. Detailed information is shown in Table 2.2.

Figure 2.7 shows the installation of a load cell in the laboratory for cable tension measurement. The load cell is of type TCLM-1B (Tokyo Sokki Kenkyujo Co. 2001), with a digital strain meter of type TC-31K by TML (Zheng and Chen 2000).

The load cell can provide more accurate measurement of a single cable in the construction stage of a bridge (Wang 1997). However, the installation and movement of a hydraulic jack is heavy in labour and not convenient. This method is generally not adopted for an in-service cable after the bridge has been completed.

2.2.4 ELECTROMAGNETIC METHOD

Lhermet et al. (1998) designed and constructed a prototype of electromagnetic stress sensors for monitoring cables and prestressed concrete structures. The sensor uses the reverse magnetostrictive effect found in high elastic limit steels and in prestressed concrete. This effect is characterized by the variation of the steel's magnetic permeability as a function of its internal stress. Consequently, the internal stresses in these high elastic limit steels can be found by measuring their permeability. The permeability can be measured indirectly by measuring the inductance of a coil placed around or near the cable. This sensor is believed to operate continuously for several decades even in hostile environments. These kind of sensors have demonstrated accuracy's of better than 1% in measuring cable tension (Wang et al. 2001a, 2001b).

2.2.5 COMPARISON BETWEEN DIFFERENT METHODS

When compared with the other three methods for cable tension measurements, it is concluded that the vibration-method is more suitable for in-service cables. Table 2.3 shows that the vibration method is cheaper and requires less labor and time cost than the other three methods.

2.3 DYNAMICS OF SAGGED CABLE

Theories on cable dynamics have been developed and extensive efforts have been made on analytical and experimental investigations in free and forced cable vibration. An elastic sagged cable containing high geometric nonlinearity exhibits different dynamic properties identified from a taut string or an inextensible chain. The taut string is an idealized cable with the static configuration of a straight line and a constant static tension. The inextensible chain is a simplified model of a cable with relatively large sag, in which the longitudinal elastic stretch of the cable geometric configuration is ignored. In order to obtain a theoretical basis for further study on the cable condition assessment, the theoretical and experimental studies on dynamics of a sagged cable in both linear and nonlinear fields are reviewed.

2.3.1 THEORY OF CABLE DYNAMICS

2.3.1.1 History of cable dynamics study

Development of cable theory can be roughly divided into six stages: (i) taut string theory; (ii) theory for inextensible cable with sag-to-span ratio effect; (iii) theory considering both cable elasticity and sag; (iv) theory accounting for cable inclination, cable elasticity, and sag; (v) a relatively complete cable theory accounting for cable flexural rigidity (bending stiffness), inclination, elasticity, sag; and (vi) the nonlinear theory of cable dynamics.

The taut string/wire was the earliest cable attracting the attention of researchers who included Brook Taylor, D'Alembert, Euler, Johann and Daniel Bernoulli (Starossek 1994). The partial differential equation of transverse vibration

of a taut cable was first derived in 1750 by D'Alembert (Triantafyllou 1984a). Several years later in 1788, Lagrange and others found its solution in consideration of an inextensible and massless string with lumped masses (Starossek 1994). However, apart from Lagrange's work on the equivalent discrete system, solutions for the sagged cable were unknown at that time.

Considerations of cable sag and elasticity are closely related, as cables with large sag-to-span ratio can be treated as inelastic for materials with high elastic stiffness (Irvine 1981). The solution for sagged cables first appeared in 1868 in work undertaken by Routh following preliminary studies by Stokes and Röhrs. Nearly eighty years later, cable elasticity was first considered in 1942 by Klöppel and Lie, based on the results derived by Rannie and Von Karman (Irvine 1981). However, up until the 1970s, no theoretical or experimental work had been carried out to explain why the frequencies of the symmetric in-plane modes of an inextensible sagged cable do not coincide to the corresponding one of a taut string by reducing the sag to zero. This problem was solved by Irvine and Caughey in 1974 for horizontal cables with a sag-to-span ratio within 1/8 (Irvine and Caughey 1974).

Irvine extended his theory to inclined cables (Irvine 1978). However, in Irvine's theory, the weight component parallel to the cable chord was neglected. A more precise solution was given by Triantafyllou in 1984 (Triantafyllou 1984a). In this work, spatial variability of dynamic tension and weight component parallel to chord were taken into consideration.

Recent research efforts have been made on the flexural rigidity of cables. To accurately identify cable tension force from measured frequencies, Zui et al. (1996) derived practical formulation for cable vibration accounting for the flexural rigidity. Parametric studies were carried out by Mehrabi and Tabatabai (1998) to investigate

the interaction effects of the sag and the flexural rigidity on the modal frequencies of cables (Mehrabi and Tabatabai 1998).

Another focus of cable dynamics in recent research is nonlinear cable vibration. During the past quarter century, nonlinear free and periodic vibration of cables has been studied by numerous researchers (Hagedorn and Schafer 1980; Luongo et al. 1982; Luongo et al. 1984; Al-Noury et al. 1985; Takahashi and Konishi 1987; Benedettini and Rega 1987; Tadjbakhsh and Wang 1990; Rao and Iyengar 1991; Perkins 1992; Benedettini et al. 1995; Lee and Perkins 1995a, 1995b; Xiao and Druez 1996; Luongo and Piccardo 1998). In these studies, the phenomena of softening and hardening, jumping, internal resonance, sub- and super harmonic resonances were observed. Cable nonlinear dynamics is particularly important for the study of large amplitude vibrations, which have been reported to attack cables in a large number of bridges worldwide.

Several researchers including Irvine (1981), Triantafyllou (1984b), Straossek (1994) and Yu (1997), undertook earlier reviews on the history of cable dynamics study.

2.3.1.2 Linear cable vibration

In order to evaluate cable tension by dynamic methods, the relationship between the dynamic properties (i.e., natural frequencies) and cable tension should be established. Theories on this subject vary from the simplest one based on the string equation to a very complicated one recently developed by Mehrabi and Tabatabai (1998).

Based on the string equation, the cable tension can be expressed as Equation (2.1). Effects of cable sag and elasticity on its vibration were investigated by several

researchers (Starossek, 1994). An approximate solution to the in-plane vibration of an elastic cable hanging between two points at the same level was obtained by Irvine and Caughey (1974). The effect of elasticity was also investigated systematically by the same authors.

Irvine and his coworker's studies can be briefly summarized as follows. The underlying assumption is that stretching is small so that the dynamic tension is almost unvaried throughout the cable length and varies only with time. Sag introduces a catenary-related variation that is small for small sag-to-span (<1/8) ratios. They found that the antisymmetric modes are given by the taut string solution and that natural frequencies of the symmetric modes are the roots of the equation:

$$\tan\left(\frac{k_n L}{2}\right) - \frac{k_n L}{2} - \frac{4}{\lambda^2}\left(\frac{k_n L}{2}\right)^3 = 0 \tag{2.9}$$

$$k_n = \omega_n / \sqrt{H/m} \tag{2.10}$$

and,

$$\lambda^2 = \left(\frac{mgl}{H}\right)^2 \frac{L}{L_e} \cdot \frac{EA}{H} \tag{2.11}$$

$$L_e \approx L\left[1 + \frac{1}{8}\left(\frac{mgL}{H}\right)^2\right] \tag{2.12}$$

in which ω_n is the circle natural frequency of the nth symmetric in-plane mode of the cable and g is the acceleration due to gravity. The quantity λ^2 is proportional to the elastic stiffness and is the most crucial parameter. For infinite elastic stiffness, λ^2 is infinite and the above equation reduces to:

$$\tan\left(\frac{k_n L}{2}\right) - \frac{k_n L}{2} = 0 \tag{2.13}$$

for an inextensible chain. For zero elastic stiffness, the taut string result, Equation (2.9), is obtained. For intermediate values of λ^2, the first symmetric natural frequency can be anywhere between 1π and 2.86π. Furthermore, when λ^2 is between $[2(n\text{-}1)\pi]^2$ and $(2n\pi)^2$, the natural frequencies of symmetric in-plane modes are lower than those of corresponding anti-symmetric modes, which are independent of λ^2. With increment of λ^2 to $(2n\pi)^2$, the natural frequencies of symmetric in-plane modes tend to those of corresponding anti-symmetric modes and at $\lambda^2=(2n\pi)^2$ they equal each other. When λ^2 is greater than $(2n\pi)^2$, the natural frequencies of symmetric in-plane modes become larger than the corresponding anti-symmetric modes. This phenomenon is known as *frequency crossover*, which marks the transition of dynamic characteristics of a cable from a taut string to an inextensible chain. Near the transition points of $\lambda^2=(2n\pi)^2$, the nth symmetric in-plane mode shape of a cable is significantly changed while the nth antisymmetric in-plane mode shape keeps the same. When $\lambda^2 = 4\pi^2$, the first symmetric natural frequency equals the first antisymmetric one. Experimental validation of the frequency crossover phenomenon was also given by Irvine and Caughey (1974). The results were extended to the forced vibration of a horizontal cable (Irvine and Griffin 1976) and the free vibration of an inclined cable (Irvine 1978). In the latter, a transformation of axes was applied and a sag parameter λ_e^2 for inclined cable was introduced:

$$\lambda_e^2 = \left(\frac{mgL_e}{H_e}\cos\alpha\right)^2 \frac{L_e}{L_{ee}}\frac{EA}{H} \tag{2.14}$$

$$L_{ee} = L_e\left[1+\frac{1}{8}\left(\frac{mgL_e}{H_e}\cos\alpha\right)^2\right] \tag{2.15}$$

The inclination angle is α and L_e is the inclined span. For inclined cables, Equations (2.9) and (2.10) are revised by replacing L with L_e, and H with H_e, i.e.

$$\tan\left(\frac{k_n L_e}{2}\right) - \frac{k_n L_e}{2} - \frac{4}{\lambda^2}\left(\frac{k_n L_e}{2}\right)^3 = 0 \tag{2.16}$$

$$k_n = \omega_n / \sqrt{H_e / m} \tag{2.17}$$

The above approximate equations for inclined cables obtain satisfactory results when both the cable sag and inclination are small. However, Irvine's solution cannot capture an important property of inclined cables known as the *frequency avoidance* phenomenon, which can only be observed by recovering one item, the weight component parallel to cable, dropped from Irvine's equation. This work was done later by Triantafyllou (1984a).

Triantafyllou (1984b) derived a more precise asymptotic solution for free vibration of an inclined elastic cable with a small sag. This work allowed elastic waves but kept the assumption of quasi-static stretching of the cable along the cable tangential direction. It was found that a frequency avoidance might replace a frequency crossover when the sag parameter λ_e^2 of an inclined cable is near $(2n\pi)^2$. When hybrid modes composed of the corresponding nth symmetric and antisymmetric modes of the cable are observed within a certain region around the cable sag parameter of $(2n\pi)^2$, the phenomenon is called frequency avoidance, in which a mixture of symmetric and antisymmetric forms, and the frequencies of them may be close but never equal to each other at the frequency avoidance point, or the transition point of $(2n\pi)^2$. When frequency avoidance occurs, there is a transition region in which the first symmetric mode and the first antisymmetric mode become hybrid and after this region they exchange mode properties. In the frequency

avoidance range, both symmetric and antisymmetric mode shapes are significantly changed and large dynamic tension may arise in both modes (Triantafyllou and Grinforgel 1986).

The reason to induce frequency avoidance was then investigated. Burgess and Triantafyllou (1988) believed that the reason lies on the unsymmetric static profile of an inclined cable due to cable inclination. As a result, the larger the cable inclination is, the more obvious the frequency avoidance phenomenon will be observed. Cheng and Perkins (1992) even found that frequency avoidance also occurs on a horizontal cable. They observed that the frequency avoidance in a horizontal cable when a lumped mass attached on the cable does not locate at midspan, destroys the symmetry of the horizontal cable profile.

In addition, to the analytical methods of Irvine and Triantafyllou for elastic cables with small sag and small amplitude motion, many other methods, including analytical, asymptotic and numerical ones, have been developed for various applications. The two main analytical methods are the dynamic stiffness method and the closed-form transfer matrix method. The dynamic stiffness method was developed by Velestsos and Darbre (1983), Darbre (1989) and Starossek (1991, 1993) based on the earlier work of Davenport and Steels (1965) which studied boundary induced cable vibrations. Most recently, this method has been used to deal with the displaceable boundaries and the effects of cable damping (Kim and Chang 2001). The transfer matrix procedure has been used by Simpson (1966) for determining in-plane natural frequencies of multispan transmission lines, in which the cable was dealt as a taut string. A closed-form transfer matrix method was explored by Cheng and Perkins (1992a, 1992b, 1994) to calculate the linear response of a suspension cable with multi-mass arrays. This method can be used for a large cable sag-to-span

regime. Lin and Perkins (1995) dropped the quasi-static stretching assumption and obtained three-dimensional results for free vibration of a sagged cable. Their results showed that three kinds of mode transitions may exist in in-plane vibration of a horizontal cable with lumped masses: elastic mode crossovers are similar to those occurring from a bare cable while the third crossover only exists in cable/mass systems with significant sag. To deal with both small and large sag-to-span ratio, an asymptotic solution was derived by Triantafyllou (1985). In addition, several finite element methods (e.g., West et al. 1975; Carson and Emery 1976; Henghold and Russell 1976; Gambhir and Batchelor 1978; Ahmadi-kashani 1989) were developed to capture dynamic characteristics and dynamic behaviour of sagged cables through a numerical procedure, especially for cables with large sag.

Though it is clear that the influence of cable extensibility is negligible for short cables, because λ tends to 0, the effects of flexural rigidity and torsional stiffness become significant in such situations. As a result, extensive efforts have been made to consider the flexural rigidity, sag-span ratio, inclination and extensibility by Zui et al. (1996). Mehrabi and Tabatabai (1998) also considered the influence of intermediate springs and/or dampers and supporting conditions on cable frequencies and obtained a unified difference equation for cable vibration. In their work, the equation of motion of the cable in the vertical direction is taken as:

$$EI\frac{\partial^4 v(x,t)}{\partial x^4} - T\frac{\partial^2 v(x,t)}{\partial x^2} - h\frac{\partial^2 y}{\partial x^2} + k'v + c'\frac{\partial v}{\partial t} + m\frac{\partial^2 v(x,t)}{\partial t^2} = 0 \qquad (2.18)$$

where, $v(x,t)$ is deflection in the vertical direction, T is cable tension in the chord direction; h *is the* derivative cable force caused by vibration; $k' = k'(x)$ is spring constant per unit length at x; $c' = c'(x)$ is viscous damping factor per unit length at x. This equation is identical to that used by Zui et al. (1996) when the external spring

and damping terms are dropped. Based on this equation, the eigenvalue problem is induced by assuming the fixed-end boundary conditions. The eigenvalue problem is then solved numerically.

2.3.1.3 Nonlinear cable vibration

Nonlinear cable vibration is a very complex and interesting problem. Rich phenomena have been observed in nonlinear cable vibration, which may be induced by different kinds of excitation sources and can be analyzed by using different mathematical tools. Interesting phenomena known as softening and hardening, jumping, internal resonance, super- and sub-harmonic response and static drift have been observed in this field. Nonlinear cable vibration is related to wind-and-rain-induced cable vibration and aerodynamic instability (Verwiebe 1998); parametric oscillation induced by cable support (bridge deck and tower) motion (Pinto da Costa et al. 1996); and cable internal resonance between in-plane modes or between in-plane and out-of-plane modes (Yamaguchi and Fujino 1998). Methods employed for solving these problems include the perturbation method, the Ritz-Galerkin method, the finite element method (FEM), and more recently the incremental harmonic balance (IHB) method.

Before reviewing the developments in nonlinear cable vibration, some characteristics of a general nonlinear dynamic system are firstly described to provide basic knowledge for understanding the behaviour of the nonlinear cable oscillation. (i) *softening, hardening, and jumping phenomena.* Softening is a nonlinear oscillation behaviour in which the nonlinear resonance peak in the frequency-response curve will deviate towards the left side of the linear one. Contrarily, the hardening behaviour leads to right bending of the nonlinear response curve from the linear one. Jumping is related to the multiple-value solutions for a nonlinear dynamic system

with non-zero damping. (ii) *super- and sub-harmonic resonances*. Super-harmonic resonance is characterized by higher order harmonics, i.e. second or third order harmonics. Sub-harmonic resonance is characterised by sub-harmonics, i.e. one-half, one-third, sub-harmonics in the resonance; (iii) *Internal resonances* relate to the strong interaction/coupling between two modes when they have commensurable or near commensurable frequencies.

Several earlier works (Leonard and Recker 1972; Carson and Emery 1976; Migliore and Webster 1979) undertaken on nonlinear cable vibrations made use of numerical techniques in terms of finite element discretization and numerical integration methods. However, numerical methods are inefficient in performing parametric studies and very time consuming to obtain convergent solutions. To gain a better understanding of cable nonlinear dynamic behaviour, several approximate analytical-numerical methods have been developed since the 1980s.

Analytical-numerical methods are developed for simplified cable models with one to four degrees-of-freedom in analyzing nonlinear cable vibration by using the perturbation method and the Ritz-Galerkin method. Simplified into a single-degree-of-freedom (SDOF) model, the cable oscillation may exhibit some phenomena like hardening, softening, jumping, super- and sub-harmonic resonances of a vibration mode. A multiple-degrees-of-freedom model should be employed when the modal coupling between different modes needs to be considered. However, it is the single-degree-of-freedom model that provides the basic ideas in solving the spatially and temporally coupled nonlinear equations of a sagged cable. For example, the combined spatial and temporal differential equations are firstly discretized via a Ritz-Galerkin procedure and the resulting motion equations are solved in terms of perturbation methods or numerical integration.

Early researches on nonlinear cable oscillation are based on single-degree-of-freedom models, which can be employed to analyze the cable oscillation with only one mode, in-plane or out-of-plane, symmetric or unsymmetric, involved. Behaviours such as hardening, softening, jumping, super- and sub-harmonic resonances may be observed with such a model. Hagedorn and Schäfer (1980) reduced the partial differential equations of nonlinear in-plane free vibration of a flat undamped suspension cable into one ordinary equation via a Ritz-Galerkin procedure and obtained an approximate solution for a single-degree-of-freedom oscillation of a single mode, the first symmetric or antisymmetric in-plane mode. Following a similar approach, Luongo et al. (1984) investigated the nonlinear in-plane free vibrations of a flat horizontal undamped cable and carried out substantial parametric studies. Significant effect of the cable geometrical nonlinearity on the cable response was found in their researches. Both the hardening and softening behaviours were observed and found to be dependent on the relative contributions of the quadratic and cubic nonlinearities. They concluded that the hardening behaviour is dominated by the cubic nonlinearities and often occurs when the cable has a lower sag parameter λ^2 or higher amplitude of oscillation. The softening behaviour is due to quadratic nonlinearities and only occurs for a sagged cable with lower amplitude oscillation. These conclusions coincide with those obtained by Rega et al. (1984) by using a numerical procedure.

By considering damping in the model, a system with hardening or softening behaviour may exhibit a new phenomenon, jumping. Benedettin and Rega (1987) considered nonlinear in-plane forced vibration of a horizontal cable under an external harmonic excitation using a single-degree-of-freedom model and studied the effect of internal cable damping on nonlinear response of the cable. The jumping phenomenon

of the cable response was observed in their research and, subsequently, multiple-value solutions were obtained. They found one unstable and two stable periodic solutions near the resonance for a taut cable and five periodic solutions for a sagged cable. Their results clearly indicated that increments of internal cable damping can effectively reduce the vibration amplitude and restrain the nonlinearity occurring from cable vibration.

Sub- and super-harmonic resonances are also observed in nonlinear cable oscillation. Benedettini and Rega (1989a) investigated the nonlinear in-plane forced vibration of a horizontal cable and discussed the secondary external resonances of the cable resulting in second- and third-order super-harmonics and, in another paper (Benedettini and Rega 1989b), one-half- and one-third sub-harmonics respectively. Significant interaction between the two main super-harmonic components was found as a result of their research.

In the above studies, the multiple scales method was accomplished in terms of ordering internal cable damping and excitation amplitude, and provided a way to investigate both external and internal resonances of a cable. However, nonlinear pure planar vibration of a cable only occurs under special conditions. In most cases non-planar coupled vibration of a cable is caused by nonlinear dynamic tension produced during cable vibration.

The interaction between the in-plane and out-of-plane modes is related to another important phenomenon, internal resonance. The modal interaction (coupling), especially the internal resonance, may occur in the nonlinear oscillation of cables and other continuous systems when the linear frequencies of systems satisfy commensurate or nearly commensurate conditions (Nayfeh 2000). The modal interaction and internal resonance may result in harmful large-amplitude responses in

the low-frequency modes when subjected to a high-frequency excitation, and provide energy exchange among the modes.

A multiple-degree-of-freedom model using at least two-degrees-of-freedom should be used for analyzing the interaction between multiple vibration modes. By using a simplified two-degrees-of-freedom model, Luonge and his coworkers (1980, 1982) studied the forced combined nonlinear in-plane and out-of-plane vibration of a flat horizontal undamped cable. In their simplified model, the dynamic tension arising from the cable was only related to the in-plane mode of vibration and a second order multiple scales method was adopted. The results showed that internal resonance between in-plane and out-of-plane modes of vibration may occur when the ratio between the frequencies of a linear in-plane mode to the corresponding linear out-of-plane mode is 2:1. The effect of dynamic tension in a horizontal cable associated with both in-plane and out-of-plane displacements was investigated by Al-noury and Ali (1985) through a more accurate two-degree-of-freedom model. They demonstrated that the modal coupling happened between the in-plane vertical and out-of-plane transverse modes when they had close resonant modes. Modal coupling leads to a beating-type exchange of energy between in-plane and out-of-plane modes (Benedettini et al. 1986). By assuming weak nonlinearity and using a multiple scales method, Rao and Iyengar (1991), and Lee and Perkins (1992a) studied the non-planar cable vibration by using a two-degree-of-freedom model. This model consisted of one symmetric in-plane mode and one symmetric out-of-plane mode of a horizontal cable with sag parameter near the frequency crossover. A 2:1 internal resonance between the in-plane and out-of-plane frequencies of oscillations (i.e. the in-plane natural frequency $\approx$ two times the out-of-plane natural frequency) was found under in-plane periodic excitations. The 2:1 internal resonance was also examined by

Perkins (1992) in terms of a multiple scales method based on a two-degree-of-freedom model and experimental investigation where a horizontal cable was excited by tangential oscillation at a support of the cable.

The perturbation method used in previous studies is only suitable to weakly nonlinear systems. Takahashi and Konishi (1987a) proposed a method combining the Galerkin method in the space domain with the harmonic balance method in the time domain for the three dimensional nonlinear forced vibration of horizontal and inclined cables, which may contain large sag-to-span ratios and strong nonlinearity. However, in their work only the nonlinear pure in-plane or pure out-of-plane free vibrations were studied. In their companion paper (Takahashi and Konishi 1987b), the out-of-plane parametric vibration caused by the in-plane vibrations of a cable under an in-plane periodic excitation was discussed and compared with the experimental results of Yamaguchi (1978). However, the modal interaction between in-plane and out-of-plane modes was neglected. According to their work, the in-plane nonlinear vibration was first approached in terms of a single-degree-of-freedom model based on one in-plane mode. The obtained in-plane solutions were then substituted into the linearized out-of-plane vibration equation and a multiple-degree-of-freedom approach based on multiple out-of-plane modes was applied, by which the Hill equations for parametric excitation system were derived. Similar research was also carried out by Takahashi (1991). In his research, the unstable regions for out-of-plane vibration of a cable under in-plane parametric excitation were established.

In order to search for more internal resonances, Lee and Perkins (1992b, 1995b) established a three-degree-of-freedom model for nonlinear vibration of a horizontal cable, in which one in-plane mode and two out-of-plane modes were

included. Under planar excitation, three types of internal resonances were captured through a multiple scales perturbation analysis. These included two separated 1:1 (i.e. the in-plane natural frequency ≈ the out-of-plane natural frequency) and 2:1 internal resonances and one simultaneous 2:2:1 internal resonance (i.e. the in-plane natural frequency ≈ the second out-of-plane natural frequency ≈ two times the first out-of-plane natural frequency), which consist of three periodic solutions. Including the pure in-plane response, there are four classes of periodic solutions found in cable vibration. In their companion paper (Lee and Perkins 1995a) experimental investigation was carried out and the observed results qualitatively agreed with their theoretical predictions. However, the quantitative comparison between them was not successful due to limitation of the experimental conditions.

Furthermore, Benedettini and Rega (1994) and Benedettini et al. (1995) developed a more complex four-degree-of-freedom model counting for two in-plane and two out-of-plane modes, one symmetric and another antisymmetric to investigate cable nonlinear vibration subject to both non-planar harmonic distributed forces and horizontal support motions. The method of multiple scales via a Galerkin procedure was applied and rich internal resonances associated with eight classes of steady-state regular motions of the cable were observed for the cable with the sag parameter near the first frequency crossover point.

The above research indicated that the in-plane and out-of-plane vibrations of a cable can be strongly coupled through quadratic and cubic nonlinearities in some conditions. The interactions may contain abundant internal resonances, which need to be investigated further. According to the linear dynamic theory of a sagged cable, the frequency crossover or avoidance is a special feature of the cable identified from a string or a chain. At the frequency crossover or avoidance points, the natural

frequencies of the corresponding symmetric or antisymmetric in-plane modes have closed value, which is almost two times the natural frequency of the same order out-of-plane mode. In this case, under pure in-plane excitation, the out-of-plane oscillation of a cable becomes a parametric excitation problem due to in-plane vibration and some significant resonances (Nayfeh and Balachandran 1989; Nayfeh and Mook 1995) between the in-plane and out-of-plane modes may occur. Rega and his coworkers (1984) focused on the frequency crossover phenomenon in their research and the results showed that nonlinear oscillations of the cable near the first frequency crossover point might produce an infinite number of crossover points related to the vibration amplitude of the cable.

All the studies discussed above have greatly helped in the understanding of cable nonlinear behaviour. However, these studies are still insufficient as viewed from the facts: (i) The great majority of the studies have been confined to shallow cables suspended between two fixed supports at the same level. Only a few studies have addressed nonlinear free and periodic oscillations of inclined cables (Takahashi and Konishi 1987); (ii) Almost all the studies applied the Galerkin procedure by making use of linearized modal deflection functions to yield a discretized model with a few (two to four) degrees of freedom, and then conducted a perturbation analysis to obtain solutions. However, the work by Pakdemirli et al. (1995) and Rega et al. (1999) showed that treatment of the discretized system in modal coordinates might result in inaccurate results compared to direct treatment of the governing partial differential equations in some circumstances.

2.3.2 EXPERIMENTAL WORKS AND FIELD TESTS

Experiments have played an important role in the development of cable theories. Numerous experiments have been carried out to validate the cable theories by many investigators during the last three decades. Some of the laboratory and field tests are reviewed in this section.

To validate the linear theory on the free vibration of a suspended cable, Irvine and Caughey (1974) measured the vibration modes of a fine copper wire approximately 2 m long with two ends fastened at the same level. The so-called crossover phenomenon, which had been predicted by their theory, was firstly observed in this experiment. This phenomenon was also experimentally confirmed by other investigators, e.g., experiments on the vibration of taut and slack marine cables in water and in air by Ramberg and Griffin (1977). Though the crossover phenomena was predicted theoretically to be replaced by the frequency avoidance phenomena for inclined cables with some certain parameters (Triantafyllou 1984a), experimental evidence is still not available to support this prediction.

To obtain experimental evidence to support their theory on cable/mass suspensions, Cheng and Perkins (1994) made quantitative measurements of the response of a suspension cable by using standard modal testing techniques in the laboratory. Optical displacement probes were used to measure lower frequency/lower amplitude motions (0~14 Hz) while higher frequency/lower amplitude motions (14~22 Hz) were measured using two miniature accelerometers. Discrepancies in frequencies between the testing results and the theoretical prediction were observed in some cases and explained to attribute to the nonlinearity in cable material behaviour and/or the inaccuracy in measuring the cable tension. However, this explanation is NOT verified. Again, attempts by Lee and Perkins (1995a) to quantitatively match the experimental results to the theoretical ones were

unsuccessful. The difficulties in making such comparisons can be attributed to two main sources: i) the inability to precisely measure the cable axial stiffness, and ii) the constraints produced by the external exciter.

The effects of environmental factors (e.g. temperature change) and the bending stiffness were found significant in some situations. In discussing the mechanical characteristics of damaged cables and temporary strengthening during the replacement of cables in two cable-stayed bridges, variations of about 1.5% in cable forces of a bridge during a period of 20 months were explained to be attributed to thermal changes (Prato et al. 1997). By using magnetic induction measurements, loss of about 9% of the cross section was found for the worst case in some cables and cable damage was not restricted to the anchor zones. The effectiveness of the force measurements was limited due to the lack of records from the end of construction to provide an initial reference state. It was found that it is of utmost importance to develop and calibrate a numerical model of the bridge to enable interpretation of all data collected during the repair process. According to this research, the numerical model together with deflection and force measurements allows further insight into bridge behaviour. In another case, Smith and Johnson (1999) conducted a field test to determine the fundamental frequency of each of the 192 stay cables of the Fred Hartman Bridge. A 45-second time record of acceleration due to ambient excitation was analyzed. An automated analysis was desired, but variations in ambient excitation presented in the spectra led to an interactive analysis in which frequency peak differences were determined, sorted, and averaged to produce an experimental fundamental frequency for each cable. Difficulties in applying this approach to the shorter cables highlighted differences between shorter and longer cable response behaviours. Resulting fundamental frequencies from eight nominally identical sets of

24 cables were compared and "outliers", which indicated possible loss of stiffness and therefore damage, were identified. The average of the eight sets was also compared with predictions from a finite element beam model and a vibrating string model. The cable flexural stiffness was considered using beam elements in the finite element model. The test results matched well with the finite element predictions for both long and short cables and the vibrating string predictions only for longer cables. This implies that bending stiffness indeed influences the natural frequencies of cable vibration, especially when the cable is relatively short.

2.4 VIBRATION-BASED MODEL UPDATING

2.4.1 INTRODUCTION

Model updating concerns the correction of finite element models by processing measurement data from the dynamic response of structures. The purpose of model updating is to modify the mass, stiffness, damping parameters and other mechanical and geometrical parameters of the numerical model in order to obtain better agreement between numerical results and test data.

Discrepancies between the prediction of a model and the measurements of the corresponding structure may come from both the model and the measurements. There are three kinds of model errors (Mottershead and Firswell 1993): (i) *model structure errors*, which are liable to occur when there is uncertainty concerning the governing physical equations, e.g., the governing equation of strongly nonlinear systems; (ii) *model parameter errors*, which would typically include the application of inappropriate boundary conditions and inaccurate assumptions used in order to

simplify the model; (iii) *model order errors*, which arise in the discretization of complex systems and can result in a model of insufficient order. The model order may be considered as a part of the model structure. The measurement errors may arise due to different reasons such as aliasing and spectral leakage in FFT techniques, errors in curve fitting, nonlinearity of transducer, additional mass and stiffness of instruments and transducers. Model updating aims to minimize model errors by using measurements, which may also contain errors, so that an accurate model is obtained. As a result of model updating, an accurate model is expected to (Zhang and Wei 1999): (i) produce the same modal frequencies, mode shapes, and even frequency response functions (FRFs) within or even beyond the testing frequency band; (ii) accurately predict responses under different load cases; (iii) obtain the distribution of dynamic stresses; and (iv) represent the physical and geometrical properties of the real structures.

Historically, model updating is related to *system identification* and *parameter estimation* originating in control engineering. Some convenient and powerful tools, such as the filtering estimators like Wiener, Kolmogorov and Kalman filters, Volterra and Wiener series in non-parametric identification of nonlinear systems, the auto regressive moving average (ARMA) models and the maximum likelihood method have been developed or implemented. In structural dynamics, experimental modal analysis may be regarded as a special area of system identification for the determination of modal properties from vibration tests and are called *modal identification*. The identified modal properties are then used to validate or update finite element models.

The problem of parameter identification can be reduced to a twofold mathematical exercises: (i) development of a mathematical model of the structure

being capable of correctly reproducing frequencies and mode shapes with proper parameter values; and (ii) updating the model to reproduce measurement taken in dynamic tests. The change in the natural frequency of mode i of a structure due to any change is a function of the constitutive parameters, $\boldsymbol{p} = \{p_1, p_2, \ldots, p_n\}$. Hence the natural frequencies can be used to identify these parameters. In fact, both natural frequencies and mode shapes are sensitive to changes in system parameters such as mass and stiffness and thus have been used in monitoring the overall condition of structures (Ogawa and Abe 1980; Gudmundson 1982; Crohas and Lepert 1982; Nataraja 1983).

Identification methods have been developed to adjust the stiffness and mass parameters in a structural model so that measured data can be reproduced. One way to correct a stiffness matrix involves the use of the sensitivity (perturbation) method to define a relationship between the change in the parameters and in the modal data (Collins et al. 1974; Stetson 1975; Steston and Palma 1976; Taylor 1977; Chen and Garba 1980; Sandstrom and Anderson 1982; Hoff et al. 1984; Kim et al. 1983; Kuo and Wada 1987). Another approach to adjust the analytical stiffness matrix of a structure using measured modal data involves the use of constrained optimization to get the stiffness matrix and simultaneously satisfy a set of constraints (Baruch 1978, 1982; Kabe 1985; Lapieere and Ostiguy 1990).

By employing the eigenvalue sensitivity analysis, Hassiotis and Jeong (1995) used equations relating the change in the stiffness of each element to the changes in the frequencies for estimating the stiffness reduction of frame and beam structures. Morassi and Rovere (1997) discussed the effect of defining a correct reference model and suggesting some working hypotheses on localizing damage in a steel frame. Salawu (1997) provided an extensive review of damage detection techniques in

structures based on changes of natural frequencies and concluded that the approach is potentially useful for routine integrity assessment of structures. It is noticed from the above papers that the number of frequencies used varies from two to ten and the number of the unknowns varies from two to forty. Theoretically, when the number of unknowns is less than the number of the frequencies measured in the problems, an extra optimality criterion needs to be introduced. Selection of such a criterion is, to some extent, arbitrary. Most recently, Fabrizio and Capecchi (2001) indicated that the damage identification problems are frequently overdetermined. They addressed the importance of determining the minimum amount of frequencies necessary to obtain a unique solution.

There is a tremendous amount of literature on the vibration-based method. A brief overview is given below.

2.4.2 MODE PAIRING

Both an analytical model and an experimental test can be used to produce modal data. Due to errors in the model and the test, the modal data from the two sources are different from each other. To calculate these differences, each measured mode should be paired with the corresponding one from an analytical model. The parameters and measurements should be scaled to improve the conditioning of the matrix inversion (Ojavlvo 1989) generally appearing in further processing. Several simple criteria constructed for pairing the tested and calculated eigenpairs are reviewed in this subsection.

As measured mode shapes generally have less degrees of freedom than the analytical model, either eigenvector expansion should be adopted for measurements

or model reduction should be used for the analytical model. Both the eigenvector expansion and model reduction methods are discussed in the next subsection.

2.4.2.1 Modal assurance criterion (MAC)

The modal assurance criterion (MAC) was initially proposed by Allemang and Brown (1982). However, several other investigators have suggested use of the MAC in modal updating (West 1986; Wolff and Richardson 1989). The MAC is defined as:

$$\mathrm{MAC}_{i,j} = \frac{(\phi_{Ai}^T \phi_{ij})^2}{(\phi_{Ai}^T \phi_{Ai})(\phi_{ij}^T \phi_{ij})}, \qquad i = 1,2,...n;\ j = 1,2,...,m \tag{2.19}$$

where, ϕ_{Ai} and n are the ith mode shape vector and the order of the analytical model, respectively; ϕ_{ij} and m are the jth mode shape vector and the number of modes from tests, respectively. Obviously, with normalized ϕ_{Ai} and ϕ_{ij}, each element in MAC will be a scalar ranging from 0 to 1. Once the MAC matrix is obtained ϕ_j is readily paired with mode r, which induces the largest value in the jth row of the MAC matrix. However, due to errors in both modelling and tests, MAC_{rj}, the largest element of jth row of MAC, may be much lower than 1. In this circumstance, other methods should be used to accept or reject the result of the pairing.

2.4.2.2 Mode shape error criterion

The summation of the squared errors between two mode shapes can also be used to pair modes (Zhang 1999). The summation of squared mode shape errors is defined as:

$$E_{i,j} = \frac{1}{n_d}\sqrt{\Delta\phi_{ij}^T \Delta\phi_{ij}}, \qquad i = 1,2,...n;\ j = 1,2,...,m \tag{2.20}$$

$$\Delta\phi_{ij} = \phi_{Ai} - \phi_{ij} \tag{2.21}$$

where, ϕ_{Ai} and n are the ith normalized mode vector and the order of the analytical model, respectively; ϕ_{ij} and m are the jth normalized mode vector and the number of modes from tests, respectively; and n_d is the number of dimension of the mode vector. Once the matrix E is obtained ϕ_{ij} will be paired with mode r, which induces the smallest value in the jth row of the matrix E. Similar to MAC, matrix E is susceptible to errors in both modelling and tests.

2.4.2.3 Frequency error criterion

It is well known that natural frequencies can be obtained with much higher accuracy than mode shapes. The relative errors between the measured and calculated frequencies can be used for pairing modes, i.e.

$$\varepsilon = (\omega_{t,i} - \omega_{A,j}) / \omega_{A,j} \tag{2.22}$$

where, $\omega_{t,i}$ and $\omega_{A,j}$ are the measured natural frequency of mode i from the test and the calculated natural frequency of mode j from the analytical model, respectively. The smallest error indicating a pair. This criterion is straightforward and simple. However, when the structure has closely spaced frequencies, this method should be combined with other criterions using mode shapes, such as the MAC and the mode shape error criterions.

2.4.3 TEST INCOMPLETENESS

In practice, only limited discrete measurements may be obtained from both laboratory and field tests for the structure responses. The measurements are also limited to the concerned frequency range when dynamic responses are considered. In

fact, it is usually not feasible to measure the response of a structure at all of the degrees of freedom nor is it usually possible to collect data from all of the vibration modes that the model possesses. The two kinds of test incompleteness are referred to as '*spatial sparseness*' and '*modal incompleteness*', respectively (Hjelmstad 1996).

Before discussing test incompleteness, the process for solving a normal inverse problem in modal analysis is provided as follows. The basic equations in modal analysis are:

$$\boldsymbol{K\Phi} = \boldsymbol{M\Phi\Lambda} \tag{2.23}$$

$$\boldsymbol{\Phi}^T\boldsymbol{M\Phi} = \boldsymbol{I} \tag{2.24}$$

$$\boldsymbol{\Phi}^T\boldsymbol{K\Phi} = \boldsymbol{\Lambda} \tag{2.25}$$

where, $\boldsymbol{K}$ is the stiffness matrix, $\boldsymbol{M}$ is the mass matrix; $\boldsymbol{I}$ is the unity matrix; $\boldsymbol{\Phi}$ is the eigenvector matrix and $\boldsymbol{\Lambda}$ is the modal stiffness matrix. Equation (2.23) is the control equation of the eigenvalue problem of the structure. Equations (2.24) and (2.25) are the orthogonality conditions for mass and stiffness matrices, respectively. It is noticed that in Equation (2.24) the eigenvector matrix is normalized with respect to mass. When both the measured modal eigenvector matrix, $\boldsymbol{\Phi}$, and the spectral matrix, $\boldsymbol{\Lambda}$, are obtained as a square, non-singular matrix with the same dimension as the analytical model, the mass matrix $\boldsymbol{M}$ and the stiffness matrix $\boldsymbol{K}$ are readily obtained by:

$$\boldsymbol{M} = (\boldsymbol{\Phi}^T\boldsymbol{\Phi})^{-1} \tag{2.26}$$

$$\boldsymbol{K} = (\boldsymbol{\Phi}^T\boldsymbol{\Lambda}\boldsymbol{\Phi})^{-1} \tag{2.27}$$

However, when test incompleteness occurs, the eigenvalue problem described by Equations (2.23 to 2.25) becomes under-determined. Thus, there are infinite $\boldsymbol{M}$

and $\boldsymbol{K}$ that may contend the three equations. To obtain one unique solution for analysis, there are two options. The first is to add additional equations and the second is to limit the unknowns. Depending on the different ways adopted by the two options, different methods have been developed for model updating. Some practical methods adopted in model updating to deal with test incompleteness are reviewed in the following.

2.4.3.1 Spatial sparseness

Basically two methods, known as eigendata expansion and model reduction, may be used to overcome the problem of spatial sparseness in model updating. In eigendata expansion the unmeasured quantities are computed based on measurements by some interpolation techniques. These techniques include *spline fitting* (Chung and Craig 1985; O'Callahan et al. 1985; Mitchell and Pardoen 1988), *physical interpolation* (Berman et al. 1980; Berman and Nagy 1983; O'Callahan et al. 1985), the addition of known mass and stiffness (Nalitolela et al. 1990; Dems and Mróz 2001) and changing boundary conditions (Lallement and Cogan 1992). The model reduction methods include *static reduction* (Guyan 1965; Irons 1965; Henshell and Ong 1975; Downs 1980; Shan and Raymund 1982; Mata 1987), *physical reduction* (O'Callahan 1989; Suarez and Singh 1992; Zhang and Li 1995), *modal reduction* (Kammer 1987) and *mixed reduction* (O'Callahan et al. 1989; Zhang and Wei 1995a).

2.4.3.2 Modal incompleteness

Compared with the numerous available researches dealing with spatial sparseness, papers devoted to modal incompleteness are few and far between. Heylen (1982) implicitly constructed the complete space by replacing one part of the inverse

mass/stiffness matrix of the original analytical mass/stiffness matrix with the counterpart of tests. The formulation is simple and direct:

$$\boldsymbol{M}^{-1} = \boldsymbol{M}_A^{-1} - \boldsymbol{M}_{A,sub}^{-1} + \boldsymbol{M}_{t,sub}^{-1} \tag{2.28}$$

where, $\boldsymbol{M}$ is the updated mass matrix and $\boldsymbol{M}_A$ is the original mass matrix (the matrix of the analytical model before updating). As one part of $\boldsymbol{M}_A$, $\boldsymbol{M}_{A,sub}$ corresponds to those degrees of freedom where test data is available, and $\boldsymbol{M}_{t,sub}$ is the mass matrix in the subspace spanned by the measured vectors. $\boldsymbol{M}_{A,sub}$ and $\boldsymbol{M}_{t,sub}$ are defined by:

$$\boldsymbol{M}_{t,sub}^{-1} = \boldsymbol{\Phi}_t \boldsymbol{\Phi}_t^T \tag{2.29}$$

$$\boldsymbol{M}_{A,sub}^{-1} = \boldsymbol{\Phi}_{A,sub} \boldsymbol{\Phi}_{A,sub}^T \tag{2.30}$$

in which $\boldsymbol{\Phi}_t$ is the measured eigenvector matrix and $\boldsymbol{\Phi}_{A,sub}$ is the corresponding analytical eigenvector. The updated stiffness matrix $\boldsymbol{K}$ can be obtained in a similar way, i.e.

$$\boldsymbol{K}^{-1} = \boldsymbol{K}_A^{-1} - \boldsymbol{K}_{A,sub}^{-1} + \boldsymbol{K}_{t,sub}^{-1} \tag{2.31}$$

$$\boldsymbol{K}_{t,sub}^{-1} = \boldsymbol{\Phi}_t \boldsymbol{\Lambda}_t^{-1} \boldsymbol{\Phi}_t^T \tag{2.32}$$

$$\boldsymbol{K}_{A,sub}^{-1} = \boldsymbol{\Phi}_{A,sub} \boldsymbol{\Lambda}_{A,sub}^{-1} \boldsymbol{\Phi}_{A,sub}^T \tag{2.33}$$

where, $\boldsymbol{\Lambda}_t$ is the measured spectral matrix and $\boldsymbol{\Lambda}_{A,sub}$ is the corresponding spectral matrix of the analytical model. Assuming that the model updating only slightly changes the original model, Chen (1985) avoided the time consuming, and sometimes ill conditioned, matrix inversion calculation in Equations (2.28) and (2.31). Some other implicit methods are available in the literature by Zhang and Wei (1991, 1992). An explicit method for generating complete modal space was

developed by Zhang and coworkers (Zhang et al. 1989; Zhang and Wei 1991; Zhang and Li 1992; Zhang 1998; Zhang and Wei 1996).

2.4.4 MODAL SENSITIVITY

Most methods for model updating take a form as (Mottershead and Friswell 1993):

$$\delta \mathbf{z} = \mathbf{S}\delta \mathbf{p} \tag{2.34}$$

where, $\delta\mathbf{p}$ is the perturbation in the parameter; $\delta\mathbf{z}$ is the perturbation in the measured output and **S** is the sensitivity matrix containing the first derivative of the eigenvalue and mode shapes with respect to the parameters. When **S** and $\delta\mathbf{z}$ are obtained, $\delta\mathbf{p}$ can be solved from Equation (2.34). Two types of method, namely the direct and the indirect/modal methods have been developed for the calculation of **S**. Zhang and Li (1993) discussed the relationship between the two methods.

2.4.4.1 Direct methods

Direct methods refer to those methods which obtain the derivatives of eigendata by directly calculating partial derivatives of the eigenvector Equation (2.23). The original work relating to this kind of method is given by Fox and Kapoor (1968). However, this method requires inversing a full matrix. Nelson (1976) introduced a new method, which could retain the sparsity of the finite element matrices, to obtain the general solution for the problem. The method was then further developed by Dailey (1986) and Mills-Curran (1988). Mills-Curran (1990) pointed out a deficiency of this method in the circumstances of repeated eigenvalues. The method by Zhang and Wei (1990) based on the matrix perturbation principle is much simpler than Nelson's method. Another direct method by Zhang and Wei (1997) is

the mixed method, which is much faster than other methods when the derivatives of multiple modes are to be calculated. The method by Fox and Kapoor (1968) is presented here to show the basic idea of direct methods.

Fox and Kapoor (1968) calculated the derivative of the ith eigenvalue, λ_i, with respect to the jth parameter, p_j, by taking the derivative of the corresponding eigenvector equation in Equation (2.23), to give:

$$\left(\frac{\partial \boldsymbol{K}}{\partial p_j} - \lambda_i \frac{\partial \boldsymbol{M}}{\partial p_j}\right)\varphi_i - \frac{\partial \lambda}{\partial p_j}\boldsymbol{M}\varphi_i + (\boldsymbol{K} - \lambda_i \boldsymbol{M})\frac{\partial \varphi_i}{\partial p_j} = 0 \tag{2.35}$$

Left multiplying by the transpose of the eigenvector, φ_i, and using mass orthogonality (Equation 2.24) and the original definition (Equation 2.23) of the eigensystem produces:

$$\frac{\partial \lambda}{\partial p_j} = \varphi_i^T \left(\frac{\partial \boldsymbol{K}}{\partial p_j} - \lambda_i \frac{\partial \boldsymbol{M}}{\partial p_j}\right)\varphi_i \tag{2.36}$$

The calculation for this expression is easy and requires only the ith eigenvalue and eigenvector. Eigenvector derivatives can be obtained by using Equation (2.35) and the derivative of the mass orthogonality equation, i.e.

$$\begin{bmatrix} \boldsymbol{K} - \lambda_i \boldsymbol{M} \\ \lambda_i \varphi_i^T \boldsymbol{M} \end{bmatrix} \frac{\partial \varphi_i}{\partial p_j} = \begin{Bmatrix} \frac{\partial \lambda}{\partial p_j}\boldsymbol{M}\varphi_i - \left(\frac{\partial \boldsymbol{K}}{\partial p_j} - \lambda_i \frac{\partial \boldsymbol{M}}{\partial p_j}\right)\varphi_i \\ \frac{1}{2}\lambda_i \varphi_i^T \frac{\partial \boldsymbol{M}}{\partial p_j}\varphi_i \end{Bmatrix} \tag{2.37}$$

Left multiplying with $[\boldsymbol{K}\text{-}\lambda_i\boldsymbol{M},\ \lambda_i\boldsymbol{M}\varphi_i]$ on both sides, the derivatives of a single-root eigenvector can be obtained by solving the resulting linear algebraic equations.

2.4.4.2 Indirect methods

The basic idea of indirect methods is to assume that the derivatives of eigenvectors are linear combinations of the eigenvectors (Fox and Kapoor 1968), i.e.

$$\frac{\partial \varphi_i}{\partial p} = \sum_{j=1}^{k} A_{ij} \varphi_j \qquad i = 1,2,...,k \tag{2.38}$$

where, p is the concerned parameter; k is the number of modes measured from a test or calculated from an analytical model and A_{ij} is the coefficient to be solved. Substituting the above equation into Equation (2.35) and premultiplying the equation by φ_k^T, we get:

$$A_{ik} = \frac{\varphi_k^T (K' - \lambda_i M') \varphi_i}{\lambda_i - \lambda j}, \qquad k \neq i \tag{2.39}$$

A_{ii} can be obtained using Equation (2.38) and the mass orthogonality equation, i.e.

$$A_{ii} = \frac{1}{2} \varphi_i^T M' \varphi_i \tag{2.40}$$

It should be noted that k is generally smaller than the number of degrees of freedom of the analytical model, so that the eigenvector derivatives obtained from Equation (2.38) may have great errors due to modal incompleteness. From recent work (Zhang 1995, 1996), these errors can be reduced.

2.4.5 FINITE ELEMENT MODEL UPDATING

2.4.5.1 Sensitivity based methods

There are two kinds of sensitivity based methods in implementation, one is to determine updating factors of substructures, and the other is to update design parameters. To update substructure factors, the mass and stiffness matrices are expressed as (Zhang and Lallement 1987):

$$\boldsymbol{M} = \sum_{i}^{l} \boldsymbol{M}_i = \sum_{i}^{l} \alpha_{mi} \boldsymbol{M}_{Ai} \tag{2.41}$$

$$\boldsymbol{K} = \sum_{i}^{l} \boldsymbol{K}_i = \sum_{i}^{l} \alpha_{ki} \boldsymbol{K}_{Ai} \tag{2.42}$$

The measured eigendata is also a function of parameters, $\alpha_{m,i}$ and $\alpha_{k,i}$, i.e.

$$\lambda_t = \lambda_A + \sum_{i}^{l} \frac{\partial \lambda_A}{\partial \alpha_{mi}} \Delta\alpha_{mi} + \sum_{i}^{l} \frac{\partial \lambda_A}{\partial \alpha_{ki}} \Delta\alpha_{ki} \tag{2.43}$$

$$\varphi_t = \varphi_A + \sum_{i}^{l} \frac{\partial \varphi_A}{\partial \alpha_{mi}} \Delta\alpha_{mi} + \sum_{i}^{l} \frac{\partial \varphi_A}{\partial \alpha_{ki}} \Delta\alpha_{ki} \tag{2.44}$$

in which, $\Delta\alpha_{mi}=\alpha_{mi}-1$, $\Delta\alpha_{ki}=\alpha_{ki}-1$. Equation (2.34) can be obtained with S being the Jacobian matrix:

$$\mathbf{S} = \begin{bmatrix} \frac{\partial \varphi_A^1}{\partial \alpha_{m1}} & \cdots & \frac{\partial \varphi_A^1}{\partial \alpha_{ml}} & \frac{\partial \varphi_A^1}{\partial \alpha_{k1}} & \cdots & \frac{\partial \varphi_A^1}{\partial \alpha_{kl}} \\ \vdots & & \vdots & \vdots & & \vdots \\ \frac{\partial \varphi_A^k}{\partial \alpha_{m1}} & \cdots & \frac{\partial \varphi_A^k}{\partial \alpha_{ml}} & \frac{\partial \varphi_A^k}{\partial \alpha_{k1}} & & \frac{\partial \varphi_A^k}{\partial \alpha_{k1}} \\ \frac{\partial \lambda_A^1}{\partial \alpha_{m1}} & \cdots & \frac{\partial \lambda_A^1}{\partial \alpha_{m1}} & \frac{\partial \lambda_A^1}{\partial \alpha_{k1}} & \cdots & \frac{\partial \lambda_A^1}{\partial \alpha_{k1}} \\ \vdots & & \vdots & \vdots & & \vdots \\ \frac{\partial \lambda_A^k}{\partial \alpha_{m1}} & \cdots & \frac{\partial \lambda_A^k}{\partial \alpha_{m1}} & \frac{\partial \lambda_A^k}{\partial \alpha_{k1}} & \cdots & \frac{\partial \lambda_A^k}{\partial \alpha_{k1}} \end{bmatrix}_{(N+1)k\times 2l} \tag{2.45}$$

$$\Delta \mathrm{p} = \begin{bmatrix} \Delta\alpha_{m1} \\ \vdots \\ \Delta\alpha_{ml} \\ \Delta\alpha_{k1} \\ \vdots \\ \Delta\alpha_{kl} \end{bmatrix}_{2l\times 1}, \quad \Delta \mathrm{z} = \begin{bmatrix} \varphi_t^1 - \varphi_A^1 \\ \vdots \\ \varphi_t^k - \varphi_A^k \\ \lambda_t^1 - \lambda_A^1 \\ \vdots \\ \lambda_t^k - \lambda_A^k \end{bmatrix}_{(N+1)k\times 1}, \tag{2.46}$$

When the number of parameters and measurements are not equal, the sensitivity matrix **S** is not square. Chen and Garba (1980) considered the undetermined case. The parameter vector nearest to the original analytical parameters was sought which reproduced the required measurement change. When it becomes overdetermined, a least squares or weighted least squares technique may be used. Hart and Yao (1977) and Ojalvo et al. (1989) have given further details. The change in the parameters are calculated as:

$$\Delta \mathbf{p} = \left[\mathbf{S}^T \mathbf{S}\right]^{-1} \mathbf{S}^T \Delta \mathbf{z} \tag{2.47a}$$

$$\Delta \mathbf{p} = \left[\mathbf{S}^T \mathbf{V}^{-1} \mathbf{S}\right]^{-1} \mathbf{S}^T \mathbf{V}^{-1} \Delta \mathbf{z} \tag{2.47b}$$

for the least squares and weighted least squares respectively. The matrix **V** is a positive definite weighting matrix that is usually related to the estimated variance of the measured data.

Similar approaches are used to update design parameters (Collins et al. 1972; Collins et al. 1974) and physical parameters (Dascotte and Vanhonacker 1989; Dascotte 1990; Robinson 1992; Dascotte 1992). Piranda et al. (1991) discussed the practical implementation of these methods, including the choice of measurement locations, the criteria for convergence and automatic mode pairing. The use of the second order sensitivity was discussed by some investigators (Kim et al. 1983; Brandon 1984; Kuo and Wada 1987; Ojalvo and Pilon 1991).

2.4.5.2 Lagrange multiplier

Berman and Baruch were among some of the earliest investigators to use the Lagrange multiplier in order to update the finite element model (Berman 1979; Berman and Wei 1980; Berman and Wei 1981; Baruch 1982a; Berman Nagy 1983; Baruch 1984). In Berman-Baruch's method, a constrained minimum problem is constructed. The solution of the minimum problem will get a solution which contends both mass and stiffness orthogonal equations and is the nearest one to the original analytical model in the sense of weighted Euclidian distances. As the mass orthogonal Equation (2.24) is only related to the eigenvectors, the mass matrix is firstly determined and then the stiffness matrix. For the mass matrix updating, the minimum problem is described as (Berman and Nagy 1983):

$$\left\| M_A^{-1/2}(M - M_A)M_A^{-1/2} \right\| = \mathbf{min} \tag{2.48}$$

$$\Phi_t^T M \Phi_t = I \tag{2.49}$$

By using λ_{ij} as the Lagrange multiplier, the above problem is equivalent to minimizing the objective function:

$$J = \left\| M_A^{-1/2}(M - M_A)M_A^{-1/2} \right\| + \sum_{i=1}^{m}\sum_{j=1}^{m} \lambda_{ij}(\Phi_t^T M \Phi_t - I)_{ij} \tag{2.50}$$

The minimization procedure results in the updated mass as:

$$M = M_A + M_A \Phi_t m_A^{-1}(I - m_A)m_A^{-1}\Phi_t^T M \tag{2.51}$$

where m_A is defined by:

$$m_A = \Phi_t^T M \Phi_t \tag{2.52}$$

Similar to the process for determining M, an updated stiffness matrix can be obtained by minimizing the following objective function:

$$J = \left\| M_A^{-1/2}(K - K_A)M_A^{-1/2} \right\| + \sum_{i=1}^{m}\sum_{j=1}^{m} \lambda_{Kij}(K\Phi_t^T - M\Phi_t \Lambda)_{ij} + \\ + \sum_{i=1}^{m}\sum_{j=1}^{m} \lambda_{Tij}(K - K^T)_{ij} \tag{2.53}$$

Here the Lagrange multipliers are used to enforce the eigenvector equation and stiffness symmetry. The updated stiffness is obtained as:

$$K = K_A + (\Delta + \Delta^T) \tag{2.54}$$

where,

$$\Delta = \left[\frac{1}{2} M\Phi_t (\Lambda_t + k_A) - K_A\Phi_t \right] \Phi_t^T M \tag{2.55}$$

$$k_A = \Phi_t^T K_A \Phi_t \tag{2.56}$$

Berman-Baruch's method suffers in losing the sparsity of a finite element system and the connectivity of the matrix elements. The question of structural connectivity was discussed in general by Berman (1989). Kabe (1985) argued that the objective function should not be related to the absolute value of elements in the mass/stiffness matrix. He believed that the objective function should be based on the relative change of the matrix element, and therefore he proposed the minimization of the objective function:

$$J = \left\| I - I \otimes \Gamma \right\| \tag{2.57}$$

where, the i,jth term of I is given by:

$$I = \begin{cases} 1 & \text{if } K_{Aij} \neq 0 \\ 0 & \text{if } K_{Aij} = 0 \end{cases} \tag{2.58}$$

The matrix Γ is to be determined such that:

$$\boldsymbol{K} = \boldsymbol{K}_A \otimes \Gamma \tag{2.59}$$

where, $\otimes$ is the element by element (scalar) matrix multiplication operator. The minimization of J is subject to Lagrange multiplier constraints such that Γ is symmetric, and the eigenvector equation is satisfied exactly. The solution of the above problem is quite complex and the process of obtaining the solution is computationally expensive. Further research was undertaken by Kammer (1988) to improve the computational efficiency. Other researches concerning the connectivity of the mass/stiffness include those by Smith and Beattie (1991) and Gordis et al. (1986).

2.4.6 UNCERTAINTY

Uncertainty is related to the errors in both the measurements and the analytical model. Statistical techniques should be adopted to deal with uncertainties. Collins et al. (1972, 1974) presented a method to provide a Bayesian estimation of structural parameters. A Baysian estimator is based on Bayes' formula, which calculates the probability density function (PDF) of the parameters, including the measured information (the posterior PDF), in terms of the PDF of parameters before updating (the prior PDF). Many papers gave examples of use of the Collins's method (Dascotte 1990; Dascotte and Vanhonacker 1989; Robinson 1982; Thomas et al. 1986).

2.5 OPTIMIZATION TOOLS

'Optimization is the process of making something better' (Haupt and Haupt 1998). For model updating based on dynamic tests, the model parameters, or stiffness and mass matrix are optimised in a finite element model, so that the model may produce the same results as in tests. This target is hardly achievable due to the uncertainty in tests and the approximation of a model to a real structure. An optimal model is defined as one of the models, which produces the closest results to the output of tests. Optimization tools are used to find such a model.

For all optimization algorithms, the basic function is minimum seeking, i.e. the minimum value of the cost function is obtained by searching the cost surface (all possible function values). There are many textbooks that describe optimization methods (e.g., Press et al. 1992; Cuthbert 1987). Boyer and Merzbach (1991) provided a review of this subject.

The most simple, however clumsy, way to optimization is to compare all possible values of the function to find the global minimum. An extremely large number of evaluations of the function are required to catch the minimum, i.e.

$$N = \prod_{i=1}^{M} Q_i \tag{2.60}$$

where, N is the total number of different parameter combinations; M is the number of different parameters and Q_i the number of different values that parameter i can attain. It is obvious that this method takes an extremely long time to find the global minimum. This method can also be used for continuous parameters with fine sampling. Unfortunately, missing the global minimum is always at risk due to undersampling, which tends to occur when the cost function takes a long time to

evaluate. Hence, exhaustive searches may be practical for a small number of parameters in a limited searching space.

A very brief review of the development of other optimization strategies is given in this section.

2.5.1 CATEGORIES OF OPTIMIZATION

Haupt and Haupt (1998) divide the optimization algorithms into six categories as:

1. Trial-and-error optimization refers to the process of adjusting parameters that affect the output without knowing much about the process generating the output. In contrast, mathematical function optimization assumes that we can describe a process by a mathematical formula, in which various mathematical methods are applied to the function to find the optimum solution.
2. When there is only one parameter to be optimized, the problem is one-dimensional and can be solved easily. Many multidimensional optimization approaches, which tend to be increasingly difficult as the number of dimensions increases, generalize to a series of one-dimensional approaches.
3. Dynamic optimization depends on time whereas the static one is independent of time.
4. Optimization can also be distinguished by either discrete or continuous parameters.
5. Parameters often have limits or constraints. Constrained optimization incorporates parameter equalities and inequalities into the cost function. Unconstrained optimization allows the parameters to take any value. A

constrained parameter is often converted into an unconstrained parameter through a transformation of variables. Most numerical optimization routines work better with unconstrained parameters.

6. Some algorithms try to minimize the cost by starting from an initial set of parameter values. These minimum seekers easily get stuck in local minima but tend to be fast. They are the traditional optimization algorithms and are generally based on calculus methods. Moving from one parameter set to another is based on a determinant sequence of steps. On the other hand, random methods use some probabilistic calculations to find parameter sets. They tend to be slower but have greater success at finding the global minimum.

2.5.2 ANALYTICAL OPTIMIZATION

When a function and its parameters are continuous, the extrema of a function are located where the gradient of the function equals zero, i.e.

$$\nabla f = 0 \tag{2.61}$$

the roots of the above equations may contain both the maxima and minima. It is proven that when the Laplacian of the function is greater than zero:

$$\nabla^2 f > 0 \tag{2.62}$$

the extremum corresponds to a minimum. Unfortunately, searching the list of minima is required to obtain the global minimum, which makes the calculation of $\nabla^2 f$ redundant. Instead, f is evaluated at all the extrema, then the list of extrema is searched for the global minimum. This approach quickly finds a single minimum, but

a further search should be taken to find the global minimum. If there are too many parameters, it is difficult to solve $\nabla f = 0$.

When there are equality constraints for a cost function, the method known as Lagrange multipliers is adopted, i.e.

$$\begin{aligned} &\min f(x) \\ &s.t.\, g_m(x_1, x_2, \ldots) \end{aligned} \tag{2.63}$$

A new function, which is equivalent to the above problem concerning the solution of the minima, is then constructed as (Borowski and Borwein 1991):

$$F(x_1, x_2, \ldots) = f(x_1, x_2, \ldots) + \sum_{m=1}^{M} \lambda_m g_m(x_1, x_2, \ldots) \tag{2.64}$$

When gradients are taken in terms of the new parameters, λ_m, the constraints are automatically satisfied.

Techniques were needed to find the minimum of cost functions having no analytical gradients, such as in game theory. Kangorovich, von Neumann and Leontief have solved linear problems in several research fields (Anderson 1992). In 1947, Dantzig introduced the simplex method, which has been the workhorse for solving *linear programming* problems (Williams 1993). This method has been widely implemented in computer codes since the mid-1960s. *Integer programming* is an extension of linear programming in which some of the parameters can only take integer values (Williams 1993). Nonlinear techniques were also developed. Karush extended *Lagrange multipliers* to describe constraints defined by equalities and inequalities, so a much larger category of problems could be solved (Pierre 1992). Since the 1950s, Newton's method and the method of steepest descent have been commonly used.

The approach of the methods mentioned above is similar to using refined surveying tools, which unfortunately does not guarantee a global minimum to be found. Therefore, searching for a global minimum needs new algorithms and is discussed below:

2.5.3 NATURAL OPTIMIZATION

The genetic algorithm and simulated annealing are relatively new among the outstanding algorithms which have emerged over the last 30 years. The genetic algorithm models natural selection and evolution, while simulated annealing models the annealing process. Both methods generate new points in the search space by applying operators to current points and statistically moving toward more optimal places in the search space and have met with tremendous success in a number of areas. They rely upon an intelligent search of a large but finite solution space using statistical methods. Both algorithms do not require taking cost function derivatives and can, therefore, deal with discrete parameters and non-continuous cost functions. They represent processes in nature that are remarkably successful at optimizing natural phenomena.

2.5.3.1 Simulated annealing

Based on ideas formulated in the early 1950s, simulated annealing was introduced by Kirkpatrick and coworkers (1983). This method simulates the annealing process in which a substance is heated to a temperature above its melting temperature, then cooled gradually to produce a crystalline lattice. This crystalline lattice, composed of millions of atoms perfectly aligned, is a beautiful example of nature finding an optimal structure, in which its energy probability distribution is minimized. However, when cooling proceeds too quickly, the substance becomes an

amorphous mass with a higher than optimum energy state and forms no crystals. This state implies that *quencher* has occurred. Careful controlling of the rate of temperature change is the key for crystals to be formed.

The algorithmic analogue to the annealing process involves initializing a first guess state, then 'heating' it by updating the parameters. The cost function represents the energy level of the substance. The key issue for the annealing algorithm is a control parameter, analogous to the temperature, controlling the rate of descent of the algorithm into the optimum cost function value. This control parameter determines the step size, so that at the beginning of the process, the algorithm is forced to make large changes in parameter values and the changes become gradually small after a certain number of iterations. The control parameter should not be too large so that the algorithm has a chance to find the correct area before trying to get to the lowest point in the area. Control parameters resulting in too small step sizes should also be avoided; otherwise the algorithm will become extensively computational. This algorithm has essentially 'solved' the traveling salesman problem (Kirkpatrick et al. 1983) and has been applied successfully to a wide variety of problems.

2.5.3.2 Genetic algorithm

The genetic algorithm is another type of natural method. It consists of a subset of evolutionary algorithms modeling biological processes to optimize highly complex cost functions. The method was developed by Holland (1975) over the course of the 1960s and 1970s and finally popularized by Goldberg (1989).

In a genetic algorithm, an initial population/generation composed of many parameter combinations is firstly generated randomly in the solution space. The corresponding cost function values are then evaluated and weighted/ordered to

determine the weight of each parameter combination. A new population/generation is then created with a group of pairs from existing parameter combinations, which are generally called genes. The advantages of a genetic algorithm are that it (Haupt and Haupt 1998):

(1) optimizes with continuous or discrete parameters;

(2) doesn't require derivative information;

(3) simultaneously searches from a wide sampling of the cost surface;

(4) deals with a large number of parameters;

(5) is well suited for parallel computers;

(6) optimizes parameters with extremely complex cost surfaces; they can jump out of a local minimum;

(7) provides a list of optimum parameters, not just a single solution;

(8) may encode the parameters so that the optimization is done with the encoded parameters; and

(9) works with numerically generated data, experimental data, or analytical functions.

These advantages are intriguing and produce stunning results when traditional optimization approaches fail miserably.

2.5.4 SELECTION OF METHOD

Traditional methods have been well tuned to quickly find the solution of a well-behaved convex analytical function with only a few variables. For these problems the optimizer should use past experience and employ the analytical

optimization methods. In addition, for problems that are not extremely difficult, other methods may find the solution faster than the genetic algorithm and the simulated annealing.

However, many realistic problems require modifying a lot of parameters to find the optimal solution, which is frequently beyond the capability of traditional methods. Under these circumstances, referring to natural methods, such as the annealing and the genetic algorithms, can improve the situation.

2.6 SUMMARY

This Chapter provides a literature review on five relatively independent subjects including cable vibration in cable-supported bridges, cable tension measurements, dynamics of sagged cables, vibration-based model updating procedures, and local and global optimization tools, with reasonable overlaps amongst them. Cable vibrations in cable-stayed bridges are reviewed in order to understand what kinds of cable vibrations may exist in practical sagged structural cables. A survey of measurement methods for cable tension testing used in modern cable-stayed bridges is then carried out and the problems existing from previous studies are discussed in detail. Both linear and nonlinear dynamics theories of a sagged cable are then reviewed to provide a theoretical background for further study on linear and nonlinear vibration of cables. The finite element (FE) methods for cable structures are then briefly reviewed for the purpose of selecting or creating an element suitable for cable vibration analysis. Both local and global optimization methods are surveyed to select suitable ones for the problem concerned. The existing frequency-based model updating procedures are then investigated to make

perceptions about state-of-art technology and uncover the parameter identification of stay cables.

The literature review makes it clear that there are great demand in several interconnected research subjects related to cable condition assessments. These subjects include linear and nonlinear modeling for cable dynamics, vibration-based cable tension testing and optimization methods for cable parameter identification. The subsequent Chapters will consequently deal with these subjects. Chapters three, four and five concentrate on the linear and nonlinear modeling for cable dynamics and Chapters six and seven deal with parameter identification of cables by using both local and global optimization methods.

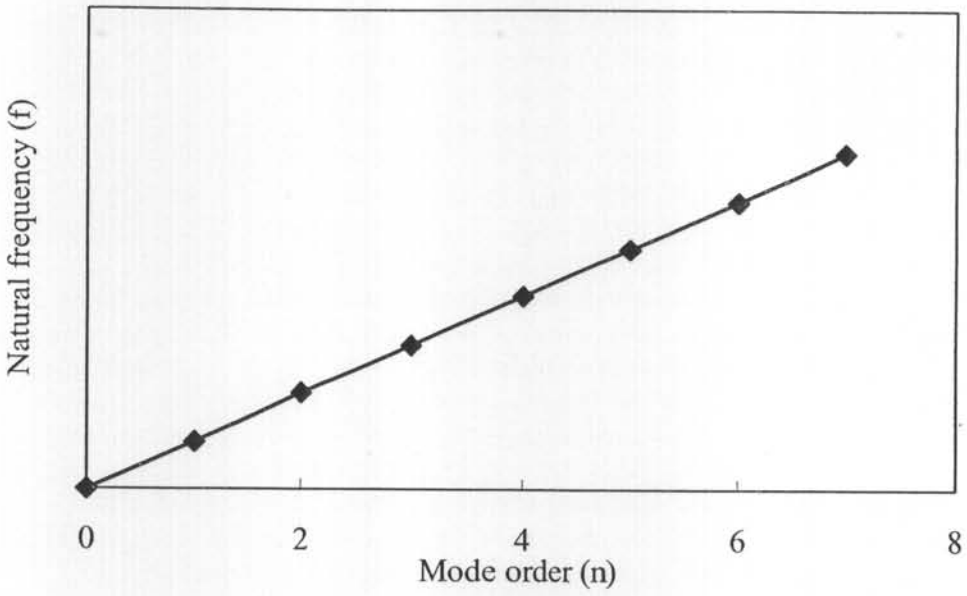

Figure 2.1 Linear relationship between mode order and natural frequency

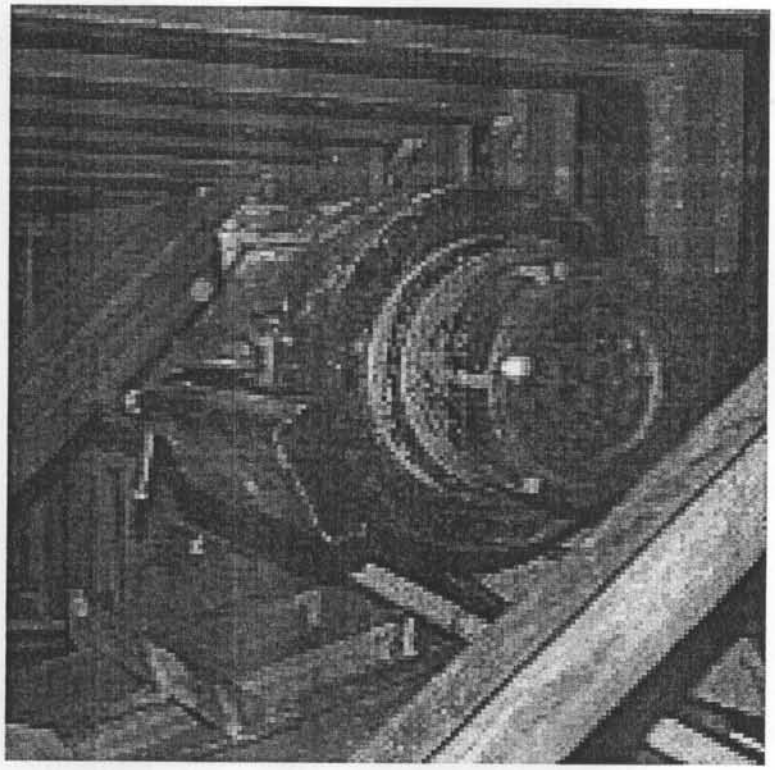

Figure 2.2 Hydraulic jack used in tensioning cable (Ogawa Bridge, Kajima Corporation, 1995)

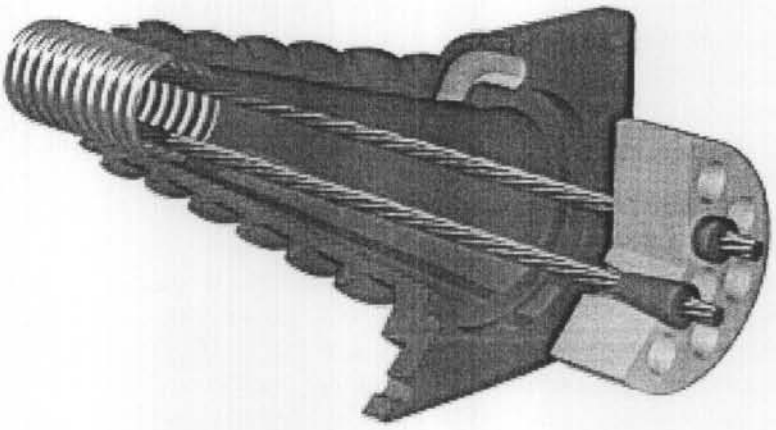

Figure 2.3 Stay cable (Yobuko Bridge, SE Corporation, Japan, 1988)

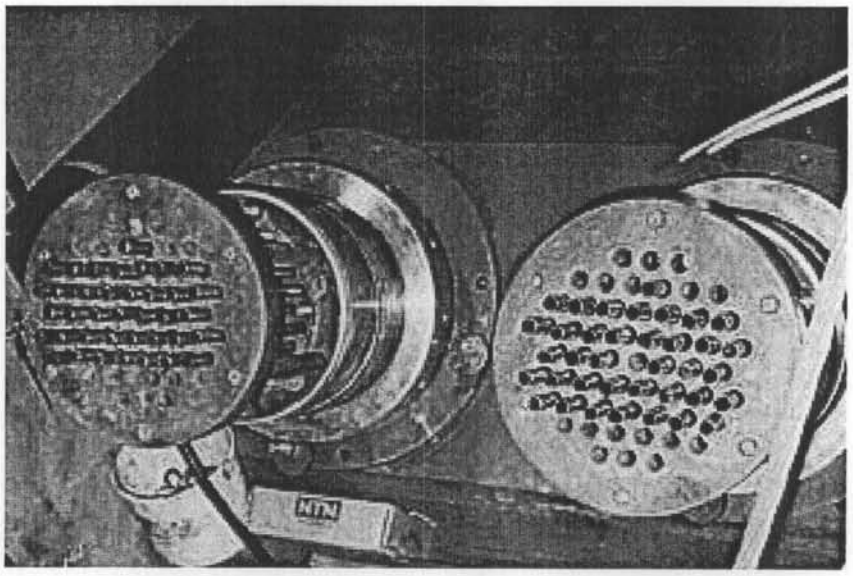

Figure 2.4 Cable anchorage in Ting Kau Bridge, Hong Kong.

Figure 2.5 Load cell: LC1011

Figure 2.6 Load cell: TCLP-NB

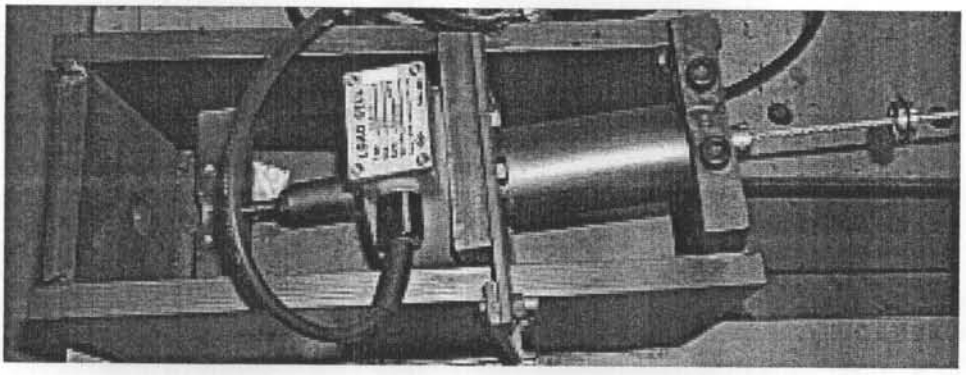

Figure 2.7 Load cell TCLM-1B (TML) in use for cable tension measurement

Table 2.1 Comparison between measured and designed cable tension (kN)

Number	Measurement	Error	Number	Measurement	Error	Design
WB24	13627	5.3%	HB24	12302	-4.9%	12942
WB23	12672	-2.3%	HB23	11951	-7.9%	12970
WB22	12737	-0.3%	HB22	13293	4.1%	12775
WB21	13295	3.6%	HB21	12863	0.2%	12838
WB20	11240	-5.0%	HB20	11988	1.3%	11837
WB19	12161	2.0%	HB19	12075	1.2%	11928
WB18	11658	-2.2%	HB18	11795	-1.1%	11923
WB17	10555	-5.7%	HB17	11137	-0.6%	11199
WB16	10218	-0.2%	HB16	10133	-1.0%	10238
WB15	9349	-7.1%	HB15	9052	10.0%	10061
WB14	8338	-7.3%	HB14	8051	-10.5	8998
WB13	7388	-11.0%	HB13	7811	-5.9%	8299
WB12	7666	-2.8%	HB12	7200	-8.7%	7888
WB11	6751	-9.0%	HB11	7315	-1.4%	7418
WB10	7025	-4.0%	HB10	6929	-5.3%	7318
WB9	6462	-3.4%	HB9	6341	-5.2%	6691
WB8	6581	-0.9%	HB8	6604	-0.5%	6639
WB7	6637	7.7%	HB7	6413	4.1%	6161
WB6	6104	0.1%	HB6	6290	3.2%	6096
WB5	6135	1.9%	HB5	5988	-0.5%	6019
WB4	5647	5.1%	HB4	6165	3.6%	5953
WB3	5176	-3.4%	HB3	5307	-0.9%	5357
WB2	5166	0.9%	HB2	4990	-2.6%	5122
WB1	6253	-3.6%	HB1	6475	-0.2%	5487
W0	8590	8.6%	H0	8373	5.8%	7911
WR1	5937	3.1%	HR1	5831	1.2%	5760
WR2	4817	-5.6%	HR2	4574	-10.4%	5105
WR3	5451	-2.4%	HR3	5509	-1.3%	5583
WR4	6240	1.3%	HR4	6052	-1.7%	6158
WR5	5862	-6.4%	HR5	6435	2.8%	6261
WR6	6906	7.3%	HR6	6414	-0.4%	6437
WR7	6696	1.5%	HR7	6858	4.0%	6596

WR8	6379	-3.6%	HR8	6328	-4.4%	6618
WR9	5898	-12.7%	HR9	6167	-8.8%	6758
WR10	6788	-5.7%	HR10	6918	-3.9%	7195
WR11	6872	-5.3%	HR11	6544	-9.9%	7259
WR12	7613	-7.3%	HR12	7444	-9.4%	8214
WR13	8394	-6.3%	HR13	7908	-11.7%	8959
WR14	8522	-5.8%	HR14	8162	-9.8%	9045
WR15	10212	0.6%	HR15	10061	-0.9%	10153
WR16	10286	-0.1%	HR16	9843	-4.4%	10301
WR17	11012	2.4%	HR17	10279	-4.4%	10751
WR18	10286	1.8%	HR18	11254	2.0%	11038
WR19	11012	-2.8%	HR19	11747	2.1%	11510
WR20	11237	-5.0%	HR20	11783	-0.2%	11806
WR21	11867	-0.8%	HR21	11964	0.0%	11960
WR22	12182	0.8%	HR22	12417	2.7%	12085
WR23	12049	-3.9%	HR23	12749	1.7%	12532
WR24	12370	-3.0%	HR24	12152	-4.7%	12750

Table 2.2 Parameters of load cells

Company	TML (Tokyo Sokki Kenkyujo Co.)	Omegadyne Inc.
Type	TCLP – NB	LC1011
Range	10 N – 2 MN	0 N – 9 MN
Accuracy	0.2% - 0.5%	0.05%
Price	N. A.	US$6,200, or HK$50,000

Table 2.3 Comparison of different methods for in-service cable tension measurements

	Cost	Labor	Time Required
Hydraulic Jack	Expensive	Heavy	Long
Load Cell	Expensive	Heavy	Long
Electro-Magneto Sensor	Expensive	Heavy	Long
Vibration-Based	Cheap	Not heavy	Short

CHAPTER 3

DYNAMIC ANALYSIS OF LARGE-DIAMETER SAGGED CABLES TAKING INTO ACCOUNT FLEXURAL RIGIDITY

3.1 INTRODUCTION

This chapter deals with the forward problem of cable dynamics, which is the basis for developing a vibration-based tension force evaluation procedure for bridge cables using measured multimode frequencies. An investigation on accurate finite element modeling of large-diameter sagged cables taking into account flexural rigidity and sag-extensibility is carried out. A three-node curved isoparametric finite element is formulated for dynamic analysis of bridge stay cables by regarding the cable as a combination of an 'ideal cable element' and a fictitious curved beam element in the variational sense. With the developed finite element formulation, parametric studies are conducted to evaluate the relationship between the modal properties and cable parameters lying in a wide range covering most of the cables in existing cable-supported bridges, and the effect of cable bending stiffness and sag on the natural frequencies. A case study is eventually provided to compare the measured natural frequencies of main cables of the Tsing Ma Bridge and the computed frequencies with and without considering cable bending stiffness. The results show that ignoring bending stiffness gives rise to unacceptable errors in predicting higher-order natural frequencies of the cables, and the proposed finite element formulation

provides an accurate baseline model for cable tension identification from measured multimode frequencies.

Different from existing models, the proposed model for the dynamic analysis of large-diameter sagged cables is a general one in the sense that it is capable of taking into account flexural rigidity, accurate cable profile (sag effects), intermediate dampers and supports, dynamic cable tension and different boundary conditions. Existing models for cable dynamic analysis are good at dealing with some of the above points but not all of them.

3.2 FORMULATION

3.2.1 BASIC ASSUMPTIONS

Two sets of assumptions are used for the nonlinear pure cable model and the linear beam model, respectively. Regarding the cable as a combination of an idealized pure cable' and a 'fictitious beam' in formulation derivation has three features: (i) Two independent elements provides easier understanding on formulation; (ii) Independent use of each model becomes possible, as is required in some circumstances. The pure nonlinear cable model may be used independently for analyzing the internal resonances occurring mainly on the lower order modes, which is hardly influenced by the cable flexural rigidity; (iii) Evaluation on the effects of cable parameters on responses becomes more convenient.

I. *Basic assumptions on the nonlinear pure cable*

(1) The cable material is linearly elastic, characterized by the elastic modulus E;

(2) The elastic cable is perfectly flexible so that it is capable of developing stresses only in the direction normal to the cross section;

(3) The normal stress is uniform over the cross-sectional area;

(4) Though the displacement may be arbitrarily large, the strains are assumed small, which means that the cross-sectional area does not change during deformation; and

(5) The radius of the cable curvature is large with regarding to its cross section dimension.

Under these assumptions, the cable may deform from an unstreched state into its static equilibrium configuration corresponding to the static load (including the cable self-weight). The deformation procedure may be iteratively simulated using the nonlinear cable model derived hereafter.

It is noticed that the derivation of the model is based on an initial equilibrium configuration as shown in **Figure 3.1**. This initial configuration may be obtained by simulating the cable deformation from an unstreched state without any load into the new configuration with the static load applied. It is obvious that such a simulation can be done by employing the model with a straight profile as the initial configuration for the cable. The only problem in this case is that the unstreched cable cannot afford any transverse load. Nevertheless, this problem can be avoided by stretching the cable before the first iteration with a large enough tension and unload this extra tension later in the iteration procedures.

II. *Basic assumptions for linear beam model*

The basic assumptions for the Timoshenko beam are adopted for the spatial curved beam model. Because the out-of-plane deflection and the axial torsion are coupled for a spatial curved beam, the torsional deformation is taken into consideration. Thus the basic assumptions for the beam model are:

(1) The material is linearly elastic, characterized by the elastic modulus E;

(2) A plane section originally normal to the neutral axis remains plane, but not necessarily remains normal to the neutral axis; and

(3) The curvature radius of the beam is large with regarding to its cross section dimension.

3.2.2 THREE-NODE CURVED ELEMENT OF SAGGED CABLE

Without losing generality, the cable static equilibrium profile is assumed in the x-y plane as shown in **Figure 3.1**. This initial (static) configuration is defined by $x(s)$ and $y(s)$, here s denotes the arc length coordinate. Let L, E, A and m be the cable length, modulus of elasticity, cross-sectional area, and mass per unit length respectively. In static equilibrium state, the cable is subjected to dead load and the static tension is $H(s)$. The cable is then subjected to the action of dynamic external forces $p_x(s, t)$, $p_y(s, t)$, and $p_z(s, t)$. The dynamic configuration of the cable is described by the displacement responses $u(s, t)$, $v(s, t)$, and $w(s, t)$ measured from the position of static equilibrium in the x-, y- and z-directions respectively. Let

$$\boldsymbol{U} = \{\, u(s,t) \;\; v(s,t) \;\; w(s,t) \,\}^T \tag{3.1}$$

$$\boldsymbol{P} = \{\, p_x(s,t) \;\; p_y(s,t) \;\; p_z(s,t) \,\}^T \tag{3.2}$$

By using the Lagrangian strain measure, the cable extensional strain due to dynamic loads, ignoring flexural rigidity, can be expressed as

$$\varepsilon = \varepsilon_0 + \varepsilon_l = \frac{d\boldsymbol{X}^T}{ds}\frac{\partial \boldsymbol{U}}{\partial s} + \frac{1}{2}\cdot\frac{\partial \boldsymbol{U}^T}{\partial s}\frac{\partial \boldsymbol{U}}{\partial s} \tag{3.3}$$

where

$$\boldsymbol{X} = \{x(s) \;\; y(s) \;\; 0\}^T \tag{3.4}$$

$\boldsymbol{X}$ is the static equilibrium coordinate vector. The finite element formulation is derived from the Hamilton's principle

$$\delta H = \delta \int_{t_1}^{t_2} \int_0^L (Q - V) ds dt + \int_{t_1}^{t_2} \int_0^L \delta W ds dt = 0 \tag{3.5}$$

in which Q is the kinetic energy density; V is the elastic strain energy density; W is the virtual work density associated with the dead load, dynamic excitation and damping force. They are expressed as

$$Q = \frac{m}{2} \cdot \frac{\partial \boldsymbol{U}^T}{\partial t} \frac{\partial \boldsymbol{U}}{\partial t} \tag{3.6a}$$

$$V = V_i + \frac{EA}{2} \cdot \varepsilon^2 + H(s) \cdot \varepsilon \tag{3.6b}$$

$$\delta W = \delta \boldsymbol{U}^T \left(\boldsymbol{q} + \boldsymbol{P} - \boldsymbol{c} \frac{\partial \boldsymbol{U}}{\partial t} \right) \tag{3.6c}$$

where V_i is the elastic strain energy density held in the initial (static) configuration; $\boldsymbol{q}$ is the dead load vector existent in the initial state; $\boldsymbol{P}$ is the external force vector, and $\boldsymbol{c}$ is the viscous damping coefficient matrix, which is express as

$$\boldsymbol{c} = \begin{bmatrix} c_x & 0 & 0 \\ 0 & c_y & 0 \\ 0 & 0 & c_z \end{bmatrix} \tag{3.7}$$

Substituting Equations (3.6) and (3.3) into Equation (3.5) yields

$$\begin{aligned} \delta I = \delta \int_{t_1}^{t_2} \int_0^L \Bigg[& \frac{m}{2} \cdot \frac{\partial \boldsymbol{U}^T}{\partial t} \cdot \frac{\partial \boldsymbol{U}}{\partial t} - V_i - \frac{EA}{2} \cdot \left(\frac{d\boldsymbol{X}^T}{ds} \cdot \frac{\partial \boldsymbol{U}}{\partial s} + \frac{1}{2} \cdot \frac{\partial \boldsymbol{U}^T}{\partial s} \cdot \frac{\partial \boldsymbol{U}}{\partial s} \right)^2 - \\ & - H \cdot \left(\frac{d\boldsymbol{X}^T}{ds} \cdot \frac{\partial \boldsymbol{U}}{\partial s} + \frac{1}{2} \cdot \frac{\partial \boldsymbol{U}^T}{\partial s} \cdot \frac{\partial \boldsymbol{U}}{\partial s} \right) \Bigg] ds dt + \\ & + \int_{t_1}^{t_2} \int_0^L \delta \boldsymbol{U}^T \cdot \left(\boldsymbol{q} + \boldsymbol{P} - \boldsymbol{c} \cdot \frac{\partial \boldsymbol{U}}{\partial t} \right) ds dt = 0 \end{aligned} \tag{3.8}$$

Here the displacement vector U is selected to fulfill the boundary conditions and initial conditions. By integrating Equation (3.8) by parts and accounting for the static equilibrium configuration, we have

$$\delta I = \int_{t_1}^{t_2} \int_0^L \delta U^T \left\{ m \cdot \frac{\partial^2 U}{\partial t^2} - EA \cdot \frac{\partial}{\partial s}\left[\left(\frac{dX^T}{ds}\frac{\partial U}{\partial s} + \frac{1}{2} \cdot \frac{\partial U^T}{\partial s}\frac{\partial U}{\partial s} \right)\left(\frac{dX}{ds} + \frac{\partial U}{\partial s} \right) \right] \right.$$
$$\left. \frac{\partial}{\partial s}(H \cdot \frac{\partial U}{\partial s}) + c\frac{\partial U}{\partial t} - P \right\} ds dt = 0 \qquad (3.9)$$

An isoparametric curved element with three-nodes is introduced to describe the cable. As shown in **Figure 3.2**, the shape functions in the natural coordinate system are given by

$$N_1 = \frac{1}{2}(1-\xi) - \frac{1}{2}(1-\xi^2), \quad N_2 = 1-\xi^2, \quad N_3 = \frac{1}{2}(1+\xi) - \frac{1}{2}(1-\xi^2) \qquad (3.10a,b,c)$$

and the coordinates and the displacement functions are expressed as

$$x = \sum N_i x_i \qquad (3.11a)$$

$$y = \sum N_i y_i \qquad (3.11b)$$

$$u = \sum N_i u_i \qquad (3.12a)$$

$$v = \sum N_i v_i \qquad (3.12b)$$

$$w = \sum N_i w_i \qquad (3.12c)$$

where x_i, y_i (i = 1, 2, 3) are the nodal coordinates; and the nodal displacement vector is defined as

$$\{U_j\} = \{\{U\}_{j1}^T \{U\}_{j2}^T \{U\}_{j3}^T\}^T$$
$$= \{u_{1j} \quad v_{1j} \quad w_{1j} \quad u_{2j} \quad v_{2j} \quad w_{2j} \quad u_{3j} \quad v_{3j} \quad w_{3j}\}^T \qquad (3.13)$$

By rewriting Equation (3.12) as

$$\begin{aligned} U &= \{u\ v\ w\}^T = [N_1 I\ \ N_2 I\ \ N_3 I]\{\{U\}_{j1}^T \{U\}_{j2}^T\ \{U\}_{j3}^T\}^T \\ &= [N]\{U_j\} \end{aligned} \tag{3.14}$$

and substituting Equations (3.11) to (3.14) into Equation (3.3), we get the following expressions

$$\varepsilon_0 = [B_0]\{U_j\} = [\{B_{01}\}\ \{B_{02}\}\ \{B_{03}\}]\{U_j\} \tag{3.15a}$$

$$\varepsilon_l = [B_l]\{U_j\} = [\{B_{l1}\}\ \{B_{l2}\}\ \{B_{l3}\}]\{U_j\} \tag{3.15b}$$

$$\{B_{0i}\} = \frac{1}{J^2}\{x'N_i'\ \ y'N_i'\ \ 0\} \tag{3.15c}$$

$$\{B_{li}\} = \frac{1}{2J^2}\{u'N_i'\ \ v'N_i'\ \ w'N'\} \tag{3.15d}$$

where the prime denotes the derivative with respect to ξ and, J is the Jacobian determinant, i.e

$$J = ds/d\xi \tag{3.16}$$

Substituting Equations (3.13) to (3.15) into Equation (3.8), after some manipulation, yields

$$\begin{aligned} \delta\Pi = \int_{t_1}^{t_2} \sum \delta\{U_j\}^T \{[M_j]\{\ddot{U}_j\} + [C_j]\{\dot{U}_j\} + \\ + [K_{0j} + K_{aj} + K_{lj}(\{U_j\}) + K_{2j}(\{U_j\}\{U_j\}^T)]\{U_j\} - \{P_j\}\} dt \\ = 0 \end{aligned} \tag{3.17}$$

from which the governing equation of motion of element j is obtained as

$$[M_{ej}]\{\ddot{U}_{ej}\} + [C_{ej}][\dot{U}_{ej}] + [K_{0ej} + K_{aej} + K_{1ej}(\{U_{ej}\}) + K_{2ej}(\{U_{ej}\}\{U_{ej}\}^T)]\{U_{ej}\} = \{P_{ej}\} \tag{3.18}$$

in which,

$$[M_{ej}] = mJ \int_{-1}^{+1} [N]^T [N] d\xi \tag{3.19a}$$

$$[C_{ej}] = J \int_{-1}^{+1} [N]^T [c] [N] d\xi \tag{3.19b}$$

$$\{P_{ej}\}=J\int_{-1}^{1}[N]^T\{P\}d\xi \tag{3.19c}$$

$$[K_{0ej}]=EAJ\int_{-1}^{1}[B_0]^T[B_0]d\xi \tag{3.19d}$$

$$[K_{1ej}]=EAJ\int_{-1}^{1}\left([B_l]^T[B_0]+2[B_0]^T[B_l]\right)d\xi \tag{3.19e}$$

$$[K_{2ej}]=2EAJ\int_{-1}^{1}[B_l]^T[B_l]d\xi \tag{3.19f}$$

$$[K_{\sigma ej}]=\frac{1}{2J}\int_{-1}^{1}H[N']^T[N']d\xi \tag{3.19g}$$

The global equation of the cable is then obtained through assembling the element mass matrix, damping matrix, stiffness matrix, and nodal load vector by the standard assembly procedure. It is noted that in Equation (3.19) the stiffness matrix includes linear stiffness term (K_0), the quadratically nonlinear stiffness term (K_1), the cubically nonlinear stiffness term (K_2) and the geometric stiffness term (K_σ).

To validate the model for its capability in nonlinear analysis, the free cable profile of the main span of the Tsing Ma Suspension Bridge, Hong Kong, is calculated by using the present model. The main span is of 1377.0 m long, the horizontal component of the cable tension is 122,642 kN in the blue print, the cross sectional area is 0.759278 m^2 and the elastic modulus is 200 GPa in the blue print. The calculation begins with a straight cable of about 1390 m long under an initial tension of 122,642 kN. Then the cable is subject to its dead load (self-weight) and deform from the original state. The calculation processes iteratively and the cable profile finally converges to a catenary configuration, which is proven to be the analytical solution for the problem with the parameters given above. The displacement at the midspan is 112 m, which is more than one hundred times the cable cross section diameter, and the angle change at the left end before and after

deformation is 18 degree. It is evident from the example that the nonlinear pure cable model derived here pertains to large displacement – large rotation behavior.

3.2.3 FORMULATION FOR FLEXURAL RIGIDITY

The additional stiffness contribution due to the flexural rigidity of cable is derived by assuming a fictitious curved beam. The curved beam element is same as shown in **Figure 3.2**, but a new local coordinate system in terms of tangential and normal axes is introduced for the convenience of formulation to relate displacements with stress resultants. As illustrated in **Figure 3.3**, the displacements at any node i are expressed as

$$\{\delta\}_i = \{u_i \; v_i \; w_i \; \theta_{ti} \; \theta_{si} \; \theta_{zi}\}^T \tag{3.20}$$

where u_i is the in-plane displacement in tangential direction; v_i is the in-plane displacement in transverse direction; w_i is the displacement in z-direction; θ_{ti} is the total rotation in tangential direction; θ_{si} is the angle of twist; and θ_{zi} is the total rotation of transverse bending. Similar to Equation (3.13), the displacement vector is expressed with isoparametric interpolation functions as

$$\{U\} = \{u \; v \; w \; \theta_t \; \theta_s \; \theta_z\}^T = [N_1 \mathrm{I} \;\; N_2 \mathrm{I} \;\; N_3 \mathrm{I}]\left\{\{\delta\}_1^T \;\; \{\delta\}_2^T \;\; \{\delta\}_3^T\right\}^T = [N]\{\delta\} \tag{3.21}$$

The strain vector is written as

$$\{\varepsilon\} = \{\kappa_z \; \kappa_t \; \alpha \; \gamma_{vs} \; \gamma_{ws}\}^T \tag{3.22}$$

where κ_z and κ_t are the in-plane and out-of-plane curvature changes, respectively; α is the cross-sectional torsion change; γ_{vs} and γ_{ws} are the shear strains. The strain-displacement relation can be expressed as

$$\kappa_z = \frac{\partial \theta_z}{\partial s} + \frac{1}{R} \cdot \frac{\partial u}{\partial s} \tag{3.23a}$$

$$\kappa_t = -\frac{\partial \theta_s}{\partial s} - \frac{\theta_t}{R} \tag{3.23b}$$

$$\alpha = \frac{\partial \theta_t}{\partial s} - \frac{\theta_s}{R} \tag{3.23c}$$

$$\gamma_{vs} = \frac{\partial v}{\partial s} - \theta_z \tag{3.23d}$$

$$\gamma_{ws} = \frac{\partial w}{\partial s} + \theta_s \tag{3.23e}$$

in which R is the curvature radius of the element. It should be noted that R is not a constant for a sagged cable. It is calculated using the formula

$$R = \frac{\left[1 + (dy/dx)^2\right]^{\frac{3}{2}}}{d^2y/d^2x} \tag{3.24}$$

Combining Equations (3.21) and (3.23) yields

$$\{\varepsilon\} = [\boldsymbol{B}]\{\delta\} = \left[[\boldsymbol{B}_1]\ [\boldsymbol{B}_2]\ [\boldsymbol{B}_3]\right]\{\delta\} \tag{3.25}$$

in which $\boldsymbol{B}_i$ (i = 1, 2, 3) is expressed as

$$[\boldsymbol{B}_i] = \frac{1}{RJ} \cdot \begin{bmatrix} N_i' & 0 & 0 & 0 & 0 & R \cdot N_i' \\ 0 & 0 & 0 & -R \cdot N' & -J \cdot N_i & 0 \\ 0 & 0 & 0 & -J \cdot N_i & R \cdot N_i' & 0 \\ 0 & R \cdot N_i' & 0 & 0 & 0 & -RJ \cdot N_i \\ 0 & 0 & R \cdot N_i' & JR \cdot N_i & 0 & 0 \end{bmatrix} \tag{3.26}$$

Figure 3.4 shows the stress-resultants at node i. The stress–strain relation is given by

$$\begin{aligned} \{\sigma\} &= \{M_z\ M_s\ T\ V_z\ V_s\}^T \\ &= \text{diag}[EI_z\ EI_s\ GJ_s\ \beta GA\ \beta GA]\{\varepsilon\} \\ &= [\boldsymbol{D}]\{\varepsilon\} \end{aligned} \tag{3.27}$$

With Equations (3.25) and (3.27), the additional element stiffness matrix due to cable flexural rigidity is derived in a similar way as

$$[K_0] = J\int_{-1}^{1}[B]^T[D][B]d\xi \tag{3.28}$$

The additional stiffness matrix given in Equation (3.28) is obtained by referring to the local coordinate system. It should be transformed into the element stiffness relation in the global *x-y-z* coordinate system before performing assembly to obtain overall stiffness matrix. Likewise, the element stiffness matrix given in Equation (3.19), with 9×9 dimension, only accommodates the translational degrees of freedom. It should be expanded in the assembly process as an 18×18 matrix to cater for the rotation degrees of freedom.

3.3 PARAMETRIC STUDIES

The proposed formulation has been encoded into a versatile finite element program. In this section, parametric studies are conducted to evaluate the effect of bending stiffness and sag-extensibility on natural frequencies, and the relation between the modal properties and cable parameters for a wide parameter range. A numerical verification is first carried out through comparing the computed results by the proposed method with the analytical results available in literature. Mehrabi and Tabatabai (Mehrabi and Tabatabai 1998) formulated a differential equation for solution of free vibration of suspended cables by use of finite difference technique. This approximate formula accounted for cable bending stiffness and sag-extensibility, but was based on the assumption of flat sag and invariability of dynamic tension along cable length. The following dimensionless parameters have been adopted to characterize the bending stiffness and sag-extensibility respectively

$$\xi = L\sqrt{\frac{H_h}{EI}} \tag{3.29a}$$

$$\lambda^2 = \frac{LEA}{H_h L_e}\left(\frac{mgL}{H_h}\right)^2 \tag{3.29b}$$

where H_h is the horizontal component of cable static tension force; I is the moment of inertia of cable cross section; and

$$L_e = \int_0^L \left(\frac{ds}{dx}\right)^3 dx \cong L\left[1 + \frac{1}{8}\left(\frac{mgL}{H_h}\right)^2\right] \tag{3.30}$$

Four suspended cables with the same length of 100 m but different sag-extensibility (λ^2) and bending-stiffness (ξ) parameters are analyzed. Table 3.1 shows the parameters of the four cables. Cable 1 ($\lambda^2 = 0.79$, $\xi = 605.5$) has a moderate sag and a low bending stiffness; Cable 2 ($\lambda^2 = 50.70$, $\xi = 302.7$) has a large sag and an average bending stiffness; Cable 3 ($\lambda^2 = 1.41$, $\xi = 50.5$) has a moderate sag and a high bending stiffness; Cable 4 ($\lambda^2 = 50.70$, $\xi = 50.5$) has a large sag and a high bending stiffness.

Table 3.1 Material and geometric parameters of four cables

Cable No.	λ^2	ξ	m (kg/m)	g (N/kg)	L (m)	H (10^6N)	E (Pa)	A (m^2)	J_s (m^4)
1	0.79	605.5	400.0	9.8	100.0	2.90360	1.5988e+10	7.8507e-03	4.9535e-06
2	50.70	302.7	400.0	9.8	100.0	0.72590	1.7186e+10	7.6110e-03	4.6097e-06
3	1.41	50.5	400.0	9.8	100.0	26.13254	2.0826e+13	7.8633e-03	4.9204e-06
4	50.70	50.5	400.0	9.8	100.0	0.72590	4.7834e+08	2.7345e-01	5.9506e-03

Table 3.2 Comparison of computed frequencies of in-plane modes (Hz)

Cable No.	λ^2	ξ	String theory		Finite difference formula		Present method	
			1st mode	2nd mode	1st mode	2nd mode	1st mode	2nd mode
1	0.79	605.5	0.426	0.852	0.440	0.853	0.441	0.854
2	50.70	302.7	0.213	0.426	0.428	0.464	0.421	0.460
3	1.41	50.5	1.278	2.556	1.399	2.679	1.400	2.682
4	50.70	50.5	0.213	0.426	0.447	0.464	0.438	0.461

Modal properties of the four cables are evaluated by the proposed finite element formulation. The static profiles of the cables are assumed as parabolas. Sixty equi-length cable elements are used in the computation. Table 3.2 presents a comparison of predicted natural frequencies of the first two in-plane modes obtained by the taut string theory, the finite difference formula and the proposed method. It is observed that for all the four cases the results by the proposed method coincide well with those by the finite difference formula. Both the methods take into account sag-extensibility and bending stiffness. It is found from the table that the computed natural frequencies from the taut string equation (ignoring sag-extensibility and bending stiffness) are quite different from those calculated by the proposed method and the finite difference formula, indicating a considerable influence of sag-extensibility and bending stiffness in these cases.

Table 3.3 Parameters of two sets of cables

	Cable set 1				Cable set 2			
	A (m^2)	H (N)	d/L	f_{1s} (Hz)	A (m^2)	H (N)	d/L	f_{1s} (Hz)
Minimum value	9.788×10^{-7}	0.1031	1/23750	0.5810	9.575×10^{-5}	9.846×10^{2}	1/2375	0.1817
Maximum value	0.14258	3.236×10^{6}	1/110	8.5284	14.258	3.236×10^{10}	1/11	2.6969

In order to relate the modal properties with cable parameters, the relation surfaces of dimensionless frequencies versus λ^2 and ξ are obtained for a wide range of structural parameters. Two cable sets are considered. The fixed cable parameters are $L = 100$ m and $E = 200$ GPa. The ranges of other changed parameters are given in Table 3.3. The parameters result in $0.001 \le \lambda^2 \le 10000$ and $10 \le \xi \le 260$ for both cable sets. The volume mass density of set 1 is kept as a constant value of $\rho = m/A = 7.86\times10^3$ kg/m^3, while the density of set 2 is appropriately altered to produce same ranges of λ^2 and ξ for set 2 and set 1. The main difference between the two sets is the

range of their sag to span ratio d/L. Both the finite difference formula and the proposed method are used to compute the relation surfaces. The cable is divided into 50 elements in the finite element solution and 100 elements in the finite difference formula, with totally 101 nodes used for each method. With the computed natural frequency f_n of the nth mode, the corresponding dimensionless frequency is defined as

$$\bar{f}_n = \frac{f_n}{f_{1s}} \tag{3.31}$$

where f_{1s} is the fundamental frequency of the corresponding stretched string which is obtained from

$$f_{1s} = \frac{1}{2L}\sqrt{\frac{H_h A}{m}} \tag{3.32}$$

Figure 3.5 shows the relation surfaces of dimensionless frequencies versus λ^2 and ξ for the 1st symmetric and anti-symmetric in-plane modes obtained by the finite difference formula. **Figure 3.6** gives the corresponding relation surfaces obtained by the proposed method. By comparing the two figures, it is seen that the results for the two fundamental modes obtained by the approximate finite difference formula and by the proposed method coincide very well with each other throughout the concerned ranges of λ^2 and ξ for cable set 1 (with low sag to span ratio). For cable set 2 (with high sag to span ratio), a good agreement is still achieved except for a small region with very high λ^2 and very low ξ where the relation surfaces display a slight difference with each other. **Figure 3.7** provides a comparison of the relation surfaces of two high-order modes obtained by the two methods. It is observed that in these cases the results deviate significantly from each other in the range of small ξ. The deviation of the approximate finite difference formula from the finite element results

increases with the mode order. **Figure 3.8** illustrates the relation surfaces of dimensionless frequency versus λ^2 and ξ for high-order in-plane modes of cable set 2 obtained by the proposed method. **Figure 3.9** shows the relation surfaces of out-of-plane modes of cable set 2 using the proposed method. It is obvious in **Figures 3.8** and **3.9** that the high-order frequencies of the in-plane as well as out-of-plane modes depend on both parameters λ^2 and ξ, although the change rate of the frequencies along the parametric axis of λ^2 is much smaller than that along the parametric axis of ξ. This observation is different from that made in (Mehrabi and Tabatabai 1998). These differences are attributed to the fact that the finite difference formula was derived on the assumptions of parabolic static profile, flat sag and spatial invariability of dynamic tension, while the proposed method eschews these assumptions. The above studies conclude that when high-order modal properties are required in an inverse problem, a precise finite element model is more acceptable in regard to its accuracy, versatility and reliability.

3.4 CASE STUDIES

3.4.1 TSING MA BRIDGE CABLES

The Tsing Ma Bridge, as shown in **Figure 3.10**, is a double deck suspension bridge with a main span of 1377 m and an overall length of 2160 m (Beard 1995). The two main cables of the bridge are 36 m apart and have a cross section of 1.1 m in diameter after compacting. The central span deck and the Ma Wan side span deck are suspended at 18 m intervals by hangers to the main cables. The Tsing Yi side span deck is instead supported from the ground by three concrete piers spaced at 72 m

centers. As a result, the main cables on the Tsing Yi side span are free cables without bridge deck suspended. The modal properties of the Tsing Ma Bridge in different construction stages (including the erection completion stage) have been measured through a series of ambient vibration survey (Ko et al. 2000). One stage under measurement is the freely suspended cable stage. In this stage, only the tower-cable system was erected but none of deck segments has been hoisted into position. The main cables on all the three spans were free cables in this stage. The modal parameters of the main cables on the main span and the Tsing Yi side span in this stage are analyzed by the proposed method and compared with the measurement results for verification. The cable length and sag are 1397.8 m and 112.5 m for the suspended main span cable, and 329.1 m and 5.7 m for the inclined Tsing Yi side cable. The horizontal component of the tension force is 122,642 kN for both the cables. The main span cable is partitioned into 77 elements and the Tsing Yi side span cable is partitioned into 17 elements. The computation is conducted by assuming the cable supports as pinned ends and fixed ends respectively. Tables 3.4 and 3.5 list the natural frequencies of the first three in-plane and out-of-plane modes of the two cables. It is seen that the computed natural frequencies agree favorably with the measurement results.

Table 3.4 Natural frequencies of main span cable in freely suspended cable stage (Hz)

Mode No.	Out-of-plane modes			In-plane modes		
	1st	2nd	3rd	1st	2nd	3rd
Computed: pinned ends	0.0522	0.1040	0.1557	0.1008	0.1471	0.2081
Computed: fixed ends	0.0528	0.1052	0.1578	0.1020	0.1488	0.2091
Measurement	0.0530	0.1050	0.1560	0.1020	0.1430	0.2070

Table 3.5 Natural frequencies of Tsing Yi side span cable in freely suspended cable stage (Hz)

Mode No.	Out-of-plane modes			In-plane modes		
	1st	2nd	3rd	1st	2nd	3rd
Computed: pinned ends	0.2352	0.4696	0.7154	0.3527	0.4693	0.7216
Computed: fixed ends	0.2450	0.4946	0.7534	0.3569	0.4943	0.7593
Measurement	0.2360	0.4770	0.7400	0.3430	0.4780	0.7310

After completion of the bridge construction, a total of about 300 sensors, including four accelerometers on the main cables, have been permanently installed on the Tsing Ma Bridge for structural health and condition monitoring (Lau et al. 1999). The tension forces of the Tsing Yi side span free cables can be therefore monitored by means of vibration measurement. In order to examine the effect of cable bending stiffness on the modal properties, the natural frequencies of the Tsing Yi side span free cable in the erection completion stage are predicted using the proposed method (considering cable bending stiffness) as well as the pure cable model (ignoring cable bending stiffness), and then compared with the measurement results in the same stage from ambient vibration survey. The cable length and sag in this stage are 331.5 m and 1.8 m. The horizontal component of the tension force is 405,838 kN. The cable is divided into 200 elements in computation. **Figure 3.11** shows a comparison of the natural frequencies of the first 19 in-plane and out-of-plane modes obtained by the proposed method, the pure cable model and ambient vibration measurement. Because the accelerometer for ambient vibration measurement was located close to a modal node of the 8th and 16th modes as shown in **Figure 3.12**, the natural frequencies of these two modes could not be measured with high fidelity. It is observed from **Figure 3.11** that the predicted natural

frequencies by the proposed method agree very well with the measurement results, whereas the natural frequencies predicted using the pure cable model gradually deviate from the measured values with the increase of mode order. The maximum error is as large as 30% for the first 20 modes. This example proves again the significant influence of cable bending stiffness on higher-mode frequencies and the necessity of using an accurate model for multimode-based cable tension and parameter identification.

3.4.2 TING KAU BRIDGE CABLES

Due to large flexibility, relatively small mass and extremely low damping, structural cables are susceptible to vibration in dynamic conditions. For example, unexpectedly large oscillation occurring in bridge stay cables under specific combinations of wind and rain has been observed in a number of cable-stayed bridges worldwide (Poston 1998). This has resulted in increasing application of passive and semi-active dampers in cable-stayed bridges for cable vibration mitigation. For a bridge cable attached with dampers, the existing analytical or approximate formulae are difficult to accurately identify the tension force due to their inability in dealing with damper stiffness effect. The present finite element method does not suffer from this restriction. Modal analysis of the damper-attached Ting Kau bridge cables by the proposed method is provided here as an example.

As shown in **Figure 3.13**, the Ting Kau Bridge is a multi-span cable-stayed bridge with three monoleg towers supporting two main spans of 448 m and 475 m and two side spans of 127 m each (Bergermann and Schlaich 1996). In this bridge, eight longitudinal stabilizing cables with a length of up to 465 m have been used to strengthen the slender central tower. Passive dampers have been installed between

the cables and deck near the lower ends in the cable planes. The dampers were connected perpendicular to the cables at the location of 19.2 m cable length measured from the lower ends. The length and sag of the longitudinal stabilizing cable are 464.9 m and 8.3 m respectively. The horizontal component of the cable tension force is 2391.5 kN. The cable is divided into 200 elements in computation. **Figure 3.14** illustrates the relation curves of the cable natural frequency versus spring (damper) stiffness for the first six in-plane modes. The maximum frequency discrepancy with and without considering damper stiffness is respectively 2.22%, 4.35%, 4.28%, 4.35%, 4.34% and 4.35% for the six modes. This means that if each natural frequency of the six modes is used to evaluate tension force from the taut string equation, the maximum identification error of tension force stemming from the damper stiffness effect will be 4.44%, 8.70%, 8.56%, 8.70%, 8.68% and 8.70% respectively. This also demonstrates the importance of a versatile finite element model for tension force evaluation of cables connected with dampers. In addition, it is possible and feasible to simultaneously identify the cable tension force and damper stiffness by use of a precise finite element model and measured multimode frequencies.

3.5 DISCUSSION

It should be noticed that the stiffness matrix of a cable depends on the cable tension force. In the present study, a nonlinear static analysis is performed to obtain the stiffness matrix associated with the dead-load deformed shape and then a linear dynamic analysis is followed. In the derived stiffness matrix formula in Equation 3.19(d) for linear dynamic analysis, it is noticed that the stiffness is only related to

the static tension H. But in the traditional cable theory (Irvine 1981; Mehrabi and Tabatabai 1998) we could find a dynamic tension component h in the governing equation (e.g., Equation (1) by Irvine 1981) and its contribution to stiffness. In fact, however, this dynamic tension component $h(t)$ and its contribution to stiffness can be represented by cable axial strain energy ($EA\varepsilon^2/2$). Because the cable theory was established based on the development of inextensible chain formula, it introduced the dynamic tension concept instead of the axial strain energy concept for clarity. In fact, when the governing equations and stiffness matrix are derived from the modern variational principle and finite element formulation, using axial strain energy instead of dynamic tension can get more direct and more general results. The explicit relation between the $h(t)$ and axial strain energy has been established for cable nonlinear dynamic analysis (Ni et al. 2000). Returning to the present study, the item on the right-hand-side of Equation (3.19d) just reflects the stiffness contribution of axial strain energy, i.e., of the dynamic tension $h(t)$. More significantly, the conventional cable governing equation using the concept of dynamic tension (e.g., see reference by Mehrabi and Tabatabai 1998) is derived based on the assumption that the tension is spatially invariable along the cable length. However, the formula derived in the proposed study relaxes this constraint. Therefore, the finite element formulation given in this chapter not only accounts for the contribution of the so-called dynamic tension term to stiffness, but also allows for more general description of tension distribution along the cable.

3.6 SUMMARY

In this chapter a three-dimensional finite element formulation is developed for dynamic analysis of large-diameter structural cables. The proposed formulation is suited for both suspended and inclined cables, and allows for the consideration of cable flexural rigidity, sag-extensibility, spatial variability of dynamic tension, boundary conditions, lumped masses and intermediate springs and/or dampers. This formulation provides a good baseline model for accurate identification of cable tension force and other structural parameters based on the measurement of multimode frequencies.

Parametric studies are made to evaluate the effects of cable bending stiffness and sag-extensibility on modal properties, and the relation between the natural frequencies and cable parameters for a wide parameter range. The results show that the cable bending stiffness contributes a considerable influence on the natural frequencies when the tension force is relatively small, and affects the higher-mode frequencies more significantly than the lower-mode frequencies. A comparison study of the computed and measured natural frequencies of the Tsing Ma bridge cables shows that taking into account bending stiffness is necessary for large-diameter bridge cables to obtain an accurate prediction of the natural frequencies. The predicted higher-mode frequencies for such cables without considering bending stiffness may significantly deviate from the true values. The case study of the Ting Kau bridge cables demonstrates the degree of influence of the stiffness of attached dampers on the cable modal properties and on the tension identification accuracy. It is concluded that the tension forces of long-span large-diameter bridge cables can be accurately evaluated from vibration measurement only when a precise model

accounting for cable bending stiffness, sag-extensibility and other constraints is utilized in the identification procedure.

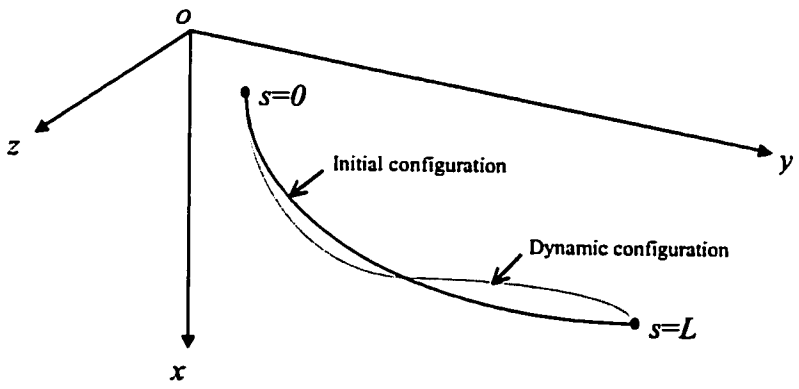

Figure 3.1 Schematic of cable configuration

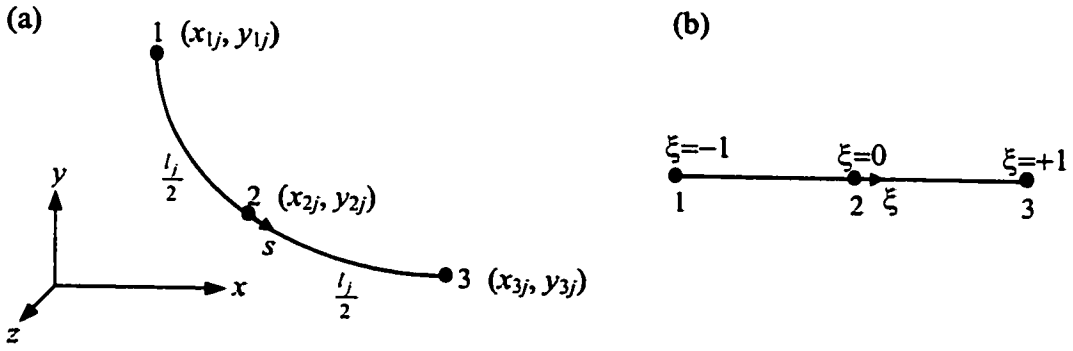

Figure 3.2 Three-node curved cable element: (a) physical coordinate; (b) natural coordinate

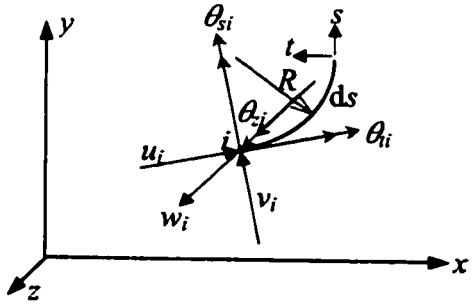

Figure 3.3 Displacements at node *i*

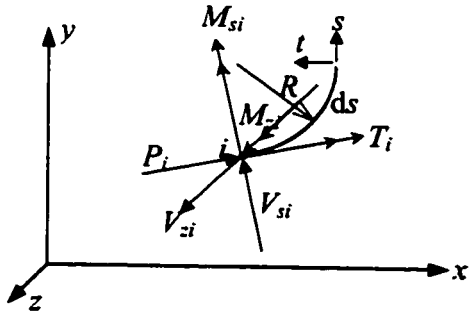

Figure 3.4 Stress-resultants at node *i*

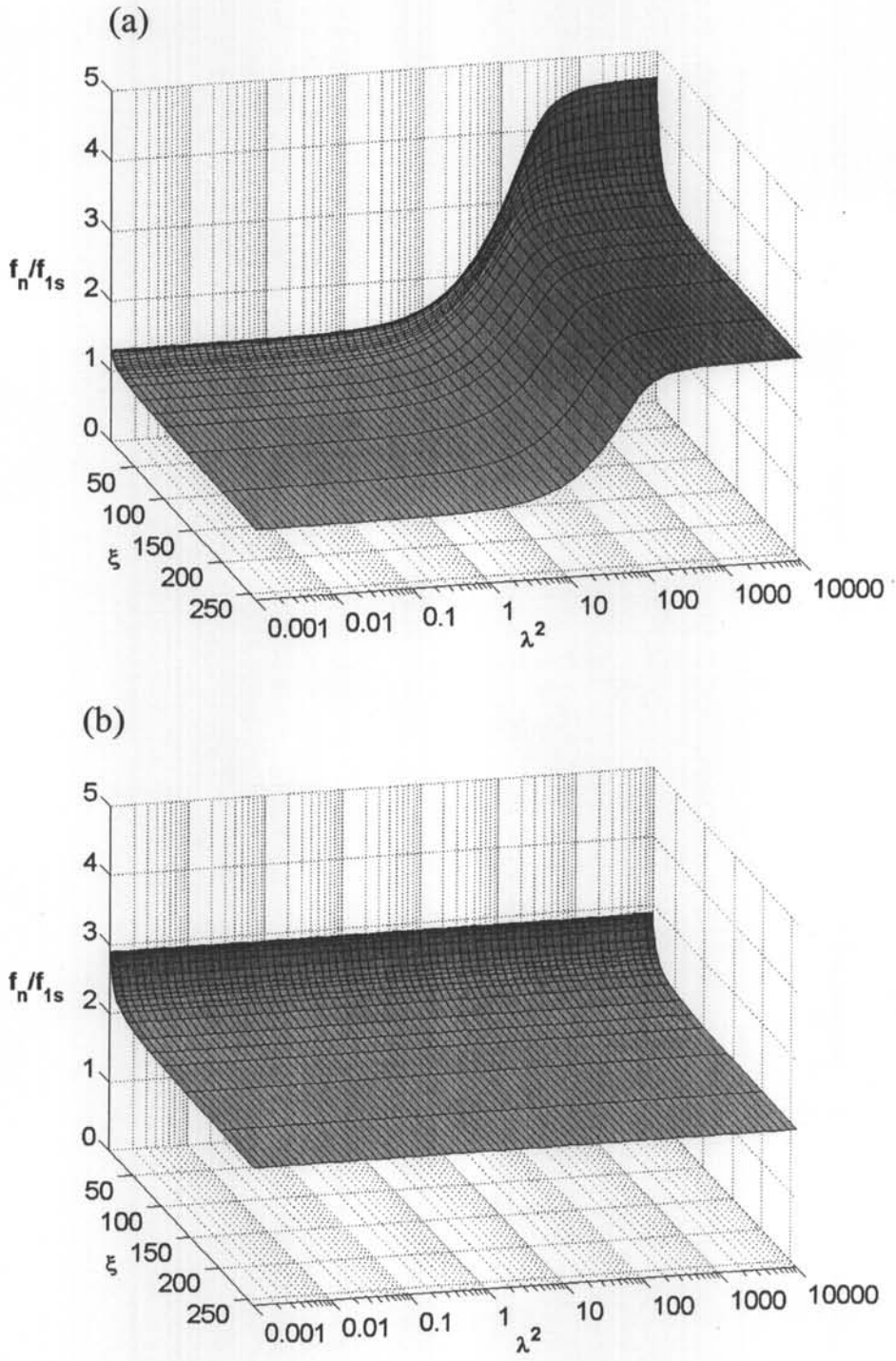

Figure 3.5 Relation surfaces of two in-plane fundamental modes obtained by finite difference formula: (a) 1st symmetric mode (cable set 1 and set 2); (b) 1st anti-symmetric mode (cable set 1 and set 2)

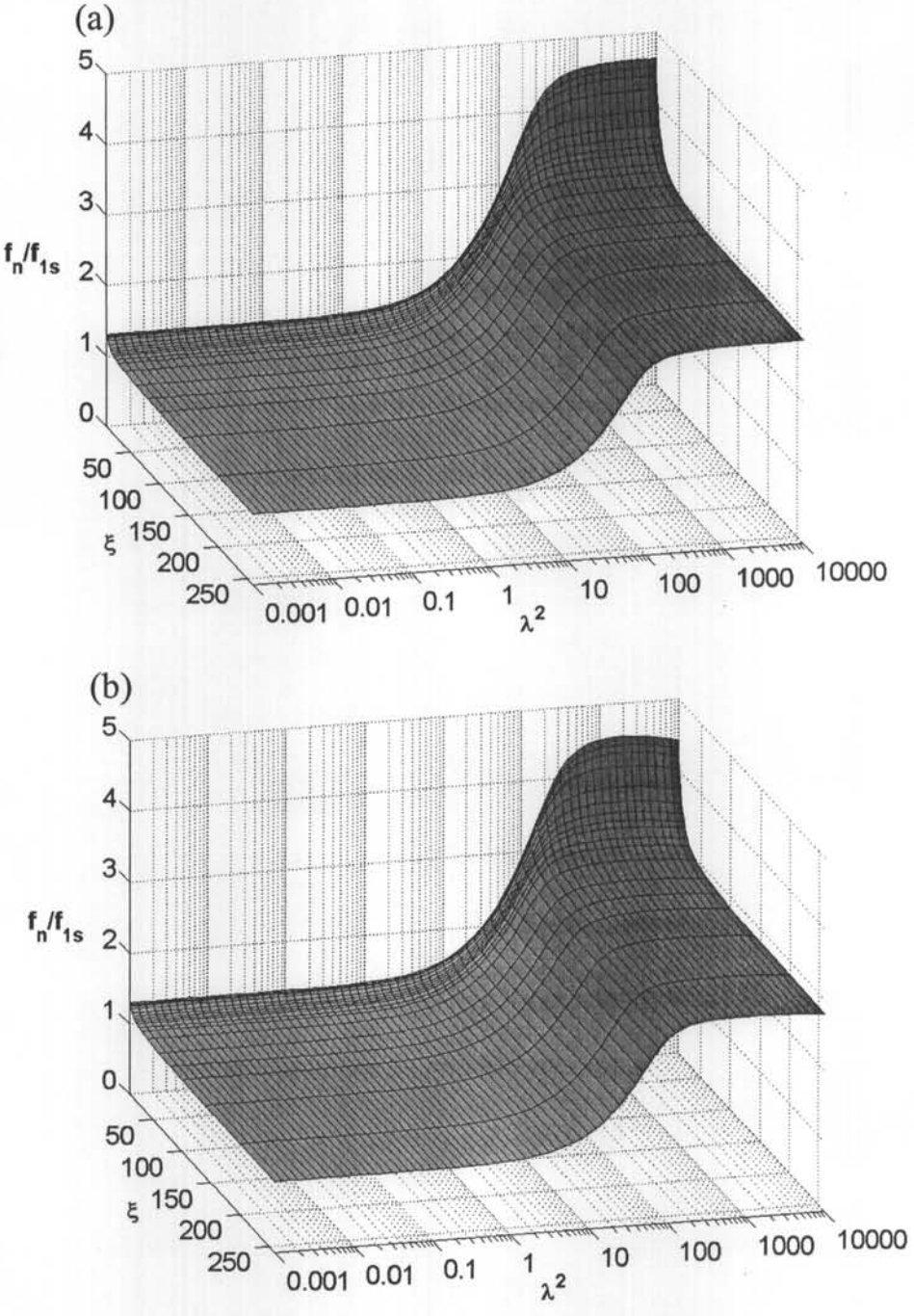

Figure 3.6 Relation surfaces of two in-plane fundamental modes obtained by the present method: (a) 1st symmetric mode (cable set 1); (b) 1st symmetric mode (cable set 2)

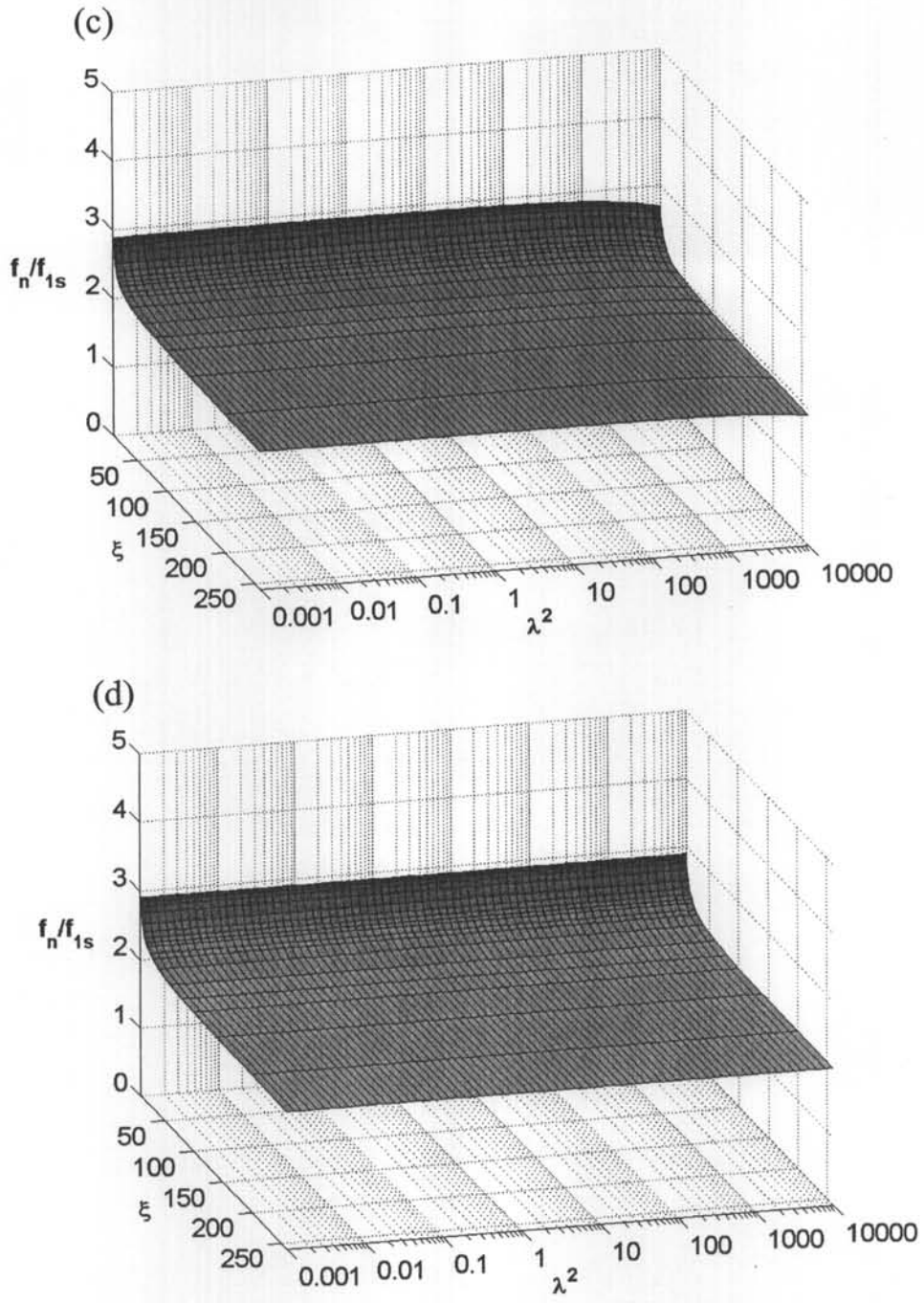

Figure 3.6 Relation surfaces of two in-plane fundamental modes obtained by the present method (Cont'd): (c) 1st anti-symmetric mode (cable set 1); (d) 1st anti-symmetric mode (cable set 2)

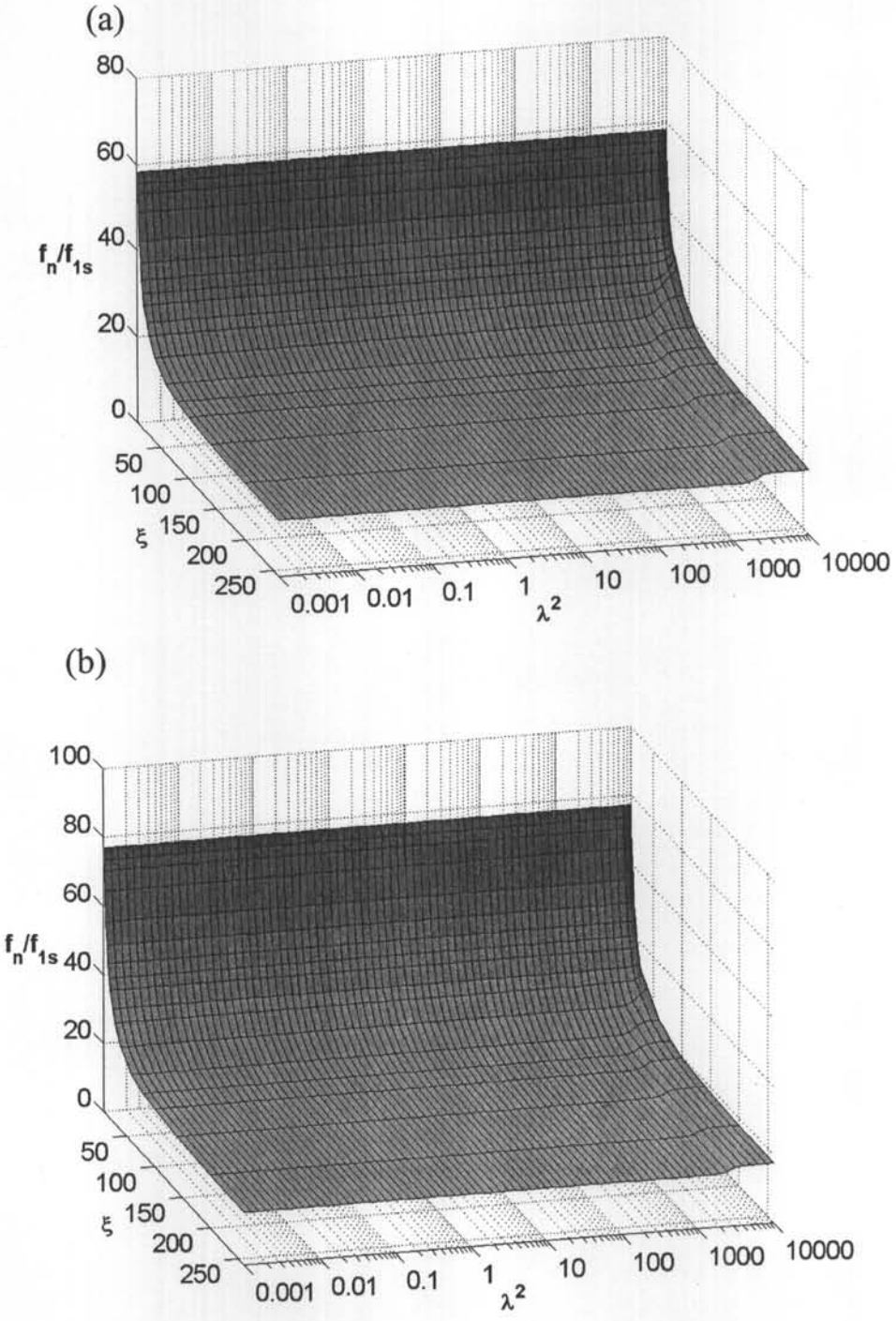

Figure 3.7 Comparison of relation surfaces of higher-order in-plane modes obtained by two methods: (a) 7th symmetric mode by finite difference formula (cable set 1 and set 2); (b) 8th symmetric mode by finite difference formula (cable set 1 and set 2)

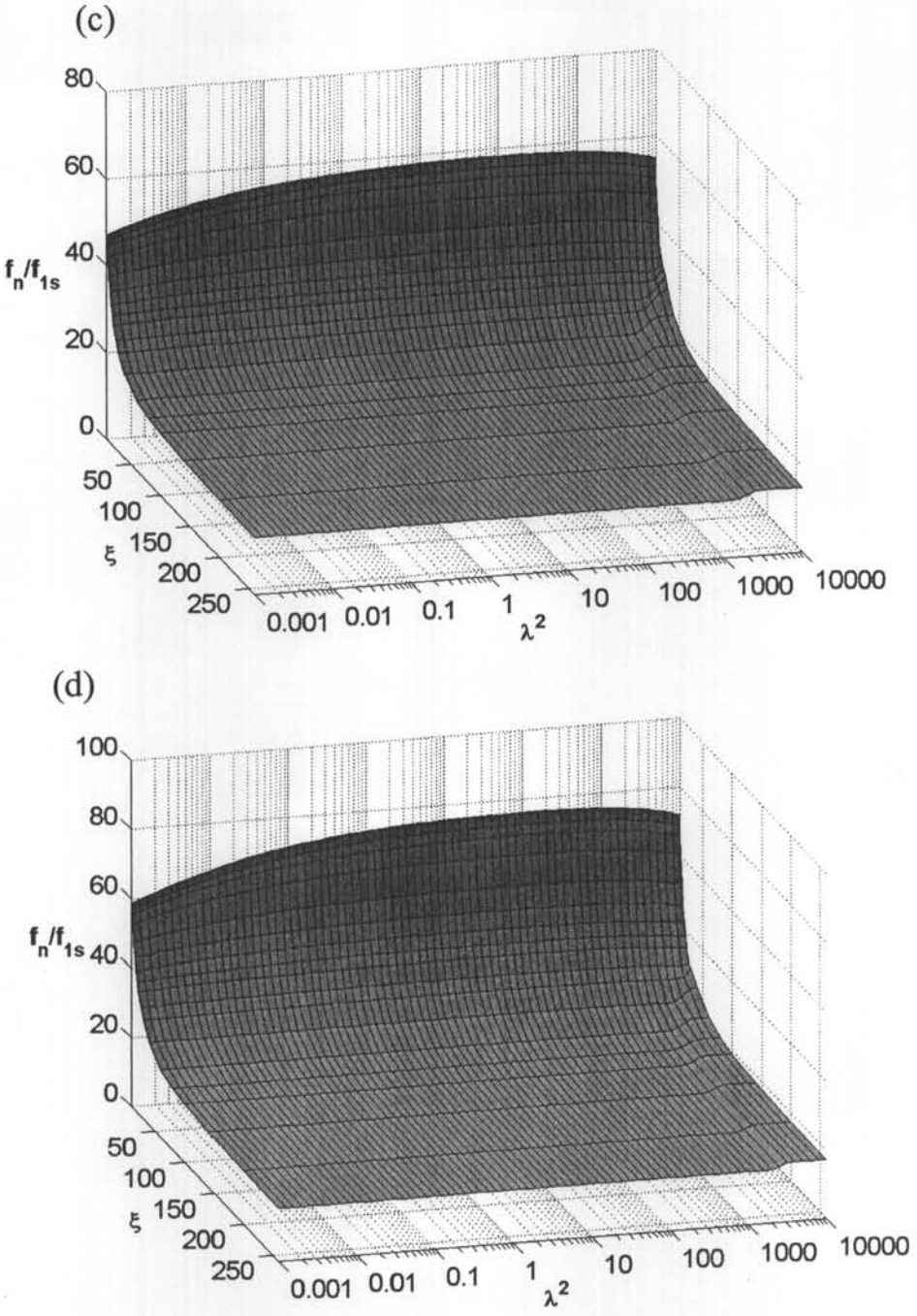

Figure 3.7 Comparison of relation surfaces of higher-order in-plane modes obtained by two methods (Cont'd): (c) 7th symmetric mode by the present method (cable set 2); (d) 8th symmetric mode by the present method (cable set 2)

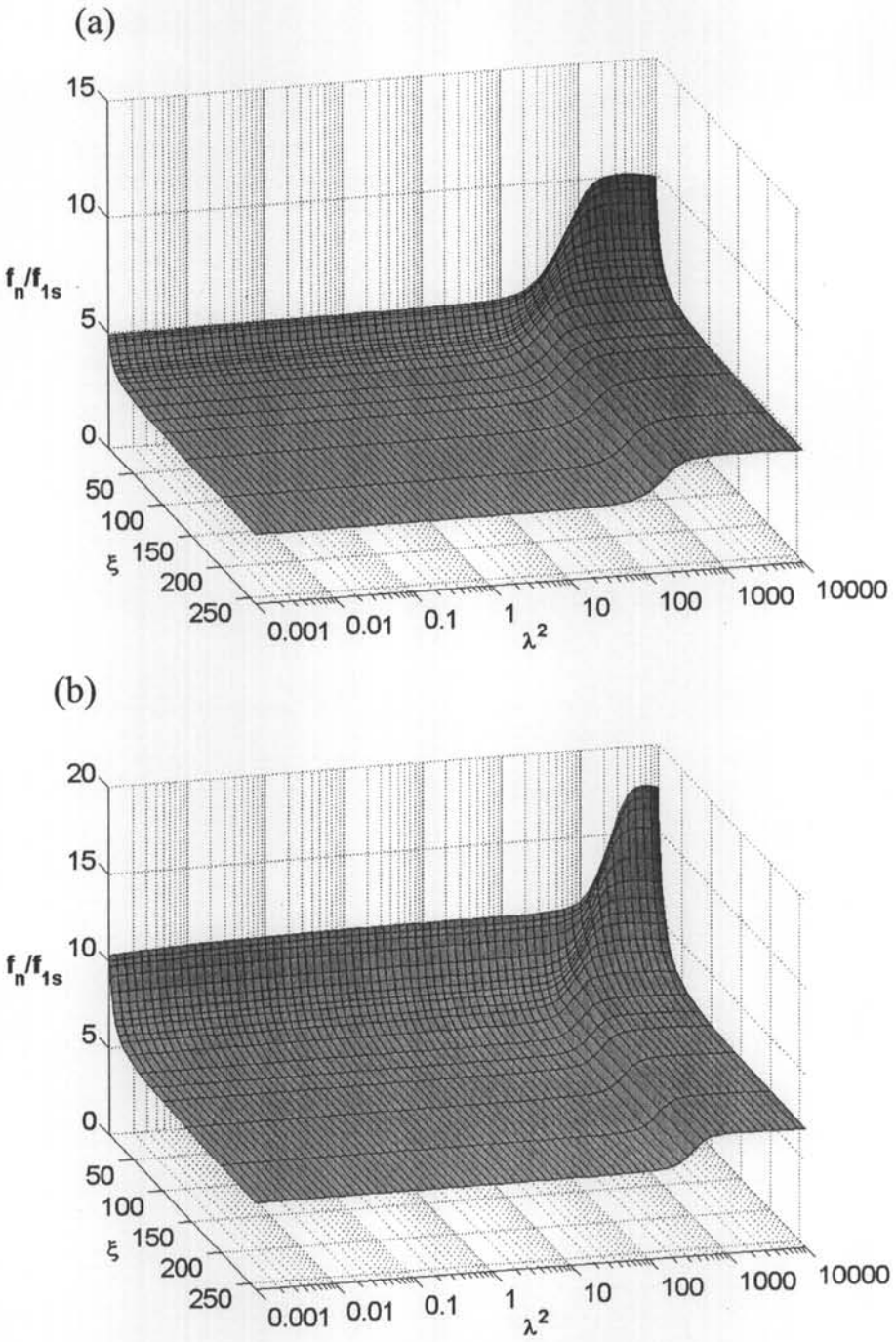

Figure 3.8 Relation surfaces of high-order in-plane modes obtained by the present method for cable set 2: (a) 2nd symmetric mode; (b) 3rd symmetric mode

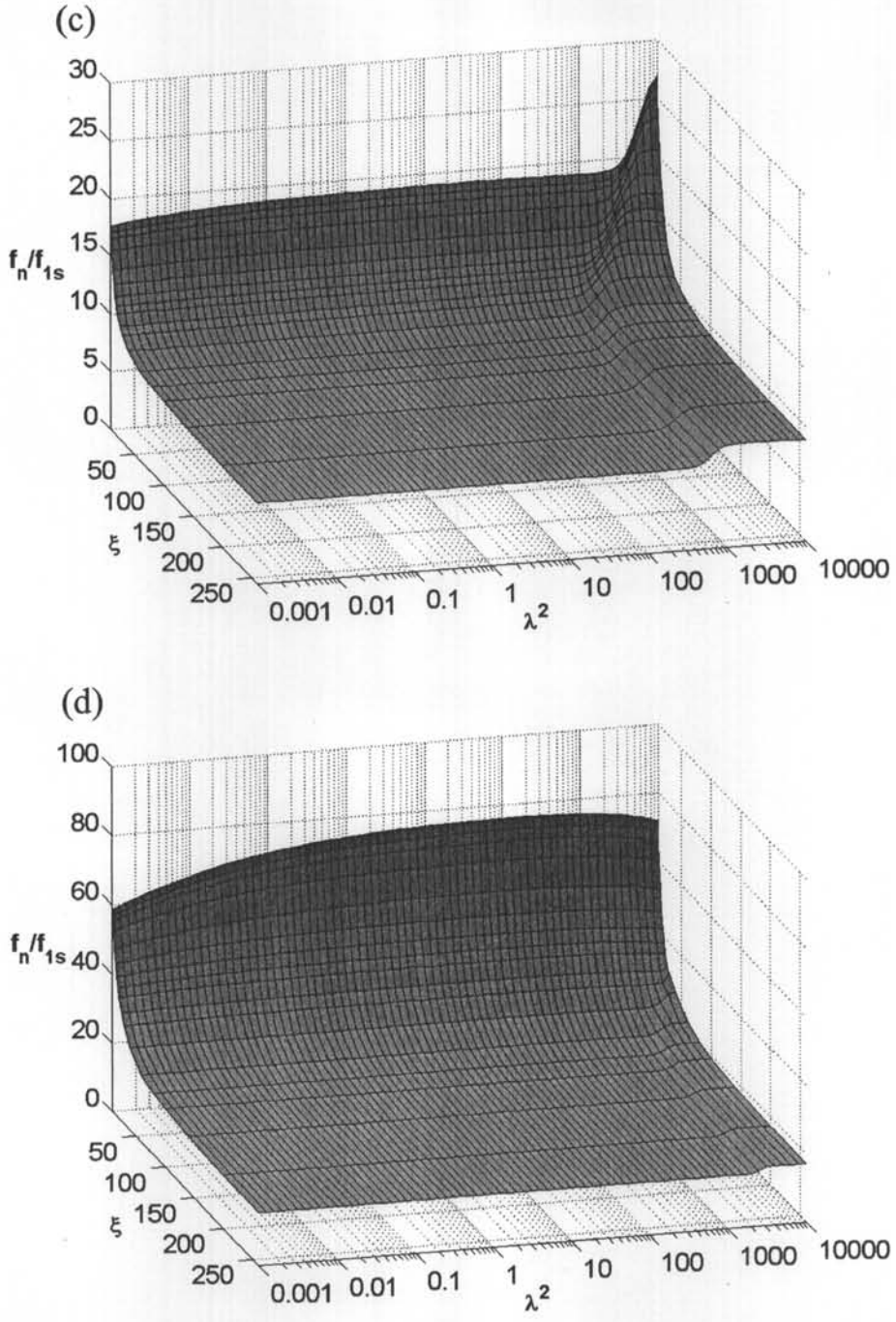

Figure 3.8 Relation surfaces of high-order in-plane modes obtained by the present method for cable set 2 (Cont'd):

(c) 4th symmetric mode; (d) 8th symmetric mode

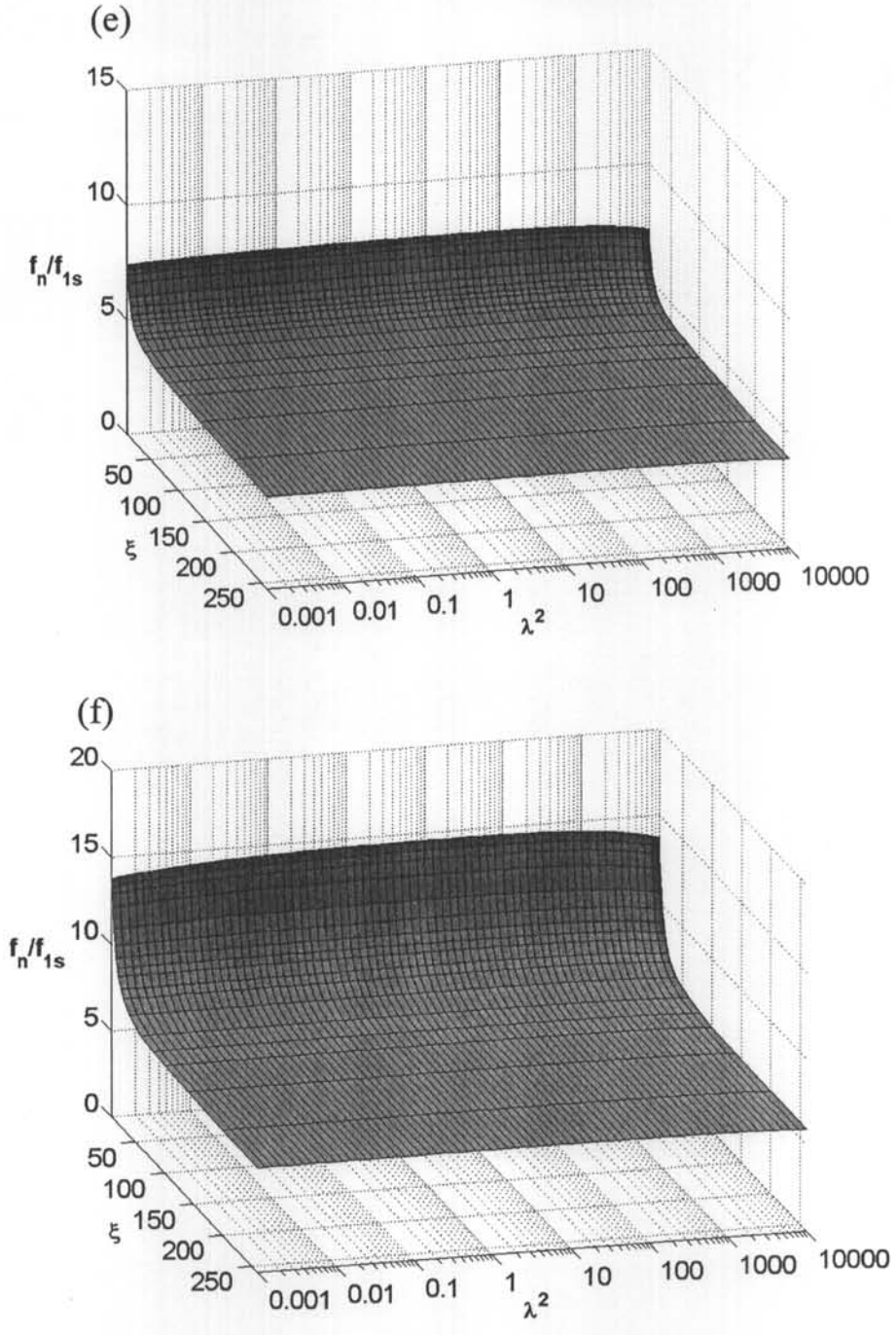

Figure 3.8 Relation surfaces of high-order in-plane modes obtained by the present method for cable set 2 (Cont'd): (e) 2nd anti-symmetric mode; (f) 3rd anti-symmetric mode

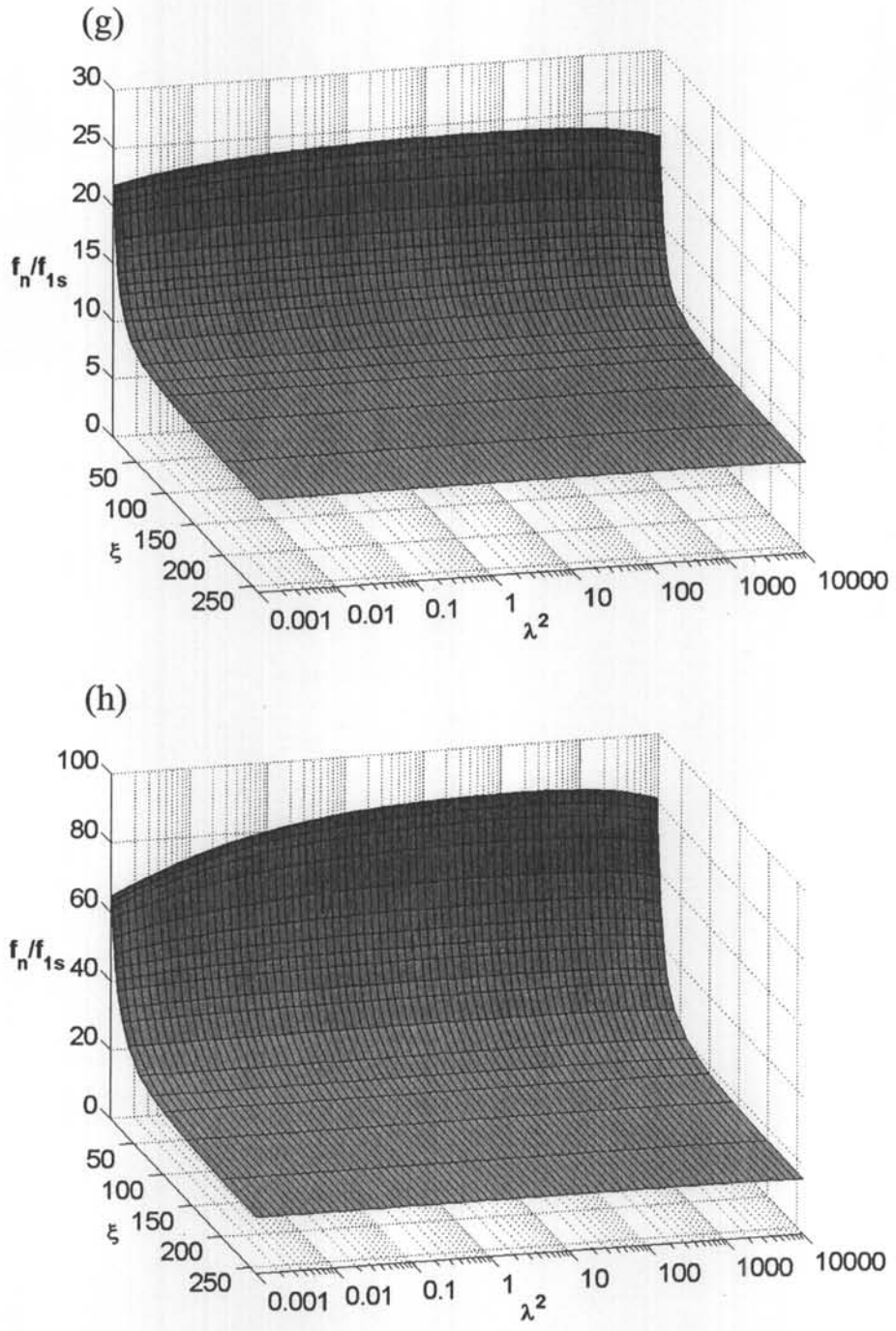

Figure 3.8 Relation surfaces of high-order in-plane modes obtained by the present method for cable set 2 (Cont'd): (g) 4th anti-symmetric mode; (h) 8th anti-symmetric mode

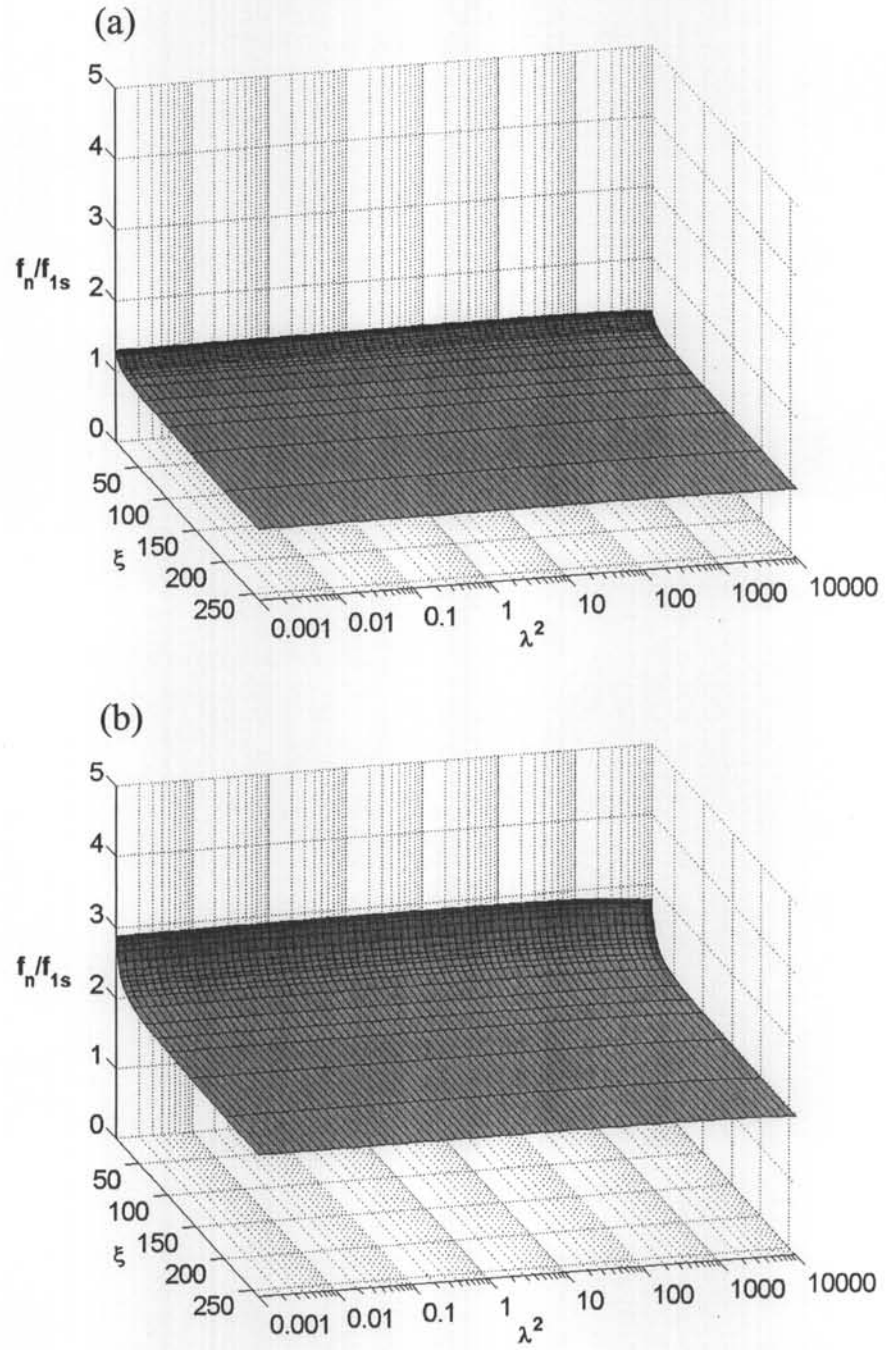

Figure 3.9 Relation surfaces of out-of-plane modes obtained by the present method for cable set 2: (a) 1st symmetric mode; (b) 1st anti-symmetric

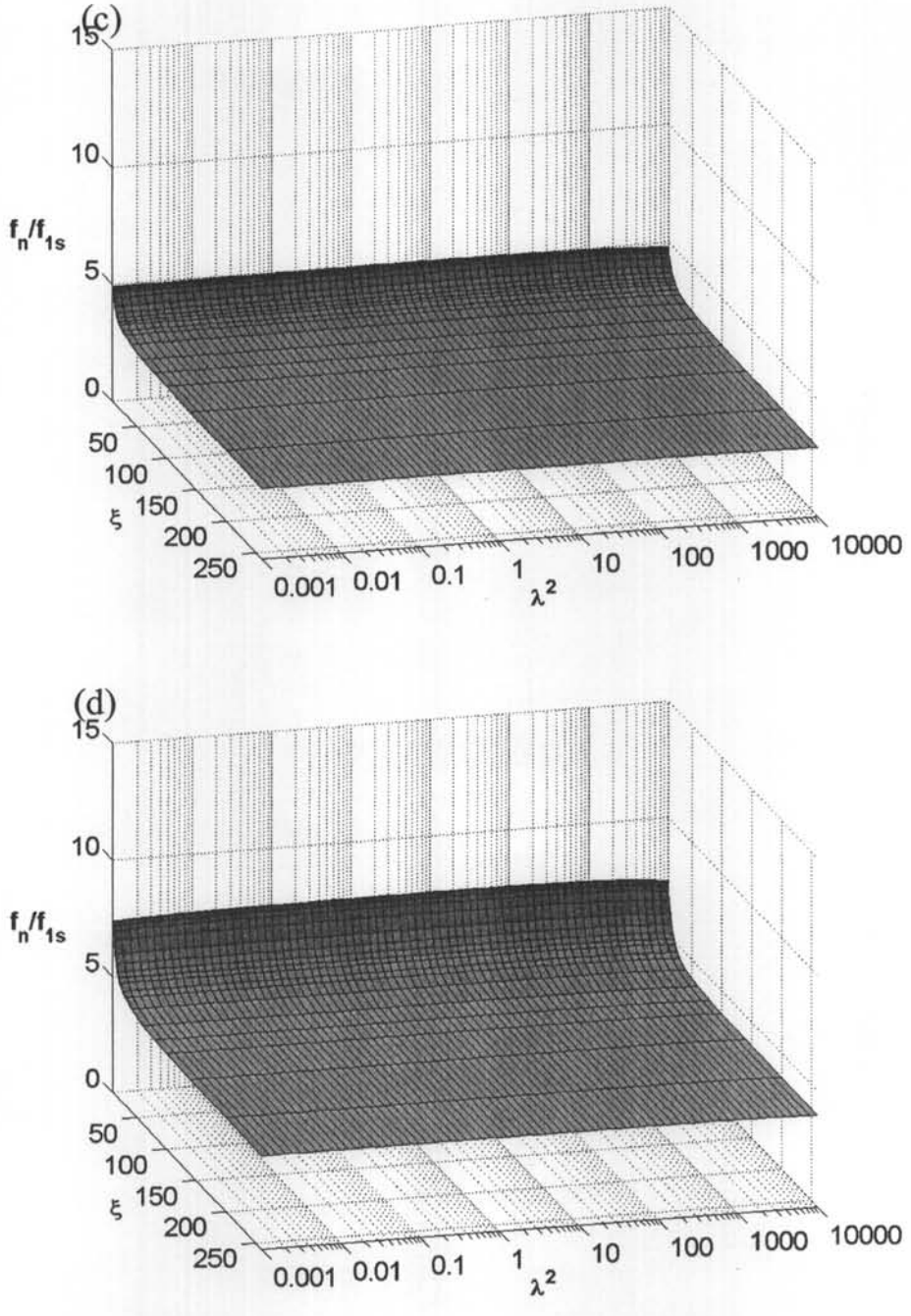

Figure 3.9 Relation surfaces of out-of-plane modes obtained by the present method for cable set 2 (Cont'd): (c) 3rd symmetric mode; (d) 8th symmetric mode

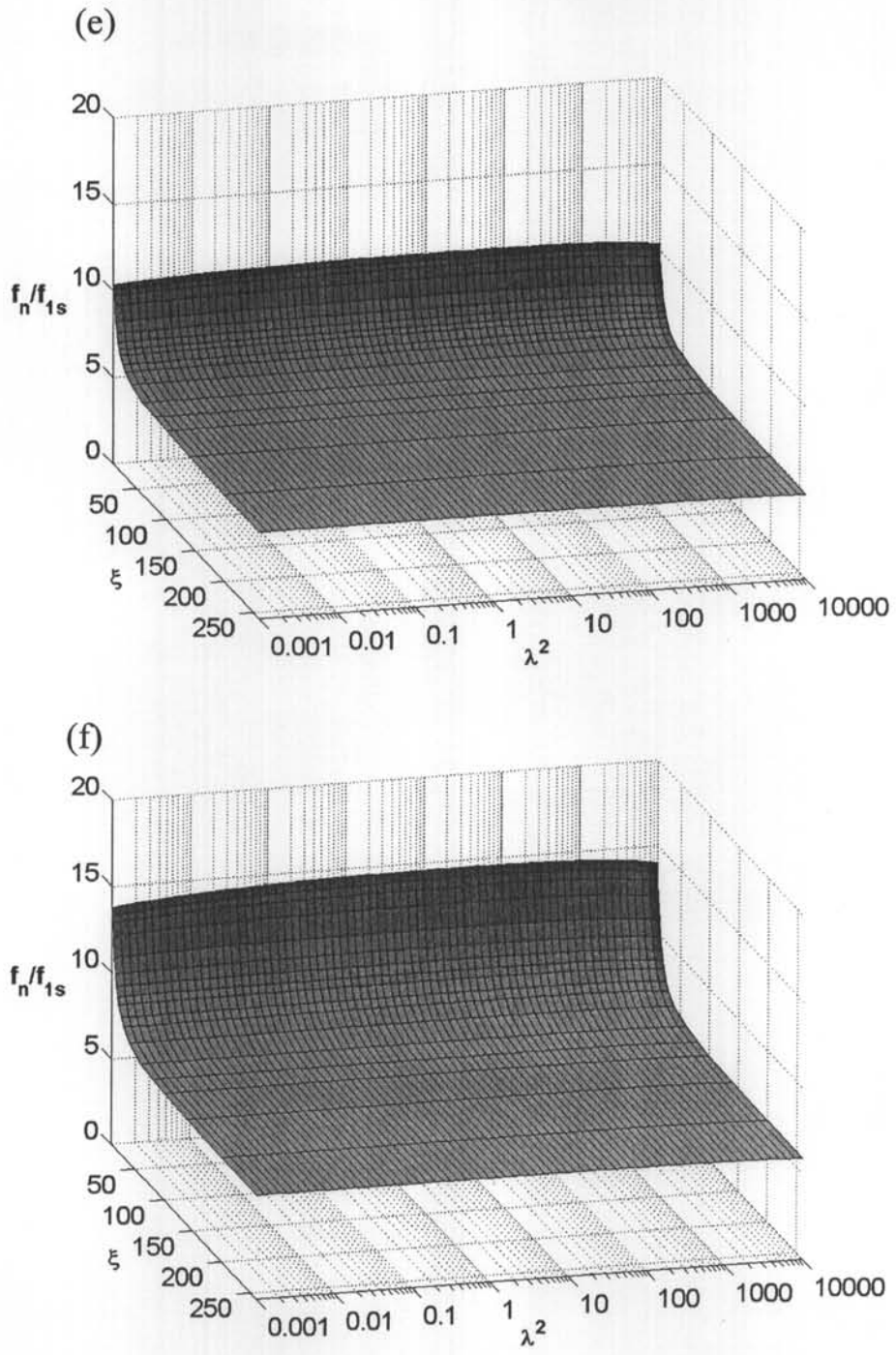

Figure 3.9 Relation surfaces of out-of-plane modes obtained by the present method for cable set 2 (Cont'd): (e) 1st anti-symmetric mode; (f) 2nd anti-symmetric mode

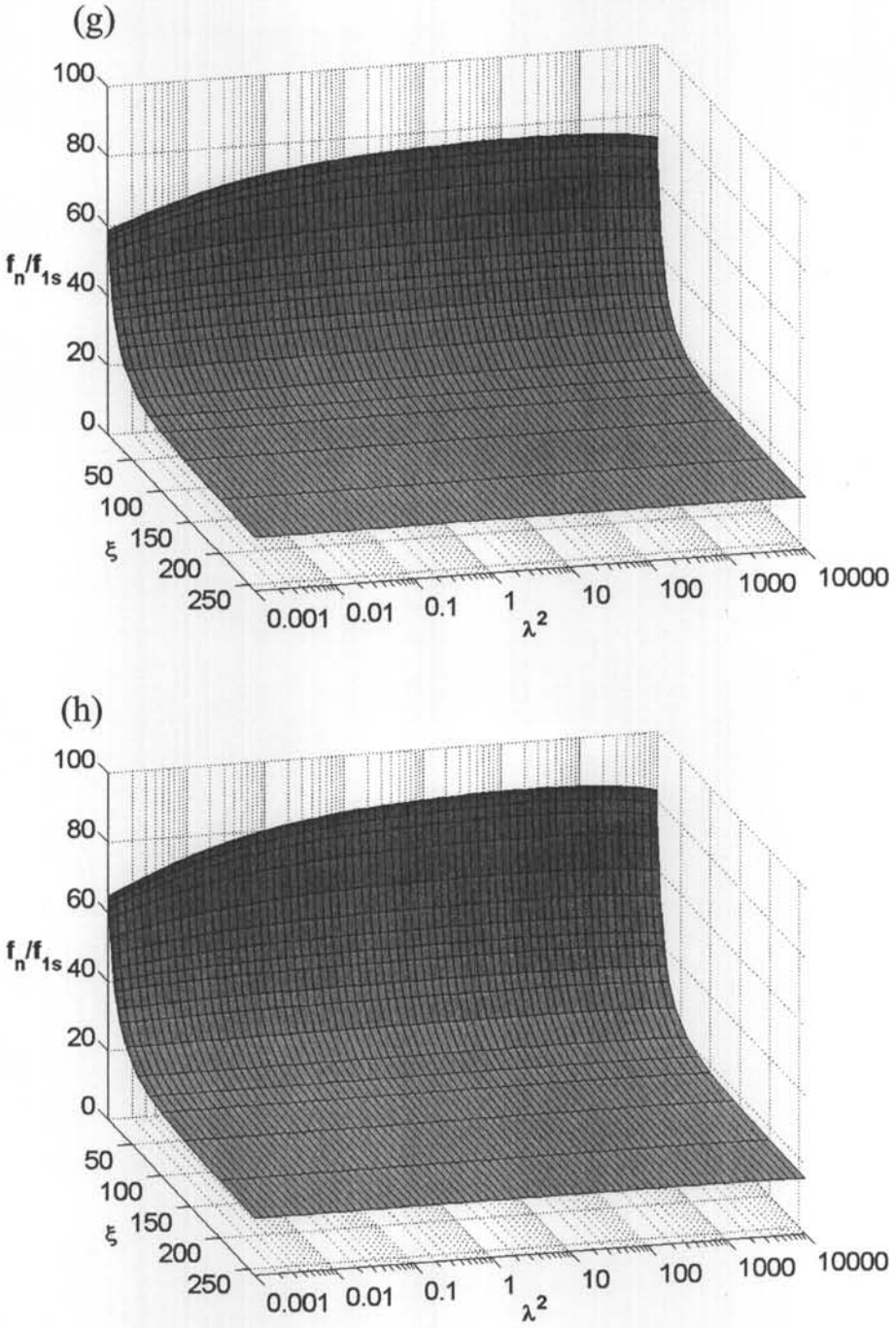

Figure 3.9 Relation surfaces of out-of-plane modes obtained by the present method for cable set 2 (Cont'd): (g) 3rd anti-symmetric mode; (h) 8th anti-symmetric mode

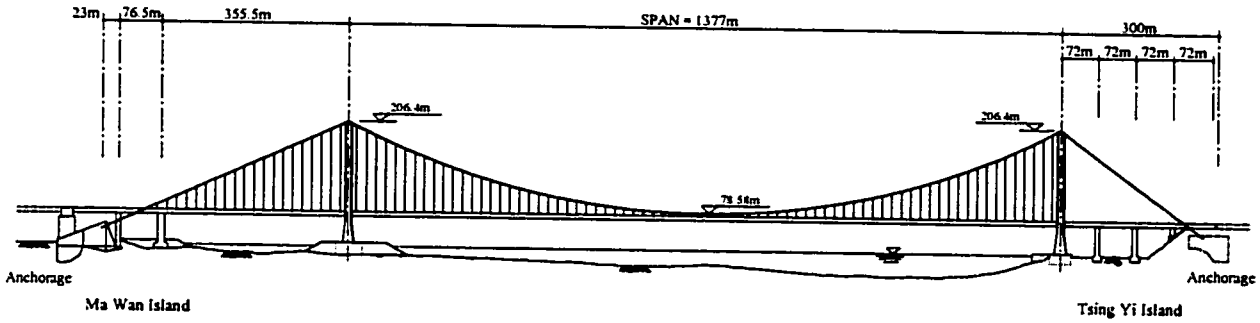

Figure 3.10 Elevation of Tsing Ma Bridge

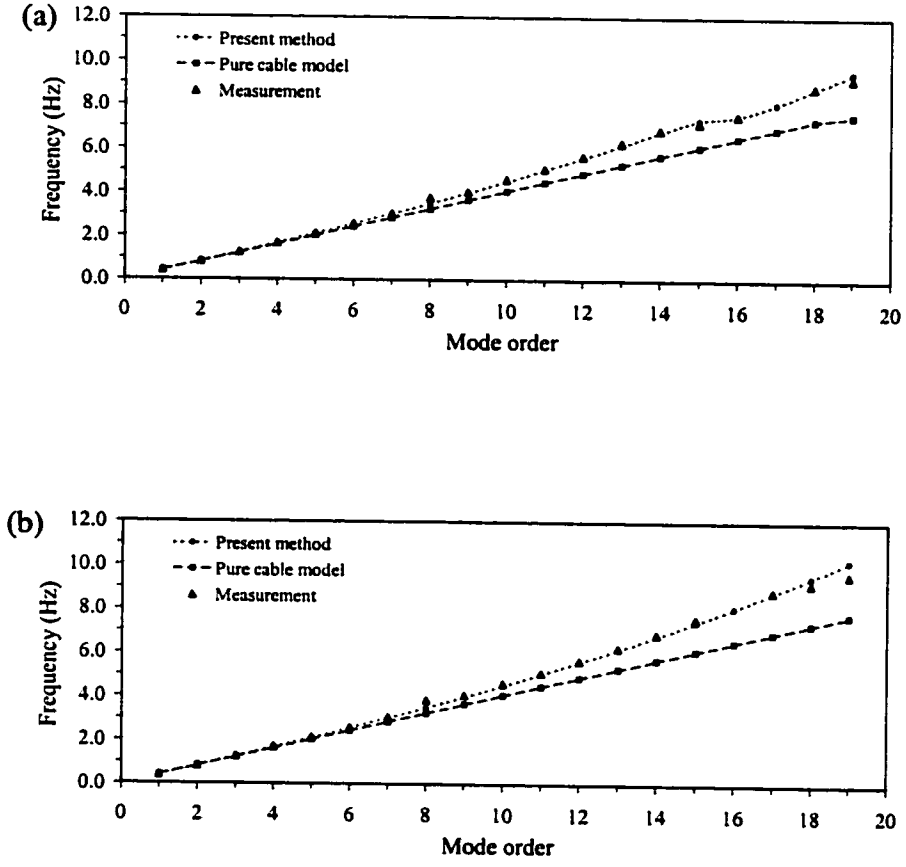

Figure 3.11 Comparison between computed and measured natural frequencies of Tsing Yi side span cable in erection completion stage: (a) frequencies of in-plane modes; (b) frequencies of out-of-plane modes

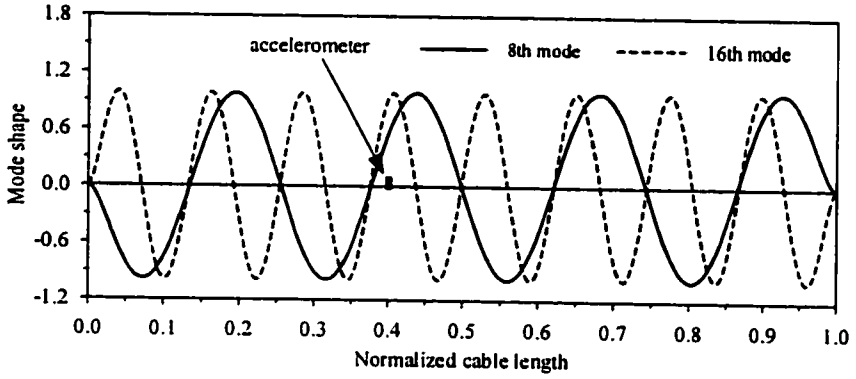

Figure 3.12 Deployment of accelerometer on cable for ambient vibration measurement

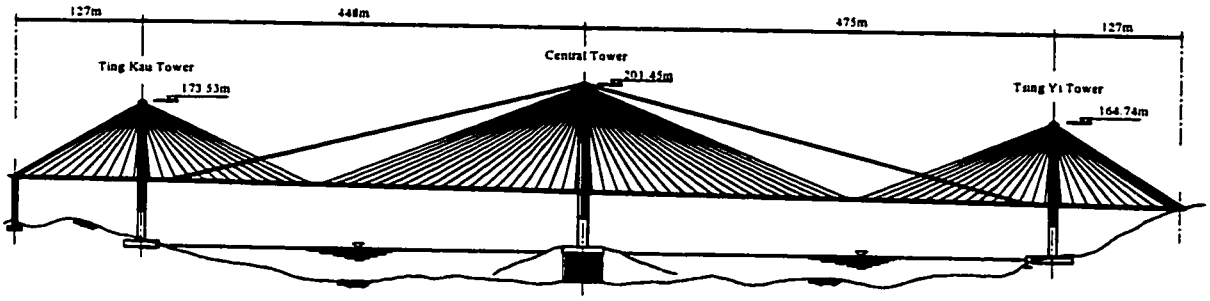

Figure 3.13 Elevation of Ting Kau Bridge

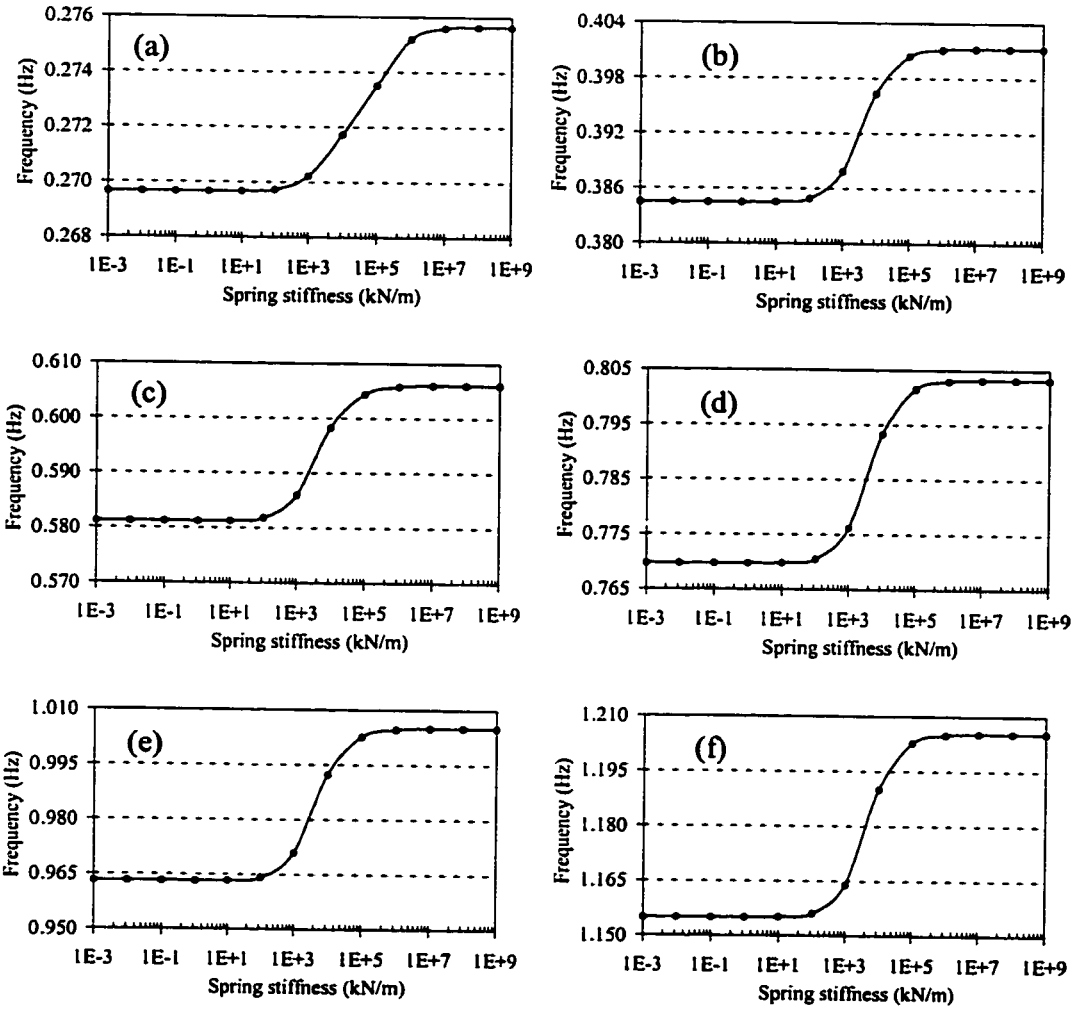

Figure 3.14 Relation diagrams of natural frequency versus spring (damper) stiffness for Ting Kau bridge stabilizing cable: (a) 1st mode; (b) 2nd mode; (c) 3rd mode; (d) 4th mode; (e) 5th mode; (f) 6th mode

Appendix: Formulation for parabolic and catenary profiles

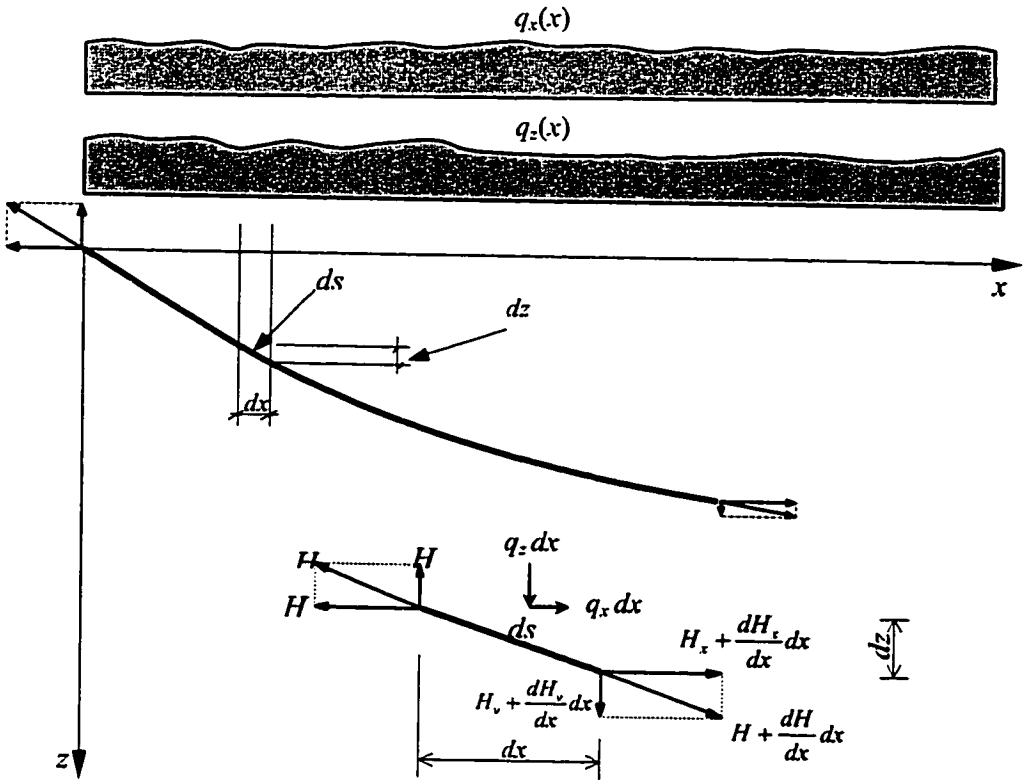

Figure 3.15 Internal and external force on a cable element.

Figure 3.15 shows a cable subjected to distributed force $q_x(x)$ and $q_z(x)$. The cable profile is defined by $z(x)$, which is to be determined according to the external load $q_x(x)$ and $q_z(x)$. As the cable is perfectly flexible, the cable tension, H, is always in the tangential direction of the cable profile. That is

$$H_v = H_h \frac{dz}{dx} \tag{A3.1}$$

The equilibrium equations of the cable are:

$$\frac{dH_h}{dx}dx + q_x dx = 0 \tag{A3.2}$$

$$\frac{dH_v}{dx}dx + q_z dx = 0 \tag{A3.3}$$

In most cases, external load on structural cables used in engineering is mainly in the vertical direction. When the horizontal external load is ignored, the cable horizontal

internal force is a constant. Substituting Equation (A3.1) in to Equation (A3.3) and dividing by dx, we get

$$H_h \frac{d^2 z}{dx^2} + q_z = 0 \tag{A3.4}$$

Two type of vertical load are the uniformly distributed force along the cable span, x, and along the cable arch length, s, respectively. The expressions of q_z in these circumstances are:

$$q_z(x) = q \quad \text{(constant } q \text{ along cable span, } x\text{)} \tag{A3.5}$$

$$q_z(x) = q\frac{ds}{dx} \quad \text{(constant } q \text{ along cable arch length, } s\text{)} \tag{A3.6}$$

By substituting Equations (A3.5) and (A3.6) into Equation (A3.4), the cable profile $z(x)$ can be obtained as the parabolic and the catenary profiles, respectively. The parabolic profiles is:

$$z(x) = \frac{q}{2H_h}x^2 + C_1 x + C_2 \tag{A3.7}$$

in which C_1 and C_2 are constants to be determined by the boundary conditions.
For the catenary profile, when $z = 0$ at $x = 0$ and $z = c$ at $x = l$, the curve is expressed as

$$z(x) = \frac{H_h}{q}\left[\cosh\alpha - \cosh\left(\frac{2\beta x}{l} - \alpha\right)\right] \tag{A3.8}$$

in which

$$\alpha = \sinh^{-1}\left[\frac{\beta(c/l)}{\sinh\beta}\right] + \beta \tag{A3.9}$$

$$\beta = \frac{ql}{2H_h} \tag{A3.10}$$

CHAPTER 4

NONLINEAR DYNAMIC BEHAVIOUR OF BRIDGE CABLES

4.1 INTRODUCTION

A new method for analyzing nonlinear steady-state oscillation of three-dimensional sagged stay cables subject to arbitrary periodic excitation is proposed in this chapter. A frequency-domain solution method to obtain the periodically forced response is developed by applying the incremental harmonic balance (IHB) technique to the finite element model constructed in the previous chapter. The proposed method is an accurate algorithm in the sense that it accommodates multi-harmonic components and no mode-based model reduction is made in the solution process. Both the frequency- and amplitude-controlled algorithms are formulated and are alternatively implemented to obtain complete frequency-response curves including unstable solutions. In recognizing that the geometric nonlinearity of cables may be of hardening or softening, the amplitude-controlled algorithm is formulated along with the frequency-controlled algorithm so that the developed method can predict both stable and unstable steady-state responses and can analyze both super- and sub-harmonic resonances and internal resonances. Case study of applying the proposed method to nonlinear dynamic behavior analysis of the Tsing Ma bridge cables is demonstrated. The analysis results show that the side-span free cables of the bridge

display distinctly different nonlinear characteristics in the construction and in the final stages. The different nonlinear behaviors of the cable in different construction stage are interpreted as the change in the relative contributions of the quadratic and cubic nonlinearities concerning with the static tension and the sag of the cable, respectively.

Though the method developed in this chapter and the analyses carried out in this and the next chapters for the nonlinear dynamics of cables do not directly contribute to the cable condition assessments, the methods presented in these two chapters, are important in dealing with such problems when the nonlinearities should be considered. The nonlinear analyses play a key role for cable condition assessment when the cable is in large amplitude vibration as a result of parametric excitation, wind-rain-excitation, galloping and wake galloping. For modern bridge health monitoring systems, the vibration data are collected in a 24-hour working mode and the data are to be processed on-line. Results of data processing provide information on the health and safety of the bridge. However, the results of cable condition assessment rely on the model adopted for the cable parameter estimation. When large amplitude oscillation occurs, the nonlinear model should be adopted.

The nonlinear model is also very important for investigation on the mechanism of wind-rain-induced vibration and parametric oscillation. For analyzing real cables in cable-stayed bridges, the interaction of girder-cables-pylons cannot be neglected in some cases. The nonlinear model developed may serve as one method for analyzing cable oscillation in such cases

4.2 PRESENTATION OF METHOD

4.2.1 FINITE ELEMENT FORMULATION

The finite element model of the inclined homogeneous cable is formulated in the previous chapter, as shown in Equations (3.1) to (3.14). Usually, to get the nonlinear dynamic response of the cable, the formulation derived in Chapter 3 should be applied with the direct integration in the time domain. Nevertheless, time integration methods are quite time consuming and are not convenient in extracting qualitative characteristics of the nonlinear cable system. The proposed method incorporates the incremental harmonic balance (IHB) technique with the finite element method. The combined use of the incremental harmonic balance (IHB) technique and the finite element method can provide a semi-analytical tool to solve the nonlinear oscillation problem of a cable system.

4.2.2 INCREMENTAL HARMONIC BALANCE TECHNIQUE

The incremental harmonic balance technique (Lau and Cheung 1981; Lau et al. 1983) is then applied to Equation (3.12). Consider a general external periodic excitation vector $\overline{\boldsymbol{P}}(t)$ with period T, and

$$T = 2\pi/\omega \tag{4.1}$$

The corresponding steady-state dynamic responses $\overline{\boldsymbol{U}}(t)$ have the same frequency. By defining dimensionless time

$$\tau = \omega t \tag{4.2}$$

the functions $\overline{\boldsymbol{P}}(\tau)$ and $\overline{\boldsymbol{U}}(\tau)$ possess the period equal to 2π. By setting $t_1 = 0$ and $t_2 = T$, Equation (3.17) becomes

$$\int_0^{2\pi} \delta\{U\}^T \{\omega^2[M]\{\ddot{U}\} + \omega[C]\{\dot{U}\} + \\ + \left[K_0 + K_\sigma + K_1(\{U\}) + K_2\left(\{U\}\{U\}^T\right)\right]\{U\} - P\} d\tau = 0 \tag{4.3}$$

where the overdot represents the differentiation with respect to the dimensionless time τ, and the bar is omitted for the sake of simplicity.

The i-th component $P_i(\tau)$ (i = 1, 2, ··· , N) of the periodic excitation vector $\boldsymbol{P}(\tau)$ can be expressed as

$$P_i(\tau) = \frac{p_{i0}}{2} + \sum_{j=1}^{L} p_{ij} \cos j\tau + \sum_{j=1}^{L} p_{ij}^{*} \sin j\tau \tag{4.4}$$

where,

$$f_i = \{p_{i0}\ p_{i1}\ p_{i2} \cdots p_{iL}\ p_{i1}^{*}\ p_{i2}^{*} \cdots p_{iL}^{*}\}^T \tag{4.5}$$

is the known harmonic component vector of $P_i(\tau)$.

The ith component $U_i(\tau)$ (i = 1, 2, ··· , N) of the steady-state response vector $\boldsymbol{U}(\tau)$ can be represented in the form of multi-harmonic solution as

$$U_i(\tau) = \frac{a_{i0}}{2} + \sum_{j=1}^{M} a_{ij} \cos j\tau + \sum_{j=1}^{M} a_{ij}^{*} \sin j\tau \tag{4.6}$$

where M ($\geq L$) is the number of harmonic terms taken into account, and

$$a_i = \{a_{i0}\ a_{i1}\ a_{i2} \cdots a_{iM}\ a_{i1}^{*}\ a_{i2}^{*} \cdots a_{iM}^{*}\}^T \tag{4.7}$$

is an unknown vector containing the first M harmonic components of $U_i(\tau)$.

With Equations (4.6) and (4.7), $\boldsymbol{U}(\tau)$ can be written as

$$\boldsymbol{U}(\tau) = [Y(\tau)]\{A\} \tag{4.8}$$

in which,

$$\{A\} = \{a_1^T \; a_2^T \cdots a_i^T \cdots a_N^T\}^T \tag{4.9}$$

$$[Y] = \text{Diag}[y^T \; y^T \cdots \; y^T] \tag{4.10}$$

$$y = \left\{\frac{1}{2} \quad \cos\tau \quad \cos 2\tau \quad \cdots \quad \cos M\tau \quad \sin\tau \quad \sin 2\tau \quad \cdots \quad \sin M\tau\right\} \tag{4.11}$$

Similarly, $P(\tau)$ can be expressed as

$$P(\tau) = [Y(\tau)]\{F\} \tag{4.12}$$

in which,

$$\{F\} = \{f_1^T \; f_2^T \cdots f_i^T \cdots f_N^T\}^T \tag{4.13}$$

where the dimensionality of f_i (i = 1, 2, ··· , N) has been augmented to be same as a_i by setting

$$p_{ij} = p_{ij}^* = 0 \quad \text{for} \, j = L+1, L+2, \cdots, M \tag{4.14}$$

Substituting Equations (4.6) and (4.12) to Equation (4.3) yields

$$\begin{aligned} \delta\{A\}^T \int_0^{2\pi} [Y]^T \{ & \omega^2[M][\ddot{Y}]\{A\} + \omega[C][\dot{Y}]\{A\} + \\ & + \left[K_0 + K_1([Y]\{A\}) + K_2\left([Y]\{A\}\{A\}^T[Y]^T\right)\right][Y]\{U\} \\ & - [Y]\{F\} \; \} d\tau = 0 \end{aligned} \tag{4.15}$$

Since the variation $\delta\{A\}^T$ is arbitrary, from Equation (4.15) it follows

$$\begin{aligned} \int_0^{2\pi} \{\Gamma\} d\tau = \int_0^{2\pi} & [Y]^T \{\omega^2[M][\ddot{Y}]\{A\} + \omega[C][\dot{Y}]\{A\} \\ & + \left[K_0 + K_1([Y]\{A\}) + K_2\left([Y]\{A\}\{A\}^T[Y]^T\right)\right][Y]\{A\} \\ & - [Y]\{F\} \; \} d\tau = 0 \end{aligned} \tag{4.16}$$

Consider a dynamic equilibrium state $\{F_0\}$, $\{A_0\}$, ω_0, $\{\Gamma_0\}$ and its neighboring solution

$$\{F\} = \{F_0\}+\{\Delta F\} \tag{4.17a}$$

$$\{A\} = \{A_0\}+\{\Delta A\} \tag{4.17b}$$

$$\omega = \omega_0 + \Delta\omega \tag{4.17c}$$

$$\{\Gamma\} = \{\Gamma_0\}+\{\Delta\Gamma\} \tag{4.17d}$$

By using the Taylor's expansion and neglecting the high-order terms, we have

$$\{\Gamma\} = \{\Gamma_0\}+\frac{\partial\{\Gamma\}}{\partial\{A\}}\{\Delta A\}+\frac{\partial\{\Gamma\}}{\partial\{F\}}\{\Delta F\}+\frac{\partial\{\Gamma\}}{\partial\omega}\Delta\omega \tag{4.18}$$

Substituting Equation (4.18) into Equation (4.16) achieves

$$[\tilde{K}]\{\Delta A\} = \{\tilde{R}\}+[\tilde{P}]\{\Delta F\}+\{\tilde{Q}\}\Delta\omega \tag{4.19}$$

in which,

$$\begin{aligned}[\tilde{K}] = & \int_0^{2\pi}[Y]^T\left[\omega_0^2[M][\ddot{Y}]+\omega_0[C][\dot{Y}]+[K_0][Y]\right]d\tau + \\ & + \int_0^{2\pi}[Y]^T\left[[C_1([A_0])]+[C_2([A_0])]\right]d\tau\end{aligned} \tag{4.20}$$

$$\begin{aligned}\{\tilde{R}\} = & -\left(\int_0^{2\pi}[Y]^T\left[\omega_0^2[M][\ddot{Y}]+\omega_0[C][\dot{Y}]+[K_0][Y]\right]d\tau\right)\{A_0\} \\ & -\left(\int_0^{2\pi}[Y]^T\left[K_1(\{A_0\})+K_2(\{A_0\}\{A_0\}^T)\right][Y]d\tau\right)\{A_0\} \\ & +\left(\int_0^{2\pi}[Y]^T[Y]d\tau\right)\{F_0\}\end{aligned} \tag{4.21}$$

$$[\tilde{P}] = \int_0^{2\pi}[Y]^T[Y]d\tau \tag{4.22}$$

$$\{\tilde{Q}\} = -\left(\int_0^{2\pi}\{Y\}^T\left[2\omega_0[M][\ddot{Y}]+[C][\dot{Y}]\right]d\tau\right)\{A_0\} \tag{4.23}$$

$$K_1(\{A_0\}) = \sum_j \frac{3EA}{2J_j^3}\int_{-1}^{+1}[N']^T[N']\{X_j\}\{A_{0_j}\}^T[Y_j]^T[N']^T[N']d\xi \tag{4.24}$$

$$K_2(\{A_0\}\{A_0\}^T)= \sum_j \frac{EA}{2J_j^3}\int_{-1}^{+1}[N']^T[N'][Y_j]\{A_{0j}\}\{A_{0j}\}^T[Y_j]^T[N']^T[N']d\xi \tag{4.25}$$

$$\begin{aligned} C_1(\{A_0\}) &= [K_1][(\{A_0\})][Y]+ \\ &\sum_j \frac{3EA}{2J_j^3}\int_{-1}^{+1}[N']^T[N']\{X_j\}\{A_{0j}\}^T[Y_j]^T[N']^T[N'][Y_j]d\xi \\ &= [K_1(\{A_0\})][Y]+\sum_j [K_{1j}(\{A_{0j}\})][Y_j] \end{aligned} \tag{4.26}$$

$$\begin{aligned} C_2(\{A_0\}) &= [K_2\{A_0\}\{A_0\}^T][Y]+\sum_j [K_{2j}(\{A_0\}\{A_0\}^T)][Y_j] \\ &+\sum_j \frac{EA}{2J_j^3}\int_{-1}^{+1}(\{A_0\}^T[Y_j]^T[N']^T[N'][Y_j]\{A_0\})[N']^T[N'][Y_j]d\xi \end{aligned} \tag{4.27}$$

$$\{U_j\}=[Y_j]\{A_j\}=(\mathrm{Diag}[y^T y^T \cdots y^T])\{A_j\} \tag{4.28}$$

The incremental equation (Equation 4.19) is a system of linear algebraic equations at each iteration step and is easy to solve. Given $\{F_0\}$, $\{A_0\}$, ω_0, ΔF and $\Delta\omega$, the values of $[\tilde{K}]$, $\{\tilde{R}\}$, $[\tilde{P}]$ and $[\tilde{Q}]$ can be readily computed directly from Equations (4.20) to (4.28) or using a FFT-based time/frequency domain alternating technique (Wang et al. 1994). Then the increments $\{\Delta A\}$ are solved from Equation (4.19). This iterative process is continued until the corrective term

$$\|\{\tilde{R}\}\| \to 0 \tag{4.29}$$

The response results of associated linear system can be taken as initial guesses for iteration. The proposed method is formulated in terms of the increments of all F, A, ω, and therefore is specially suited to parametric study. On the basis of Equation (4.19), the frequency- and amplitude-controlled algorithms can be alternatively implemented. This incremental formulation allows stepping solution along the

frequency axis ($\Delta\omega$), the response-components axes (ΔA) or the excitation-components axes (ΔF). It is particularly amenable to the solution of unstable response and bifurcation problem. For instance, when there are multiple valued responses at a certain frequency range, the response amplitude-controlled algorithm can be adopted to search the unstable branches of the frequency response curves. Following this approach, the increment of a certain component of the response harmonic vector $\{A\}$ is prescribed artificially and regarded as a known, then the frequency increment $\Delta\omega$ and other remaining response harmonic component increments are taken as unknowns and solved simultaneously from Equation (4.19).

Since accommodating multi-harmonic terms, the proposed method enables direct solution of super-harmonic resonances. This method can also analyze sub-harmonic resonances through introducing a reduced frequency. To search for the sub-harmonic resonances of the system under a periodic excitation, e.g.

$$F(t) = F_0 \cos\omega t \tag{4.30}$$

the expression of the excitation can be rewritten as

$$F(t) = F_0 \cos n\omega' t \tag{4.31}$$

in which the reduced frequency

$$\omega' = \omega/n \tag{4.32}$$

and n is a positive integer representing the order of sub-harmonics required to be considered. The periodic responses $U(t)$ can still be expressed in a standard Fourier expansion form as Equation (4.6), and then be solved directly by the present algorithms, so long as ω' substituting for ω is referred to as an excitation frequency. After the nominal primary- and super-harmonic components vector $\{a_i\}$ is solved,

the real multi-harmonic response including the sub-harmonics, is obtained as

$$U_i(t) = \frac{a_{i0}}{2} + \sum_{j=1}^{M} a_{ij} \cos\left(\frac{j\omega t}{n}\right) + \sum_{j=1}^{M} a_{ij}^{\bullet} \sin\left(\frac{j\omega t}{n}\right) \tag{4.33}$$

4.3 CASE STUDY

4.3.1 PROBLEM DESCRIPTION

The proposed method is applied to analyze nonlinear dynamic characteristics of the Tsing Ma Bridge side-span free cables at different construction stages. The Tsing Ma Bridge (Ko et al. 2000) is a suspension bridge of 1377 m main span and 2160 m overall length. The central span and the western Ma Wan side span are suspended with hangers at intervals of 18 m to the main cables. The eastern Tsing Yi side span is contrarily supported from the ground by three concrete piers spaced at 72 m centers. As a result, the Tsing Yi side-span cables are free cables in the completed Tsing Ma Bridge. Studied in the following is one Tsing Yi side-span cable in two stages: (i) tower-cable construction stage, and (ii) finally completed bridge stage. In the first stage, only the bridge towers and main cables were erected but no deck units had been hoisted into position. So all the main cables of three spans are free in this construction stage. In the second stage, the bridge has been completely erected and only the main cables in the Tsing Yi side span are free. The Tsing Yi side-span free cable in these two stages is referred to as Cable I and Cable II, respectively. Due to distinctly different cable tension, the configuration of Cable I and Cable II is different as shown in Table 4.1. All the parameter values listed in Table 4.1 are obtained from the design drawings, where L_x, L_y, ρ, E, A and H_x represent horizontal and vertical lengths of the cable, the mass density, the elasticity modulus, the cross-

sectional area, and the horizontal component of static tension, respectively. In the present study, the cable supports at both stages are regarded as fixed ends (both translation and rotation in tree directions are prohibited).

Table 4.1 Configuration of Tsing Yi side-span free cable

Parameter	Unit	Cable in construction stage (Cable I)	Cable in final stage (Cable II)
L_x	m	290.862	293.184
L_y	m	155.552	154.738
ρ	kg/m^3	7837.8	7837.8
E	GPa	200	196
A	m^2	0.75928	0.80074
H_x	kN	122640	405838

Both Cable I and Cable II are subjected to a vertical sinusoidal excitation with amplitude F and frequency f at mid-span point. It follows that

$$P(t) = F\cos 2\pi ft \tag{4.34}$$

In the response computation, each cable is divided into 10 elements with totally 21 nodes. The truncated harmonic order of the steady-state response is taken as 3, i.e., $M = 3$. Numerical test is also conducted by taking a larger order number $M = 10$. It is found that the third-order harmonics only contribute less than 2% of the total response amplitude and the harmonic components higher than the third order have a negligible influence on the cable response even in the resonant frequency ranges. It should be noted that the zero-order harmonic term (a_0) is not negligible for the cable problem as illustrated below.

The damping matrix in the finite element formulation is taken as the Rayleigh damping form with the expression

$$[C] = \alpha[M] + \beta\left([K_0] + [K_\sigma]\right) \tag{4.35}$$

4.3.2 SOFTENING

Figures 4.1 to **4.4** show the vertical dynamic responses of Cable I at mid-span point under the damping parameters $\alpha = 0.08$ and $\beta = 0.008$. **Figure 4.1** shows the frequency response curves corresponding to different excitation amplitudes. **Figure 4.2** gives a comparison of linear and nonlinear response curves under the excitation amplitude $F = 2.0\times10^6$ N. It is evident from **Figures 4.1** and **4.2** that Cable I exhibits softening nonlinearity, i.e. the resonance peak of the nonlinear oscillation is at the left side of the corresponding linear resonance peak in the frequency-response curve so that it seems the frequency of the cable is decreased, which means that the structure are 'softer' than the original one in the linear theory. The discrepancy between the linear and nonlinear primary resonant frequencies under $F = 2.0\times10^6$ N is about –5.27% (the negative sign represents softening). The response amplitude at the nonlinear resonant peak value is slightly larger than the corresponding linear value. **Figure 4.3** shows the total response amplitude (A) and static drift response ($a_0/2$) versus exciting frequency under $F = 7.0\times10^5$ N. It is seen that under simple harmonic excitation, the cable nonlinear dynamic response is not symmetric about the static equilibrium position. The nonzero mean value (called static drift) is significant in the vicinity of resonant frequency. **Figure 4.4** illustrates the corresponding first- and second-order harmonic components of the response at mid-span point. It is found that the first-order harmonic peak near the frequency 0.335 Hz in **Figure 4.6(a)** corresponds to the first in-plane modal frequency f_1 of the cable (Ko et al. 2000), while the second-order harmonic peak near the frequency 0.355 Hz in **Figure 4.6(b)** is due to the super-harmonic resonance of the third in-plane modal frequency f_3.

In order to get a deeper insight into the super-harmonic resonance philosophy, the frequency response characteristics of Cable I is re-analysed under a weaker damping condition with the coefficients $\alpha = 0.07667$ and $\beta = 0$. **Figures 4.5** and **4.6** illustrate the frequency response curve and harmonic component responses in this case with $F = 4.0\times10^5$ N. It is observed from **Figure 4.5** that the frequency response curve has an 'inflexion point' in the vicinity of 0.355Hz, which is identified as a super-harmonic resonant peak from the analysis of **Figure 4.6**. The first in-plane mode of the cable is symmetric (0.5-wave), the second mode is anti-symmetric (1-wave), and the third mode is symmetric (1.5-wave) again. As a result, the second mode and other anti-symmetric modes do not contribute super-harmonic resonance to the response at mid-span point. The 'inflexion point' in **Figure 4.5** and the sharp peak in **Figure 4.6(b)**, at about the frequency f = 0.355Hz, are due to the second-order super-harmonic resonance caused by the third modal frequency f_3, i.e., $2f \cong f_3$. Of course, there is also a second-order super-harmonic resonance corresponding to the first modal frequency f_1 at about the frequency $f \cong f_1/2 \cong 0.176$Hz as observed in the frequency response curves. However, for this specific case, the super-harmonic resonant peak at the frequency $f \cong f_1/2$ is much less than that at the frequency $f \cong f_3/2$ due to $f_3/2$ being just close to the primary resonant frequency f_1.

It should be addressed that the cable may exhibit softening as well as hardening behaviors according to relative contribution of quadratic and cubic nonlinearities. The static cable tension and the cable sag contribute to the quadratic and cubic nonlinearities, respectively. When the cable tension is relatively lower, the cubic nonlinearity plays more important role and the cable exhibit softening behavior as observed in this subsection. When the cable tension is relatively large, the quadratic nonlinearity becomes prevalent and we will find that the cable may also exhibit

hardening behavior as presented in the next subsection.

4.3.3 HARDENING

Then the nonlinear dynamic characteristics of the Tsing Yi side-span free cable in the finally completed bridge stage (Cable II) are analyzed under the same excitation as in Case I. **Figures 4.7** to **4.9** show the vertical dynamic responses of Cable II at mid-span point under the damping parameters $\alpha = 0.08$ and $\beta = 0.008$. **Figure 4.7** illustrates the frequency response curves for different excitation amplitudes. **Figure 4.8** provides a comparison of linear and nonlinear response curves under the excitation amplitude $F = 7.0\times10^5$ N. It is known from **Figures 4.7** and **4.8** that in contrast with Cable I, Cable II displays hardening nonlinearity, i.e. the resonance peak of the nonlinear oscillation is at the right side of the corresponding linear resonance peak in the frequency-response curve. The discrepancy between the linear and nonlinear primary resonant frequencies under $F = 7.0\times10^5$ N is about 5%. **Figure 4.9** plots the total response amplitude and static drift response of Cable II versus exciting frequency under $F = 2.0\times10^6$ N. Under simple harmonic excitation, the steady-state response of the cable with hardening nonlinearity is also asymmetric. **Figure 4.10** shows the corresponding first- and second-order harmonic component responses.

4.4 SUMMARY

A hybrid finite element/incremental harmonic balance method, that eschews commonly used modal reduction, is developed for analysis of nonlinear periodically forced vibration of inclined cables with arbitrary sag. By taking enough finite

elements and appropriate harmonic terms, the proposed method can obtain accurate steady-state dynamic response under single- or multi-harmonic excitation. The conventional time integration procedure is expensive in seeking frequency response curves as it may take a long transient process to reach steady state, whereas the proposed method directly resolves steady-state solutions. Moreover, the proposed method is able to completely predict unstable, multi-valued responses, as well as sub- and super-harmonic resonances in an alternating frequency- and amplitude-controlled manner. This method can also be explored to evaluate cable internal resonance in any modal combination when a certain commensurable condition is met, as discussed in the next chapter.

Though the method developed in this chapter and the analyses carried our in this and the next chapters for the nonlinear dynamics of cables do not directly contribute to the cable condition assessments, they are potential in dealing with such problems when the nonlinearities should be considered. For instance, when the condition of a cable in nonlinear oscillation, which may occur when the cable is under wind-rain-induced vibration, excited by support moving, are to be assessed, the proposed method may serve as a good candidate. The present method is readily capable of analyzing the nonlinear cable oscillation excited by support motion. When the wind- and wind-rain induced vibration are to be analyzed, the excitation force along the cable should be identified first and then the present method can be used. Due to its computational versatility, this method can be extended to analyze the interconnected cable system and the cable-damper system, which are widely adopted in modern cable-stayed bridges.

Numerical analysis results of the Tsing Ma Bridge attain to the following conclusions: (i) The Tsing Yi side-span free cable of the Tsing Ma Bridge exhibits

softening nonlinearity in the tower-cable construction stage, but diverges to display hardening nonlinearity in the finally completed bridge stage. That is, the bridge cable has distinctly different nonlinear characteristics in the two stages due to different cable static tension and configuration. The softening behavior is due to the relative large contribution of cable sag, which takes cubic nonlinearity to the oscillation, and the hardening behavior is due to the large cable tension; (ii) The steady-state periodic response of the cable under simple harmonic excitation is not symmetric about the static equilibrium position. The nonzero mean value (static drift) is significant in the resonant frequency range; (iii) In steady-state response of the cable considered, the third-order harmonics have magnitudes less than 2% of the total response amplitudes, and harmonic terms of mode 4 and above can be disregarded in the solution process; (iv) The sub-harmonic resonance of the cable can be caused by not only the primary resonant frequency but also by the higher-mode resonant frequencies. They may result in pronounced resonant peaks in the low damping case.

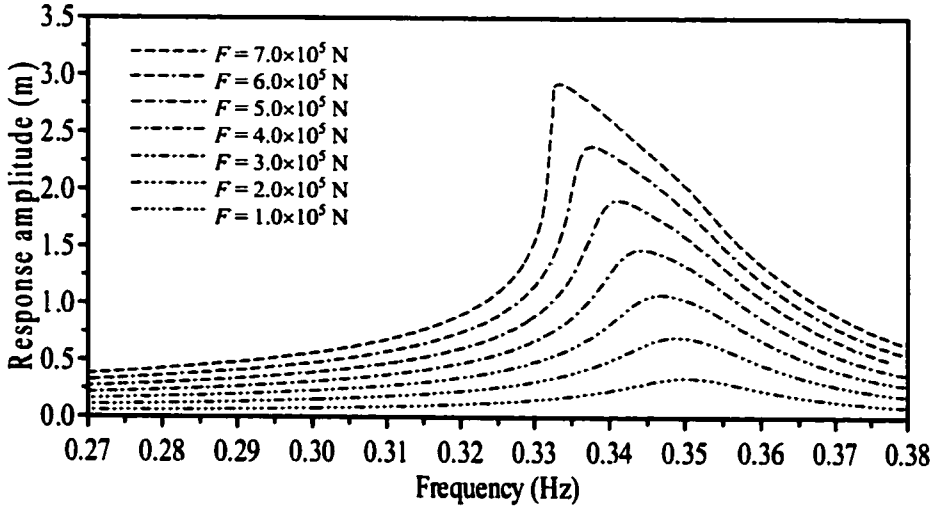

Figure 4.1 Frequency response curves of Cable I (α=0.08, β=0.008)

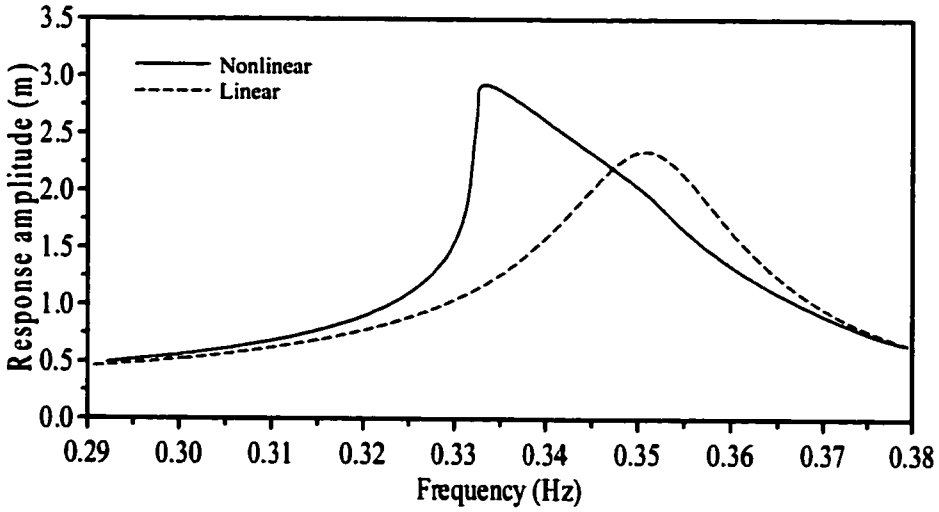

Figure 4.2 Linear and nonlinear response of Cable I ($F=2.0\times10^6$ N, α= 0.08, β=0.008)

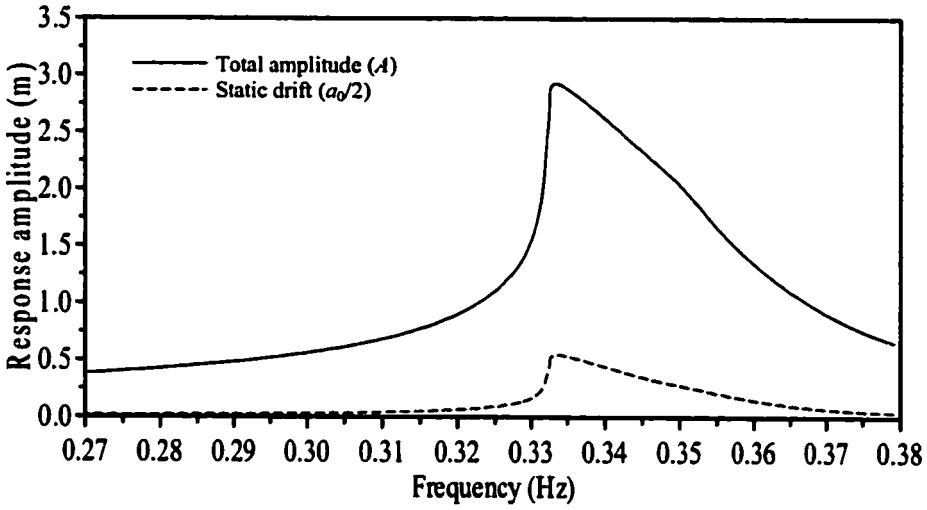

Figure 4.3 Total amplitude and static drift of Cable I ($F=7.0\times10^5$ N, $\alpha=0.08$, $\beta=0.008$)

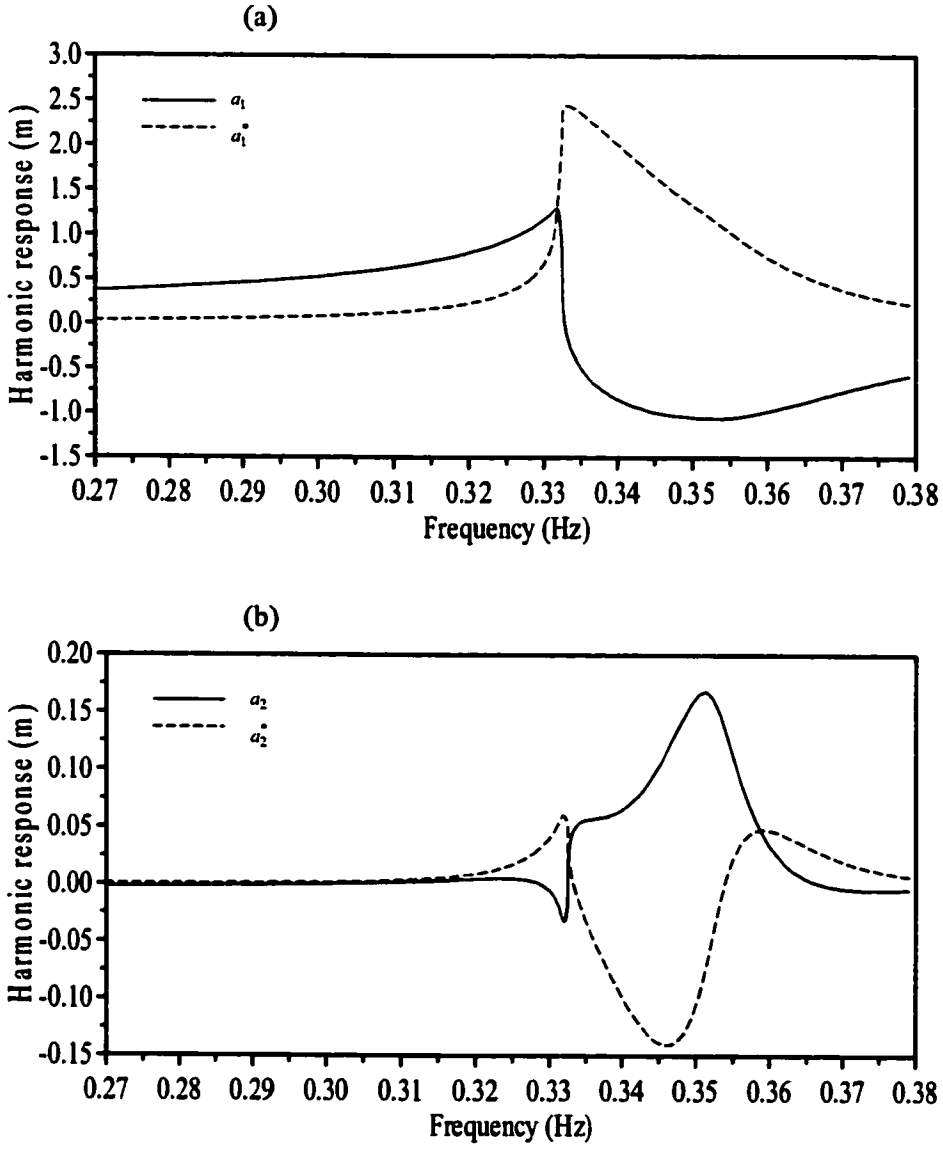

Figure 4.4 Harmonic response components of Cable I ($F=7.0\times10^5$ N, $\alpha=0.08$, $\beta=0.008$): (a) 1st order harmonic components; (b) 2nd order harmonic components

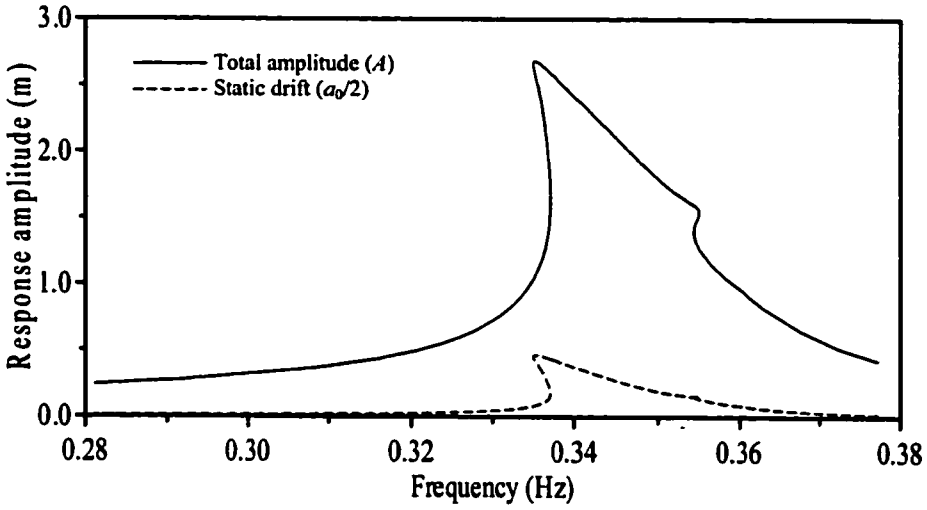

Figure 4.5 Total amplitude and static drift of Cable I ($F=4.0\times10^5$ N, $\alpha=0.07667$, $\beta=0$)

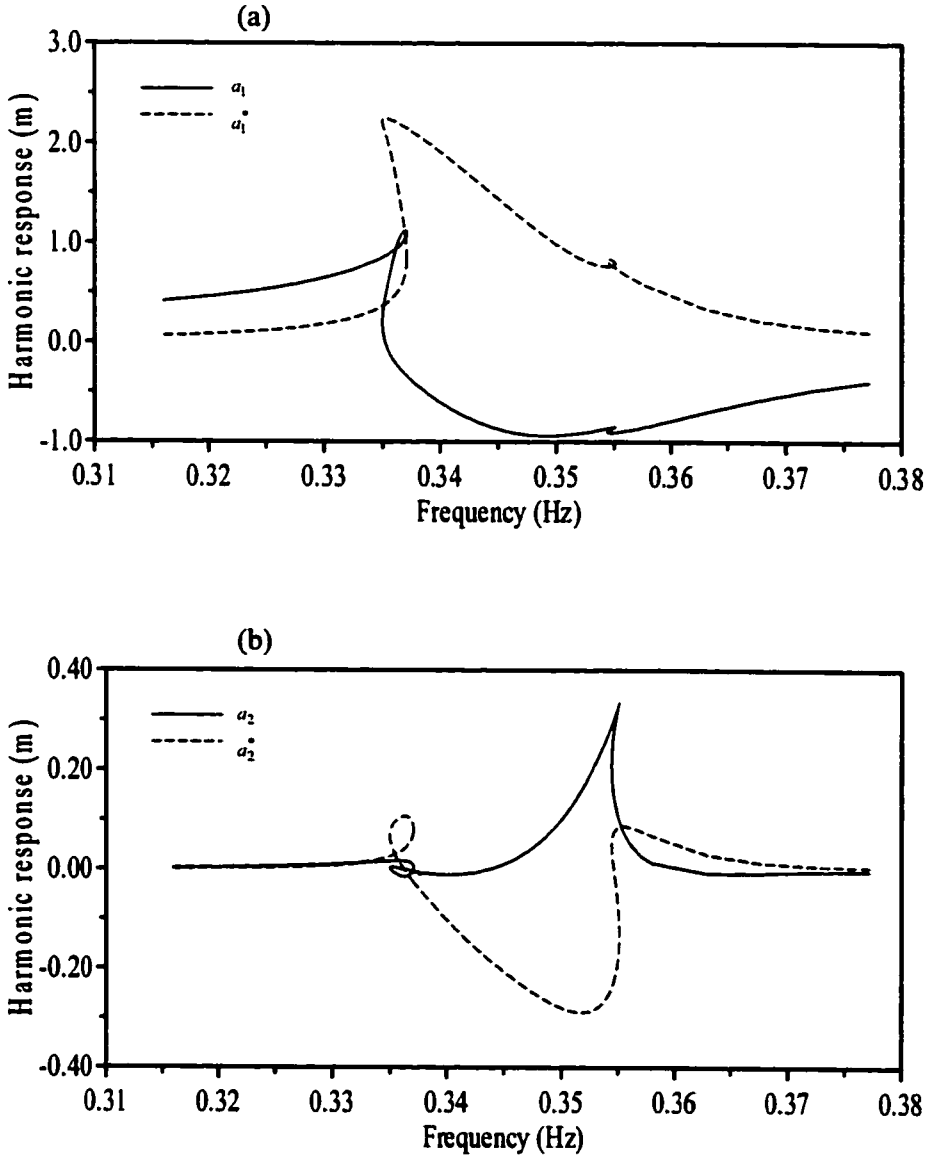

Figure 4.6 Harmonic response components of Cable I ($F=4.0\times10^5$ N, $\alpha=0.07667$, $\beta=0$): (a) 1st order harmonic components; (b) 2nd order harmonic components

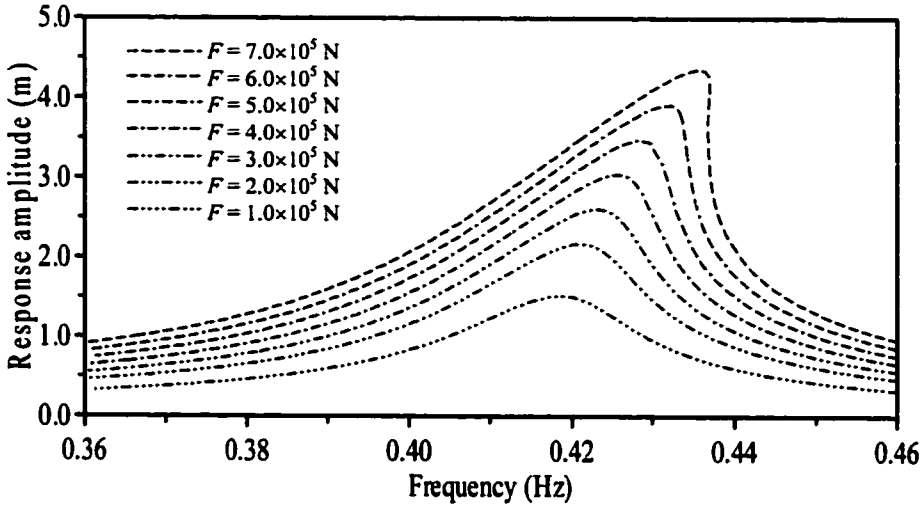

Figure 4.7 Frequency response curves of Cable II (α=0.08, β=0.008)

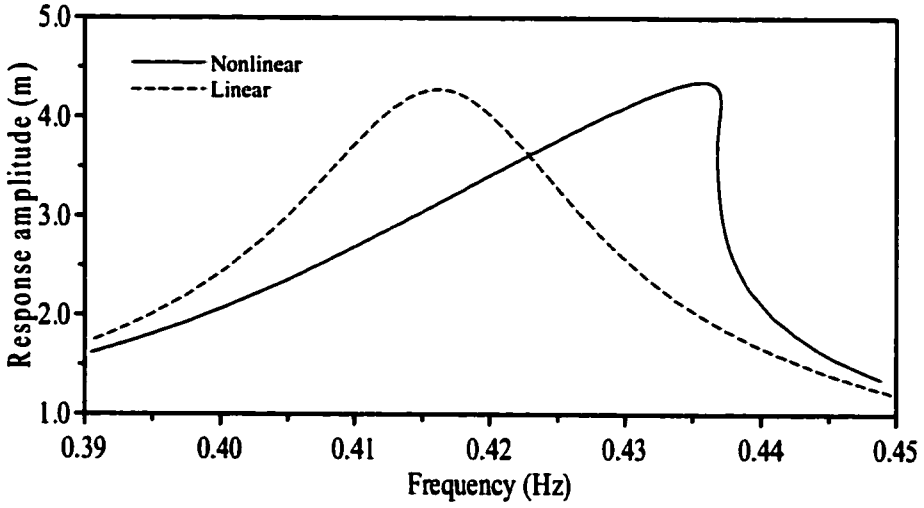

Figure 4.8 Linear and nonlinear response of Cable II (F=7.0×10^5 N, α=0.08, β=0.008)

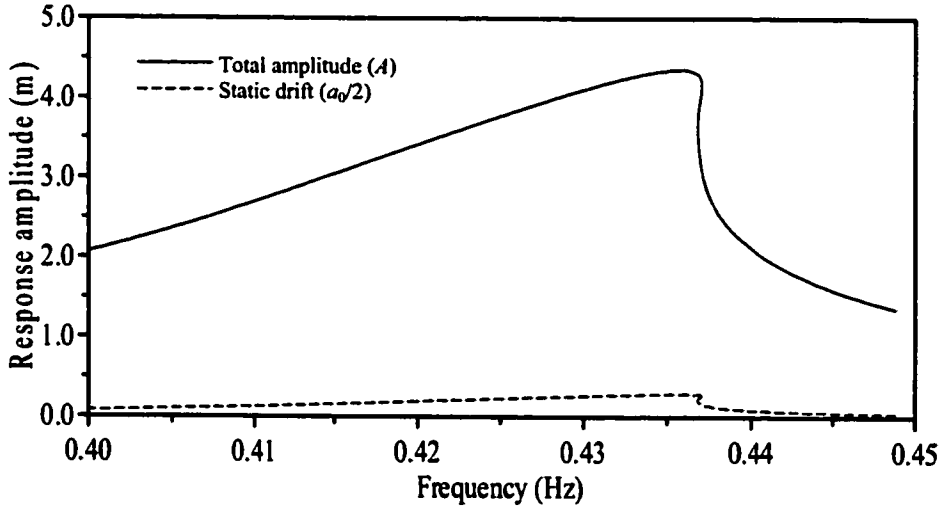

Figure 4.9 Total amplitude and static drift of Cable II ($F = 2.0 \times 10^6$ N, α = 0.08, β = 0.008)

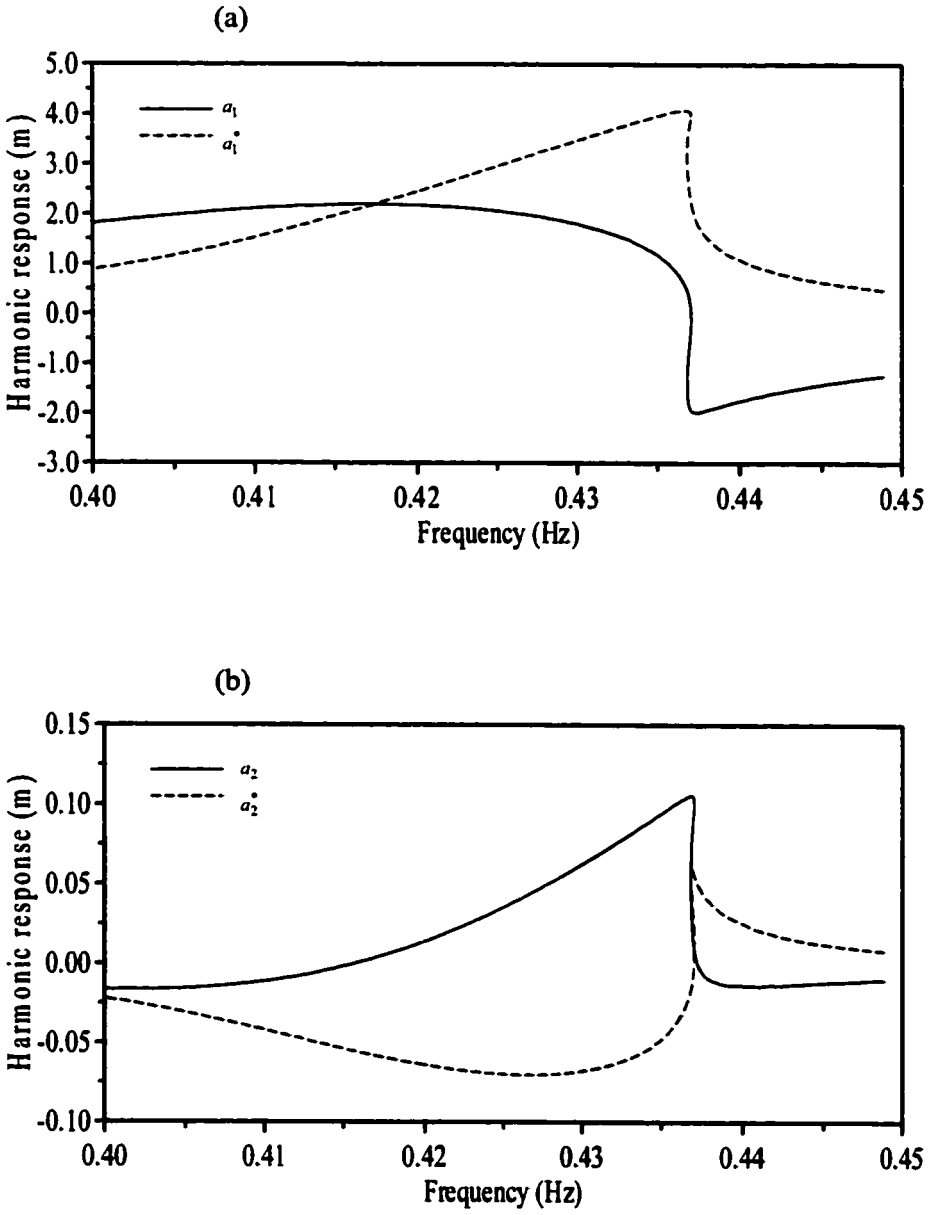

Figure 4.10 Harmonic response components of Cable II ($F=2.0\times10^6$N, $\alpha=0.08$, $\beta=0.008$): (a) 1st order harmonic components; (b) 2nd order harmonic components

CHAPTER 5

SUPER-HARMONIC AND INTERNAL RESONANCES OF A SUSPENDED CABLE

5.1 INTRODUCTION

In this chapter, the super-harmonic and internal resonance characteristics of a viscously damped cable with nearly commensurable natural frequencies are investigated by use of the method developed in the previous chapter, in which the method has shown its capability in analysis of the softening and hardening phenomena in nonlinear cable vibration. The alternating frequency/amplitude-controlled algorithm enables a complete solution for the frequency-response curves including unstable branches, sub- and super-harmonic resonances and internal resonances. A suspended cable paradigm under internal resonance condition is studied to demonstrate the capability of the presented method in analyzing modal coupling (interactions) and internal resonances.

Nonlinear response and modal interaction characteristics of the cable at different frequency regions are identified from analysis of response profiles and harmonic component features. The super-harmonic and internal resonance responses are respectively characterized based on the harmonic distribution. Under an in-plane harmonic excitation, the two-to-one internal resonance between the in-plane and out-of-plane modes and the super-harmonic resonance around the second symmetric in-plane mode are revealed. Strong nonlinear interaction among different modes in the parameter space ranging from primary resonance to super-harmonic resonance is

observed. Spatial-temporal response profiles and numerical harmonic components at different parameter ranges are presented to highlight the plentiful nonlinear response behaviors of the cable.

5.2 PROBLEM DESCRIPTION

5.2.1 PERTURBATION METHOD

Nonlinear periodically forced oscillation of elastic cables has been studied by numerous researchers based on different theoretical and experimental models, as reviewed in Chapter 2. Interesting phenomena known as internal resonance, super- and sub-harmonic response, static drift, etc., have been observed in real cables.

The perturbation method is the most widely used method in this field, which primarily includes two branches: the direct models and the mode-reduced models. In the direct models, multiple scales or other perturbation techniques are directly applied to the governing partial-differential equations and boundary conditions of distributed-parameter cable systems through expressing the solution in an expansion form of a small parameter. In the mode-reduced models, the original governing equations are first dealt with as a discretized modal model with a few (one to four) degrees of freedom by using the Galerkin method and linear modal functions, and then the method of perturbation is applied to obtain the response solution. The approach using the mode-reduced models is more universal and more efficient in analysis treatment. However, it is based on the approximate assumption that the motion of the nonlinear system has the same spatial dependence as the linearized system. The recent investigations by Pakdemirli et al. (1995) and by Rega et al.

(1999) showed that the results obtained by treating a cable system as a mode-reduced discretized model might be quantitatively and/or qualitatively erroneous.

An important phenomenon in the nonlinear dynamics of cables and other continuous systems is the modal interaction (coupling), especially the internal resonance when the linear frequencies of systems satisfy commensurate or nearly commensurate conditions (Nayfeh 2000). The modal interaction and internal resonance may result in harmful large-amplitude response in the low-frequency modes when subjected to a high-frequency excitation, and provide energy exchange among the modes. In this chapter, modal interaction and internal resonance characteristics of a suspended cable paradigm (Rega et al. 1999; Nayfeh 2000) are investigated by using the method developed in the previous chapter.

5.2.2 CABLE PARAMETERS

The cable under investigation is a suspended homogeneous elastic cable that has been studied analytically and experimentally by Rega et al. (1997, 1999). Table 5.1 shows the cable parameters, where L and d represent the cable span and the midspan sag respectively; E is the Young modulus; A is the cross-sectional area; m is the mass per unit length; H is the horizontal component of cable tension force. The cable has the in-plane (vertical) and out-of-plane (lateral) damping coefficients 0.06781 kg/m·s and 0.09689 kg/m·s respectively. Table 5.2 lists the natural frequencies of the first four in-plane and out-of-plane modes of the cable. It is seen that the cable has very close natural frequencies among the first symmetric in-plane mode (6.302 Hz), the first antisymmetric in-plane mode (6.254 Hz) and the first antisymmetric out-of-plane mode (6.320 Hz). Also, these frequencies are approximately twice the natural frequency of the first symmetric out-of-plane mode (3.165 Hz). Because of these

nearly commensurate linear frequencies, internal resonances may occur in this cable. In the present paper, we focus attention on the two-to-one internal resonance between the first symmetric in-plane mode and the first symmetric out-of-plane mode.

Table 5.1. Parameters of the cable.

L (m)	d (m)	E (MPa)	A (m^2)	mg (N/m)	H (N)
0.6005	0.0305	1340.8	1.2570×10^{-7}	0.4769	0.7048

Table 5.2. Natural frequencies of the cable (Hz).

Mode Type	1st symmetric	1st antisymmetric	2nd symmetric	2nd antisymmetric
In-plane mode	6.302	6.254	9.731	12.603
Out-of-plane mode	3.165	6.320	9.478	12.636

The cable is excited by a distributed vertical harmonic load. The symmetric in-plane excitation is expressed as

$$p_y(x,t) = p_0(1-\cos 2\pi x)\cos 2\pi ft \tag{5.1}$$

where x denotes the horizontal coordinate of the cable; f is the excitation frequency (Hz) and p_0 is the exciting force amplitude. The spatial distribution of this load is the same as the first in-plane mode shape of the cable linear vibration. The exciting force amplitude is taken as p_0 = 0.5 N in the study.

5.3 MODAL INTERACTION AND INTERNAL RESONANCE

The proposed method is applied to analyze the modal interaction and internal resonance of nonlinear steady-state response of the cable under a periodic excitation. The cable is divided into 8 curved elements with a total of 17 nodes in the

computation. The response component for each of the three degrees of freedom at a node is assumed to comprise 9 harmonic terms, i.e. $M = 4$ in Equation (4.11). **Figure 5.1** illustrates the frequency-response curves of the cable at the mid-span point, obtained by the present method. The thin solid line shows the in-plane vertical response branch at which the cable does not exhibit out-of-plane response under the in-plane excitation. The thick solid line shows the in-plane vertical response branch at which the two-to-one internal resonance happens, while the dashed line shows the corresponding out-of-plane response exhibited due to the resonance.

5.3.1 SUPER-HARMONIC RESONANCE

In order to explore the modal interaction and internal resonance characteristics, we start the response analysis at the frequency points far away from the primary resonance range, i.e. points A and B in **Figure 5.1**, and then sweep the excitation frequency toward the first in-plane resonant frequency. The in-plane vertical responses of the cable mid-span at point A (f_A = 2.080 Hz) and point B (f_B = 7.920 Hz) are obtained as

$$\begin{aligned} u_{ym}^{A}(t) = 10^{-4}(&0.08 + 5.90\cos\omega t + 0.16\sin\omega t \\ &- 0.13\cos 2\omega t + 0.02\sin 2\omega t) \quad (\omega = 2\pi f_A) \end{aligned} \tag{5.2}$$

$$\begin{aligned} u_{ym}^{B}(t) = 10^{-4}(&0.18 - 8.75\cos\omega t + 0.13\sin\omega t \\ &- 0.16\cos 2\omega t - 0.03\sin 2\omega t) \quad (\omega = 2\pi f_B) \end{aligned} \tag{5.3}$$

It is observed from Equations (5.2) and (5.3) that the responses at points A and B contain non-zero high-order harmonic terms, but the high-order harmonic components are very small in comparison with the primary-harmonic components. **Figure 5.2** illustrates the spatial-temporal profiles of horizontal and vertical response components of the cable at points A and B. In **Figures 5.2(a)** and **5.2(c)**, the diagram of displacement response versus cable length at any instant is always symmetric with

respect to the mid-span point. This means that the horizontal response components are symmetric along the cable span. All the figures appearing hereafter for the cable horizontal response show the same feature. Due to negligible effect of the high-order harmonic components, the diagram of response versus time looks like a single-harmonic response curve with its frequency same as the excitation frequency.

5.3.2 INTERNAL RESONANCE

The excitation frequency is then swept from point A to point C through points S_1 and S_2 as shown in **Figure 5.1**. Since point C, the frequency-sweeping method is tried again but no convergent solution can be obtained when only in-plane response is taken into account. In recognizing this, the solution search is then changed in the following ways: (i) continuing the frequency-sweeping solution from point C after imposing an initial out-of-plane response disturbance; (ii) starting the amplitude-sweeping solution from point C. Following the former way, we find the internal resonance from point C to point D between the in-plane and out-of-plane modes. Following the latter way, we find that the frequency-response curve can be stretched from point C to a peak point P_1 with increasing response amplitude and decreasing resonant frequency.

In the process of frequency sweeping from point C (f_C = 5.888 Hz) to point D (f_D = 6.320 Hz), out-of-plane response of the cable occurs in accompanying with the in-plane response under the in-plane vertical excitation. The thick solid line and the dashed line in **Figure 5.1** respectively show the in-plane vertical response amplitude and the out-of-plane response amplitude in this region. The simultaneously exhibited in-plane and out-of-plane responses under a pure in-plane excitation throughout the region reveal the occurrence of internal resonance between in-plane and out-of-plane

modes. **Figure 5.3** illustrates the spatial-temporal profiles of in-plane horizontal and vertical response components of the cable at three frequency points I_1 (f_{I1} = 5.890 Hz), I_2 (f_{I2} = 6.062 Hz) and I_3 (f_{I3} = 6.320 Hz) lying in this region, and **Figure 5.4** shows the spatial-temporal profiles of the corresponding out-of-plane responses. The in-plane vertical and out-of-plane horizontal responses of the cable mid-span at three frequency points are obtained as

$$u_{ym}^{I_1}(t) = 10^{-3}(0.74 + 3.61\cos 2\omega t + 3.96\sin 2\omega t + 0.03\cos 4\omega t - 0.56\sin 4\omega t) \quad (\omega = 2\pi f_{I_1}/2) \tag{5.4a}$$

$$u_{zm}^{I_1}(t) = 10^{-3}(0.00 - 1.13\cos \omega t - 1.68\sin \omega t + 0.07\cos 2\omega t - 0.04\sin 2\omega t) \quad (\omega = 2\pi f_{I_1}/2) \tag{5.4b}$$

$$u_{ym}^{I_2}(t) = 10^{-3}(0.71 - 3.63\cos 2\omega t + 3.89\sin 2\omega t + 0.04\cos 4\omega t + 0.48\sin 4\omega t) \quad (\omega = 2\pi f_{I_2}/2) \tag{5.5a}$$

$$u_{zm}^{I_2}(t) = 10^{-3}(0.00 + 0.22\cos \omega t - 0.45\sin \omega t - 0.02\cos 2\omega t - 0.01\sin 2\omega t) \quad (\omega = 2\pi f_{I_2}/2) \tag{5.5b}$$

$$u_{ym}^{I_3}(t) = 10^{-3}(0.79 + 0.39\cos 2\omega t + 5.00\sin 2\omega t + 0.45\cos 4\omega t - 0.08\sin 4\omega t) \quad (\omega = 2\pi f_{I_3}/2) \tag{5.6a}$$

$$u_{zm}^{I_3}(t) = 10^{-3}(0.00 - 0.39\cos \omega t - 5.07\sin \omega t + 0.00\cos 2\omega t + 0.23\sin 2\omega t) \quad (\omega = 2\pi f_{I_3}/2) \tag{5.6b}$$

By comparing the response configurations given in **Figures 5.3** and **5.4** and from Equations (5.4) to (5.6), it is evident that the internal resonance occurring in this region is a two-to-one internal resonance between the first in-plane mode and the first out-of-plane mode. Again, the high-order harmonic components in the internal resonance are very small and have negligible effect on the spatial-temporal response profiles shown in **Figures 5.3** and **5.4**. Thus in the internal resonance range, the three-dimensional cable response configuration can be regarded as a combination of the first symmetric in-plane mode and the first symmetric out-of-plane mode with

different phases. It is also observed in **Figure 5.5** that in the internal resonance, the static drift of the steady-state in-plane response is of significance whereas the out-of-plane response has no static drift. **Figure 5.6** shows the trajectory of the cable mid-span response at point I_3. In the phase plane, the trajectory of the out-of-plane response is symmetric with respect to the origin, while the trajectory of the in-plane response is only symmetric about the axis of zero velocity.

5.3.3 PRIMARY RESONANCE

By using the amplitude-controlled algorithm, the frequency-response curve is searched from point C to a peak response at point P_1 (f_{P1} = 5.862 Hz) through response harmonic component stepping. The in-plane vertical response of the cable mid-span at point P_1 is obtained as

$$u_{ym}^{P_1}(t) = 10^{-3}(0.85 + 3.81\cos\omega t + 4.29\sin\omega t + 0.06\cos 2\omega t - 0.71\sin 2\omega t) \quad (\omega = 2\pi f_{P_1}) \tag{5.7}$$

The frequency-response curve is also searched from point B to another peak response at point P_2 (f_{P2} = 6.240 Hz) through descending frequency sweeping. The in-plane vertical response of the cable mid-span at point P_2 is obtained as

$$u_{ym}^{P_2}(t) = 10^{-3}(0.82 - 3.58\cos\omega t + 4.28\sin\omega t + 0.11\cos 2\omega t + 0.62\sin 2\omega t) \quad (\omega = 2\pi f_{P_2}) \tag{5.8}$$

Figure 5.7 illustrates the spatial-temporal profiles of in-plane horizontal and vertical response components of the cable at points P_1 and P_2. It is known from Equations (5.7) and (5.8) and **Figure 5.7** that both the responses at points P_1 and P_2 represent the primary resonance of the first symmetric in-plane mode. These two peak responses contain large primary-harmonic components, considerable zero-order harmonic components (static drift), and very small high-order harmonic components.

5.3.4 MODAL INTERACTION

Although points P_1 and P_2 represent same primary resonance and are closely spaced, the frequency-response curve of pure in-plane response evolving from point P_1 to point P_2 takes a long distance as shown in **Figure 5.1**. The alternating frequency/amplitude-controlled algorithms are utilized to obtain the complete response trace denoted by $P_1 \rightarrow S_3 \rightarrow S_4 \rightarrow S_5 \rightarrow S_6 \rightarrow P_2$. **Figure 5.8** illustrates the evolution of phase diagrams from point P_1 to point P_2 along this trace. It is seen from the figure that albeit the starting point P_1 and the ending point P_2 have simple and almost identical phase diagrams, the responses within the trace exhibit very complicated dynamic trajectories, distinct from those at points P_1 and P_2. Strong modal interactions occur when the response is traced from point P_1 to point P_2. **Figure 5.9** illustrates the spatial-temporal profiles of horizontal and vertical response components of the cable at points S_3 (f_{S3} = 5.252 Hz), S_4 (f_{S4} = 4.880 Hz), S_5 (f_{S5} = 5.260 Hz) and S_6 (f_{S6} = 5.860 Hz) within this response region. The in-plane vertical responses of the cable mid-span at these points are obtained as

$$u_{ym}^{S_3}(t) = 10^{-3}(0.73 + 3.16\cos\omega t + 2.15\sin\omega t - 0.50\cos 2\omega t - 1.14\sin 2\omega t) \quad (\omega = 2\pi f_{S_3}) \tag{5.9}$$

$$u_{ym}^{S_4}(t) = 10^{-3}(0.87 + 0.16\cos\omega t + 2.54\sin\omega t + 2.13\cos 2\omega t - 0.08\sin 2\omega t) \quad (\omega = 2\pi f_{S_4}) \tag{5.10}$$

$$u_{ym}^{S_5}(t) = 10^{-3}(0.78 - 1.95\cos\omega t + 1.18\sin\omega t - 0.77\cos 2\omega t + 1.19\sin 2\omega t) \quad (\omega = 2\pi f_{S_5}) \tag{5.11}$$

$$u_{ym}^{S_6}(t) = 10^{-3}(0.67 - 2.76\cos\omega t + 1.64\sin\omega t - 0.50\cos 2\omega t + 0.79\sin 2\omega t) \quad (\omega = 2\pi f_{S_6}) \tag{5.12}$$

It is evident from **Figure 5.9** and Equations (5.9) to (5.12) that the responses occurring in this region involve strong modal interactions. The response profiles can

be significantly different at different points of this response region. The high-order harmonic components participate greatly in the responses. At point S_4 (f_{S4} = 4.880 Hz), the second-order harmonic amplitude (2.132×10^{-3} m) of the cable mid-span response is the same order of magnitude as the primary-harmonic amplitude (2.545×10^{-3} m). In recognizing the frequency at point S_4 (4.880 Hz) is almost half of the natural frequency of the second symmetric in-plane mode (9.731 Hz), this response region with extremely large second-order harmonic components is ascertained as second-order super-harmonic resonance of the second symmetric in-plane mode. The super-harmonic resonance is strongest in the vicinity of S_4. Along the trace $P_1 \rightarrow S_3 \rightarrow S_4$, the response transits from the primary resonance to the super-harmonic resonance; and then along the trace $S_4 \rightarrow S_5 \rightarrow S_6 \rightarrow P_2$, the response changes from the super-harmonic resonance to the primary resonance again. Response profiles of the cable at super-harmonic resonance are significantly different from those at primary and internal resonances.

5.4 SUMMARY

Nonlinear modal interaction and internal resonance of a suspended cable paradigm are numerically investigated by means of a hybrid 3-D finite element/incremental harmonic balance method. This frequency-domain solution method eschews commonly used modal reduction and can accommodate arbitrary harmonic terms. By taking enough finite elements and appropriate harmonic terms, the proposed method can obtain an accurate description of the cable nonlinear steady-state dynamic response characteristics under either simple or multi-harmonic excitation. This method is suited for both suspended and inclined cables with sag-to-

span ratios not limited to being small, and allows for the consideration of boundary conditions, lumped masses, supporting motion, and intermediate springs and/or dampers. The proposed method is promising for the analysis of cable nonlinear modal interactions (coupling) and internal resonances because it accommodates multi-harmonics and retains mathematical tractability in the description of spatial degrees of freedom and multi-modes. Due to its numerical accuracy, this method can be also used in some situations to verify the solutions obtained from other approximate analytical methods.

Based on the study of modal interaction and internal resonance characteristics of a suspended cable paradigm, the following conclusions are drawn: (i) A two-to-one internal resonance of the cable between the first in-plane mode and the first out-of-plane mode is revealed; (ii) A second-order super-harmonic resonance of the second symmetric in-plane mode is found in the cable; (iii) The static drift (zero-order harmonic component) of the in-plane response at the primary, super-harmonic and internal resonances is significantly large; (iv) There is no static drift in the out-of-plane response of the cable when activated by the two-to-one internal resonance; (v) Strong modal interactions occur in the transition between the primary and the super-harmonic resonances; (vi) Response profiles of the cable at the super-harmonic resonance are significantly different from those at the primary and internal resonances.

Though the analyses carried out for the nonlinear dynamics do not directly contribute to the cable condition assessments, they are potential in dealing with such problems when the nonlinearities should be considered. In this chapter, it is noticed that different kind of modal interactions of cable nonlinear oscillations are quantitatively distinguished by the different harmonic terms (Equations 5.2 to 5.13)

and qualitatively characterized by different spatial-temporal profiles (**Figures 5.2** to **5.9**). When the measured nonlinear oscillation of a real cable can be accurately simulated through the proposed method, it is evident that the nonlinear dynamic cable tension can be obtained and the cable condition can be assessed. However, this can only be done when both the excitation and the nonlinear oscillation of the cable have been measured providing the cable to be assessed is in steady state oscillation.

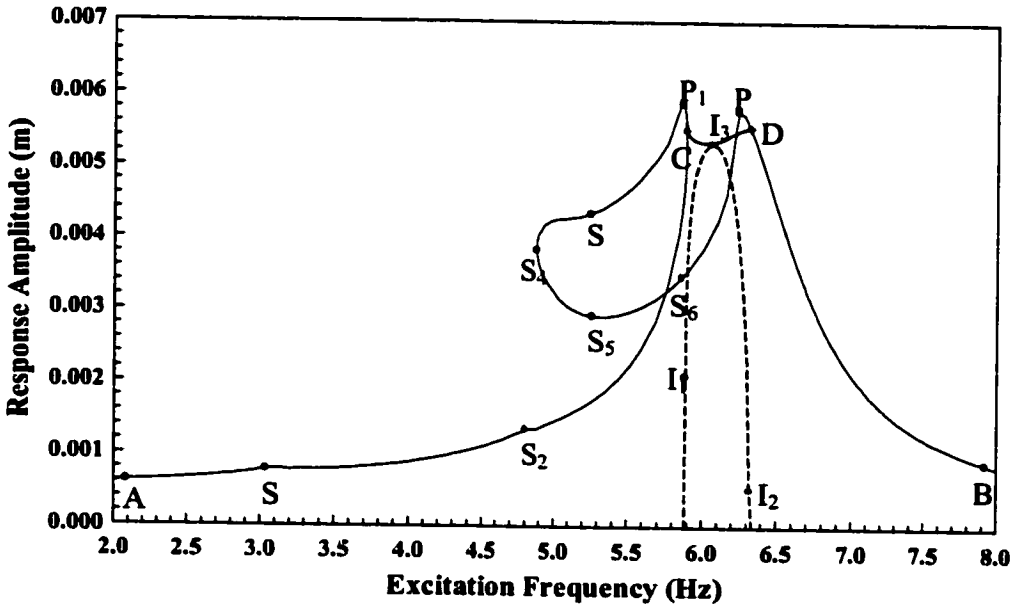

Figure 5.1 Frequency-response curves of cable nonlinear vibration.

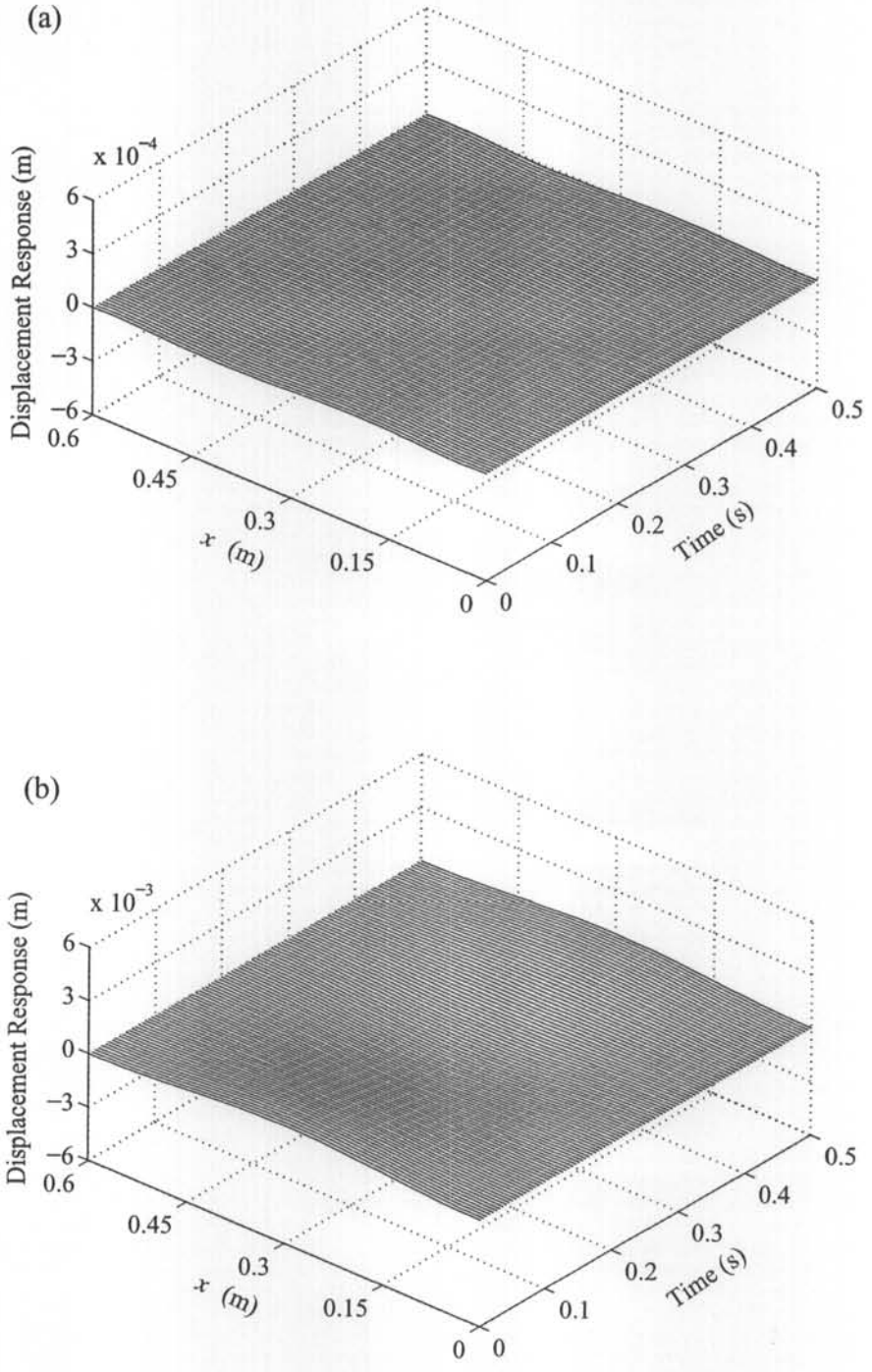

Figure 5.2 In-plane response at points A and B:

(a) horizontal component at point A;

(b) vertical component at point A

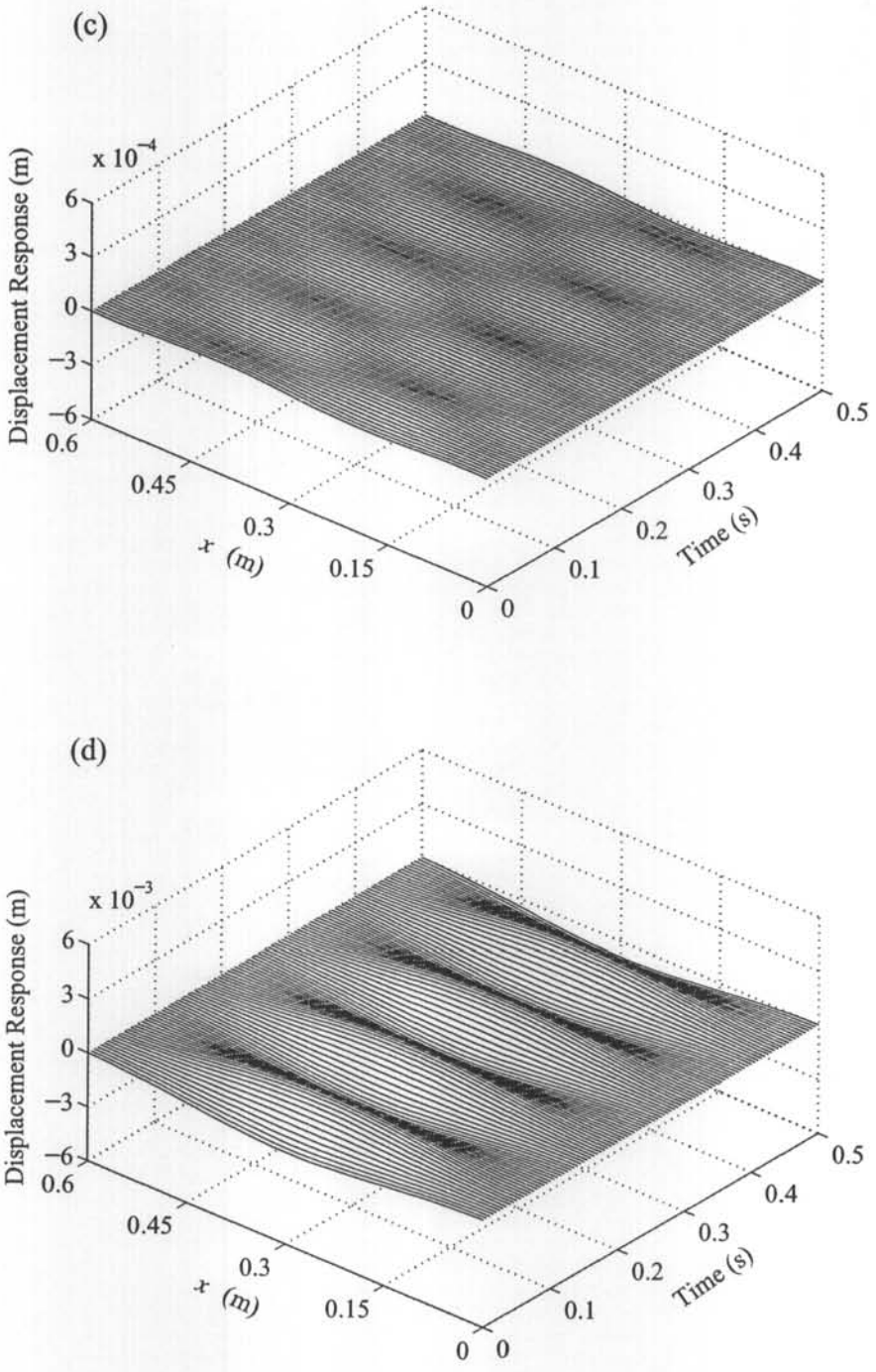

Figure 5.2 In-plane response at points A and B (Cont'd):

(c) horizontal component at point B;

(d) vertical component at point B

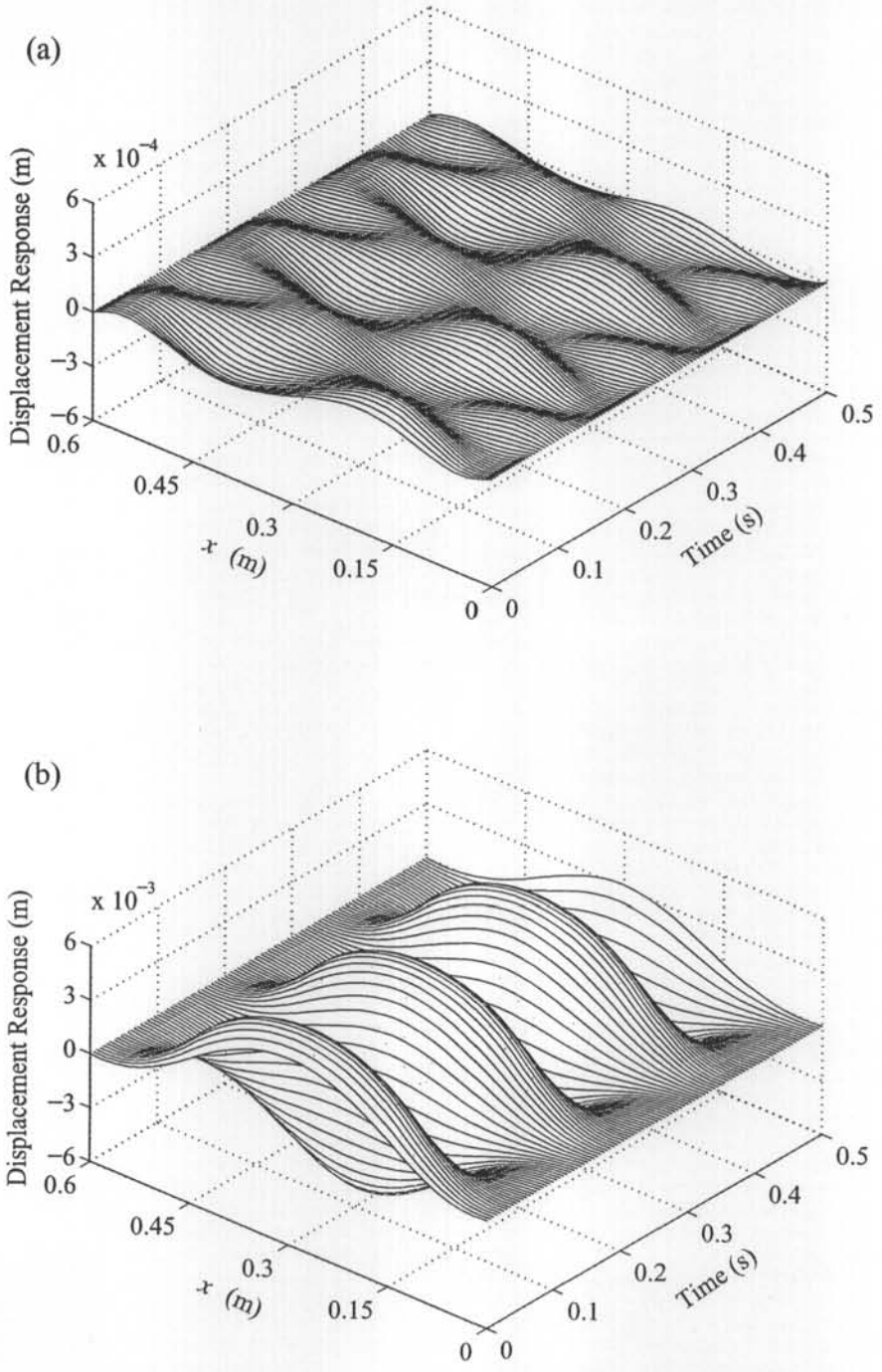

Figure 5.3 In-plane response at internal resonance:

(a) horizontal component at point I1;

(b) vertical component at point I1;

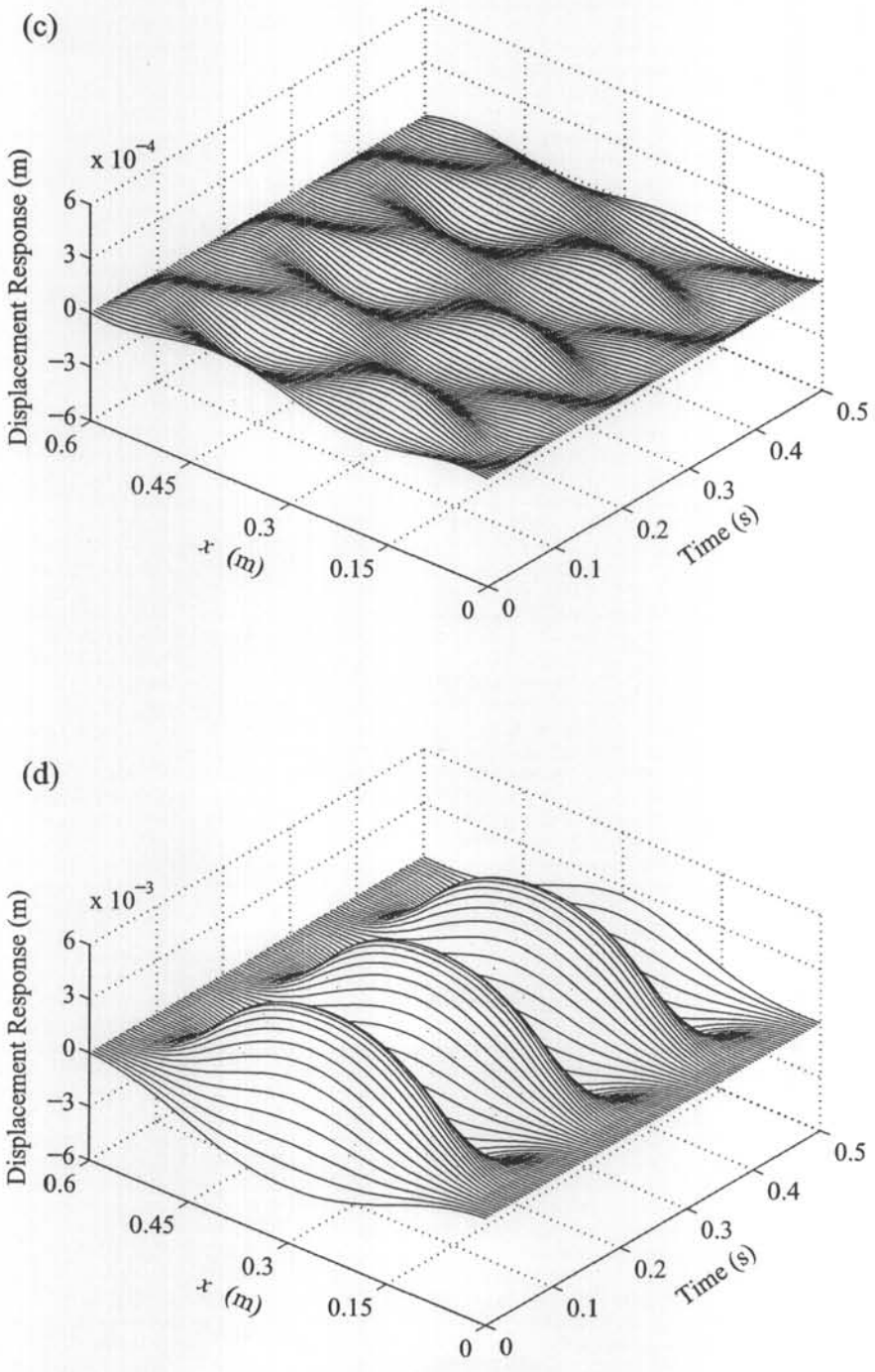

Figure 5.3 In-plane response at internal resonance (Cont'd):

(c) horizontal component at point I2;

(d) vertical component at point I2

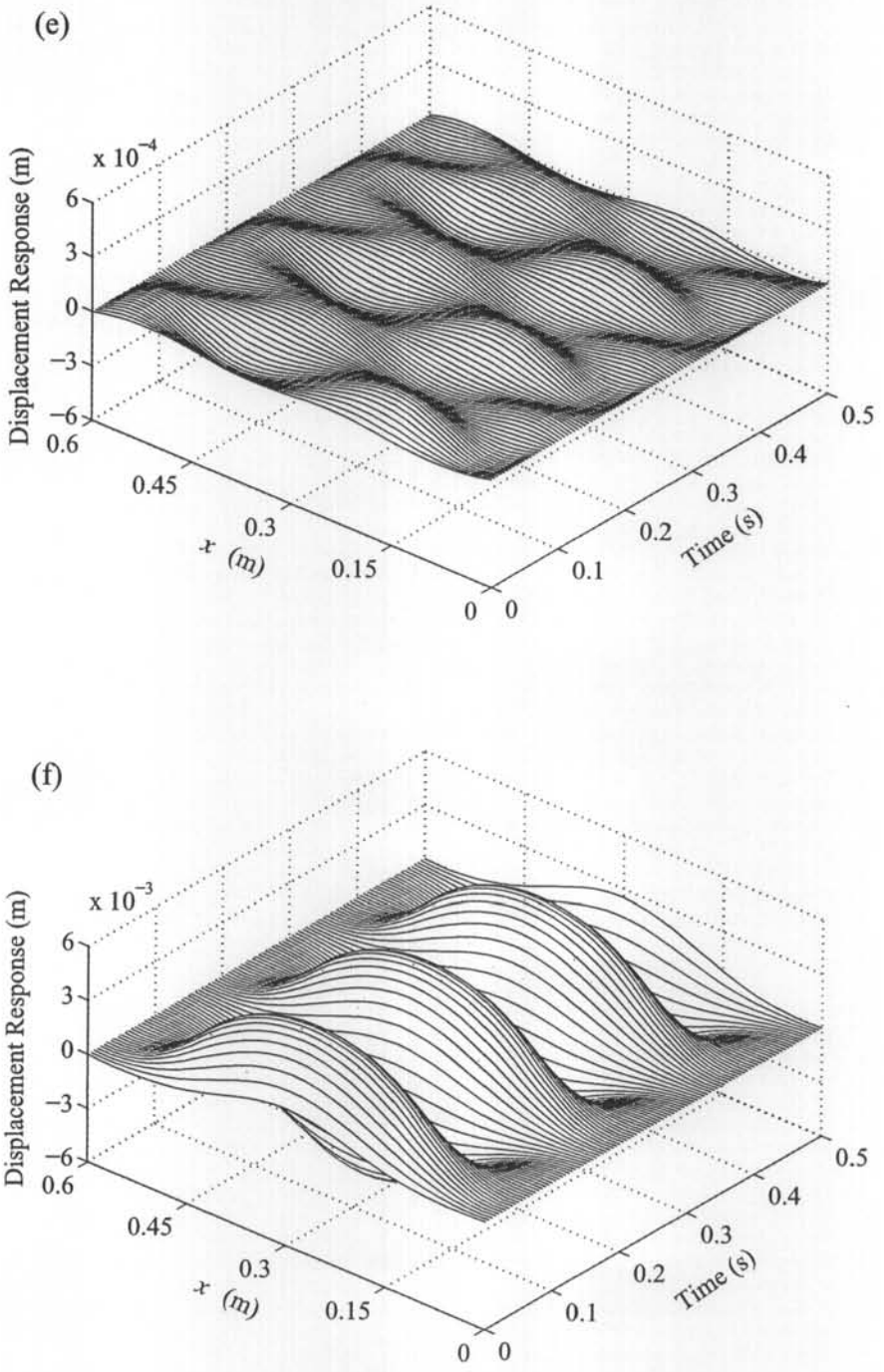

Figure 5.3 **In-plane response at internal resonance (Cont'd):**

(e) horizontal component at point I3;

(f) vertical component at point I3.

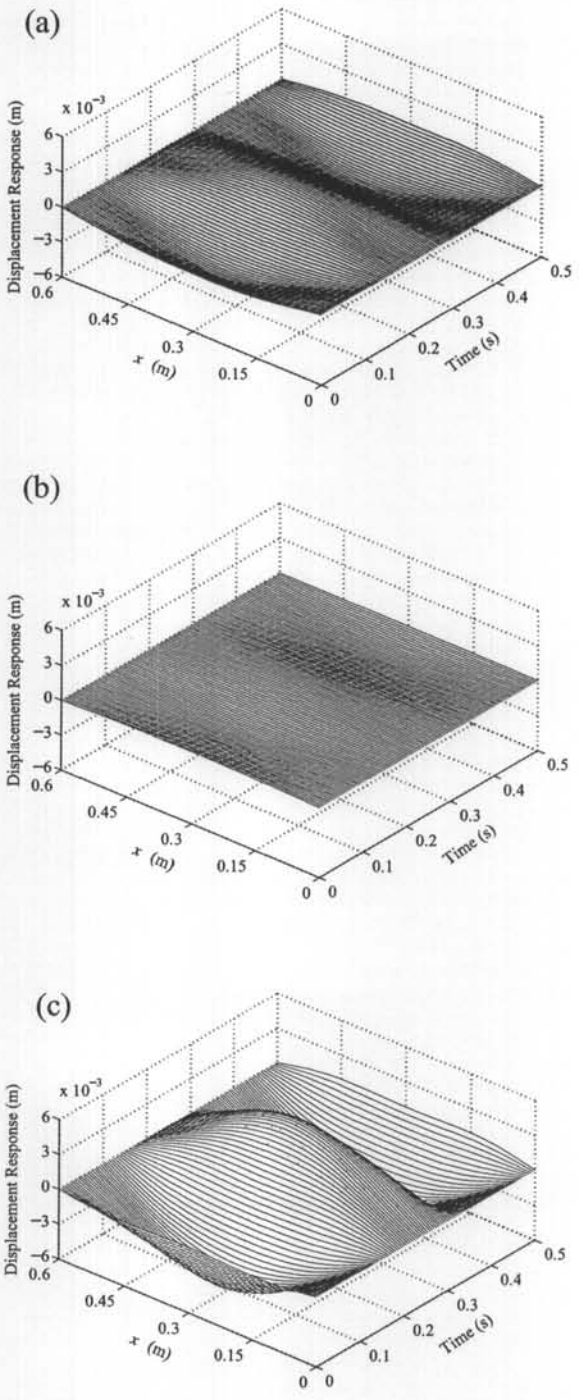

Figure 5.4 **Out-of-plane response at internal resonance:**

(a) at point I_1;

(b) at point I_2;

(c) at point I_3.

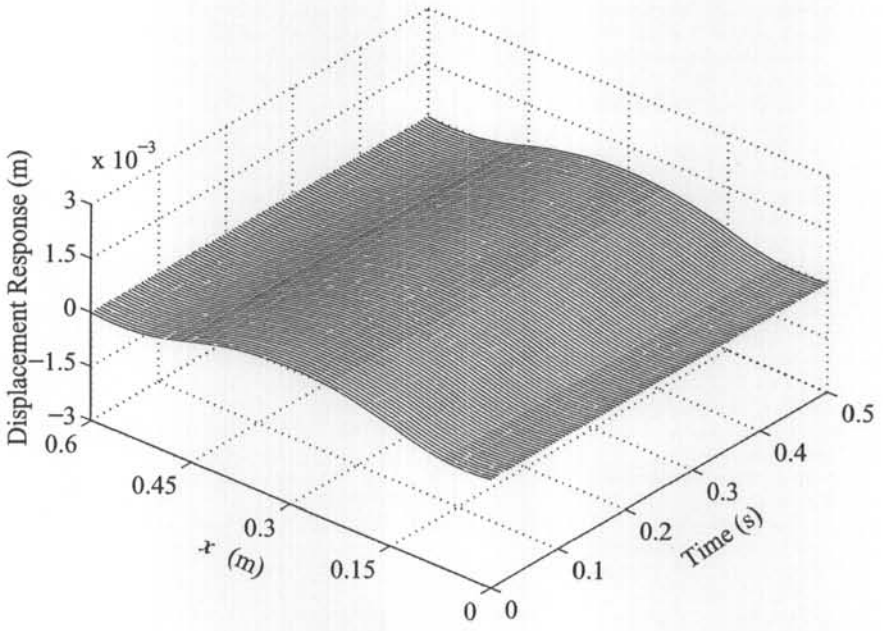

Figure 5.5 Static drift of in-plane vertical response at point I3.

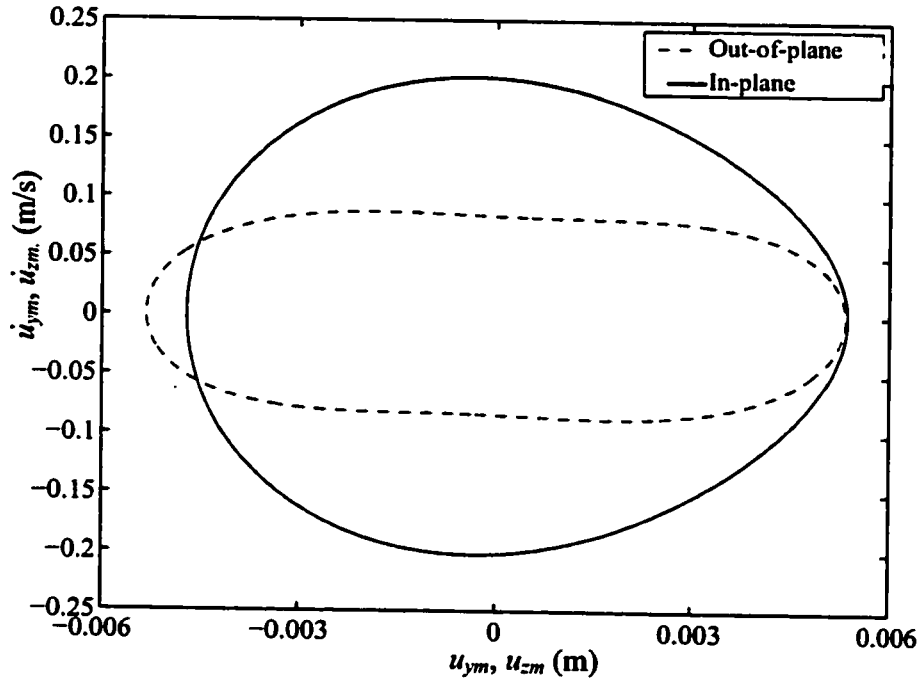

Figure 5.6 Phase diagrams of mid-span response at point I3.

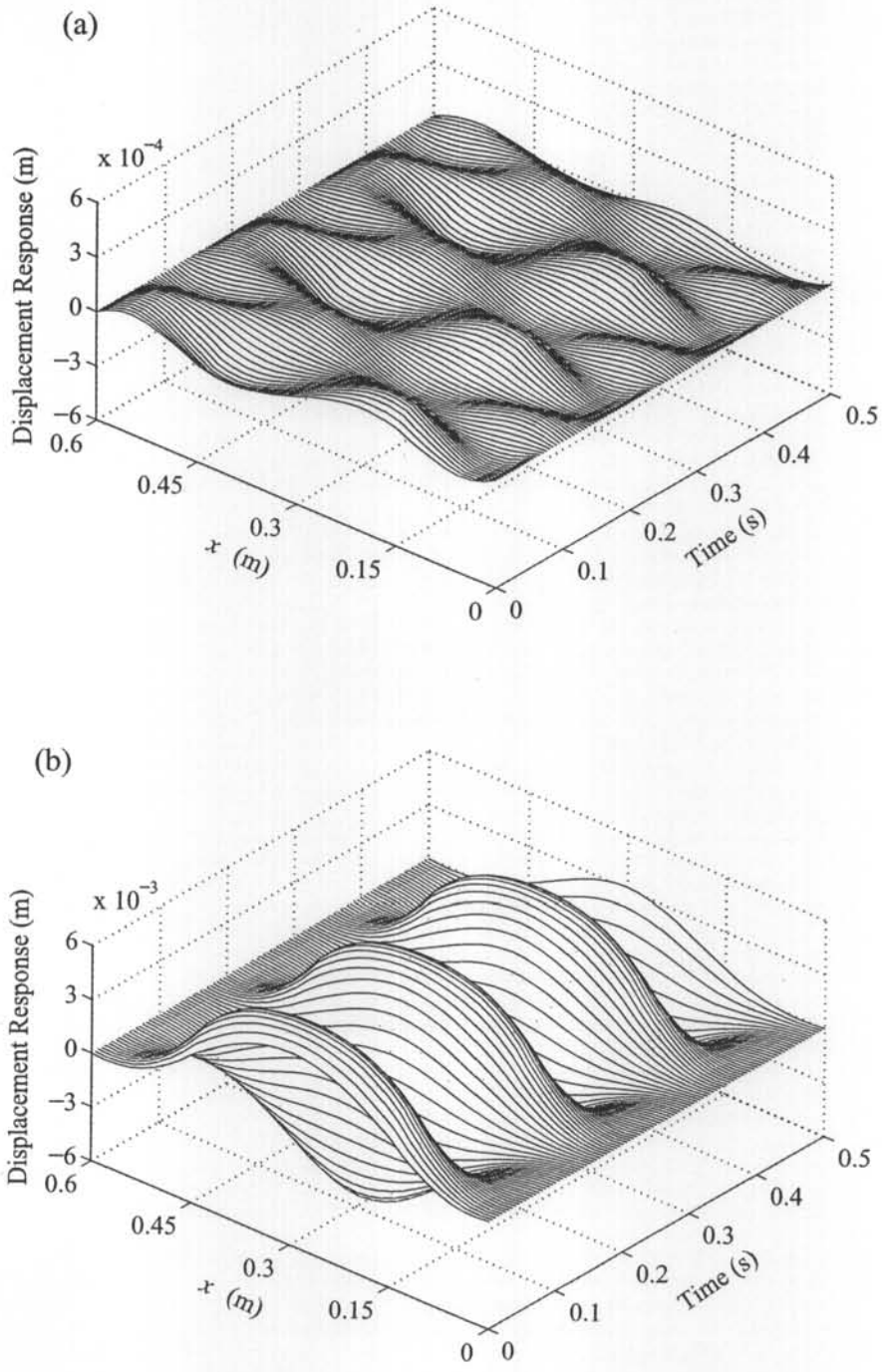

Figure 5.7 **In-plane response at primary resonance:**

(a) horizontal component at point P_1;

(b) vertical component at point P_1;

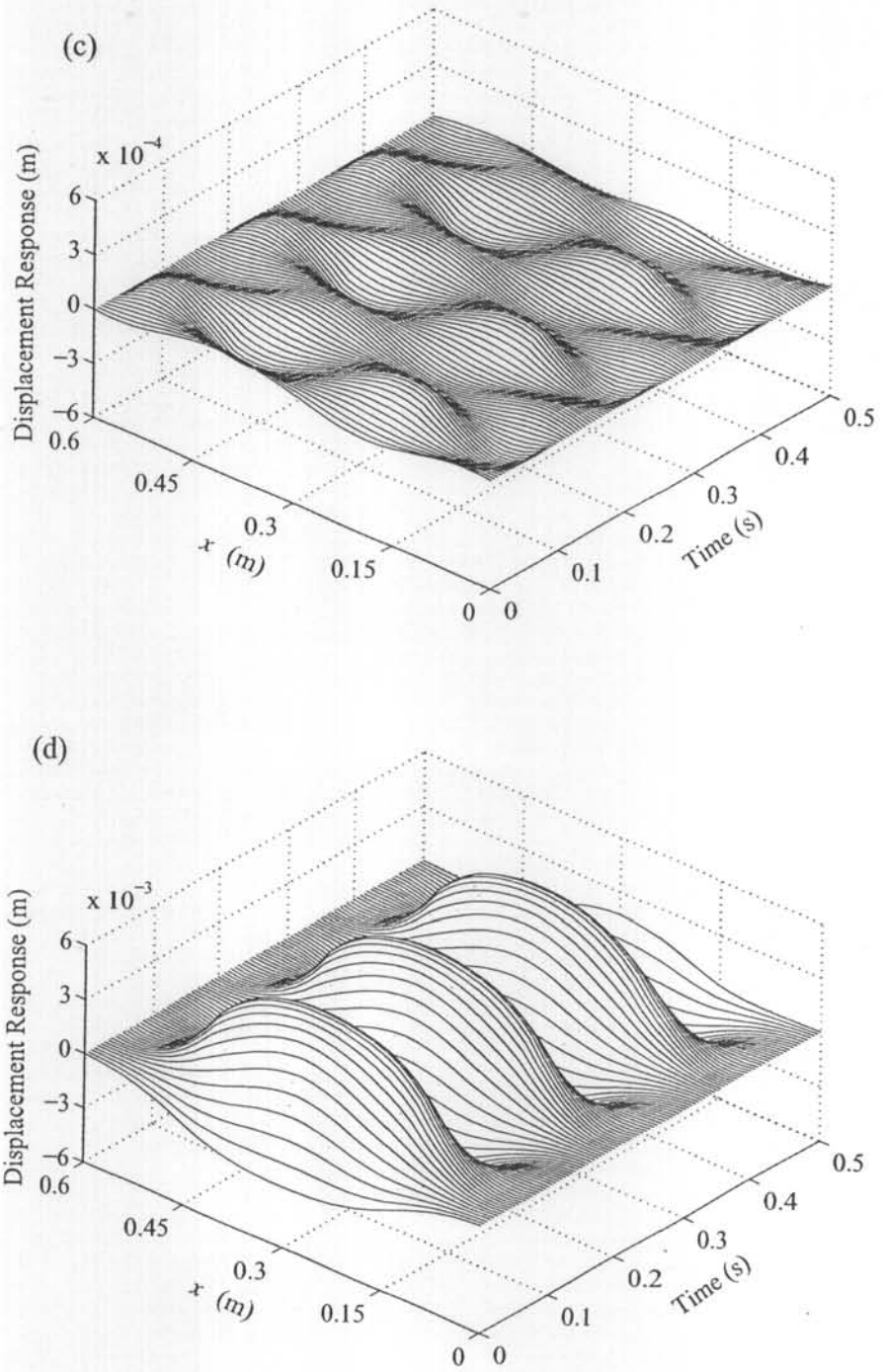

Figure 5.7 **In-plane response at primary resonance (Cont'd):**

(c) horizontal component at point P_2;

(d) vertical component at point P2.

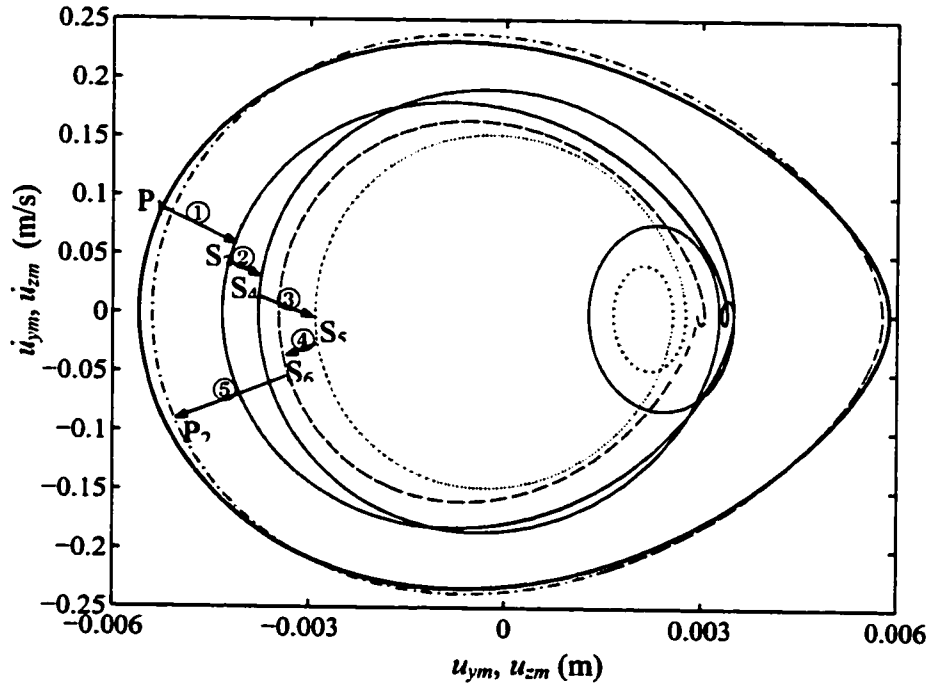

Figure 5.8 **Phase diagrams of mid-span response between two primary resonant points.**

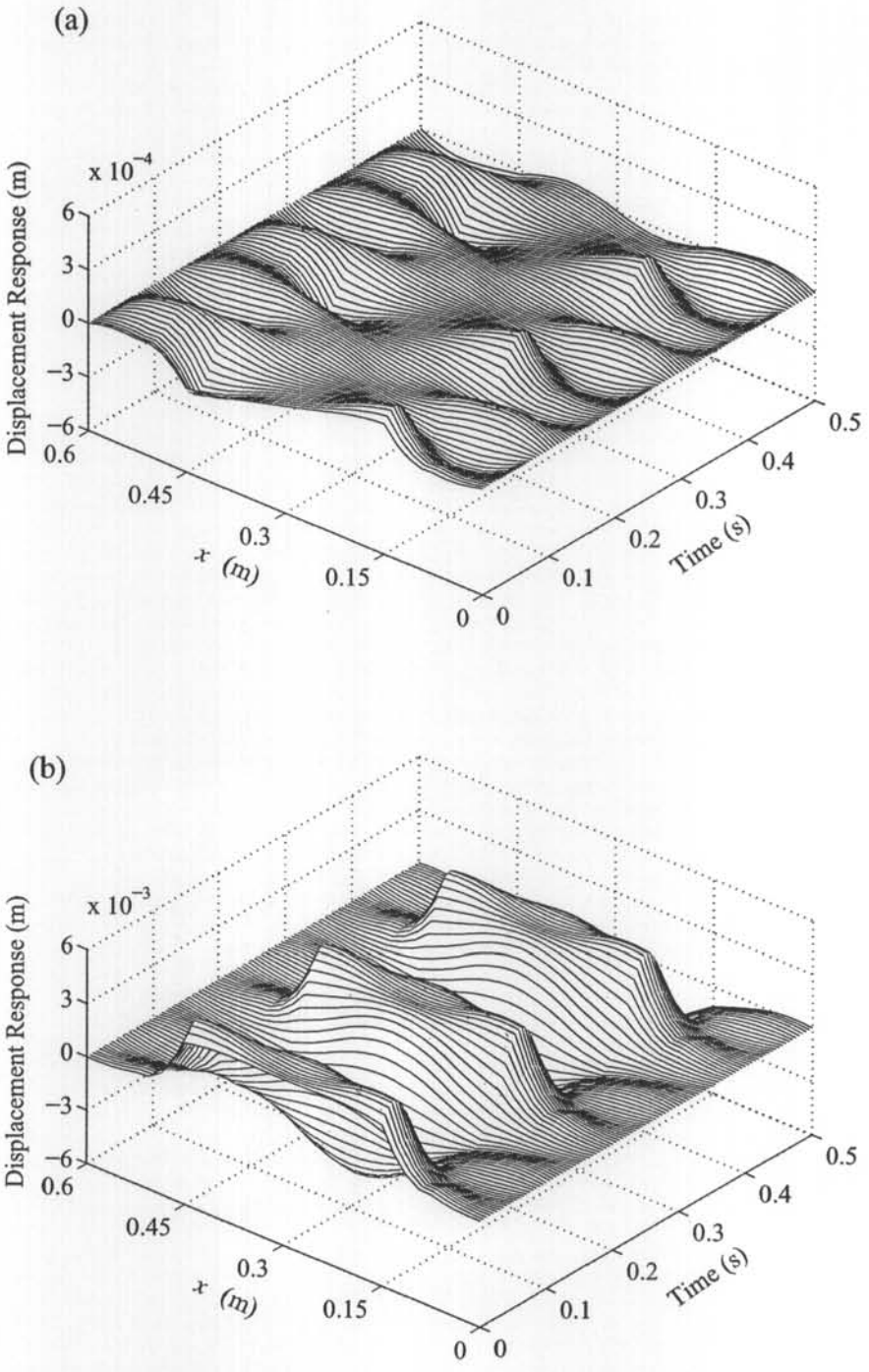

Figure 5.9 In-plane response at super-harmonic resonance:

(a) horizontal component at point S_3;

(b) vertical component at point S_3;

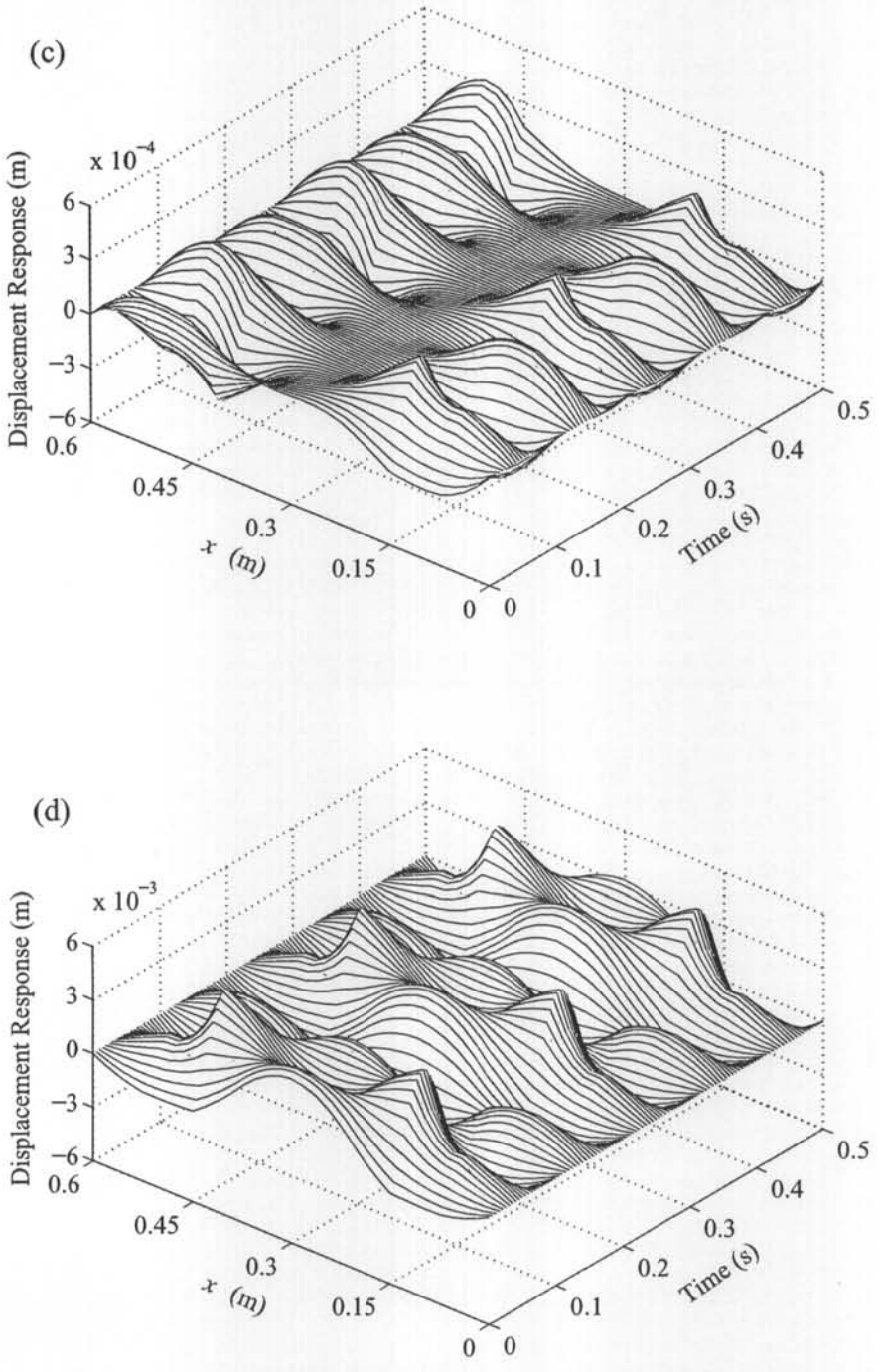

Figure 5.9 **In-plane response at super-harmonic resonance (Cont'd):**

(c) horizontal component at point S4;

(d) vertical component at point S4;

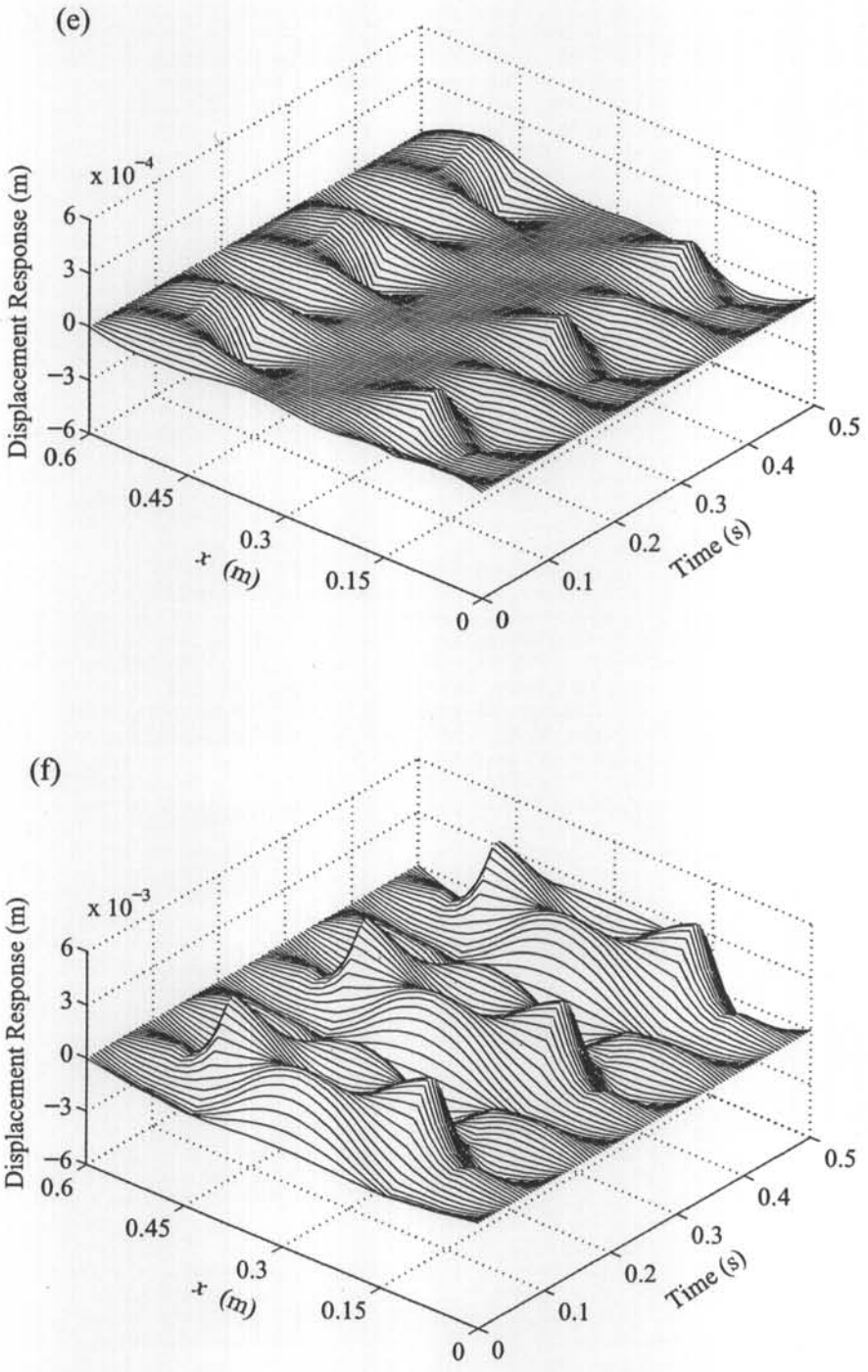

Figure 5.9 **In-plane response at super-harmonic resonance (Cont'd):**

(e) horizontal component at point S5;

(f) vertical component at point S5;

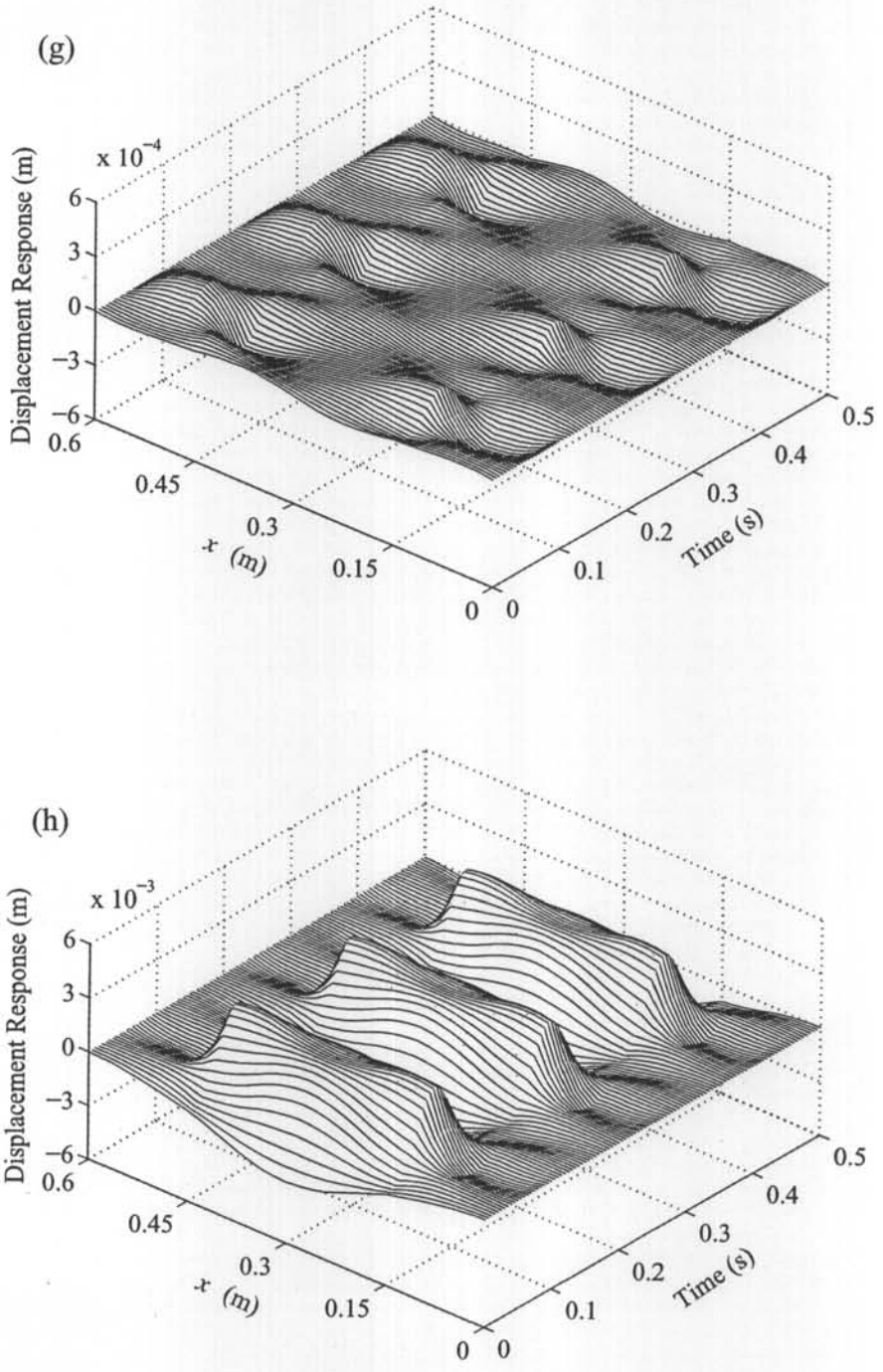

Figure 5.9 In-plane response at super-harmonic resonance (Cont'd):

(g) horizontal component at point S6;

(h) vertical component at point S6.

CHAPTER 6

PARAMETER ESTIMATION OF STRUCTURAL CABLES USING AMBIENT VIBRATION DATA: LOCAL OPTIMIZATION

6.1 INTRODUCTION

This chapter describes the parameter estimation of stay cables in the cable-stayed Dongting Lake Bridge, Hunan, P. R. China, based on ambient vibration tests, which provide dozens of natural frequencies for each cable before and after installation of magneto-rheological (MR) dampers. The parameters are estimated by means of the interior-reflective Newton method which is used to for a local optimization of the cost function value constructed with the errors between the measured and analytical natural frequencies by the nonlinear least-squares (NLS) method. The global optimization will be discussed in the next chapter.

The identification of cable tension is discussed in this chapter. Since cables are the most important structural members in cable-supported bridges, researchers and engineers have long explored the measurement and estimation of cable tension. Cable tensions may be obtained by using a ring load-cell, measuring the force in tension jack or the elongation of the cable during tensioning, carrying out topographic measurements, and installing strain gauges in the strands (Cunha et al. 2001). However, as discussed by Casas (1994), in spite the simplicity in theory, each of these methods is complex in its practical application and, in some cases, the level

of accuracy is insufficient. A relatively simple and inexpensive method to estimate cable tension is based on theory of cable dynamics, which was systematically investigated by Irvine (1981) and recently developed by other researches, such as Zui et al. (1996) and Mehrabi and Tabatabai (1998).

Generally, the natural frequency is used as input for cable tension evaluation. Structural cables employed in a cable-supported bridge may be of several hundreds; for example, more than two hundred stay cables are used in the Dongting Lake Bridge, Hunan, P. R. China. For a large number of cables employed in a cable-stayed bridge, it is not realistic to measure the cable modal shapes or using static tests for in-service cables. Fortunately, a large amount of the natural frequencies of the cables can be economically obtained with high accuracy by just monitoring one to two points of each cable. This may give the reason why extensive efforts (Takahashi et al. 1983; Kroneberger-Stanton and Hartsough 1992; Yen et al. 1997; Russell and Lardner 1998; Brownjohn et al. 1999; Smith and Johnson 1999; Wang et al. 1999; Cunha et al. 2001) have been made on measuring the cable tension of in-service cable-supported bridges and other cable structures by using vibration-based methods. However, most of these applications use only the vibration taut string theory which is not suitable for very long cables used in modern cable-supported bridges due to the effects of sag, flexural rigidity and end support conditions. Furthermore, most applications take the cable tension as the only unknown parameter in the estimation approaches, considering typically one natural frequency only. As mentioned by the author and coworkers (Zheng et al. 2001), the inaccuracy of other parameters, which is one kind of modeling error, may affect significantly the cable tension estimation. The accurate values of other parameters need to be known prior to the estimation employing only one frequency and the accuracy and reliability of this frequency

should be strictly defined. In recognizing the above facts, simultaneous estimation of the tension force and other cable parameters by using measured frequencies should be the direction to go.

For the parameter estimation of a structural cable, the number of unknowns is quite small whereas the frequencies available from tests are quite rich. That means the parameter estimation of a cable is overdetermined in some circumstances. In the present chapter, by using dozens of frequencies, several approaches are developed to identify the cable constitutive parameters, including the most concerned one, the cable tension. An important issue of this study is that the effects of weight and parameter selections in the estimation are revealed. Another issue of the present research lies in the investigation on error distribution, which is one important aspect in evaluating estimations besides the minimization in cost functions. The investigation in two kinds of intermediate cable supports, namely the deck-cable connection and the MR damper system, reveals that their effects on the cable parameter estimation are small.

6.2 IDENTIFICATION METHOD

The purpose of this section is to construct a nonlinear least squares (NLS) problem for the identification of cable parameters through frequency measurements. Firstly, the relationship between the model parameters and the analytical cable frequencies are implicitly constructed by an analytical model. Secondly, the cost function to be minimized is defined as the weighted sum of squared frequency errors. Before carrying out the identification, the values of parameters originally assigned to the model are adopted as initial guesses from which the parameters are modified iteratively to minimize the objective function.

6.2.1 ANALYTICAL MODEL

The proposed identification strategy is to develop an accurate model in which all important cable parameters are involved and updated simultaneously to achieve consistency between the analytical and measured natural frequencies for many modes. For this purpose, a precise finite element model, which account for cable flexural rigidity, sag-extensibility, spatial variability of dynamic tension, boundary conditions, lumped masses and intermediate springs and/or dampers, has been formulated in Chapter 3. and is used herein as reference model for parameter optimisation. This finite element model can be expressed as

$$\boldsymbol{M}\ddot{\boldsymbol{U}} + \boldsymbol{C}\dot{\boldsymbol{U}} + \boldsymbol{K}\boldsymbol{U} = \boldsymbol{F} \tag{6.1}$$

where $\boldsymbol{M}$, $\boldsymbol{C}$ and $\boldsymbol{K}$, are mass, damping and stiffness matrices of able, respectively; $\boldsymbol{U}$ and $\boldsymbol{F}$ are nodal displacement and external force vectors, respectively. The overdot denotes the derivative with respect to the time t. The matrices $\boldsymbol{M}$ and $\boldsymbol{K}$ are obtained from the finite element formulation and are implicit functions of cable parameters.

$$\boldsymbol{K} = \boldsymbol{K}(r_1, r_2, \ldots r_n) \tag{6.2a}$$

$$\boldsymbol{M} = \boldsymbol{M}(r_1, r_2, \ldots r_n) \tag{6.2b}$$

where $r_1, r_2, \ldots, r_n$ are the cable parameters. For the undamped free vibration, Equation (6.1) is reduced into an eigenvalue problem

$$\boldsymbol{K}\varphi_j = \lambda_j \boldsymbol{M}\varphi_j \tag{6.3}$$

where λ_j is the jth order eigenvalue and φ_j is the corresponding eigenvector. The circular frequency ω_j of the cable is obtained as

$$\omega_j = \sqrt{\lambda_j} \tag{6.4}$$

The natural frequency is obtained as

$$f_j = \omega_j / 2\pi \tag{6.5}$$

Equations (6.2) to (6.5) define an implicit relation between the natural frequencies and the cable parameters, i.e.,

$$f_j = f_j(H, EI, L_x, L_y, m, EA, GA, GJ, k) \tag{6.6}$$

where H, EI, L_x, Ly, m, EA, GA, GJ and k denote the horizontal component of cable tension, the flexural rigidity, the horizontal and vertical projections of cable length, the mass density per unit cable length, the tension rigidity, the shear rigidity, the torsional rigidity, and the stiffness of intermediate support/connection, respectively.

6.2.2 PARAMETER IDENTIFICATION

The parameter identification is defined as a nonlinear least-squares problem with the following cost function

$$J = \sum_{j=1}^{n} w_j (f_{FEM}^j - f_{MEAS}^j)^2 \tag{6.7}$$

where, f_{FEM}^j and f_{MEAS}^j are the analytical and measured natural frequencies of the jth mode; w_j is the weight factor of the error at jth mode, and n is the number of measured natural frequencies. Due to high flexibility of bridge cables, it is easy to measure several tens of natural frequencies for one cable from ambient vibration tests. All these measured natural frequencies are incorporated into Equation (6.7) for cable parameter identification. The analytical frequencies, f_{FEM}^j (j = 1, 2, ..., n), is obtained from Equation (6.6), which has encoded into a computer program to define the implicit relation between the frequency and the parameters. A precise analytical model is necessary here to accurately predict high-order modal frequencies for identification use. In this study, the NLS problem is solved by the function *lsqnonlin* in the optimization toolbox of *Matlab*®, which is used for iterative solution of the

nonlinear least-squares problem (6.7) by means of the interior-reflective Newton method (*MATLAB user's manual – version 6.0*, 2000). The convergence was defined when the change in the input (parameters) is less than a tolerance of 10^{-6}.

6.3 IMPLEMENTATION ISSUES

The implementation issues of the proposed identification strategy are explored in detail by taking the Dongting Lake Bridge as an example. The Dongting Lake Bridge is a three-tower cable-stayed bridge with two main spans of 310 m each. The bridge locates at the influx of the Dongting Lake into the Yangtze River, where the ten-minute-averaged mean wind speed of 30-year return period is 29 m/s and the maximum mean wind speed recorded is 28 m/s. Since its open to traffic in the end of 2000, the bridge has experienced severe wind-rain-induced vibration (strong oscillations under low wind speed and moderate rain) several times. The frequent occurrence of the wind-rain-induced oscillation has worried of the owner. At present, a project on full implementation of semi-active magneto-rheological (MR) dampers to totally about 200 stay cables in the bridge for wind-rain-induced vibration control is in progress (Ko et al. 2002). Working towards this objective, a series of in-situ vibration experiments have been carried out for several typical cables to understand actual dynamic performance of the cables before and after using MR dampers. In the following, the ambient vibration measurement results of a 115 m-long stay cable (denoted as A11-N) with and without MR dampers and the corresponding cable tension and parameter identification results by using the proposed method are described.

6.3.1 AMBIENT VIBRATION MEASUREMENT

Ambient vibration response of cable A11-N was measured by four accelerometers, two being deployed at 3.9 m away from the cable-deck connection point respectively for in-plane and out-of-plane response measurement; and the other two being deployed at 5.1 m away from the cable-deck connection point respectively for in-plane and out-of-plane response measurement. The measurement data in January and February 2001 are reported here. A notebook-PC-based data acquisition system was used in the field and the ambient vibration response of the cable was recorded more than one hour for each measurement. Signals from accelerometers were filtered through an anti-aliasing filter with a truncating frequency of 100 Hz and recorded at a sampling frequency of 500 Hz. Oscillations monitored during these tests were excited by ambient wind and traffic flows and thus included a wide range of frequencies rather than just several lower frequencies.

The field test data are analyzed to investigate the cable modal properties. A typical time history of the acceleration at the monitoring points is shown in **Figure 6.1**. The power spectra of the acceleration response are obtained by using FFT with a Hanning window to mitigate the power leakage. Two typical plots of the power spectral density functions of the acceleration response are shown in **Figure 6.2**. The natural frequencies are obtained by picking up the frequencies corresponding to the peaks in the response power spectra. It is obvious in **Figure 6.2** that the power spectra are capable of providing the cable natural frequencies except for those modes in the vicinity of their nodes the monitoring accelerometers located; i.e. for those frequencies near 35 Hz or 85 Hz in **Figure 6.2(a)** and frequencies near 25 Hz, 60 Hz, or 100 Hz in **Figure 6.2(b)**. Nevertheless, with the power spectra from two different locations all the natural frequencies from DC to 100 Hz of the vibration modes can

be obtained. Two characteristics of the cable dynamic property are observed: *i*) the cable exhibits an extremely high flexibility, i.e. at least the first 60-80 order vibration modes with a frequency range of 100 Hz are excited under ambient excitation from low wind speed and light traffic flows; *ii*) the modal damping ratios are found extremely low, as indicated by Ko et al. (2002).

Table 6.1 Design parameters of cable A11-N

H (kN)	EI (N·m^2)	L_x (m)	L_y (m)	m (kg/m)	EA (Pa·m^2)	GA (Pa·m^2)	GJ (N·m)
2474	9.36e+5	91.691	68.944	51.8	1.54e+9	5.76e+9	7.04

The natural frequencies of the first 66 in-plane modes and the first 66 out-of-plane modes were measured for cable A11-N from the ambient vibration measurements in January 2001 (Subset 1) and in February 2002 (Subset 2). In order to compare the measured and analytical natural frequencies, a precise three-dimensional finite element model has been developed for cable A11-N with model parameters listed in Table 6.1. The measured and analytical natural frequencies of the cable are shown in **Figure 6.3**, in which the two subtests measurement results are denoted by circle and cross, respectively, and found in good coincidence with each other. That means the ambient vibration tests provided a consistent measurement of the frequency considering the second subtest was carried out more than one month later. It is noted in **Figure 6.3** that the discrepancy between the analytical results from the taut string theory and the measurements increases when the frequency order becomes higher. This discrepancy is up to 30% for the highest several frequencies and is unacceptable from an engineering viewpoint. Therefore, it is concluded that the taut string theory are not suitable for dynamic analysis of cables like the one we investigated when the higher order frequencies need to be considered. The case for the analytical results from the FE model formulated in Chapter 3 is much better

compared to the taut string theory, as the discrepancy between the analytical results and the measurements is almost indistinguishable.

However, errors with a clear trend are still observed through figuring the absolute and relative errors of the measured and analytical frequencies are shown in **Figures 6.4** and **6.5**, respectively. The trend in the absolute and relative errors in these two figures reveal that there are some modeling errors, characterized by the smooth curves in **Figures 6.4** and **6.5**, in the FE model of the cable. The sections hereafter give detailed discussions on the updating of the FE model and the effectiveness of such updating in minimizing the errors between measured and calculated frequencies.

6.3.2 SINGLE-PARAMETER-ESTIMATION

For the purpose of comparison, the single-parameter identification is first performed. In this case only one cable parameter is taken as the unknown to be updated while other parameters are kept unvaried in their design values. Before carrying out the optimization approach, the sensitive and insensitive parameters with respect to the frequencies need to be distinguished. **Figures 6.6(a)** and **6.6(b)** show the sensitivity of the cost function with respect to individual parameters with the weight taking as unit and $1/(f_{FEM}^{j})^2$, respectively. It is observed in **Figure 6.6** the cost functions are much more sensitive with regard to four parameters, i.e., the cable tension H, the cable flexural rigidity EI, the cable length L, and the cable mass density per unit length m than other cable parameters, such as tensional rigidity EA.

Each of the four most sensitive parameters is then corrected with three single-parameter-estimation (SPE) approaches. In the first two approaches, the parameter value takes the one corresponding to a local minimum on the cost function values, as shown in **Figure 6.6(a)** and **6.6(b)**. The third approach is to use one single measured

frequency to give one estimation value of one parameter; i.e. the total 66 natural frequencies will give 66 estimations for each parameter. The changes of the parameters between the design and the estimated values from the first two approaches are shown in Table 6.2 and the statistical properties of parameter changes from the third approach are shown in Table 6.3. It is observed in Tables 6.2 and 6.3 that with different approaches the estimation results are quite different. The large standard deviation in Table 6.3 reveals that the differences within the results of the third approach are great. It is seen that all the errors trends shown in **Figure 6.7** are similar to those given in **Figures 6.4** and **6.5**. This indicates again the conventional one-parameter strategy is unable to produce accurate identification results.

Table 6.2 Parameter change by using single parameter correction (in percentage)

parameter	$\Delta H/H$	$\Delta EI/EI$	$\Delta L_x/L_x$	$\Delta m/m$
$w_i = 1$	-0.606	-3.321	0.337	0.769
$w_i = 1/f_i^2$	3.28	0.207	0.659	2.003

Table 6.3 Statistical properties of parameter changes by using single frequency estimation (in perentage)

parameter	$\Delta H/H$	$\Delta EI/EI$	$\Delta L_x/L_x$	$\Delta m/m$
mean	2.04	-0.487	-1.00	-2.02
standard deviation	3.73	1.336	1.24	2.79

How much does the above correction in a single parameter minimize the errors between the analytical and measured frequencies? The answer can be obtained from **Figure 6.7**, in which '$w_i = 1$' and '$w_i = 1/f_i^2$' correspond to the parameters taking the values in the second and third rows, respectively, and; 'mean' corresponds to the parameters taking the values in the second row of Table 6.3. The errors shown in **Figure 6.7** are the results after the cable parameters have been updated with the above three approaches. **Figures 6.7(a)**, **6.7(c)**, **6.7(e)**, and **6.7(g)** show the errors,

whereas **Figures 6.7(b), 6.7(d), 6.7(f),** and **6.7(h)** show the corresponding relative errors between the measured and calculated frequencies.

Informative and interesting observations are made from **Figure 6.7**: (i) Effects of using different approaches are similar in minimizing errors, i.e., no approach is found prevalent than others; (ii) Effects of updating different parameters are also similar in minimizing errors, i.e., no parameter is found dominant in model updating; (iii) Differences exist in the trends of the relative errors by correcting different parameters. Detailed description of the third observation is as follows. For L_x and m, as shown in **Figures 6.7(f))** and **6.7(h)**, respectively, the correction in these parameters with different approaches just results in a 'shift' in the relative errors. However, for EI, different approaches result in a 'rotation' of the relative errors, i.e., at some frequency order the relative errors seems 'unchanged' whereas the higher the mode order the greater the errors. Both the 'shift' and the 'rotation' phenomenon are observed in **Figure 6.7(b)** for the cable tension H. It is inferred from these observations that the convenient one-parameter strategy is unable to produce accurate identification results by minimizing the errors and the remedy may be a combined correction in parameters, i.e., updating multiple parameters simultaneously, as described below.

6.3.3 MULTIPLE-PARAMETER-ESTIMATION

In this case, the four most sensitive cable parameters are taken as unknown and updated simultaneously by use of the proposed multiple-parameter identification strategy. All 66 measured natural frequencies are utilized. Table 6.4 shows the identification results. It is found that the estimation of EI and m are not so sensitive as those of H and L to the weight factor. The differences between the results by using the two weight factors are 2.8% for H and 1.0% for L.

Table 6.4 Change ratio of optimized value to the design value (in percentage)

parameter	$\Delta H/H$	$\Delta EI/EI$	$\Delta L_x/L_x$	$\Delta m/m$
$w_i = 1$	7.4553	-10.5276	1.3859	-2.3320
$w_i = 1/f_i^2$	4.6195	-12.2435	0.4345	-2.3136

The results of the multiple-parameter identification strategy are compared with those of the single-parameter identification strategy. **Figure 6.8** shows the frequency errors between the measurement and the FE calculation with cable parameters resulting from the single-parameter and multiple-parameter identification strategies. It is evident from **Figure 6.8** that the optimized parameters provide an excellent agreement between the measured and computed natural frequencies for all 66 modes and yield a nearly constant error trend which implies a high confidence and reliability of identification results. The accurate and reliable values of the parameters are important in modeling the cable in further dynamic analysis, such as for research in cable vibration mitigation using MR dampers.

6.3.4 CABLE TENSION ESTIMATION

Based on a study (Zheng et al. 2001) of the influence of uncertainty in structural parameters on cable tension estimation, it has been concluded that the single-frequency approach could obtain cable tension evaluation with identical accuracy as from the multiple-frequency approach only when there is no error for other structural parameters and measurement error is small. This conclusion is experimentally verified here. Taking the previously optimized parameters except for H as 'real' structural parameters, the cable tension is identified again by using each single frequency. **Figure 6.9** illustrates the identification errors in this case and their comparison with those using design parameters. As expected, when 'real' structural parameters are adopted, the single-frequency strategy can achieve accurate tension

estimation. It is found that the result from the optimized parameters is much better than that from the design values. The former is scattered within a range of less than 3% errors compared to the initial value whereas the latter shows a clear trend in variation and covers a wide range of about 14% errors to the design one.

This implies that a good estimation in one of the cable parameters, such as the tension, can be made only when other parameters are accurately defined. However, this is not the case in practice. Therefore, the method presented in the previous section may serve as a practical and reliable approach for simultaneously identifying multiple cable parameters, including the cable tension.

6.3.5 EFFECTS OF INTERMEDIATE SUPPORTS

The cable under investigation has an attachment with the deck edge when it stretches to lower anchor and was installed with two MR dampers at a same height through a 2.5 m-high supporting pole (Ko et al. 2002). Additional stiffness stemming from these two kinds of attachments was not considered in the previous section and is addressed in this section.

6.3.5.1 Deck-cable connection

The deck-cable connection is idealized as an equivalent spring connecting the cable and the deck in the FE model. The stiffness k of the equivalent spring and the four cable parameters are then identified with the MPE approach and the results are shown in Table 6.5. The differences between the identification results of cable parameters using different weights are all less than 1.5%, better than those listed in Table 6.4. The difference of the equivalent stiffness k is less than 2% between the results from two weights. This observation further confirms the robustness of the estimation with respect to the weight in the cost function.

Table 6.5 Change ratio of optimized value to the design value (in percentage, except for k)

parameter	$\Delta H/H$	$\Delta EI/EI$	$\Delta L_x/L_x$	$\Delta m/m$	k (kN/m)
weight: $w_i = 1$	5.61	-7.00	1.28	-0.9	9764
weight: $w_i = 1/f_i^2$	4.59	-8.33	1.03	-1.38	9584

A comparison between the frequency errors resulting from the estimation approaches with and without considering the deck-cable connection stiffness is shown in **Figure 6.10**. It is noticed in **Figure 6.10** that accounting for the deck-cable connection does not reduce the frequency errors much but improve the distribution of the errors. The histogram of the frequency errors is shown in **Figure 6.11**, which shows characteristics of a normal distribution with the mean and standard deviation taking 1.5×10^{-7}, nearly nothing, and 0.054%, respectively.

The almost zero mean value, the small standard deviation and a normal distribution of relative errors provide a great confidence of the parameter estimation given in Table 6.5. Considering the uncertainty of cable parameters, the randomness of ambient excitation, the noise in measurements, the nonlinearity of cable vibration and the approximation of FE method, the normal distribution of the relative errors in the frequencies is reasonably interpreted with the central limit theorem as a result of all these factors, each of which slightly affect the frequencies. Thus, the parameters in Table 6.5 can be regarded as two sets of the best estimations of the cable parameters.

6.3.5.2 Intermediate dampers

To suppress the wind-rain-induced vibration, stay cables of many cable-supported bridges have been equipped with dampers. The dampers will add not only damping but stiffness also to the cable. Both the changes in damping and stiffness will result in the change of cable natural frequencies. However, as stated in Chapter 2,

the modal damping ratios are quite small even after damper installation on the cable. Therefore, the effect of the damping on the natural frequencies is ignored, i.e., the change in the frequency is assumed due to the equivalent spring stiffness of the damper. Following this assumption, the damper system, consisting of the damper and its support, is idealized as a spring connection between the cable and the fixed end of the support. The equivalent spring stiffness k_d of the damper system, the equivalent spring stiffness k of the deck-cable connection and the four cable parameters are then estimated with the MPE approach.

The results of the estimation are shown in Table 6.6. It is observed that the results from different weights vary less than 3%, confirming again its robustness to the weight in the cost function. An interesting observation in Table 6.6 is that the stiffness of the equivalent spring of the deck-cable connection is found to be zero, indicating the installation of the MR dampers has greatly weakened the deck-cable connection.

Table 6.6 Change ratio of optimized value to the design value (in percentage, except for k and k_d)

parameter	$\Delta H/H$	$\Delta EI/EI$	$\Delta L_x/L_x$	$\Delta m/m$	k (kN/m)	k_d (kN/m)
weight: $w_i = 1$	4.35	-5.01	1.02	-0.5	0	679
weight: $w_i = 1/f_i^2$	7.07	-7.74	1.50	-0.91	0	697

A comparison between the frequency errors resulting from the estimation approaches with and without considering k_d is shown in **Figure 6.12**. The histogram of the frequency relative errors is shown in **Figure 6.13**. It is observed in **Figure 6.12** that the consideration of the equivalent spring stiffness of the MR damper cannot make improvement much in minimizing the frequency relative errors. As shown in **Figure 6.13**, the distribution of the errors does not show a characteristic of normal distribution. All these imply that the simplification of the MR damper as a

spring may be not enough in modeling real damper behaviour. However, by comparing Tables 6.4, 6.5 and 6.6, it is found that the effects of the deck-cable connection and the intermediate damper are not significant in the estimation of cable parameters. Based on the histograms shown in **Figures 6.11** and **6.13**, it is noticed that simplifying the deck-cable connection as a spring is quite good whereas the same simplification is not so reasonable for the MR damper system. Detailed considerations are in need for modeling the dampers in further researches.

6.4 SUMMARY

By using field measurement data, the parameters of a stay cable in a real bridge are identified. The nonlinear least squares (NLS) problem is constructed by minimizing the weighted sum square of errors between the frequencies from measurements and finite element model. Both single- and multiple-parameter-estimation approaches are investigated to evaluate the effects of parameter and weight selections on the identification results. With respect to the cost function, the sensitivity of parameters is investigated and the insensitive ones are treated as constants in the estimation. The accuracy of cable tension estimation by using different methods is discussed. Based on the studies in this chapter, following conclusions are made: (i) one to two points monitoring in cable ambient vibration testes are sufficient for frequency measurements and dozens of frequency can be obtained from the tests; (ii) Single parameter updating cannot eliminate systematic errors between the measured and analytical frequencies. That means no prevalent approach or parameter is found in the single-parameter-estimation approach; (iii) The multiple-parameter-estimation approach significantly decreases the errors between the analytical and measured frequencies; (iv) The estimation of the tension, H, can be made only after other

parameters have been accurately evaluated; (v) For both the multiple parameter and single parameter cases, it is found that an accurate estimation is not sensitive to the weight of the cost function; (vi) Considering the effects of intermediate supports does not make a significant improvement in minimizing the frequency errors but enhances the confidence of the estimation.

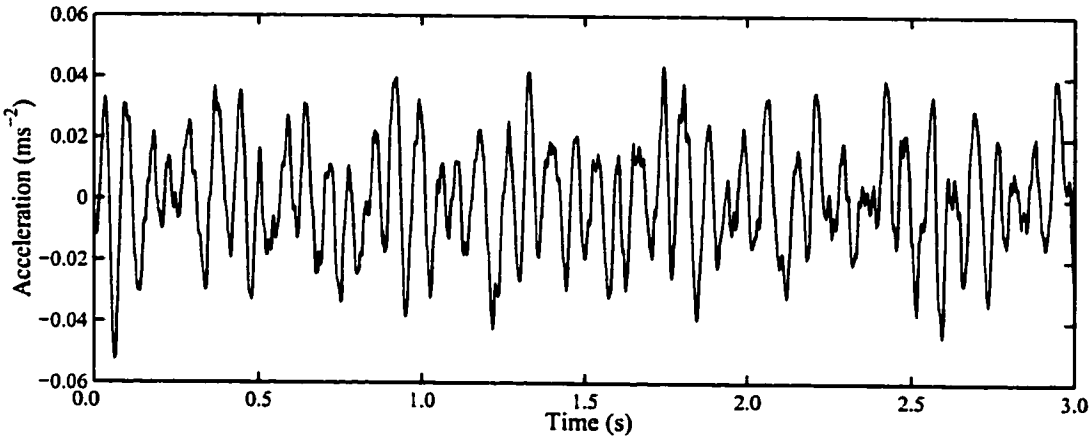

Figure 6.1 A typical time history of acceleration near the cable lower end.

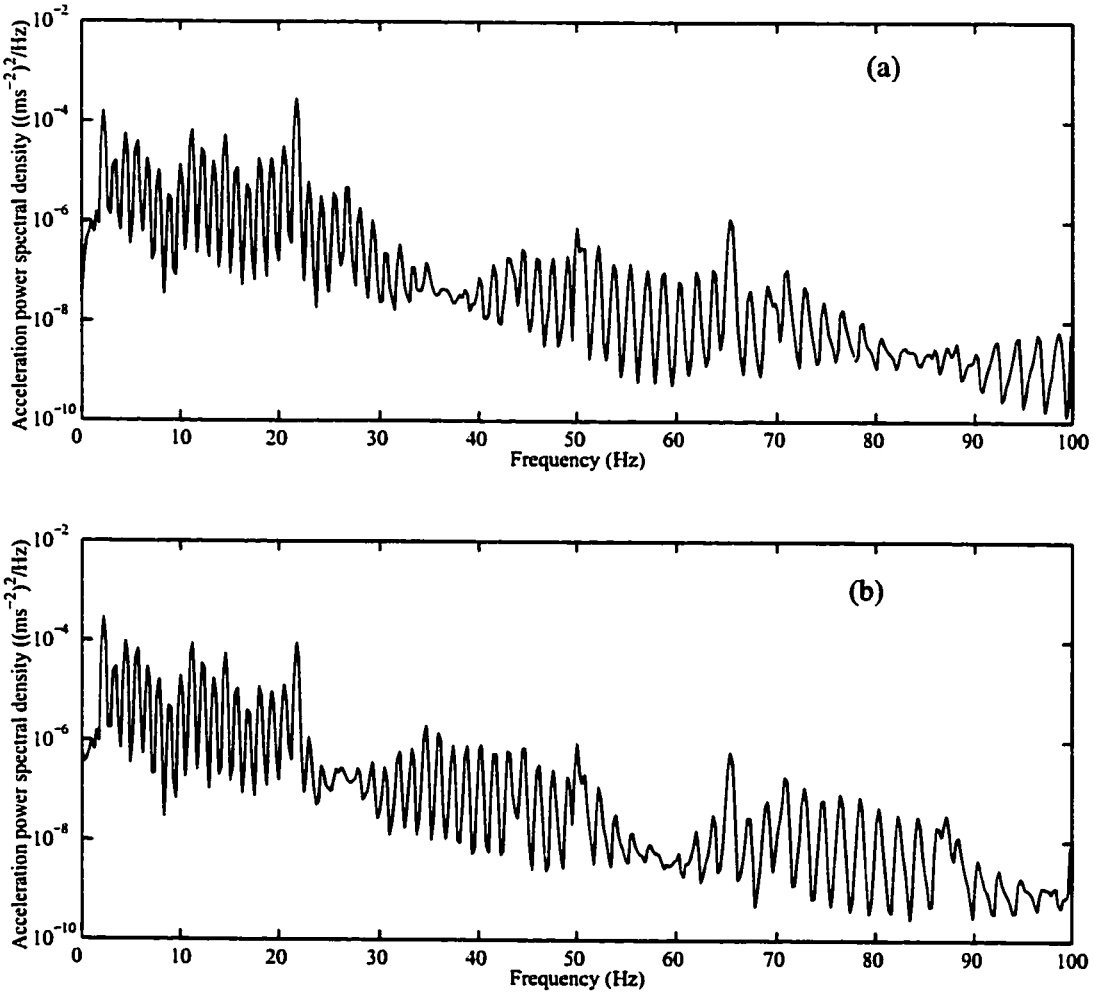

Figure 6.2 Response power spectra at different locations: (a) 3.9 m away from the deck level; (b) 5.1 m away from the deck level.

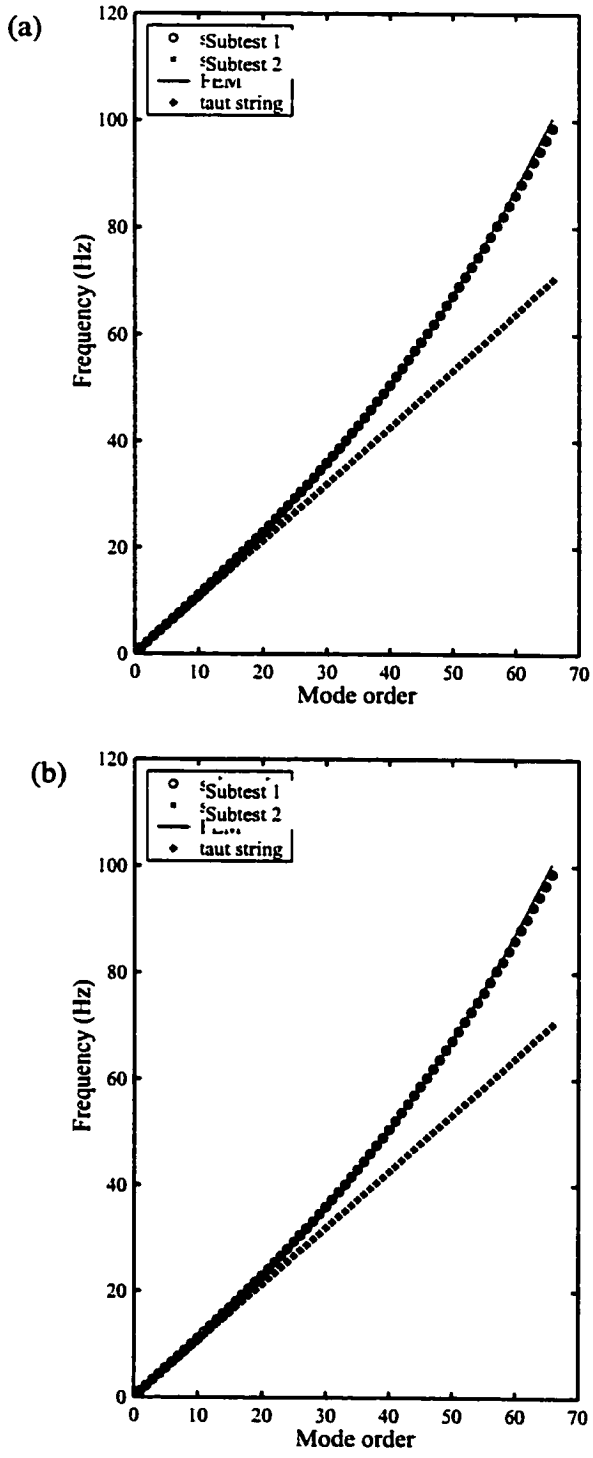

Figure 6.3 Natural frequencies of cable A11-N: (a) in-plane modes; (b) out-of-plane modes.

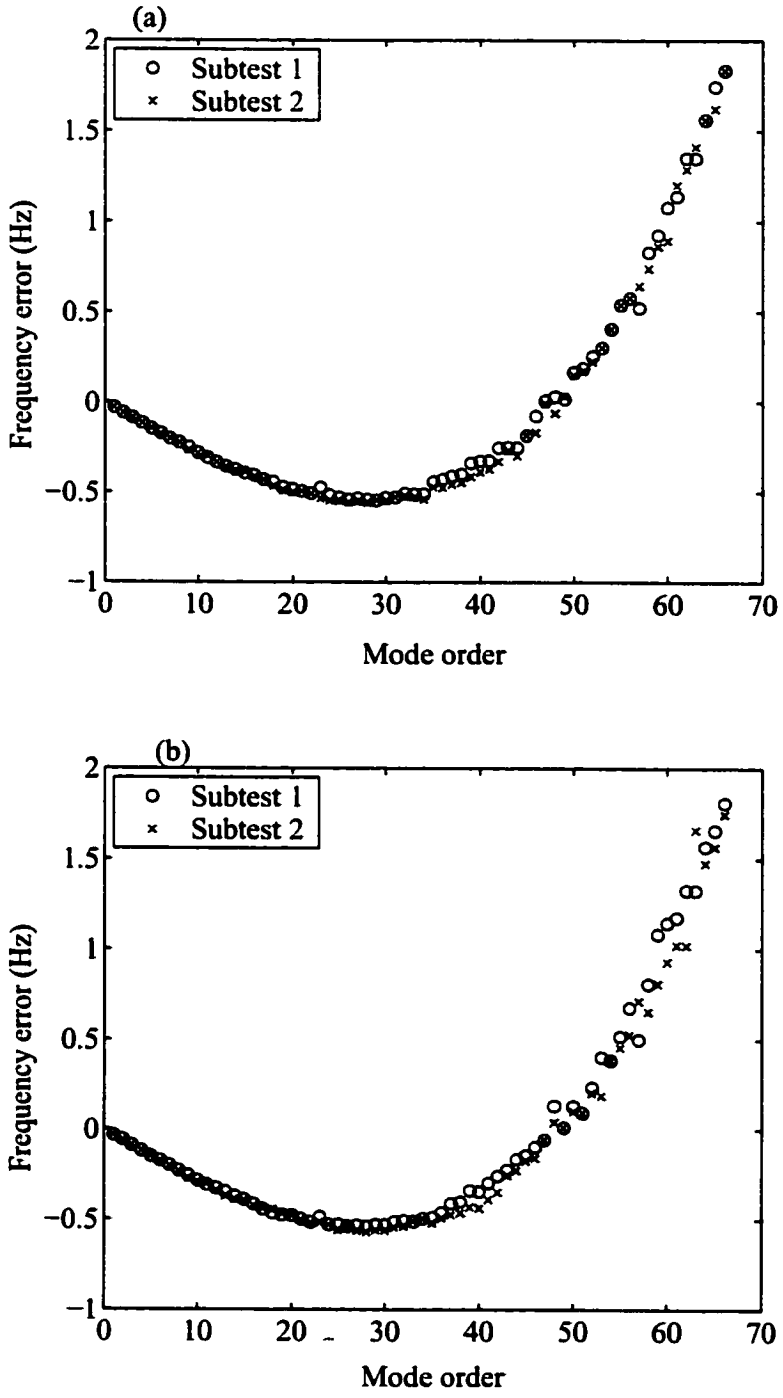

Figure 6.4 Modal frequency absolute errors between FEM and Test: (a) in-plane modes; (b) out-of-plane modes.

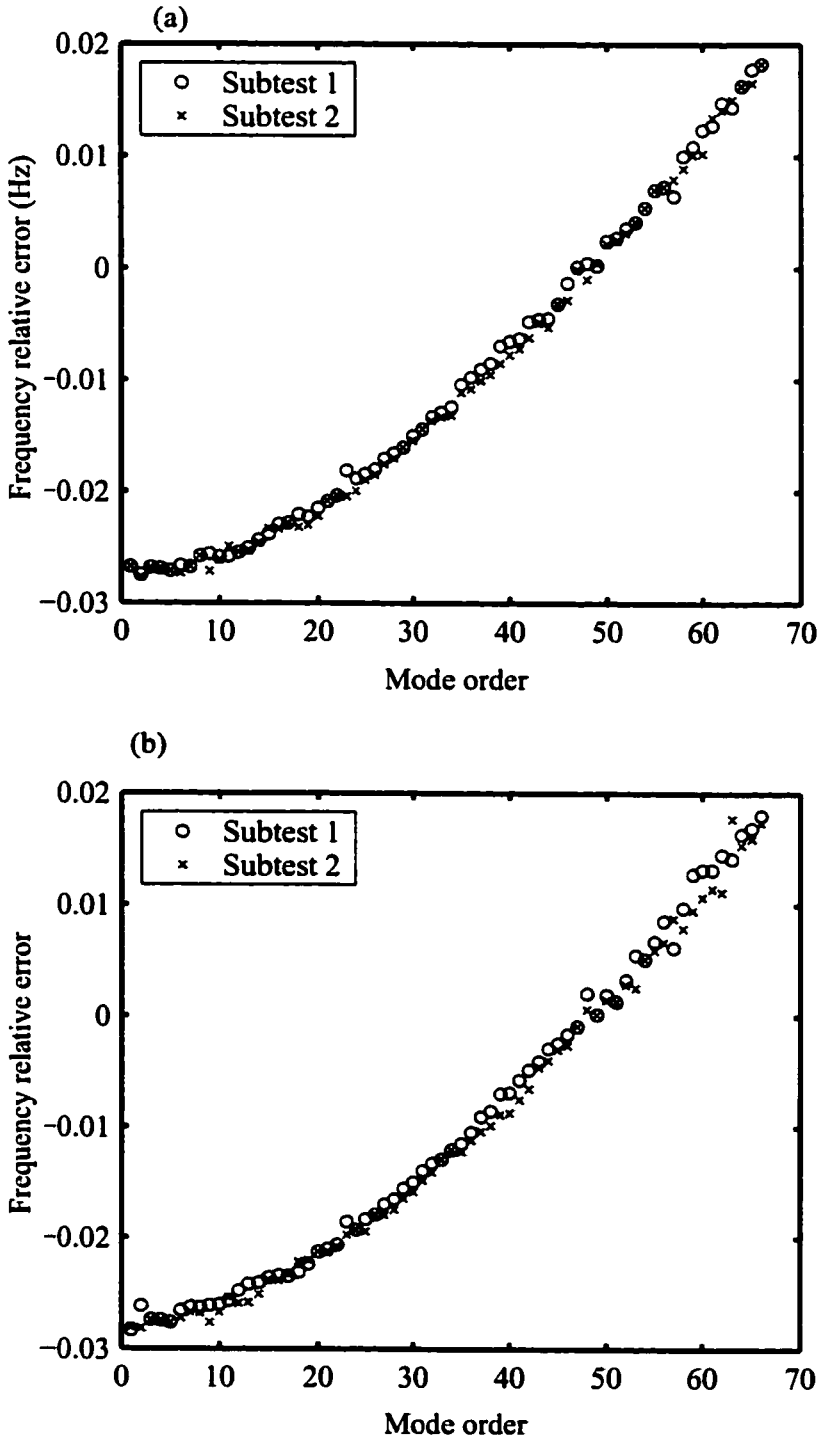

Figure 6.5 Modal frequency relative errors between FEM and Test: (a) in-plane modes; (b) out-of-plane modes.

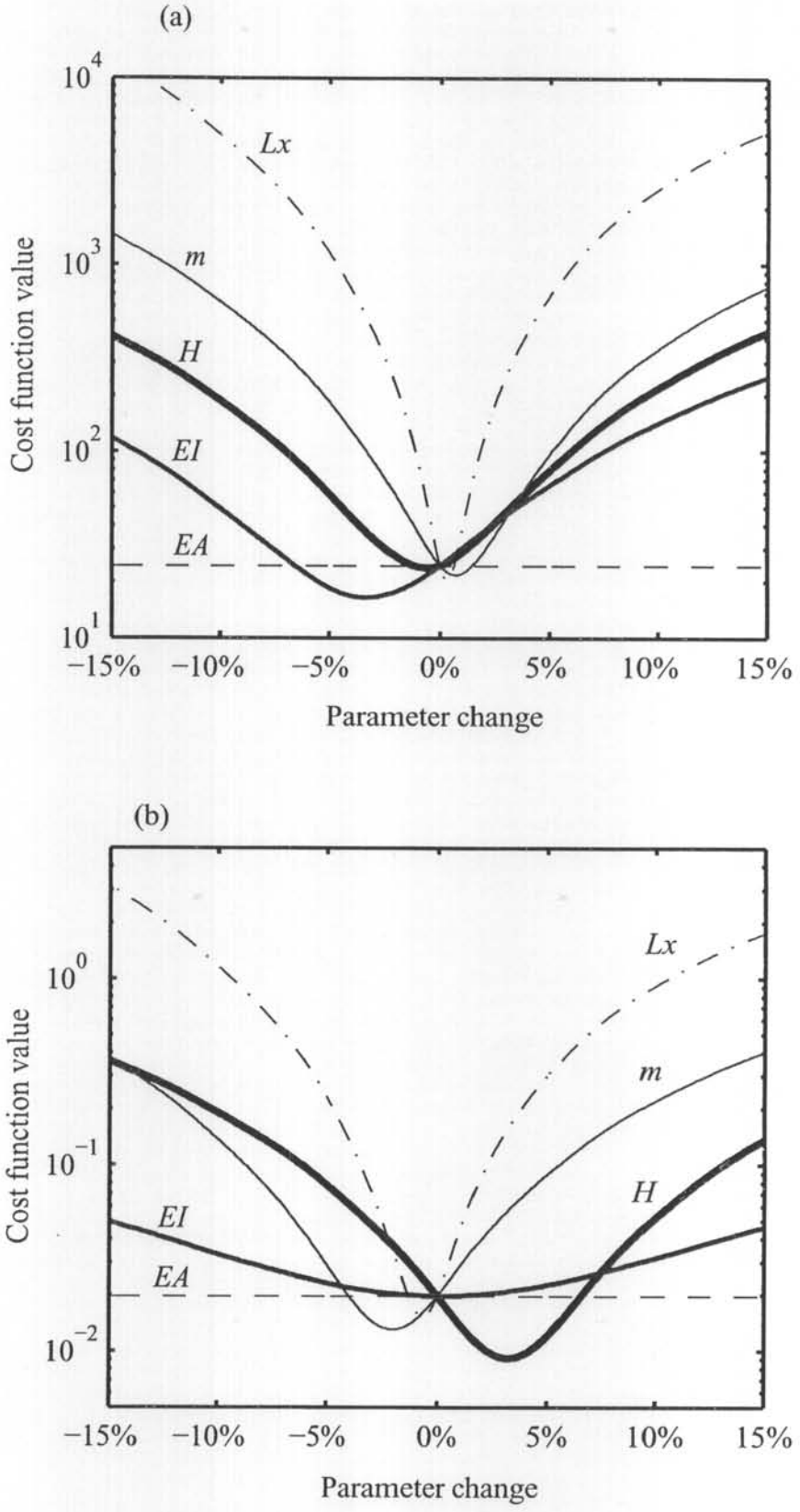

Figure 6.6 Cost function value versus cable parameters: (a) $w_i = 1$; (b) $w_i = 1/f_i^2$

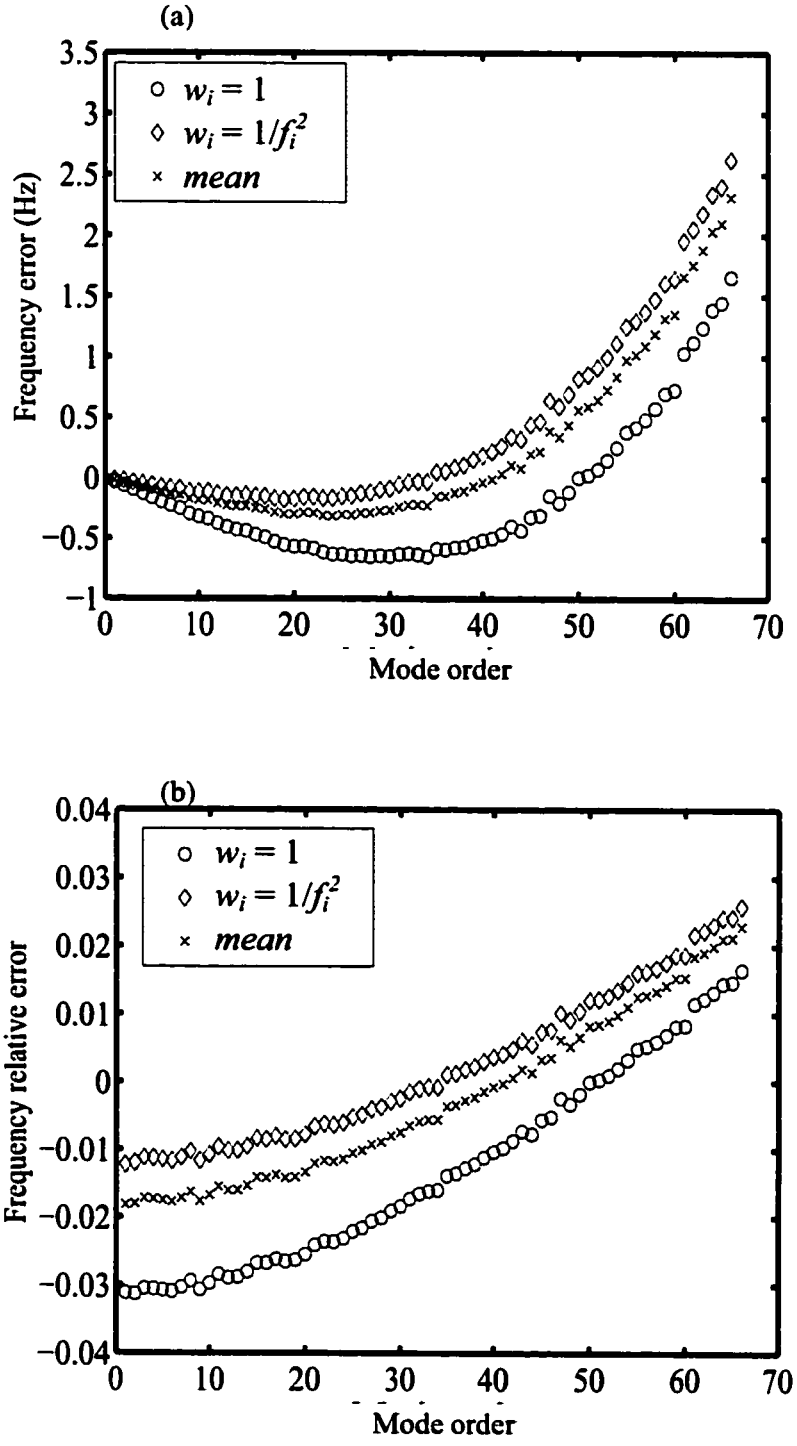

Figure 6.7 Frequency error between test and FEM results: (a) error with H updated; (b) relative error with H updated;

(c)

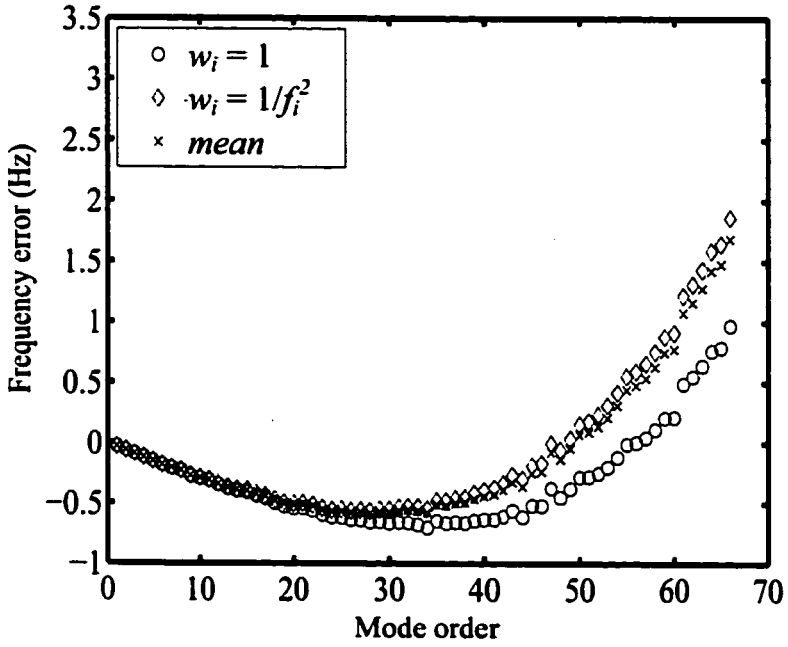

(d)

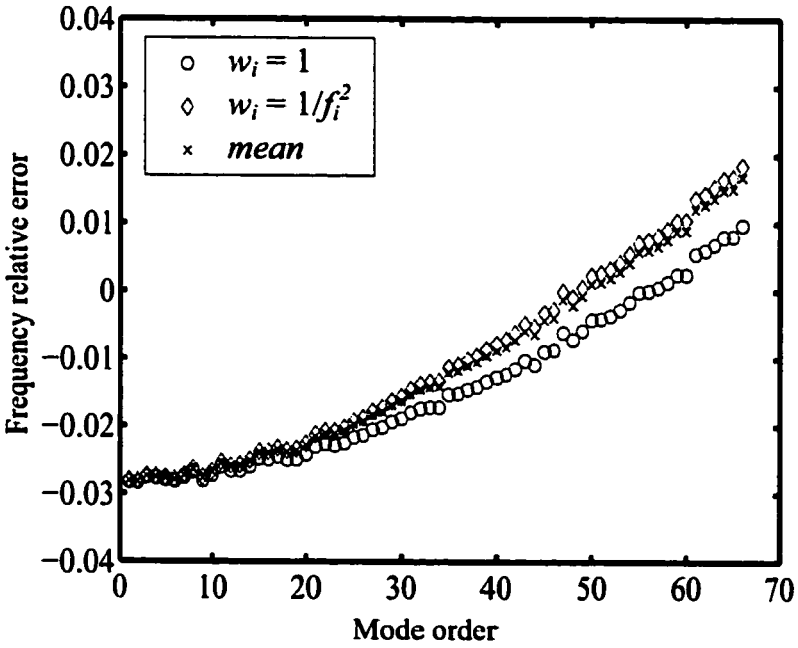

Figure 6.7 Frequency error between test and FEM results (Cont'd): (c) error with *EI* updated; (d) relative error with *EI* updated.

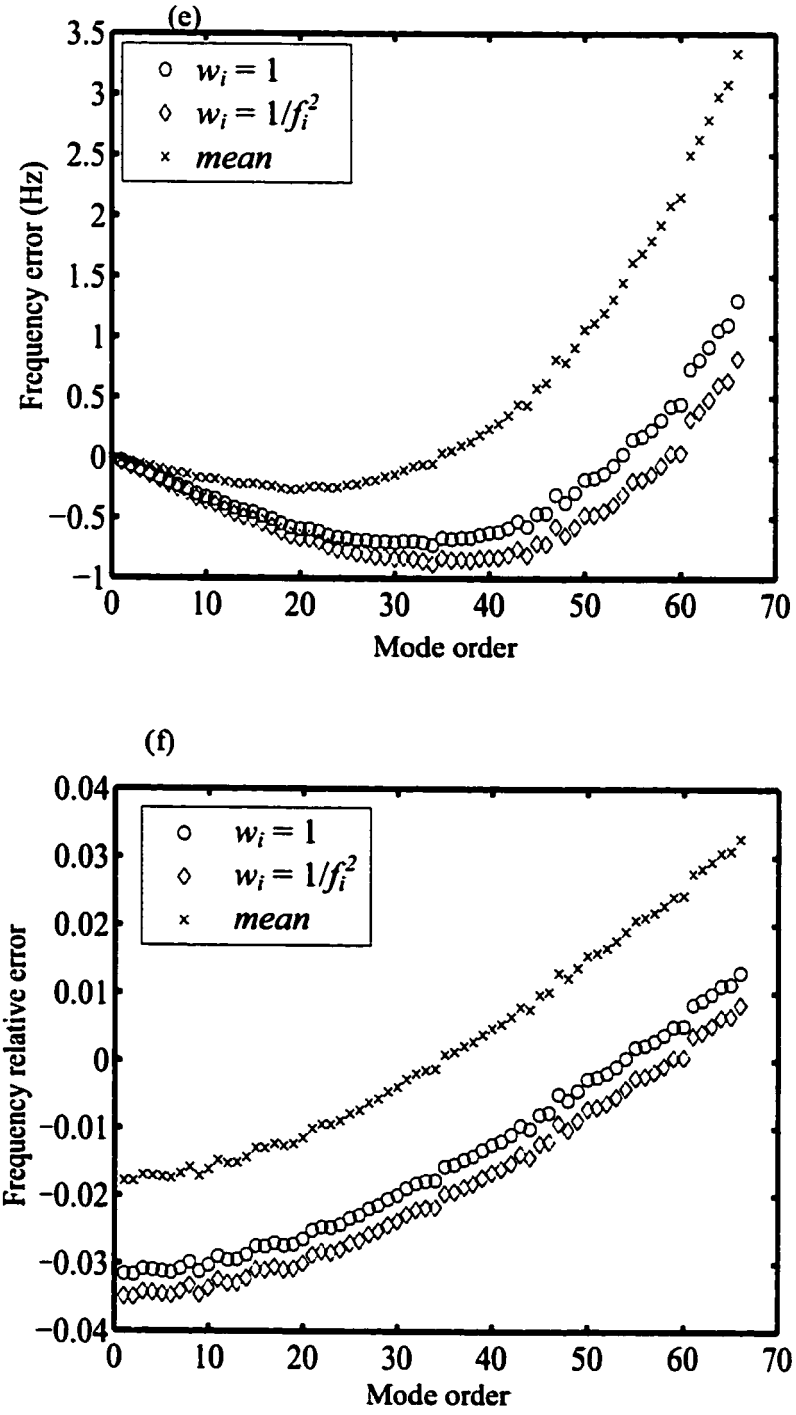

Figure 6.7 Frequency error between test and FEM results (Cont'd): (e) error with L_x updated; (f) relative error with L_x updated;

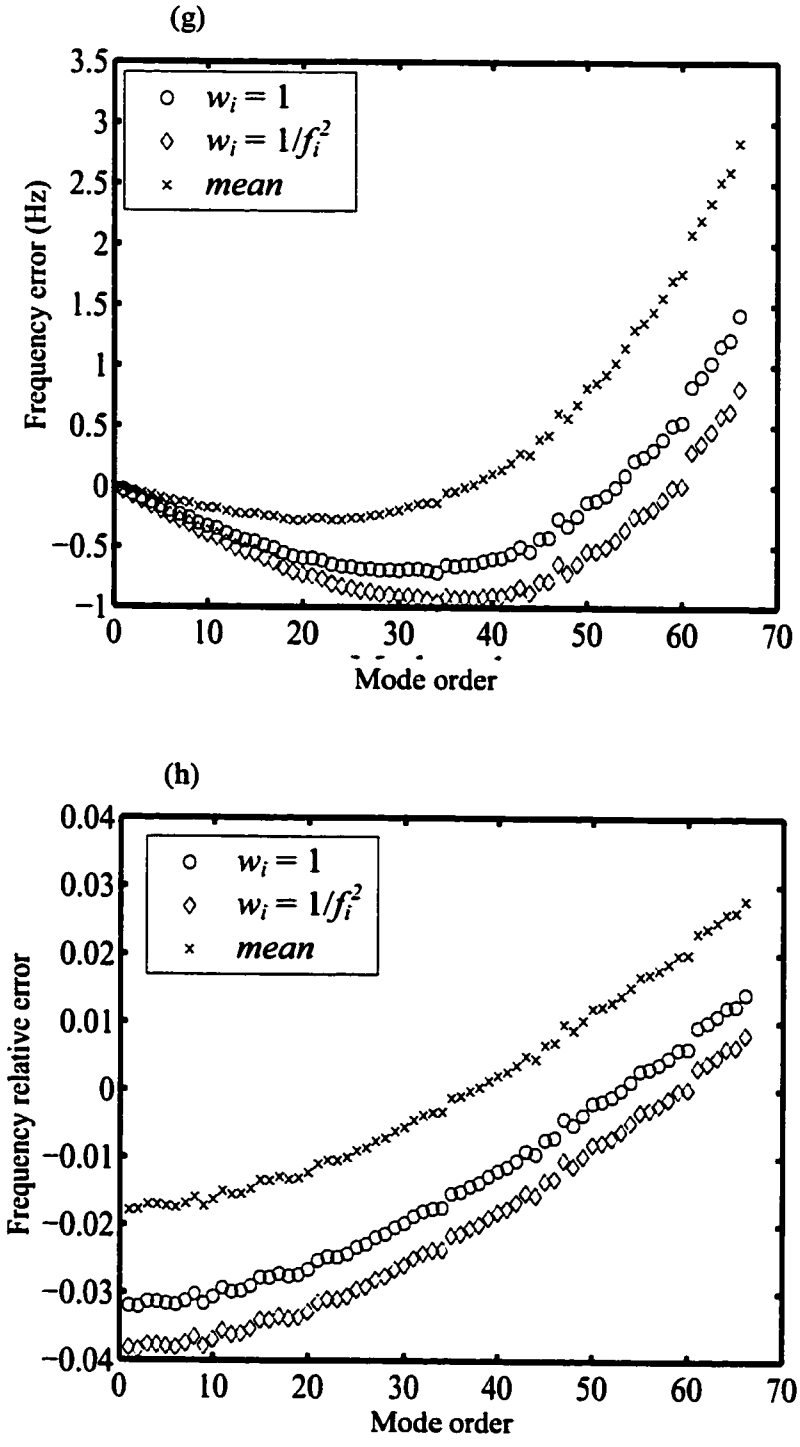

Figure 6.7 Frequency error between test and FEM results (Cont'd): (g) error with *m* updated; (h) relative error with *m* updated.

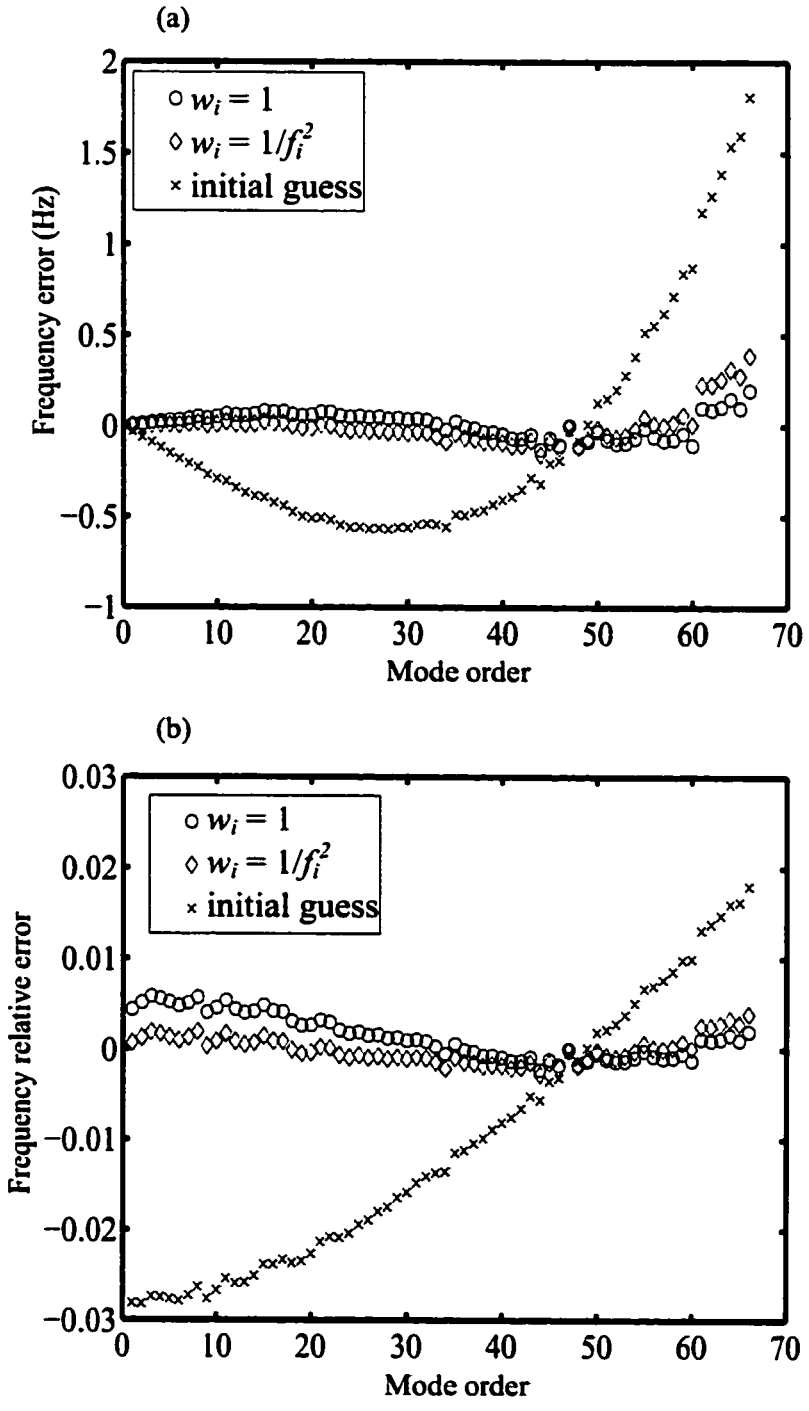

Figure 6.8 Frequency errors between measurement and FEM: (a) absolute errors; (b) relative errors

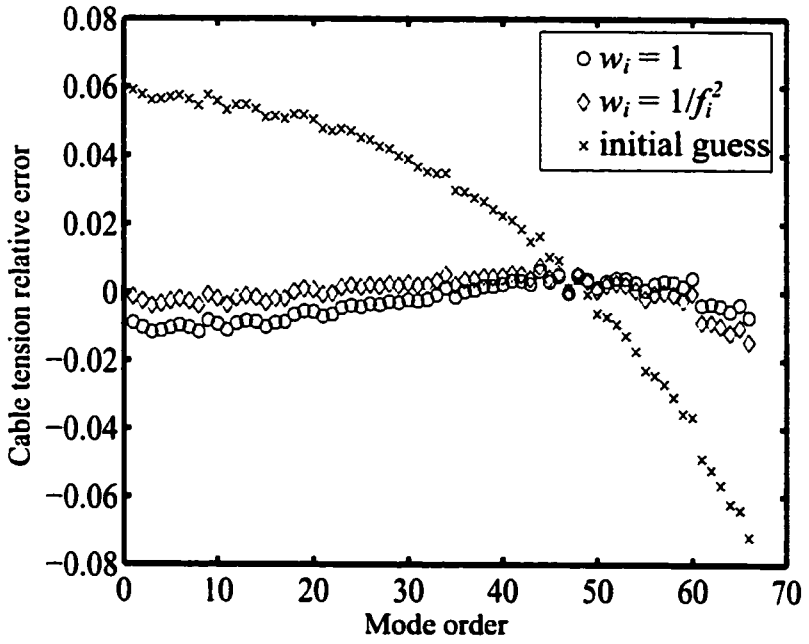

Figure 6.9 Cable tension estimation using single natural frequency with other parameters being fixed.

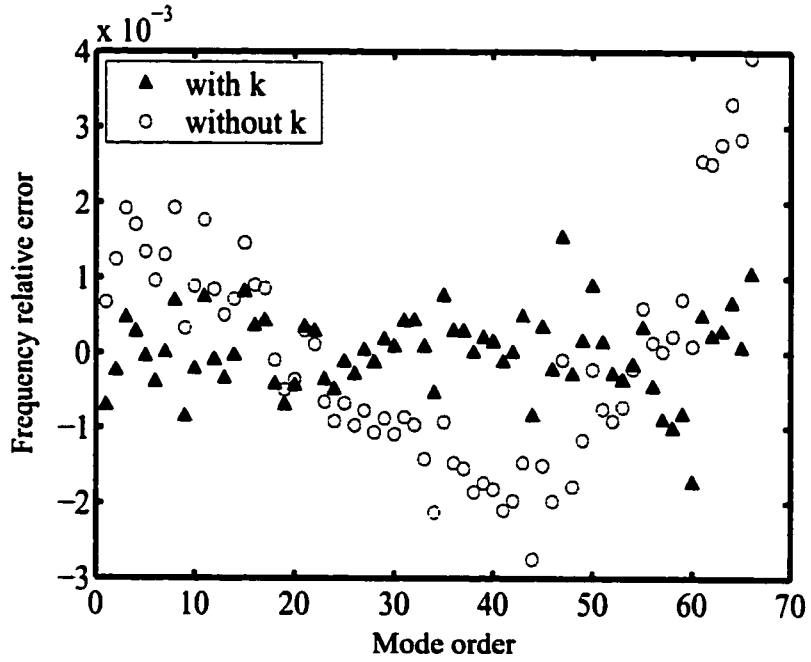

Figure 6.10 Frequency relative errors with and without considering deck-cable connection effect.

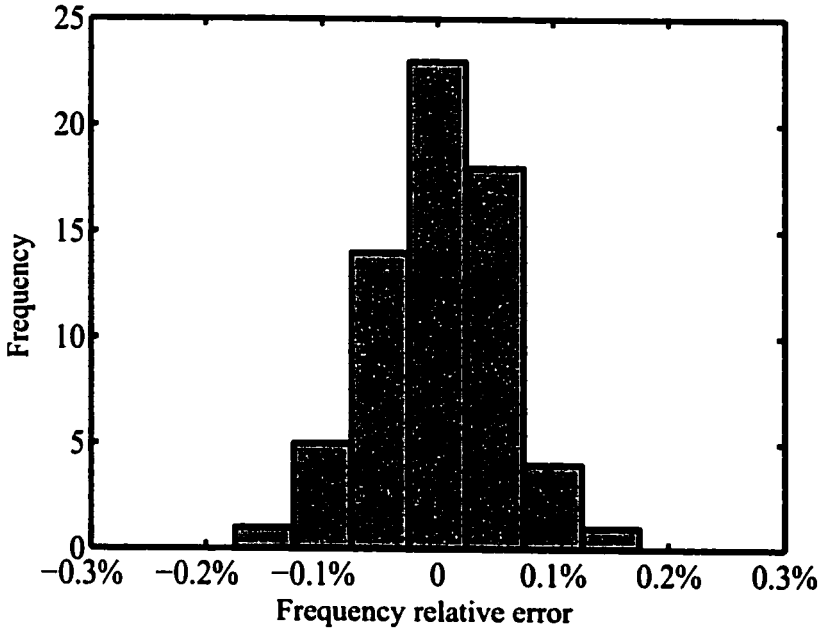

Figure 6.11 Histogram of the frequency relative errors.

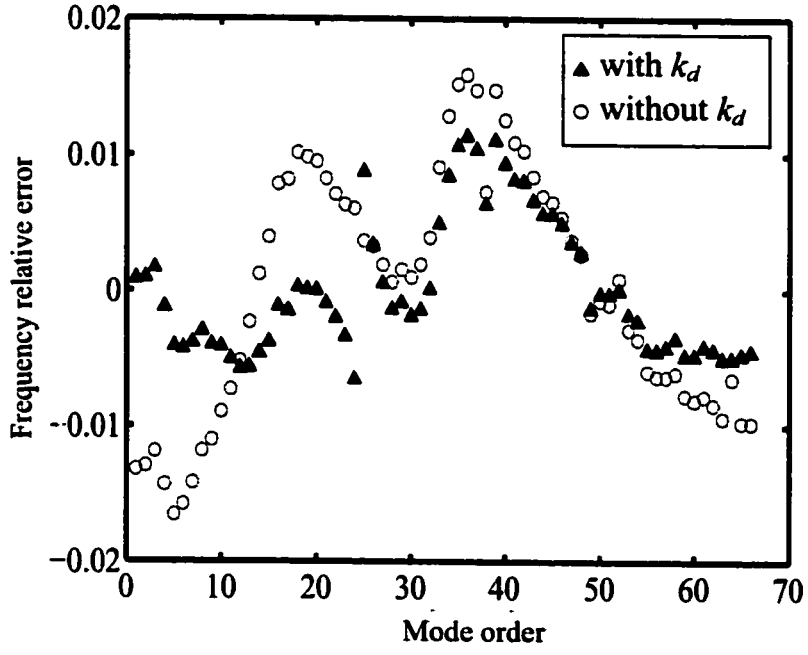

Figure 6.12 Frequency relative error with and without considering damper-cable connection effect.

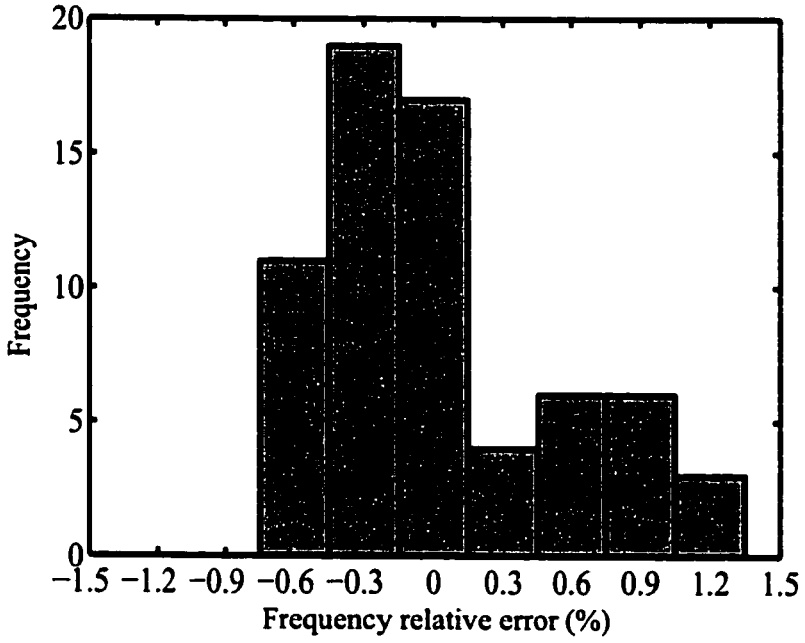

Figure 6.13 Histogram of the frequency relative errors.

CHAPTER 7

PARAMETER ESTIMATION OF STRUCTURAL CABLES USING AMBIENT VIBRATION DATA: GLOBAL OPTIMIZATION

7.1 GENERAL DESCRIPTION

This chapter focuses on the technical details of global identification of cable parameters in both simulation and real circumstances. The simulation studies are carried out for two purposes: firstly, to show the characteristics of the cost function surfaces under different noise levels and using different number of frequencies; and secondly, to obtain the statistical properties and relationships of cable parameters when uncertainty should be considered. In real circumstances three actual cables, i.e., a moderate long, 114 m, stay cable of the Dongting Lake Bridge, Changsha, P. R. China, an extremely long, 300 m, stay cable of the Ting Kau Bridge, Hong Kong, P. R. China, and an extremely heavy (with a large-diameter of 1.1 m) cable of the Tsing Ma Bridge, Hong Kong, P. R. China, are studied.

It should be noticed that the accuracy and reliability of identified cable parameters are hardly examinable directly as actually no 'real value' of the parameters are available. Nevertheless, the coincidence of the measured and

calculated frequencies using the optimal parameters may be taken as a good reference.

7.2 TECHNICAL DESCRIPTION

By using frequency measurements as inputs, the cable parameters are identified by using the exhaust search method and the genetic algorithm (GA) in the simulation. The results from both methods are compared to validate the GA in searching the global minimum for the specified problem. Then the GA is used in real circumstances. However, as the exhaust search is too time consuming, it is not adopted for the real cases.

The reason that we take modal frequencies rather than modal shapes or other measurements as inputs lies in two points: firstly, the modal frequencies can be obtained conveniently and, secondly, the measurement of frequencies is much more accurate than other parameters. The experiences from tests on real bridges shows that more than one hundred frequencies of a cable can be obtained in an ambient vibration test.

The cost function is defined by the sum of squared errors between the measured and calculated frequencies. As local minima may exist in the cost function, the genetic algorithm is selected for its potential in searching a global minimum. In the present study, the binary encoding with one-point crossover is used in the genetic algorithm. The population size is 10 and the number of generation is 50. The local minimum can be obtained by conventional methods, such as the interior-reflective Newton method.

A two-parameter case study reveals that multiple solutions exist when the number of measured frequencies is not enough to define a unique solution even without noise. The importance of uniqueness of the solution to the estimation of structural parameters has been recognized early (Udwadia and Sharma 1978) and was recently stressed by Hejemstad (1996). Non-uniqueness solutions may take barrier in searching a real solution for parameter identification problems.

The parameters of the three real cables are identified with the proposed method and the distribution of the error/noise in the frequencies is also revealed. The proposed method may serve as a general approach for cable tension estimation based on frequency measurements.

7.2.1 GENETIC ALGORITHM

As mentioned in Chapter 2, the genetic algorithm is one type of natural method for global optimization. It consists a subset of evolutionary algorithms modeling biological processes to optimize highly complex cost functions. The genetic algorithm can be concisely described as followings.

The mechanisms that link a genetic algorithm to the problem it is solving are encoding and function evaluation. Encoding is to encode solutions of the problem on chromosomes. Function evaluation is to return a measurement of the worth of any chromosome in the context of the problem.

Many techniques for encoding solutions have been invented by researches. Among them are the bit string encoding, the real number representation and the order-based representation. The selection of a technique depends on the problem to be solved and the genetic algorithm to be used. A certain amount of art is involved in such a selection and, basically, no one technique works best for all problems.

The function evaluation takes a chromosome as input and returns a number that is a measure of the chromosome's performance on the problem to be solved. The number returned from the function evaluation provides a measure of fitness that the genetic algorithm uses when selecting parents and carrying out reproduction.

A genetic algorithm mainly contains following steps (Davis 1991):

1. Initialize a population of chromosomes;
2. Evaluate each chromosome in the population;
3. Create new chromosome in the population.
4. Delete members of the population to make room for the new chromosomes;
5. Evaluate the new chromosomes and insert them into the population;
6. If time is up, stop and return the best chromosome; if not, go to 3.

Following this process of simulated evolution, an initial population of chromosomes will improve as parents are replaced by better and better children. The best individual in the final population produced can be a highly-evolved solution, which will be a good approximation of the real solution, or probably be rightly the real solution, to the problem.

7.3 NUMERICAL SIMULATION

At least two problems may arise when discussing the solution of an identification problem. Firstly, does a unique solution exist? Secondly, if a unique solution exists, is it the real solution of the problem? These two problems are studied in this section under different conditions. The effect of the number of modal

frequencies and the effect of different noise levels in the frequency measurements are investigated. In the two-parameter experiments, the global minimum is obtained on a discretized mesh, which allows exhausting search within endurable computational time.

7.3.1 SOLUTION UNIQUENESS

Cable A11-N of the Dongting Lake Bridge is used as an example to investigate uniqueness of the solution and distribution of multiple solutions, the contours of the cost function are obtained under different noise levels and using different number of frequencies, as shown in **Figures 7.1** to **7.4**, in which the triangle indicates the global minimum. The cable parameters concerned are the tension H and the flexural rigidity EI. The values of the two parameters are assumed to be within a range around the design ones, i.e, $H_0(1\pm16\%)$ for H and $EI_0(0.68\pm16\%)$ for EI, where H_0 and EI_0 are the design values of H and EI, respectively. Both parameters are assumed to take only discretized values on a 32×32 mesh of the specified region.

7.3.1.1 Noise-free measurements

The results of investigation on five selections of the number of frequencies of the in-plane modes measured are shown in **Figure 7.1**, in which the evolution of the multiple solutions to a unique one is clearly revealed. When the number of the measured frequencies varies from two to ten, the location of the minima of the cost functions on the H-EI plane almost does not change. A further increase in the number of the frequencies greatly changes the location of the minima. In the twenty frequencies case, all the three local minima are located within 10% from the EI_0 and 0.7% from the H_0. It is noticed that the case with the most frequencies (fifty frequencies) give a unique solution, and that it is the only one does so. Generally, the

more measurement frequencies provided the narrower the multiple solutions emerged, so that it is always better to have more frequencies measured.

Although multiple local minima exist on the discretized mesh, the global minimum is always the real solution, which is the only one gives a zero objective value. These results suggest that while it is possible to identify the correct solution using an enough number of measurement frequencies, the task may be corrupted by those solutions with local minimums.

7.3.1.2 Slightly contaminated measurements

The case with slightly contaminated measurements is examined. Though cases with a larger number of measurement frequencies in **Figure 7.2** again obtained the real solution, the cases with two and five frequencies failed to do so, as shown in **Figures 7.2(a)** and **7.2(b)**. That means the results by using five or less frequencies are quite sensitive to noise. In recognizing the standard deviation of the noise is only 0.05% whereas the results will have a relative error of 10% for *EI* in **Figure 7.2 (a)** and 3 % for *EI* in **Figure 7.2 (b)**, using only two to five frequencies for parameter identification is obviously not reliable. The errors in the identified parameters become larger with further increase in noise for these two cases. So that the results of these two cases are no longer presented hereafter when the noise becomes more severe.

7.3.1.3 Moderately contaminated measurements

When the frequencies were moderately contaminated by noise, as considered here for $\sigma = 0.1\%$ and $\sigma = 0.2\%$, two more interesting phenomena need to be stressed. Firstly, it is observed in **Figure 7.3 (b)** that the global minimum may not necessarily locate closer to the real solution of the objective function than a local

minimum does. That means even under exhausting search, the solution found is even not a good approximation for the real parameters. Secondly, there is a trend that some local solutions may disappear when the noise become large, as shown in **Figures 7.3(c)** and **7.3(d)**. However, contours of the cost function are similar to those shown in **Figure 7.1**, in which no noise is present. We can find in **Figure 7.3** that the case with ten frequencies, fails to identify the real solution. Nevertheless, the cases with twenty and with fifty frequencies still perform well.

7.3.1.4 Severely contaminated measurements

Under high noise levels, though only one solution is there in both **Figures 7.4 (b)** and **7.4(d)**, it is obviously the solution is not the real one. In fact, as shown in **Figure 7.4**, when the noise becomes great, all cases fail to estimate the parameters properly. However, the case using fifty frequencies still shows a good performance from the aspect that it provides good approximations for the two noise levels, within one percent in H and 5 percent in EI when $\sigma = 1\%$, and within one percent in H and fifteen percent in EI when $\sigma = 5\%$,

7.3.2 STATISTICAL ANALYSIS

7.3.2.1 Cable parameters

The design values of cable parameters, i.e., the horizontal component of cable tension, H; the elastic modulus, E; the cross sectional area, A; the mass per unit cable length, m; the horizontal and vertical projections of cable length, L_x and L_y of cable A11-N of the Dongting Lake Bridge are given in Table 7.1. These parameters are used in the numerical model as 'real' parameters.

7.3.2.2 Calculated frequencies

The calculated frequencies of the first fifty in-plane modes of the cable are shown in Table 7.2.

7.3.2.3 Monte Carlo method

The Monte Carlo method is adopted to investigate the statistical properties of the identified cable parameters, or parameter errors, and their relationship. Random numbers are generated by using the command RANDN of the Matlab® software. One sample of noise with standard normal distribution is shown in Table 7.3. The mean and standard deviation of the sample are 0.0565 and 0.7559, respectively. The random numbers with standard normal distribution are then conveniently converted into a sample of noise with a general normal distribution characterized by standard deviation σ and mean value μ. The 'measured' frequencies are numerically generated from

$$f_{MEA\,i} = f_{REAL\,i}(1+\varepsilon_i) \tag{1}$$

where $f_{REAL\,i}$ is the natural frequency of the ith mode computed from the finite element model with parameter values given in Table 7.1; and ε_i is the noise for the ith mode. The normally distributed relative errors are characterized by a standard deviation σ_ε and mean value μ_ε. In the following cases, μ_ε is assumed to be zero.

The calculated frequencies of the cable with known parameters are contaminated by noise with presumed distribution. A high level of noise under the same distribution enables the statistical analysis of the identified cable parameters. Then the relationship between the noise level and the reliability of the identified parameters is established under a statistical meaning. The correlation between the errors of different parameters is also investigated by calculating the correlation coefficients.

The 'real' frequencies are then contaminated by noise and regarded as 'measured' frequencies, which are used to identify the cable parameters. As indicated previously, when the 'measured' frequencies contains noise, the global minimum of the cost function may not necessarily indicate the 'real' solution. In other words, the identified parameters will possibly deviate from their 'real' values. Noting that such a deviation is essential in the identification problem when uncertainty cannot be avoided, it is reasonable to make statistical estimation other than a point-estimation on the cable parameters. To achieve this, random simulation should be used.

Generally, the number of independent tests should be large enough for carrying out statistical analysis by using the Monte Carlo method. In the present study, the number of independent tests is taken as 1000, that there should be one thousand tables similar to Table 7.3 to show the noise used in such a simulation process. With one thousand independent identifications, the statistical properties of the cable parameters can be conveniently obtained.

7.3.2.4 Statistical property of parameter errors

Four noise levels, i.e., σ_ε = 0.5% 1%, 2% and 5%, are considered in the simulation. The cable parameters are identified one thousand times under each noise level. Both the exhaust search and the genetic algorithm (GA) are used to identify the cable parameters.

The histograms of the relative errors of the identified parameters by using the exhaust search and the genetic algorithm are shown in **Figures 7.5** to **7.12** and **Figures 7.9** to **7.20**, respectively. **Figures 7.21** and **7.22** show the relationship between the relative errors of the cable tension and flexural rigidity with different number of measured frequencies used. The mean values and standard deviations of the relative errors of the identified parameters are given in Tables 7.4 to 7.7.

Correlations between relative errors of identified parameters are listed in Table 7.8 under different noise levels.

As the noise is generated under a presumed normal distribution the identified cable parameters are expected to be normally distributed provided that the noise is small enough to assure a linear relationship between the parameter errors and the errors in frequencies. This assumption is acceptable in most of the cases but should be rejected in some special cases, as interpreted below.

In **Figures 7.5** and **7.6**, it is observed that the cable tension errors are obviously normally distributed when the standard deviation of errors is not greater than 1.0%. This means that when the noise is small enough, i.e., in the present cases with a standard deviation not greater than one percent, the cable parameters can be identified by using both twenty and fifty frequencies while the latter produces smaller standard deviation, indicating superiority to the former. The mean values and standard deviations of the relative tension errors are listed in Tables 7.4 and 7.6, respectively. The mean values of the relative errors are found to be almost zero. The standard deviation is found to be 0.25% when taking σ_ε =0.5% and using fifty frequencies. This means that there is a 97% confidence that the relative error of the identified cable tension will be within 0.75%.

In **Figures 7.7(a)** and **7.8(a)**, the histograms no longer show a normal pattern when taking only twenty frequencies for identification. However, as seen in **Figures 7.7(b)** and **7.8(b)**, the results from fifty frequencies still show a normal distribution with mean values and standard deviations listed in Tables 7.4 and 7.6. The standard deviation is found to be 0.80% when taking σ_ε =2% and using fifty frequencies. This means that there is a 97% confidence that the relative error of the identified cable tension will be within 2.4%, still good enough from the viewpoint of engineering.

Similar observations are made in **Figures 7.9** to **7.12** for the flexural rigidity relative errors. But the standard deviations of errors of the flexural rigidity are much greater than those of the tension by comparing Table 7.6 with Table 7.7. In fact, as revealed in **Figures 7.21** and **7.22**, the errors in the two parameters are dependent on each other in a statistical way. A linear relationship is built up by fitting the points on the error in plane of H and EI. It is noticed that the relationship between the errors of two parameters are dependent on the number of the frequencies used. Using only twenty frequencies the error in flexural rigidity is about twenty times the error in tension while only five times when using fifty frequencies. The correlation coefficients between the two errors are greater than 0.95, confirming the relationship of the errors in H and EI. It is noticed that both the number of frequencies used and the level of the noise do not affect the correlation coefficients much.

7.3.3 CASE STUDIES ON THREE REAL CABLES

The design value of the parameters of three cables are listed in Table 7.10 for cable A11-N of the Dongting Lake Bridge, Table 7.11 for a Tsing Yi side span cable of the Tsing Ma Bridge, and Table 7.12 for a longitudinal stabilizing cable of the Ting Kau Bridge. As cable A11-N of the Dongting Lake Bridge is a cable with moderate length and cross section area, it is regarded as a 'Typical' stay cable used in cable-stayed bridges and referred as Cable T (Typical); the Ting Yi side span cable of the Tsing Ma Bridge is characterized by the largest cross section area around the world, consequently possessing the heaviest self-weight in stay cables, and referred as Cable H (Heaviest); the horizontal stabilizing cable of the Ting Kau Bridge is the longest cable ever used in cable-stayed bridges and is referred Cable L (Longest).

The calculated and measured frequencies of the three cables are listed in Tables 7.13 to 7.15. The tables list 66 frequencies for Cable T, 18 for Cable H and 55 for Cable L. The number of frequencies is dependant on the conditions and targets of field measurements. The measured frequencies are obtained from the power spectrum of acceleration response by using the FFT technique. The time histories of the response are all obtained by ambient vibration tests with time duration of one hour and at specified sampling frequencies, i.e., 500 Hz for Cable T, 25.6 Hz for Cable H and Cable L, respectively.

As there are no methods for accurately measuring cable tension forces (As reviewed in Chapter 2) in most cases, it is difficult to validate directly the proposed method. However, it is possible to make indirect validation, e.g., the cable tension and other cable parameters are believed to be accurately identified when the calculated frequencies from the model based on these parameters coincide with the measurements.

7.3.3.1 Dongting Lake Bridge: a typical stay cable

Cable T is cable A11-N of the Dongting Lake Bridge. The identified cable parameters are listed in Table 7.10, in which the identified flexural rigidity is found to have the largest deviation, -8.33% from the design one. The error in cable tension is 4.59%, in cable length 1.03% and in cable mass –1.38%.

Figure 7.23 shows the distribution of frequency relative errors with respect to the mode order. It is noticed in this figure that the errors are all lower than 0.2%, which demonstrate that the validity of the cable model and the accuracy of the identified parameters. **Figures 7.24** and **7.25** show the probability and the histogram of the errors. It is observed that the normal distribution, indicated respectively by the solid line and solid curve in **Figures 7.24** and **7.25**, respectively, is quite good for

describing the errors. Considering the central limit theorem, the normal distribution of the small errors, not greater than 0.2%, can be interpreted as a result of many factors, which slightly affect frequency measurements and calculations.

7.3.3.2 Tsing Ma Bridge: an extremely heavy cable

Cable H is the Tsing Yi side span cable of the Tsing Ma Bridge. The identified cable parameters are listed in Table 7.11, in which the identified cable tension is found to have the largest deviation, -2.65% from the nominal value (the nominal value of the flexural rigidity is obtained by regarding the cable as a solid steel beam with a cross section area equals the sum of the cross section areas of all wires.) The error in cable length is -1.14% and in cable mass is 1.63%. The identified flexural rigidity is identical to the nominal value.

Figure 7.26 shows the distribution of frequency relative errors with respect to the mode order. It is noticed in this figure that the errors are all lower than 0.3%, which validate the cable model and indicate the accuracy of the identified parameters. **Figures 7.27** and **7.28** shows the probability and the histogram of the errors. It is observed that the normal distribution, indicated respectively by the solid line and solid curve in **Figures 7.24** and **7.25**, is fairly good for describing the errors. In fact, the distribution is more like a uniform distribution rather than a normal one.

7.3.3.3 Ting Kau Bridge: an extremely long cable

Cable L is the longitudinal stabilizing cable of the Ting Kau Bridge. The identified cable parameters are listed in Table 7.12. The identified flexural rigidity is found to have the largest deviation, -99.99% from the nominal one. The error in cable tension is 18.85%, in length −0.83% and in mass 0.095%. The large errors in cable tension may indicate the cable is possibly overloaded from its design value.

The great errors in the flexural rigidity may mean that the cable wires may not be compacted.

Figure 7.29 shows the distribution of frequency relative errors with the respect to mode order. It is noticed in this figure that the errors are all lower than 0.4%, which validate again the cable model and indicate the accuracy of the identified parameters. **Figures 7.30** and **7.31** show the probability and the histogram of the errors. It is observed that the distribution of the errors is neither normal nor uniform.

7.4 SUMMARY

The identification of cable parameters is studied by using both simulation and real testing data. The simulation study is carried out to show the characteristics of the cost function surfaces under different conditions and to obtain the statistical properties of the cable parameters (or cable parameter errors). The real testing data from three real bridges are used to evaluate the cable conditions (identify cable parameters). In the identification process, both the exhaust search and the genetic algorithm (GA) are used for the simulation study and the GA is used for real cables.

The effects of the number of modal frequencies and the noise level on the solution uniqueness and distribution of multiple solutions are investigated. The correlation between the errors of different parameters is obtained through calculating the correlation coefficients. The distribution of frequency errors of three real cables is discussed. Based on the extensive study on both the simulation and real cases, the following conclusions are drawn: (i) Generally, the more measurement frequencies are used as input, the narrower (more accurate) the solutions are distributed. It is

always better to have more frequencies measured; (ii) Both small and large number of input frequencies works well when there is no noise or the noise is very small. However, a large number of frequencies should be employed to achieve reliable and accurate identification results when the noise level is severe. (iii) The exhaust search and the genetic algorithm (GA) provide coincident results; (iv) When the noise is small and normally distributed, the errors in the identified cable parameters are also normally distributed. However, when the noise is large, the errors no longer conform to a normal distribution; (v) The correlation between the parameters errors is strong, indicated by an absolute correlation coefficient greater than 0.95. The correlation coefficient is hardly affected by the noise or by the number of frequencies; (vi) Case studies on three real bridges validate the proposed parameter identification method for different kind of cables. The method may serve as a general approach for evaluating cable conditions, especially for cable tension calibration in real long-span cable-supported bridges.

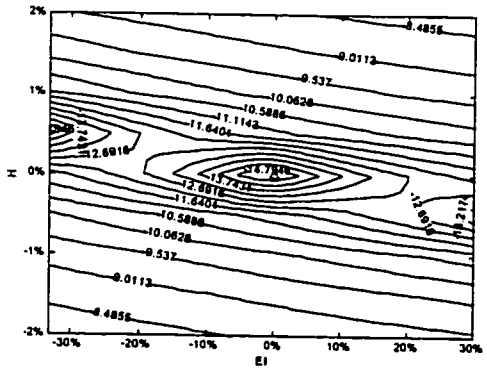

(a) Frist two frequencies used

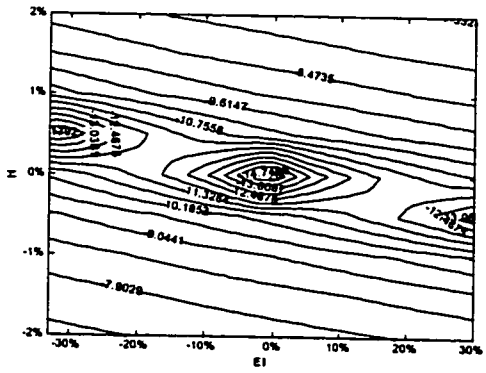

(b) First five frequencies used

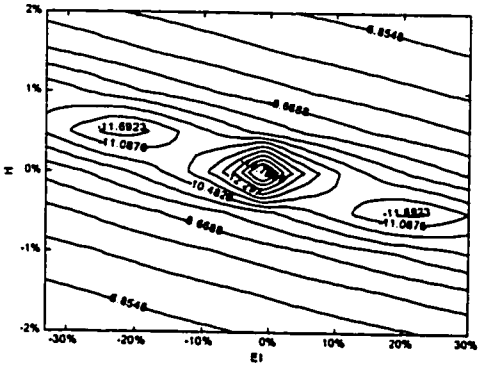

(c) First ten frequencies used

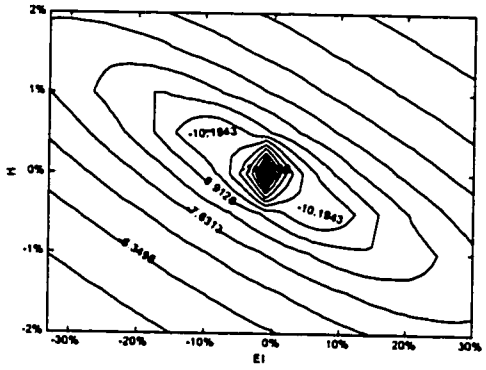

(d) First twenty frequencies used

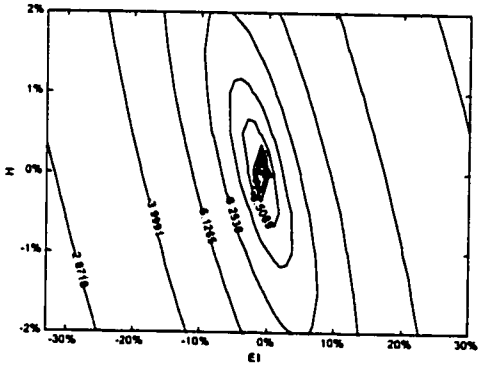

(e) First fifty frequencies used

Figure 7.1 Cost function contours with difference number of frequency measurements under noise level $\sigma = 0$

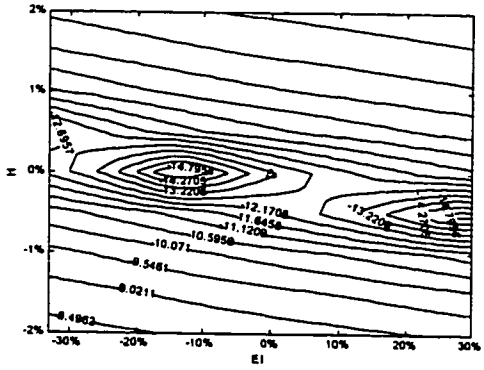

(a) Frist two frequencies used

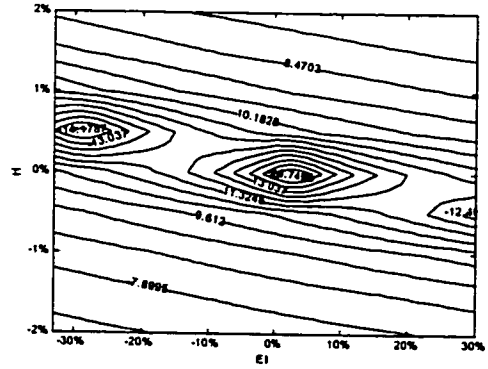

(b) First five frequencies used

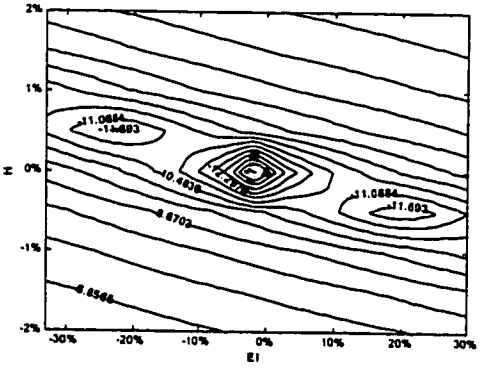

(c) First ten frequencies used

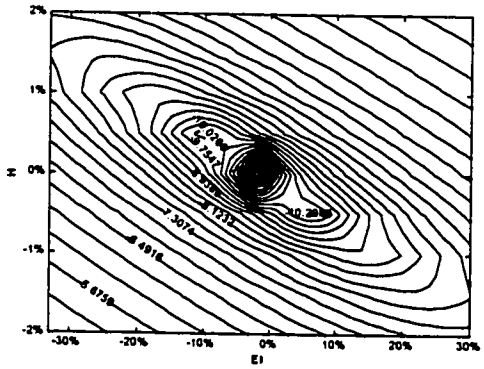

(d) First twenty frequencies used

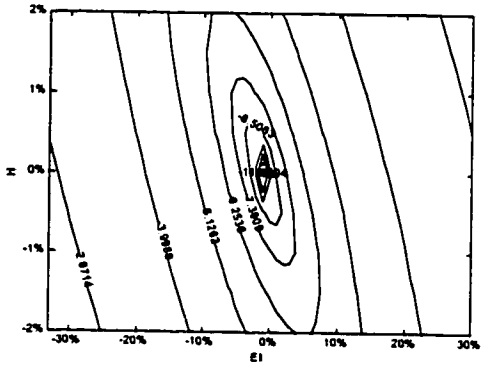

(e) First fifty frequencies used

Figure 7.2 Cost function contours with difference number of frequency measurements under noise level $\sigma = 0.05\%$

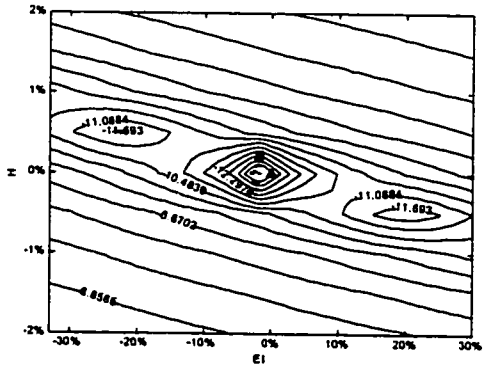

(a) First ten frequencies and σ =0.1%;

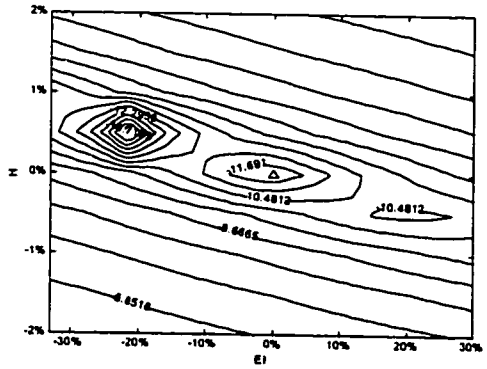

(b) First ten frequencies and σ =0.2%

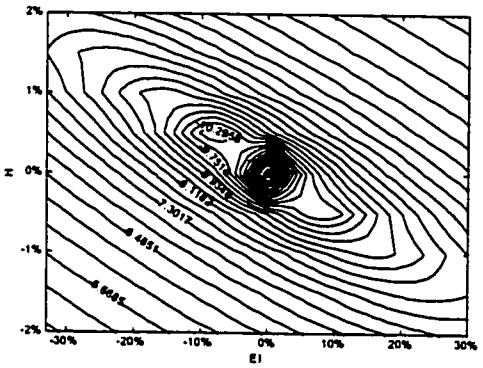

(c) First twenty frequencies, σ =0.1%;

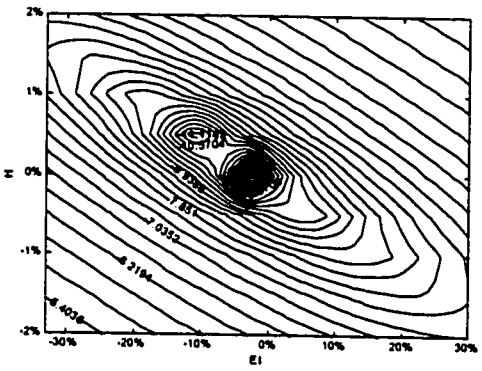

(d) First twenty frequencies, σ =0.2%

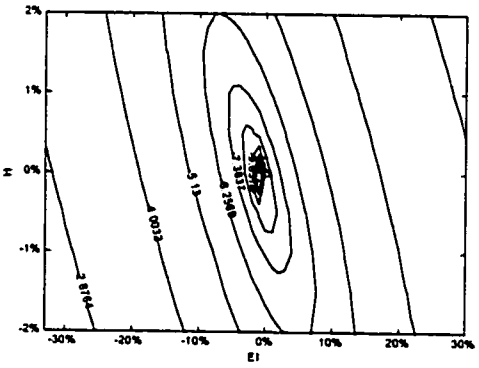

(e) First fifty frequencies and σ =0.1%;

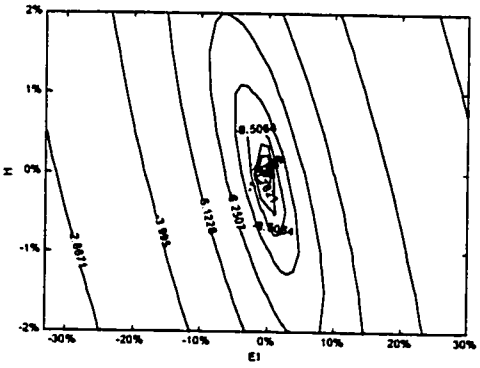

(f) First fifty frequencies and σ =0.2%

Figure 7.3 Cost function contours with difference number of frequency measurements under moderate noise

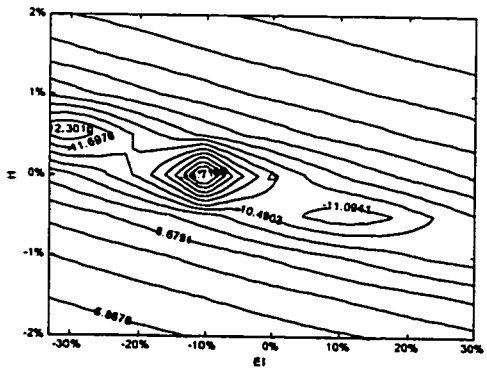

(a) First ten frequencies and σ =1%

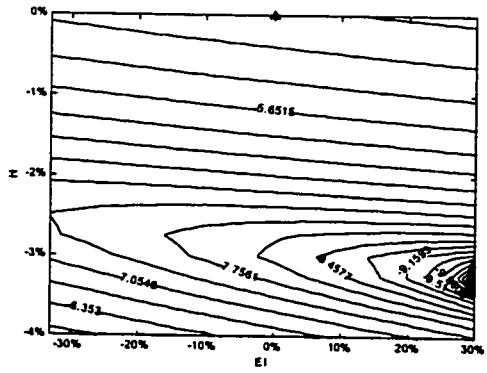

(b) First ten frequencies and σ =5%

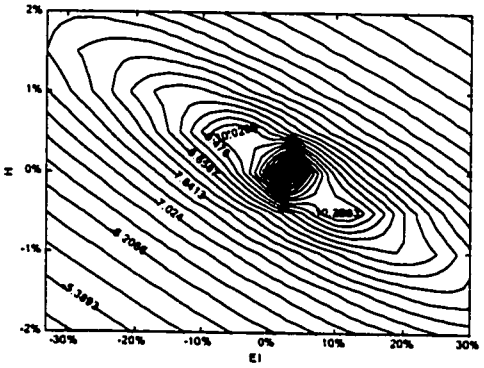

(c) First twenty frequencies and σ =1%

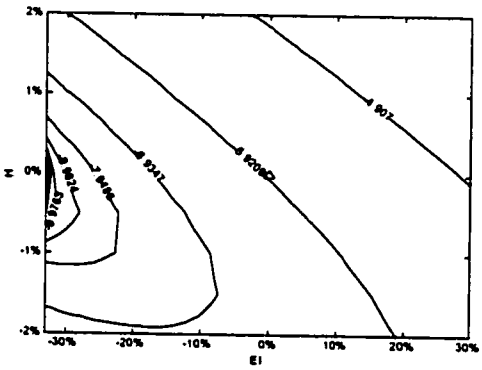

(d) First twenty frequencies and σ =5%

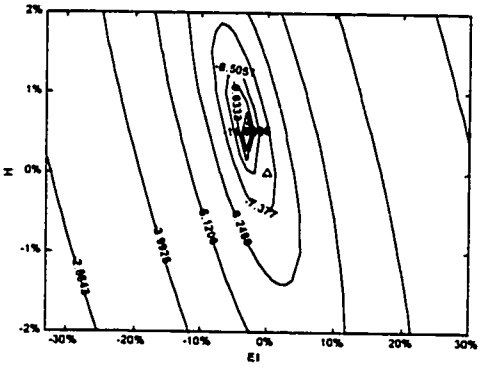

(e) First fifty frequencies and σ =1%

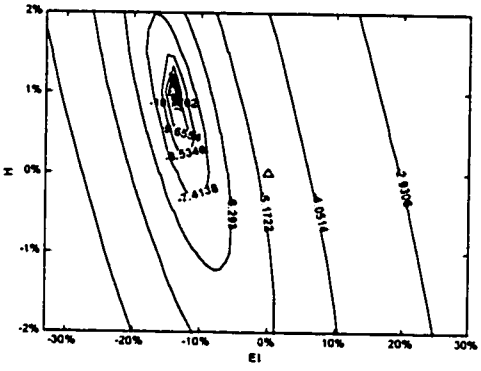

(f) First fifty frequencies and σ =5%

Figure 7.4 Cost function contours with difference number of frequency measurements under severe noise

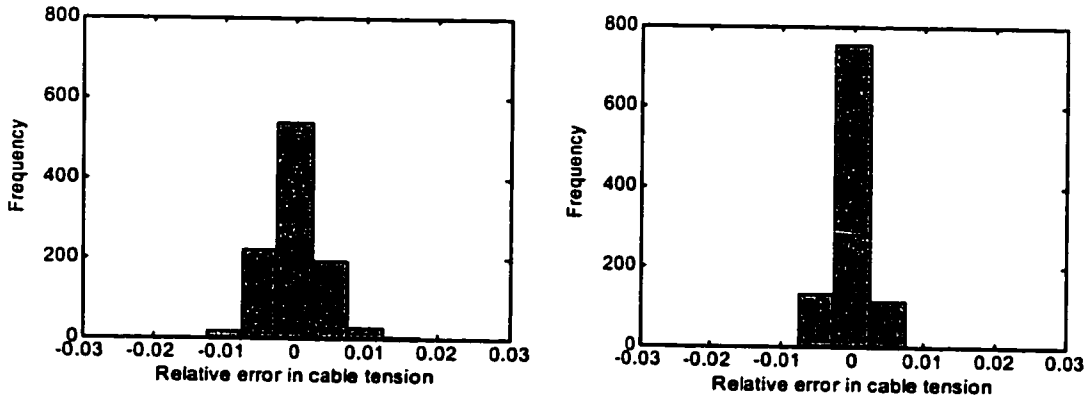

(a) twenty frequencies (b) fifty frequencies

Figure 7.5 Distribution of cable tension errors ($\sigma_\varepsilon = 0.5\%$)

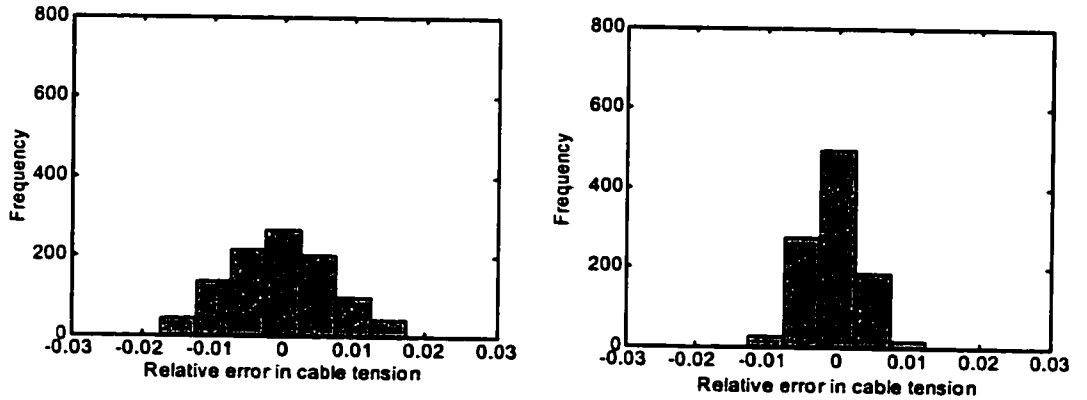

(a) twenty frequencies (b) fifty frequencies

Figure 7.6 Distribution of cable tension errors ($\sigma_\varepsilon = 1\%$)

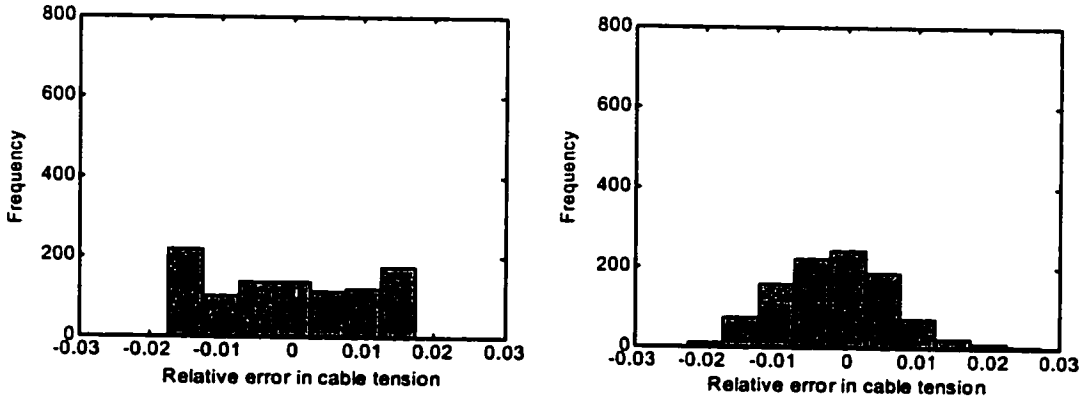

Figure 7.7 **Distribution of cable tension errors ($\sigma_\varepsilon = 2\%$): (a) twenty frequencies; (b) fifty frequencies**

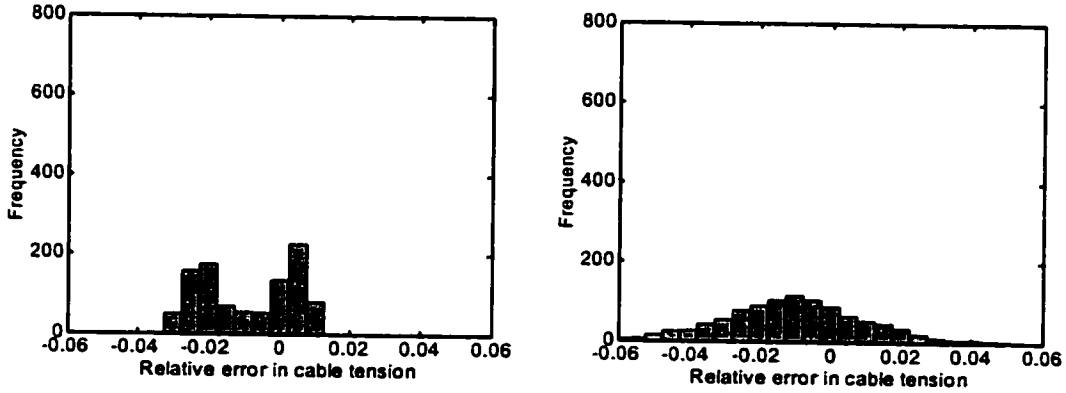

Figure 7.8 **Distribution of cable tension errors ($\sigma_\varepsilon = 5\%$) (a) twenty frequencies; (b) fifty frequencies**

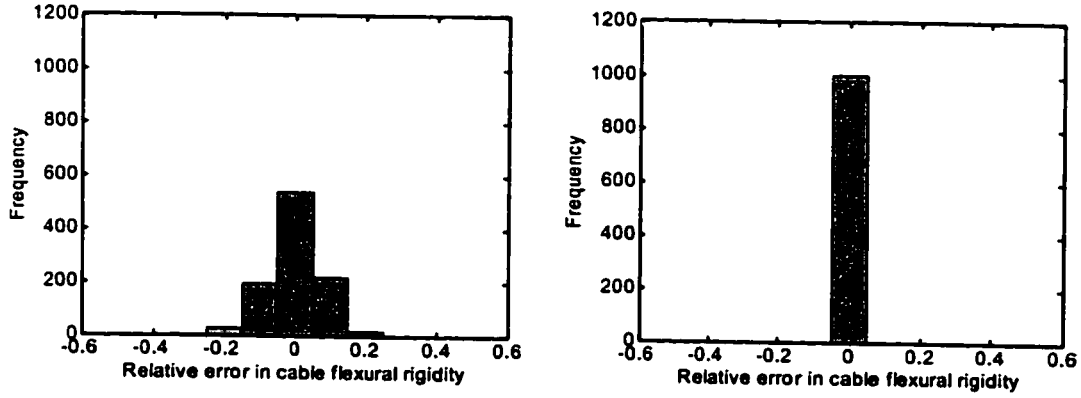

Figure 7.9 Distribution of cable flexural rigidity errors ($\sigma_\varepsilon = 0.5\%$) (a) twenty frequencies; (b) fifty frequencies

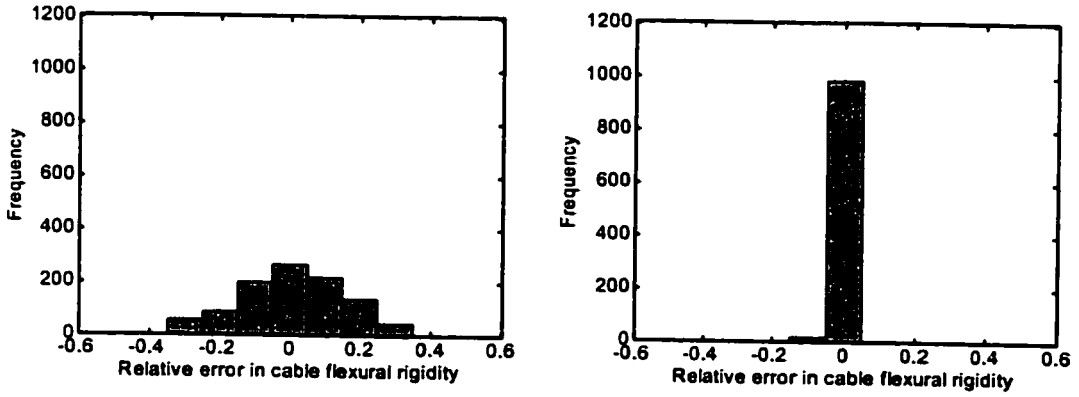

Figure 7.10 Distribution of cable flexural rigidity errors ($\sigma_\varepsilon = 1\%$): (a) twenty frequencies; (b) fifty frequencies

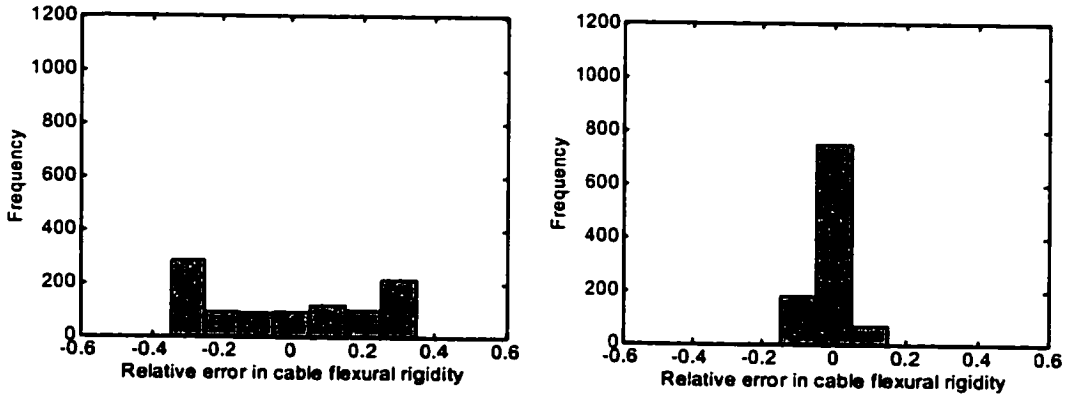

Figure 7.11 Distribution of cable flexural rigidity errors ($\sigma_\varepsilon = 2\%$): (a) twenty frequencies; (b) fifty frequencies

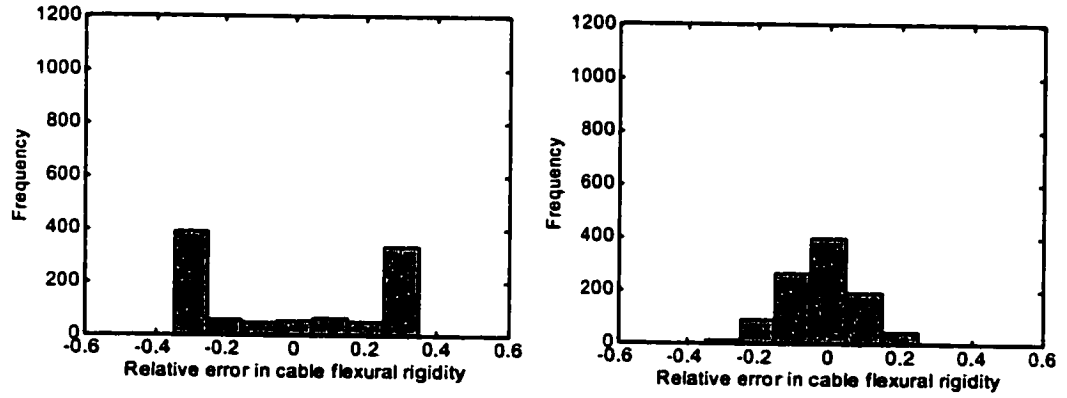

Figure 7.12 Distribution of cable flexural rigidity errors ($\sigma_\varepsilon = 5\%$): (a) twenty frequencies; (b) fifty frequencies

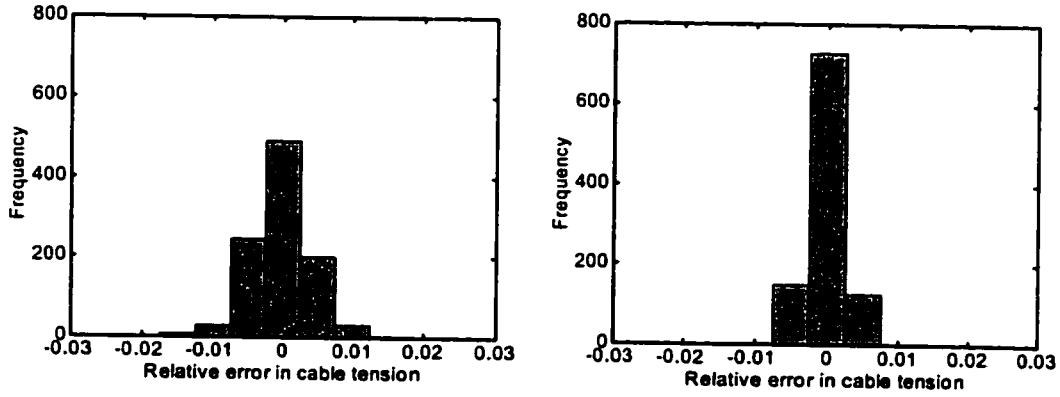

Figure 7.13 Distribution of cable tension errors ($\sigma_\varepsilon = 0.5\%$): (a) twenty frequencies; (b) fifty frequencies

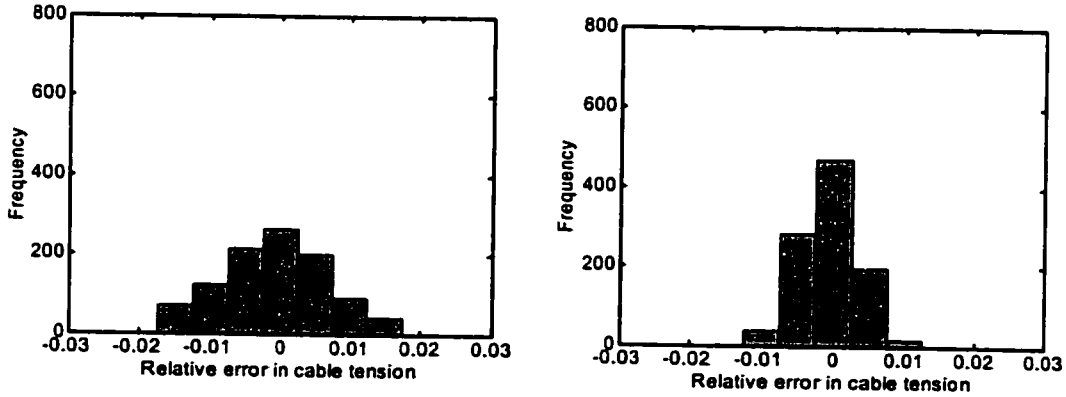

Figure 7.14 Distribution of cable tension errors ($\sigma_\varepsilon = 1\%$): (a) twenty frequencies; (b) fifty frequencies

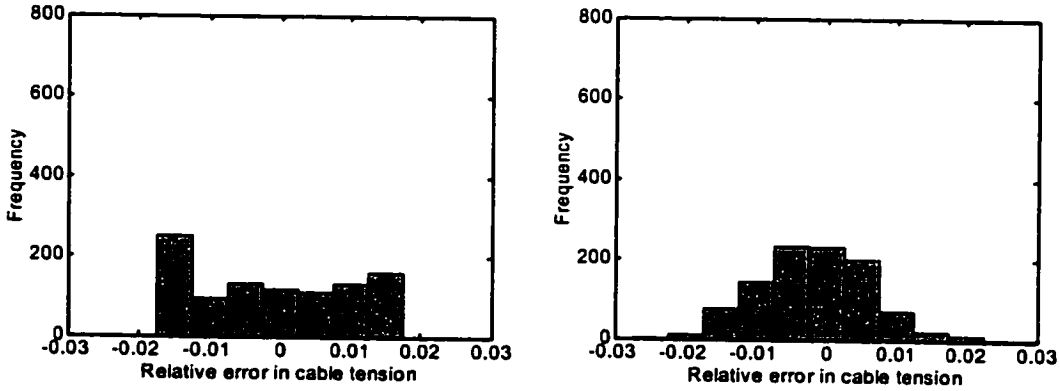

Figure 7.15 Distribution of cable tension errors ($\sigma_\varepsilon = 2\%$): (a) twenty frequencies; (b) fifty frequencies

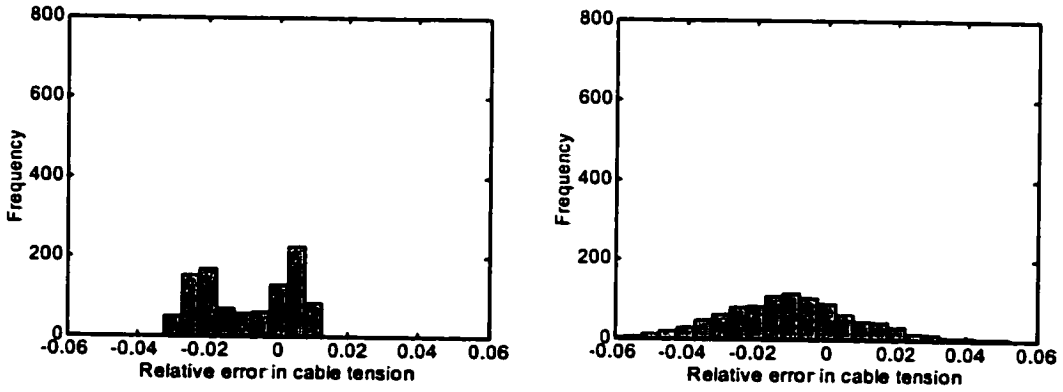

Figure 7.16 Distribution of cable tension errors ($\sigma_\varepsilon = 5\%$): (a) twenty frequencies; (b) fifty frequencies

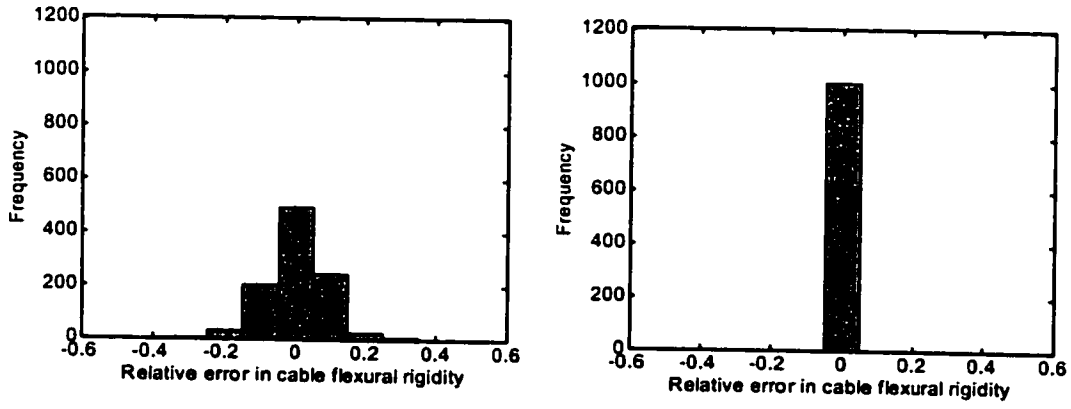

Figure 7.17 Distribution of cable flexural rigidity errors ($\sigma_\varepsilon = 0.5\%$): (a) twenty frequencies; (b) fifty frequencies

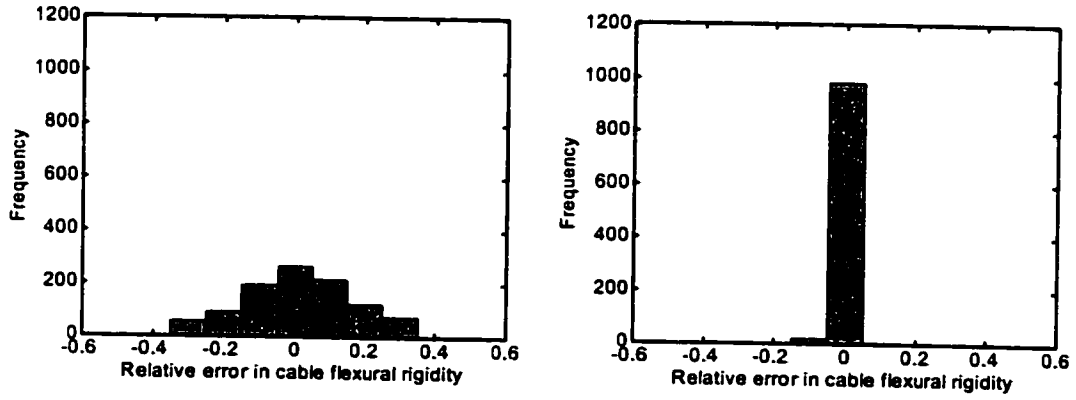

Figure 7.18 Distribution of cable flexural rigidity errors ($\sigma_\varepsilon = 1\%$): (a) twenty frequencies; (b) fifty frequencies

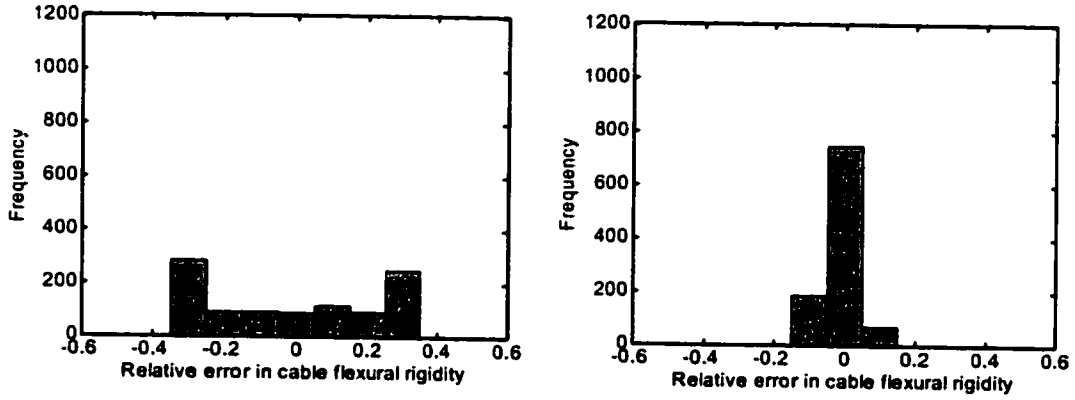

Figure 7.19 Distribution of cable flexural rigidity errors ($\sigma_\varepsilon = 2\%$): (a) twenty frequencies; (b) fifty frequencies

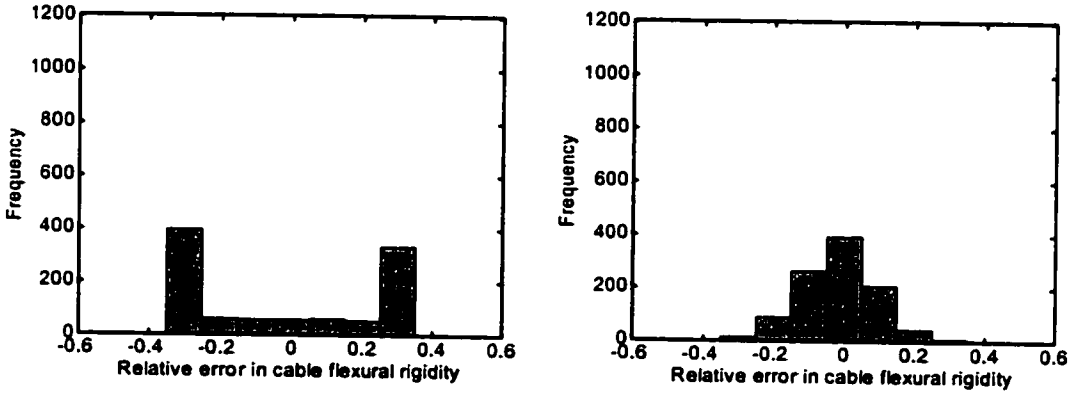

Figure 7.20 Distribution of cable flexural rigidity errors ($\sigma_\varepsilon = 5\%$): (a) twenty frequencies; (b) fifty frequencies

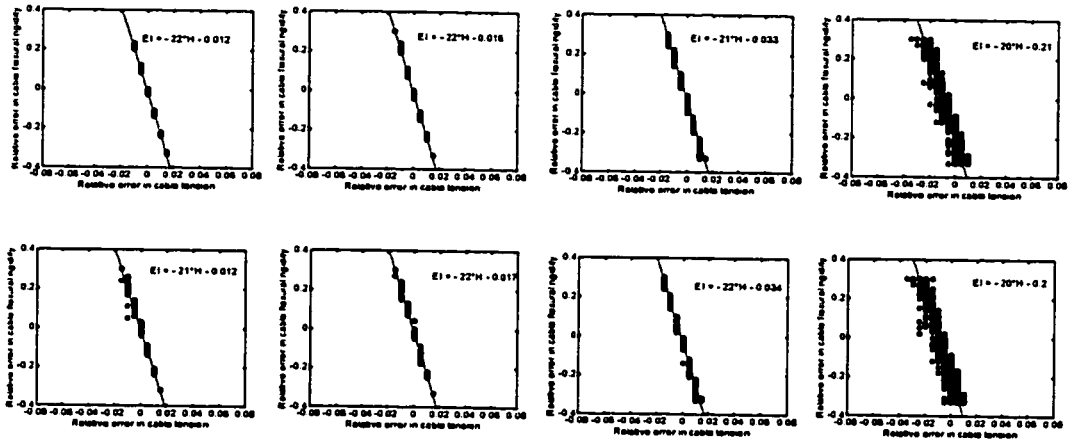

Figure 7.21 Relationship between errors of *H* and *EI* (Twenty frequencies measured)

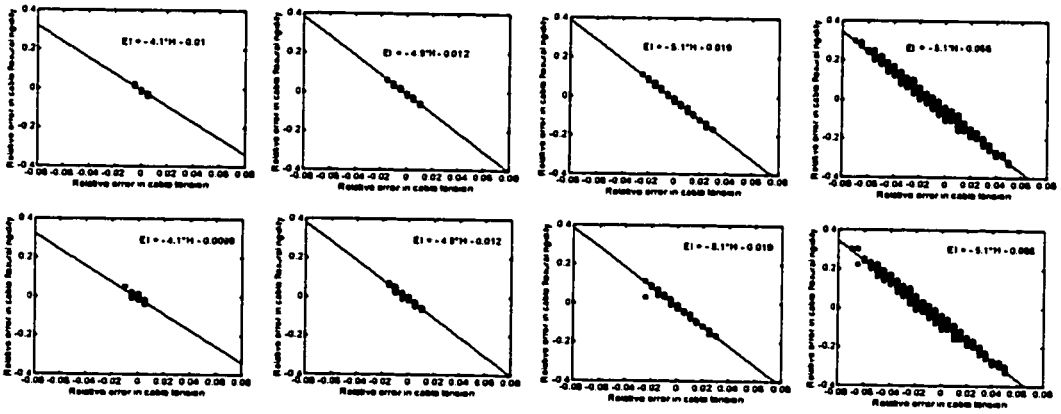

Figure 7.22 Relationship between errors of *H* and *EI* (Fifty frequencies measured)

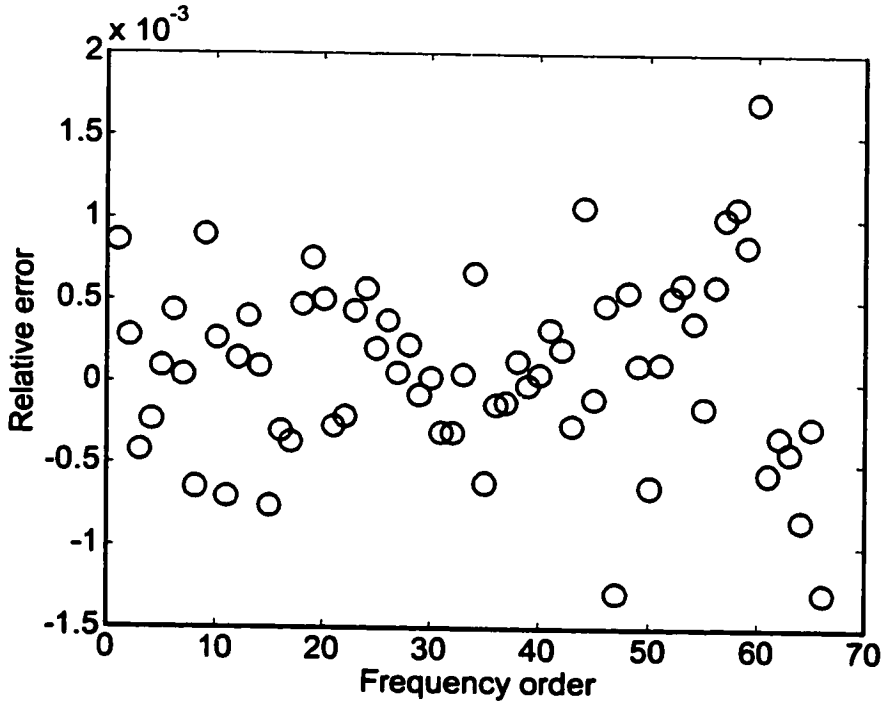

Figure 7.23 Relative frequency errors of Cable T

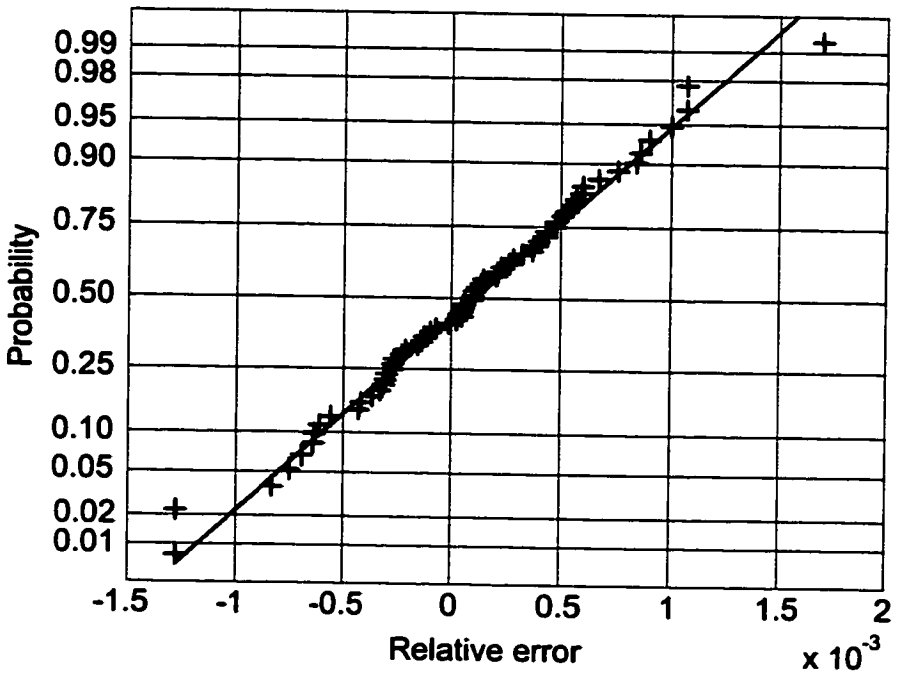

Figure 7.24 Probability of relative frequency errors of Cable T

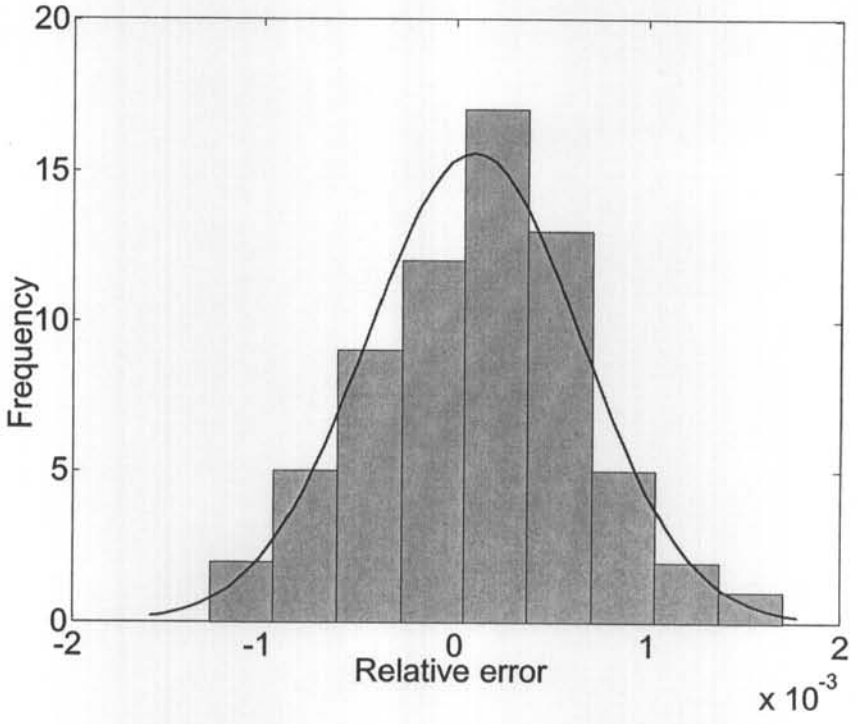

Figure 7.25 Histogram of relative frequency errors of Cable T

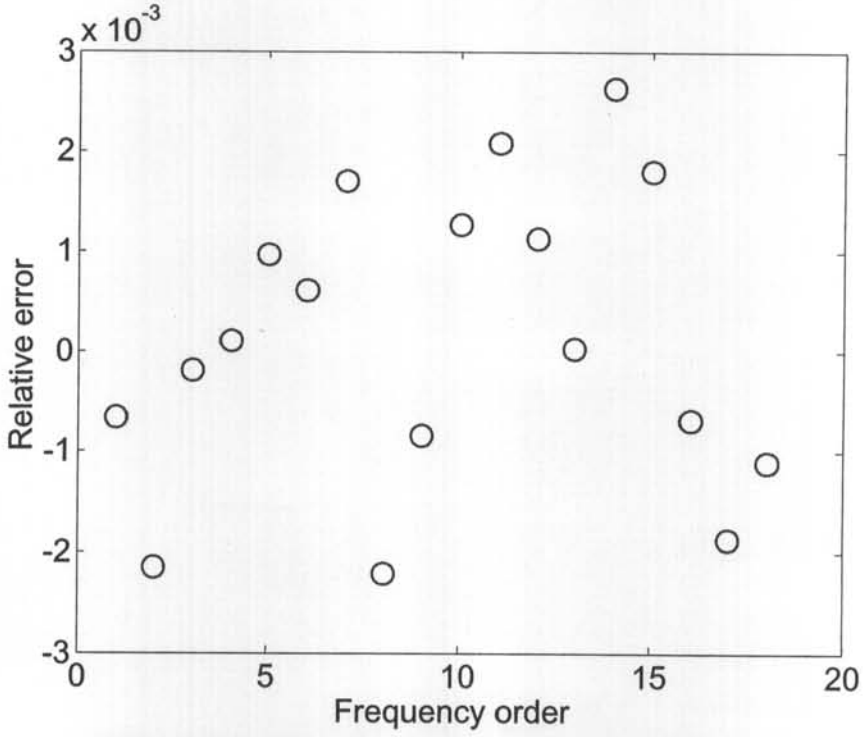

Figure 7.26 Relative frequency errors of Cable H

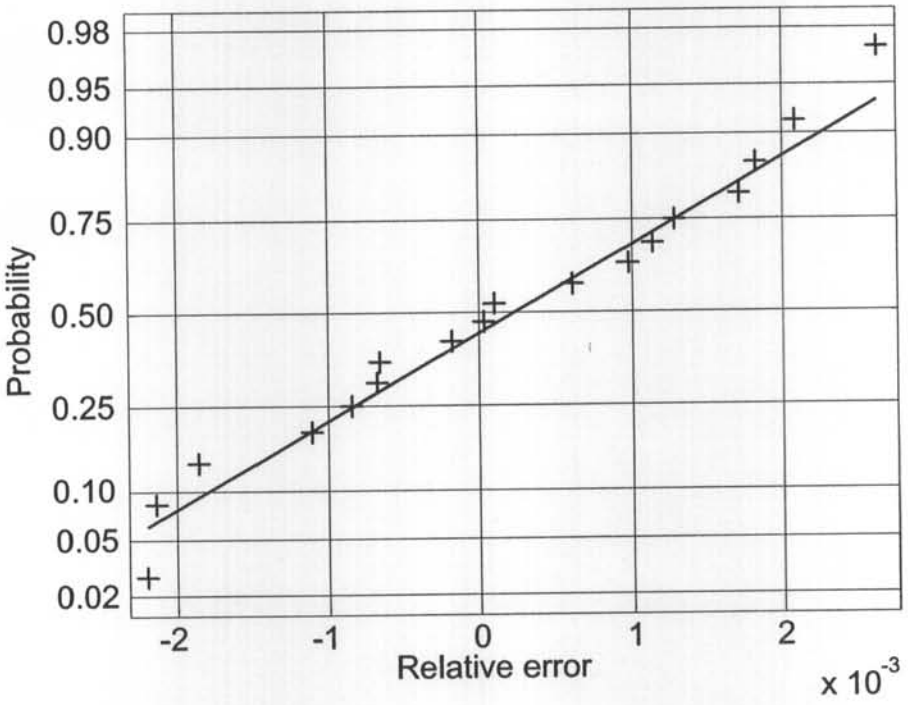

Figure 7.27 Probability of relative frequency errors of Cable H

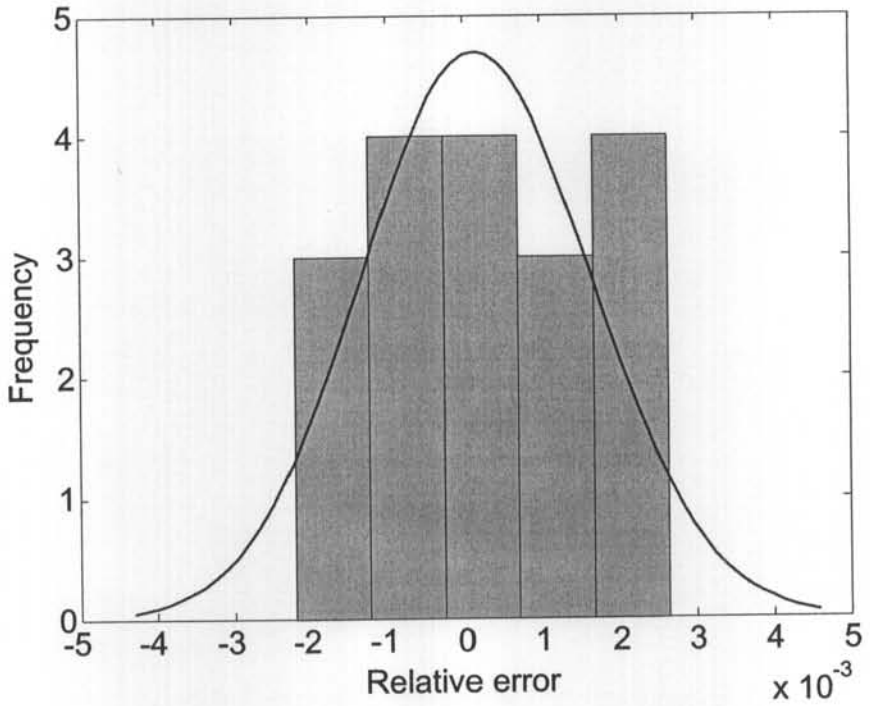

Figure 7.28 Histogram of relative frequency errors of Cable H

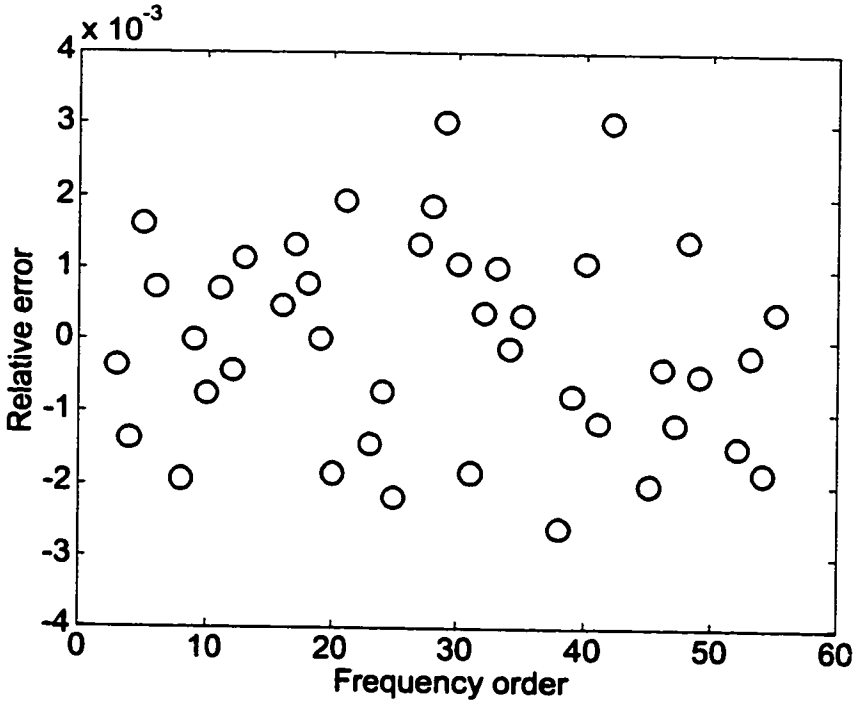

Figure 7.29 Relative frequency errors of Cable L

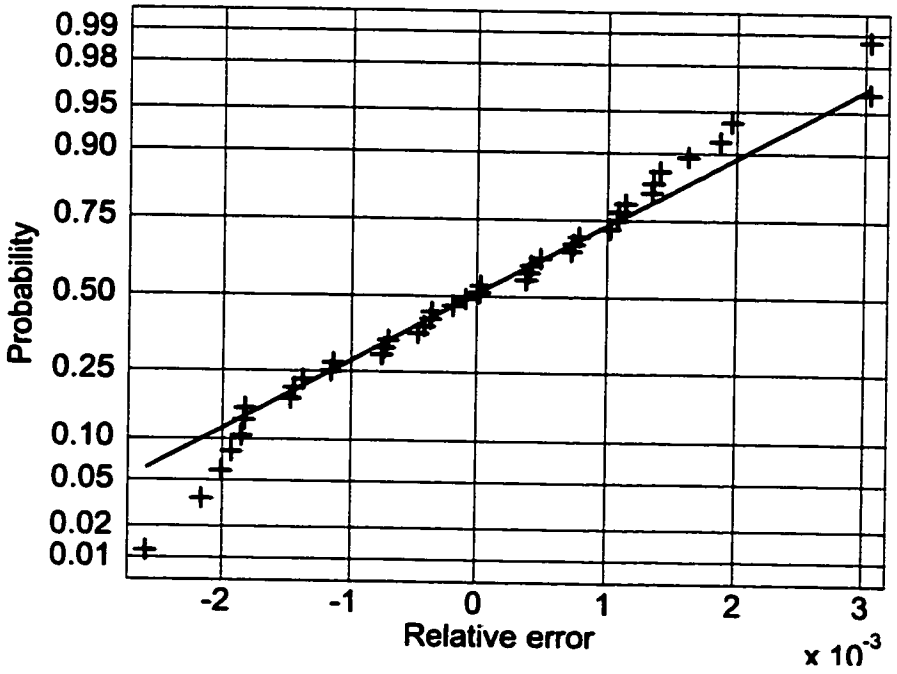

Figure 7.30 Probability of relative frequency errors of Cable L

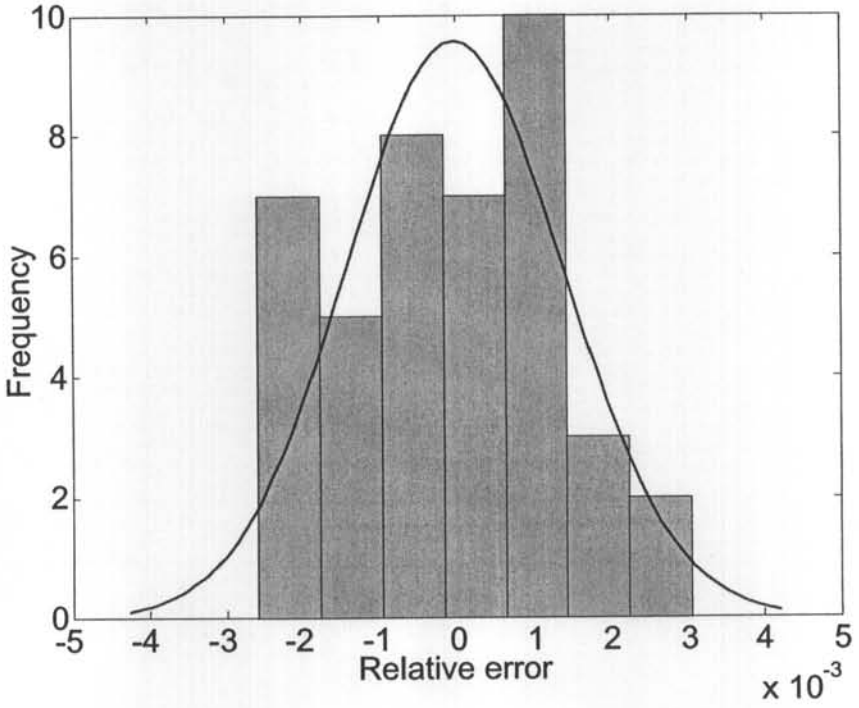

Figure 7.31 Histogram of relative frequency errors of Cable L

Table 7.1 Design parameters of cable A11-N

H (kN)	EI (N·m^2)	L_x (m)	L_y (m)	M (kg/m)	EA (Pa·m^2)	GA (Pa·m^2)	GJ (N·m)
2474	9.36e+5	91.691	68.944	51.8	1.54e+9	5.76e+9	7.04

Table 7.2 Calculated frequencies of cable A11-N of the Dongting Lake Bridge

Mode Order	1	11	21	31	41
+0	1.0815	11.9541	23.3745	35.7941	49.6130
+1	2.1539	13.0638	24.5644	37.1069	51.0855
+2	3.2323	14.1794	25.7648	38.4341	52.5757
+3	4.3118	15.3015	26.9761	39.7762	54.0841
+4	5.3936	16.4304	28.1986	41.1333	55.6108
+5	6.4778	17.5667	29.4329	42.5059	57.1562
+6	7.5651	18.7108	30.6793	43.8944	58.7206
+7	8.6558	19.8632	31.9383	45.2990	60.3043
+8	9.7506	21.0243	33.2101	46.7200	61.9076
+9	10.8498	22.1946	34.4953	48.1579	63.5308

Table 7.3 One sample of noises with standard normal distribution

Mode Order	1	11	21	31	41
+0	-1.0106	0.0000	0.5689	0.6232	0.3899
+1	0.6145	-0.3179	-0.2556	0.7990	0.0880
+2	0.5077	1.0950	-0.3775	0.9409	-0.6355
+3	1.6924	-1.8740	-0.2959	-0.9921	-0.5596
+4	0.5913	0.4282	-1.4751	0.2120	0.4437
+5	-0.6436	0.8956	-0.2340	0.2379	-0.9499
+6	0.3803	0.7310	0.1184	-1.0078	0.7812
+7	-1.0091	0.5779	0.3148	-0.7420	0.5690
+8	-0.0195	0.0403	1.4435	1.0823	-0.8217
+9	-0.0482	0.6771	-0.3510	-0.1315	-0.2656

Table 7.4 Mean relative error of identified cable tension

	Twenty frequencies		Fifty frequencies	
σ_ε	Exhaust	GA	Exhaust	GA
0.005	-5.00e-6	-2.60e-4	-9.50e-5	-1.35e-4
0.01	-4.95e-4	-8.75e-4	-5.80e-4	-6.95e-4
0.02	-5.80e-4	-0.0011	-0.0017	-0.0017
0.05	-0.0089	-0.0087	-0.0104	-0.0107

Table 7.5 Mean relative error of identified cable flexural rigidity

	Twenty frequencies		Fifty frequencies	
σ_ε	Exhaust	GA	Exhaust	GA
0.005	-0.0114	-0.0066	-0.0097	-0.0094
0.01	-0.0051	0.0016	-0.0092	-0.0086
0.02	-0.0203	-0.0105	-0.0099	-0.0105
0.05	-0.0248	-0.0291	-0.0125	-0.0108

Table 7.6 Standard deviation of relative errors of identified cable tension

	Twenty frequencies		Fifty frequencies	
σ_ε	Exhaust	GA	Exhaust	GA
0.005	0.0039	0.0043	0.0025	0.0026
0.01	0.0072	0.0075	0.0040	0.0041
0.02	0.0108	0.0110	0.0080	0.0080
0.05	0.0131	0.0131	0.0194	0.0196

Table 7.7 Standard deviation of relative errors of identified cable flexural rigidity

	Twenty frequencies		Fifty frequencies	
σ_ε	Exhaust	GA	Exhaust	GA
0.005	0.0850	0.0914	0.0103	0.0112
0.01	0.1584	0.1626	0.0201	0.0208
0.02	0.2323	0.2372	0.0409	0.0406
0.05	0.2759	0.2746	0.1003	0.1014

Table 7.8 Correlation between relative errors of tension and flexural rigidity

	Twenty frequencies		Fifty frequencies	
σ_ε	Exhaust	GA	Exhaust	GA
0.005	-0.994	-0.991	-0.988	-0.973
0.01	-0.998	-0.997	-0.978	-0.976
0.02	-0.996	-0.996	-0.994	-0.991
0.05	-0.965	-0.962	-0.992	-0.992

Table 7.9 Parameter setting of the genetic algorithm

Number of Parameters	Population Size	Maximum Generation	Number of Function Evaluation
4-5	20	100	1802

Table 7.10 Parameters of cable A11-N of the Dongting Lake Bridge:

Cable T

Parameters	Unit	Design value	Identified value	Error	Relative error (%)
L_x	m	91.691	92.635	0.944	1.03
L_y	m	68.944	69.654	0.710	1.03
H	kN	2474.000	2587.557	113.557	4.59
M	kg/m	51.800	51.080	-0.720	-1.38
EI	Nm^2	9.36×10^5	8.58×10^5	-0.78×10^5	-8.33

Table 7.11 Parameters of Tsing Yi side span cable:

Cable H

Parameters	Unit	Design value	Identified value	Error	Relative error (%)
L_x	m	293.184	289.842	-3.342	-1.14
L_y	m	154.738	152.974	-1.764	-1.14
H	kN	405,838	395,083	-10,755	-2.65
EI	Nm^2	1.0×10^{10}	1.0×10^{10}	0	0
M	kg/m	6.276×10^{3}	6.378×10^{3}	0.102×10^{3}	1.63

Table 7.12 Parameters of the longitudinal stabilizing cable of Ting Kau Bridge:

Cable L

Parameters	Unit	Design value	Identified value	Error	Relative error (%)
L_x	M	444.396	440.693	-3.703	-0.833
L_y	m	129.563	128.483	-1.080	-0.833
H	kN	1903.546	2262.308	358.762	18.847
EI	Nm^2	1.0832×10^{6}	149.949	-1.08305×10^{6}	99.986
M	kg/m	64.763	64.825	0.062	0.095

Table 7.13 Frequencies of cable A11-N of the Dongting Lake Bridge

	Frequency			Error		Relative error	
Unit	Hz	Hz	Hz	Hz	Hz	%	%
Order	Measured	Design parameter	Optimized parameter	Design parameter	Optimized parameter	Design parameter	Optimized parameter
1	1.111	1.081	1.110	-0.030	-0.001	-2.74	-0.09
2	2.213	2.152	2.212	-0.061	-0.001	-2.74	-0.03
3	3.319	3.231	3.320	-0.088	0.001	-2.66	0.04
4	4.429	4.311	4.430	-0.118	0.001	-2.67	0.02
5	5.543	5.394	5.542	-0.149	-0.001	-2.69	-0.01
6	6.661	6.481	6.658	-0.180	-0.003	-2.71	-0.04
7	7.778	7.572	7.778	-0.206	0.000	-2.65	-0.01
8	8.896	8.668	8.902	-0.228	0.006	-2.56	0.06
9	10.040	9.770	10.031	-0.270	-0.009	-2.69	-0.09
10	11.169	10.879	11.166	-0.290	-0.003	-2.60	-0.03
11	12.299	11.995	12.308	-0.304	0.008	-2.48	0.07
12	13.458	13.118	13.456	-0.340	-0.002	-2.52	-0.01
13	14.618	14.250	14.612	-0.368	-0.006	-2.51	-0.04
14	15.778	15.392	15.777	-0.386	-0.002	-2.45	-0.01
15	16.937	16.543	16.950	-0.394	0.013	-2.32	0.07
16	18.127	17.705	18.132	-0.422	0.005	-2.33	0.03
17	19.318	18.878	19.325	-0.440	0.007	-2.28	0.04
18	20.538	20.063	20.528	-0.475	-0.010	-2.31	-0.05
19	21.759	21.261	21.742	-0.498	-0.017	-2.29	-0.08
20	22.980	22.471	22.968	-0.509	-0.012	-2.21	-0.05
21	24.200	23.695	24.207	-0.505	0.006	-2.09	0.03
22	25.452	24.934	25.457	-0.518	0.005	-2.04	0.02
23	26.733	26.187	26.721	-0.546	-0.012	-2.04	-0.04
24	28.015	27.455	27.999	-0.560	-0.016	-2.00	-0.06
25	29.297	28.740	29.291	-0.557	-0.006	-1.90	-0.02
26	30.609	30.041	30.597	-0.568	-0.012	-1.86	-0.04
27	31.921	31.358	31.919	-0.563	-0.002	-1.76	-0.01
28	33.264	32.694	33.256	-0.570	-0.008	-1.71	-0.02
29	34.607	34.047	34.609	-0.560	0.002	-1.62	0.01
30	35.980	35.419	35.979	-0.561	-0.001	-1.56	0.00
31	37.354	36.810	37.365	-0.544	0.011	-1.46	0.03
32	38.757	38.220	38.769	-0.537	0.012	-1.39	0.03
33	40.192	39.650	40.190	-0.542	-0.002	-1.35	0.00
34	41.657	41.100	41.629	-0.557	-0.028	-1.34	-0.07
35	43.060	42.571	43.086	-0.489	0.026	-1.14	0.06
36	44.556	44.063	44.562	-0.493	0.006	-1.11	0.01
37	46.051	45.577	46.057	-0.474	0.006	-1.03	0.01
38	47.577	47.113	47.571	-0.464	-0.006	-0.98	-0.01
39	49.103	48.671	49.104	-0.432	0.000	-0.88	0.00
40	50.659	50.252	50.656	-0.407	-0.003	-0.80	-0.01

Table 7.13 Frequencies of cable A11-N of the Dongting Lake Bridge (Cont'd)

	Frequency			Error		Relative error	
Unit	Hz	Hz	Hz	Hz	Hz	%	%
Order	Measured	Design parameter	Optimized parameter	Design parameter	Optimized parameter	Design parameter	Optimized parameter
41	52.246	51.856	52.229	-0.390	-0.017	-0.75	-0.03
42	53.833	53.483	53.822	-0.350	-0.011	-0.65	-0.02
43	55.420	55.135	55.434	-0.285	0.014	-0.51	0.03
44	57.129	56.810	57.068	-0.319	-0.061	-0.56	-0.11
45	58.716	58.510	58.722	-0.206	0.005	-0.35	0.01
46	60.425	60.235	60.396	-0.190	-0.029	-0.31	-0.05
47	62.012	61.986	62.091	-0.026	0.079	-0.04	0.13
48	63.843	63.761	63.807	-0.082	-0.036	-0.13	-0.06
49	65.552	65.563	65.545	0.011	-0.007	0.02	-0.01
50	67.261	67.391	67.303	0.130	0.042	0.19	0.06
51	69.092	69.245	69.084	0.153	-0.008	0.22	-0.01
52	70.923	71.126	70.885	0.203	-0.038	0.29	-0.05
53	72.754	73.034	72.710	0.280	-0.044	0.38	-0.06
54	74.585	74.970	74.557	0.385	-0.028	0.52	-0.04
55	76.416	76.933	76.428	0.517	0.011	0.68	0.02
56	78.369	78.924	78.322	0.555	-0.047	0.71	-0.06
57	80.322	80.944	80.242	0.622	-0.081	0.77	-0.10
58	82.275	82.992	82.187	0.717	-0.089	0.87	-0.11
59	84.229	85.069	84.158	0.840	-0.071	1.00	-0.08
60	86.304	87.175	86.157	0.871	-0.147	1.01	-0.17
61	88.135	89.311	88.184	1.176	0.049	1.33	0.06
62	90.210	91.476	90.239	1.266	0.029	1.40	0.03
63	92.285	93.671	92.324	1.386	0.039	1.50	0.04
64	94.360	95.897	94.439	1.537	0.079	1.63	0.08
65	96.558	98.154	96.584	1.596	0.026	1.65	0.03
66	98.633	100.441	98.759	1.808	0.126	1.83	0.13

Table 7.14 Frequencies of Tsing Yi side span cable

	Frequency			Error		Relative error	
Unit	Hz	Hz	Hz	Hz	Hz	%	%
Order	Measured	Design parameter	Optimized parameter	Design parameter	Optimized parameter	Design parameter	Optimized parameter
1	0.419	0.428	0.425	0.009	0.000	2.15	0.07
2	0.833	0.842	0.835	0.009	0.002	1.08	0.21
3	1.259	1.270	1.259	0.011	0.000	0.87	0.02
4	1.690	1.705	1.690	0.015	0.000	0.89	-0.01
5	2.133	2.149	2.131	0.016	-0.002	0.75	-0.10
6	2.586	2.605	2.585	0.019	-0.002	0.73	-0.06
7	3.058	3.075	3.053	0.017	-0.005	0.56	-0.17
8	3.530	3.561	3.538	0.031	0.008	0.88	0.22
9	4.038	4.065	4.041	0.027	0.003	0.67	0.08
10	4.624	4.588	4.564	-0.036	-0.006	-0.78	-0.13
11	5.120	5.132	5.109	0.012	-0.011	0.23	-0.21
12	5.684	5.699	5.677	0.015	-0.006	0.26	-0.11
13	6.317	6.289	6.270	-0.028	0.000	-0.44	0.00
14	6.906	6.904	6.888	-0.002	-0.018	-0.03	-0.26
15	7.547	7.545	7.533	-0.002	-0.014	-0.03	-0.18
16	8.200	8.213	8.206	0.013	0.006	0.16	0.07
17	8.861	8.908	8.907	0.047	0.017	0.53	0.19
18	9.626	9.632	9.637	0.006	0.011	0.06	0.11

Table 7.15 Frequencies of the Longitudinal Stabilizing Cable of Ting Kau Bridge

	Frequency			Error		Relative error	
Unit	Hz	Hz	Hz	Hz	Hz	%	%
Order	Measured	Design Parameter	Optimized Parameter	Design Parameter	Optimized Parameter	Design Parameter	Optimized Parameter
1	0.300	0.290	0.278	-0.011	-0.022	-3.50	-7.200
2	0.408	0.379	0.414	-0.030	0.006	-7.27	1.445
3	0.625	0.574	0.625	-0.051	0.000	-8.14	0.016
4	0.828	0.758	0.829	-0.070	0.001	-8.43	0.145
5	1.039	0.949	1.037	-0.090	-0.002	-8.66	-0.164
6	1.245	1.138	1.244	-0.107	0.000	-8.59	-0.040
7	1.442	1.328	1.452	-0.114	0.010	-7.91	0.687
8	1.656	1.518	1.659	-0.138	0.003	-8.36	0.199
9	1.867	1.708	1.867	-0.159	0.000	-8.53	-0.005
10	2.073	1.898	2.075	-0.175	0.002	-8.44	0.087
11	2.284	2.088	2.282	-0.196	-0.001	-8.56	-0.066
12	2.489	2.279	2.490	-0.211	0.001	-8.47	0.024
13	2.701	2.469	2.698	-0.231	-0.003	-8.56	-0.100
14	2.880	2.660	2.906	-0.220	0.026	-7.64	0.892
15	3.079	2.851	3.114	-0.228	0.035	-7.40	1.120
16	3.323	3.043	3.321	-0.280	-0.002	-8.44	-0.045
17	3.534	3.234	3.529	-0.300	-0.005	-8.49	-0.139
18	3.740	3.426	3.737	-0.314	-0.003	-8.40	-0.072
19	3.945	3.618	3.945	-0.328	0.000	-8.30	-0.010
20	4.145	3.810	4.153	-0.335	0.007	-8.09	0.179
21	4.369	4.003	4.361	-0.366	-0.008	-8.38	-0.185
22	4.607	4.195	4.568	-0.412	-0.039	-8.93	-0.844
23	4.769	4.389	4.776	-0.380	0.007	-7.97	0.151
24	4.980	4.582	4.984	-0.398	0.004	-7.99	0.072
25	5.180	4.776	5.191	-0.404	0.011	-7.80	0.216
26	5.436	4.970	5.399	-0.466	-0.037	-8.57	-0.683
27	5.614	5.165	5.606	-0.449	-0.007	-8.00	-0.126
28	5.825	5.359	5.814	-0.466	-0.011	-7.99	-0.184
29	6.040	5.555	6.022	-0.485	-0.018	-8.03	-0.305
30	6.236	5.751	6.229	-0.485	-0.007	-7.78	-0.109
31	6.425	5.947	6.437	-0.478	0.012	-7.44	0.184
32	6.647	6.144	6.644	-0.504	-0.003	-7.58	-0.044
33	6.859	6.341	6.852	-0.518	-0.006	-7.55	-0.095
34	7.059	6.538	7.060	-0.520	0.001	-7.37	0.014
35	7.270	6.736	7.267	-0.533	-0.003	-7.34	-0.034
36	7.453	6.935	7.475	-0.518	0.022	-6.95	0.292
37	7.637	7.134	7.683	-0.503	0.046	-6.58	0.604
38	7.870	7.334	7.890	-0.537	0.020	-6.82	0.258
39	8.092	7.534	8.098	-0.559	0.006	-6.90	0.070
40	8.315	7.735	8.306	-0.580	-0.009	-6.98	-0.106
41	8.504	7.936	8.514	-0.568	0.010	-6.68	0.116
42	8.748	8.138	8.721	-0.611	-0.027	-6.98	-0.306
43	8.937	8.340	8.929	-0.597	-0.008	-6.68	-0.090
44	9.171	8.543	9.137	-0.627	-0.034	-6.84	-0.367
45	9.326	8.747	9.345	-0.579	0.018	-6.21	0.197
46	9.549	8.951	9.553	-0.597	0.004	-6.25	0.041
47	9.749	9.157	9.760	-0.592	0.011	-6.07	0.118
48	9.982	9.362	9.968	-0.620	-0.014	-6.21	-0.140
49	10.171	9.569	10.176	-0.602	0.005	-5.92	0.045
50	10.349	9.776	10.384	-0.573	0.034	-5.54	0.333
51	10.555	9.984	10.591	-0.571	0.036	-5.41	0.345
52	10.783	10.192	10.799	-0.590	0.016	-5.47	0.152
53	11.005	10.402	11.007	-0.603	0.002	-5.48	0.021
54	11.194	10.612	11.214	-0.582	0.021	-5.20	0.185
55	11.427	10.823	11.422	-0.605	-0.005	-5.29	-0.044

CHAPTER 8

CONCLUSIONS AND DISCUSSIONS

8.1 CONCLUSIONS

The experiments, analyses, results and conclusions presented in the previous chapters can be summarized as follows.

Linear dynamic analysis of structural cables

1 A three-dimensional finite element formulation is developed for dynamic analysis of large-diameter structural cables. The proposed formulation is suited for both suspended and inclined cables, and allows for the consideration of cable flexural rigidity, sag-extensibility, spatial variability of dynamic tension, boundary conditions, lumped masses and intermediate springs and/or dampers. This formulation provides a good baseline model for accurate identification of cable tension force and other structural parameters based on the measurement of multimode frequencies.

2 Parametric studies have been undertaken to evaluate the effects of cable bending stiffness and sag-extensibility on modal properties, and the relation between the

natural frequencies and cable parameters for a wide parameter range. The results show that the cable bending stiffness contributes a considerable influence on the natural frequencies when the tension force is relatively small, and affects the higher-mode frequencies more significantly than the lower-mode frequencies. A comparison study of the computed and measured natural frequencies of the Tsing Ma Bridge cables shows that it is necessary to take bending stiffness into account for large-diameter bridge cables in order to obtain an accurate prediction of the natural frequencies. The predicted higher-mode frequencies for such cables without considering bending stiffness may deviate 30% from the true value for high-order modes. The case study of the Ting Kau Bridge cables demonstrates the effect of the degree of stiffness of attached dampers on the cable modal properties and on the tension identification accuracy. It is concluded that the tension forces of long-span large-diameter bridge cables can be accurately evaluated from vibration measurement only when a precise model accounting for cable bending stiffness, sag-extensibility and other constraints is utilized in the identification procedure.

Nonlinear dynamic analysis of structural cables

3 A hybrid finite element/incremental harmonic balance method, that eschews commonly used modal reduction, is developed for analysis of nonlinear periodically forced vibration of inclined cables with arbitrary sag. By taking enough finite elements and appropriate harmonic terms, the proposed method can obtain accurate steady-state dynamic response under simple- or multi-harmonic excitation. The conventional time integration procedure is expensive in seeking frequency response

curves as it may take a long transient process to reach steady state, whereas the proposed method directly resolves steady-state solutions. Moreover, the proposed method is able to completely predict unstable, multi-valued responses, as well as sub- and super-harmonic resonances in an alternating frequency- and amplitude-controlled manner. This method can also be explored to evaluate cable internal resonance in any modal combination when a certain commensurable condition is met. Due to its computational versatility, this method should be extended to analyze the interconnected cable system and the cable-damper system, which are widely adopted in modern cable-stayed bridges.

4 Numerical analysis results of the Tsing Ma Bridge imply the following conclusions: (i) The Tsing Yi side-span free cable of the Tsing Ma Bridge exhibits softening nonlinearity in the tower-cable construction stage, but diverges to display hardening nonlinearity in the finally completed bridge stage. That is, the bridge cable has distinctly different nonlinear characteristics in the two stages due to different cable static tension and configuration; (ii) The steady-state periodic response of the cable under simple harmonic excitation is not symmetric about the static equilibrium position. The nonzero mean value (static drift) is significant in the resonant frequency range; (iii) If the steady-state response of the cable is considered, the third-order harmonics have magnitudes less than 2% of the total response amplitudes, and harmonic terms of the 4th and above modes can be disregarded in the solution process; (iv) The sub-harmonic resonance of the cable can be caused not only by the primary resonant frequency but also by the higher-mode resonant frequencies. This may result in pronounced resonant peaks in the low damping case.

5 Nonlinear modal interaction and internal resonance of a suspended cable paradigm are numerically investigated by means of a hybrid 3-D finite element/incremental harmonic balance method. This frequency-domain solution method eschews commonly used modal reduction and can accommodate arbitrary harmonic terms. By taking enough finite elements and appropriate harmonic terms, the proposed method can obtain an accurate description of the cable nonlinear steady-state dynamic response characteristics under either simple or multi-harmonic excitation. This method is suited for both suspended and inclined cables with sag-to-span ratios not limited to being small, and allows for the consideration of boundary conditions, lumped masses, supporting motion, and intermediate springs and/or dampers. The proposed method is promising for the analysis of cable nonlinear modal interactions (coupling) and internal resonances because it accommodates multi-harmonics and retains mathematical tractability in the description of spatial degrees of freedom and multi-modes. Due to its numerical accuracy, this method can also be used in some situations to verify the solutions obtained from other approximate analytical methods.

6 Based on the study of modal interaction and internal resonance characteristics of a suspended cable paradigm, the following conclusions are drawn: (i) A two-to-one internal resonance of the cable between the first in-plane mode and the first out-of-plane mode is revealed; (ii) A second-order super-harmonic resonance of the second symmetric in-plane mode is found in the cable; (iii) The static drift (zero-order harmonic component) of the in-plane response at the primary, super-harmonic and internal resonances is significantly large; (iv) There is no static drift in the out-of-

plane response of the cable when activated by the two-to-one internal resonance; (v) Strong modal interactions occur in the transition between the primary and the super-harmonic resonances; (vi) Response profiles of the cable at the super-harmonic resonance are significantly different from those at the primary and internal resonances.

Cable condition assessment

7 Cable parameters are identified by using the nonlinear least squares (NLS) method with the objective function taking the sum of squared errors between measured and calculated frequencies. By updating the constitutive parameters other than elements of stiffness matrix, the physical meaning of the finite element (FE) model is preserved. Both single- and multiple-parameter estimation procedures are used to evaluate the effects of parameters and weight selection on the estimation of parameters. Based on a case study of a real cable from the Dongting Lake Bridge, the following conclusions are made: (i) one to two point monitoring in cable ambient tests provide consistent results in the frequency measurements and dozens of frequencies can be obtained from the tests; (ii) Single parameter updating, whether employing different procedures or choosing different parameters, cannot help systematic errors between the measured and analytical frequencies. That means no prominent procedure or parameter is found in the single-parameter-estimation procedures; (iii) Multiple-parameter estimation (MPE) procedures significantly reduce the errors between the analytical and measured frequencies, which is reduced to only one tenth of the errors before identification; (iv) For both the multiple

parameter and single parameter cases, it is found that a correct estimation is not sensitive to the weight of the cost function, and; (v) Considering the effects of intermediate supports does not make significant improvements in minimizing the frequency errors but improves the confidence in the estimation.

8 Exploration of methods for cable tension identification. When employing the single-parameter estimation procedure, the cable tension cannot be accurately identified unless other parameters are accurately known prior to the identification. However, multiple-parameter estimation procedures provide a practical way to accurately estimate the cable tension as well as other cable parameters. Cable tension identified using the multiple-parameter estimation procedure is more accurate than that identified from single-parameter estimation procedures.

9 As the nonlinear least squares (NLS) method can only deal with local optimization problems, two global optimization methods, i.e. the exhaust search and the genetic algorithm (GA) are also employed for cable parameter estimation. The identification of cable parameters is studied by using both simulation and real testing data. The simulation studies are carried out to show the characteristics of the cost function surfaces under different conditions and to obtain the statistical properties of the cable parameters (or cable parameter errors) through the Monte Carlo method. The real testing data from three real bridges are used to evaluate the cable conditions (identify cable parameters). In the identification process, both the exhaust search and the genetic algorithm (GA) are used for the simulation study and the GA is used for real cables.

10 The effects of the number of modal frequencies used and the noise levels on the solution uniqueness and distribution of multiple solutions are investigated. The correlation between the errors of different parameters is obtained through calculating the correlation coefficients. The distribution of frequency errors of three real cables is obtained. Based on extensive studies of both the simulation and real cases, the following conclusions are made: (i) Generally, the more measurement frequencies used as input, the narrower (more accurate) the solutions distributed, so that it is always better to have more frequencies measured. For example, for the cables in the Dongting Lake Bridge, the Tsing Ma Bridge and The Ting Kau bridge, thirty to more than one hundred modes are used; (ii) Both small and large quantities of input frequencies works well when there is no noise or the noise is very small. However, a large quantity of frequencies should be employed to achieve reliable and accurate identification results when the noise is great; (iii) The exhaust search and the genetic algorithm (GA) provide close results; (iv) When the noise is small and normally distributed, the errors in the identified cable parameters are also normally distributed. However, when the noise is great, the errors no longer follow a normal distribution; (v) correlation between the parameter errors is strong, indicated by an absolute value correlation coefficient greater than 0.95. The correlation coefficient is not affected significantly by the noise or by the number of frequencies used; (vi) Case studies on three real bridges validate the proposed parameter identification method for different kinds of cables. The method may serve as a general approach for evaluating cable conditions, especially for cable tension calibration in real long-span cable-supported bridges.

8.2 DISCUSSIONS AND RECOMMENDATIONS

Possible applications based on the present study are to identify the cable tension, to detect reduction in effective cable cross sectional area, to determine effective cable length based on ambient vibration tests and to analyze cable nonlinear oscillations, e.g. parametric oscillation, wind-rain-induced vibration, galloping and wake galloping.

Both local and global optimization tools are used for cable parameter estimation. Though the interior-reflective Newton's method works well for the problem considered in Chapter 6, it is obvious that a local optimization tool, such as the interior-reflective Newton's method, will fail to find the global solution of the problems in Chapter 7. For the two global optimization tools used in the study, the exhaust search is generally too time consuming to be accepted when the quantity of parameters to be identified is large, whereas the genetic algorithm is practical for cable parameter estimation.

Practical steps to assess cable conditions developed in the study are: 1) a proper model, like the one developed in Chapter 3, should be established. The model should be capable of producing accurate natural frequencies for a real cable providing the cable parameters are precisely known; 2) obtain the design values of the cable parameters. If the design values are not available, make an initial guess from experience and assume it as the design values; 3) obtain the cable natural frequencies from ambient vibration tests. Suggestions for carrying out a good ambient vibration tests for this purpose are given in next paragraph. Better results will be obtained if more frequencies are obtained, and; 4) identify cable parameters by minimizing the errors between the measurements and the calculation through the genetic algorithm.

Some experiences from the ambient vibration tests carried out on the Dongting Lake Bridge may be helpful for new comers. Firstly, the author suggests to measure responses of more than two points. If response is measured at only one point, those modes, which have nodes at or near the measurement point, will be missed. When two points are used, it is suggested to separate them at a distance of about 1/60×(length of cable) with the lower point located at 1/30×(length of cable) away from the lower cable end to get the first fifty frequencies. Secondly, the author recommends measuring the response of the girder and pylon near the cable ends as far as possible. This is because there may be some coupled vibration modes of the girder-cable-pylon system. Thirdly, the author suggests to make a rough calculation on the cable natural frequencies through Equation (2.5) before the test. Based on the calculated frequencies, the anti-aliasing may be determined by taking a value of about 1.2 to 2 times the frequency of the highest order mode. Then a sampling frequency of about 2.5 to 5 times the anti-aliasing frequency can be taken. Finally, it is very important to have a data record with its length long enough. The record is expected to have a length that can provide about 100 averages at an overlap of 75% with a high enough frequency resolution in the power spectral density of the vibration responses.

There are several limitations for the method developed: (i) The multiple-parameter-identification method is developed for real cables in cable-supported bridges, so that the method is not readily applicable for those cables used in other situation, such as mining and forest harvesting; (ii) The multiple-parameter-identification method needs high order frequencies for multiple parameter estimation. However, in some situations this requirement is not practical. For example, high order modes of some short stay cables,

which may be 2 or 3 meters long, may not be excited under ambient vibration conditions. (iii) The proposed method can only deal with constitutive cable parameters. It means the cable can be defined by several global (constitutive) parameters (EI, H, L_x, L_y, m and EA). For physical parameter changes at localized region of the cable, the proposed method can only provide estimation in an average sense.

In the present study, based on ambient vibration tests the cable condition is assessed by identifying the cable parameters. Further research in this field should include the following aspects: (i) To obtain the variation of parameters of structural cables and other components of a bridge. Information regarding the variation of parameters with time is helpful for engineers to study why, to what extent and how fast does the cable state change. Nevertheless, the condition assessment carried out in this study is a static description on the state of the cable condition at the time the ambient tests were made. An on-line 24-hour vibration monitoring system for all or typical cables should be built up to get the variation of cable parameters; (ii) To estimate the service life left for the cables. To achieve this target, it is necessary to make fatigue analysis of cable wires. (iii) To incorporate other cable parameter measuring methods with the vibration-based methods. For example, the cable length may be measured by using a GIS, which would improve the accuracy of other cable parameters identified through the vibration-based method developed in this study; (iv) To investigate the effects of environment on cable conditions. For example, variation in the temperature may change length and tension of cables; (iv) To assess the condition of cable anchorage. As carried out for this study, the cable anchorage state should be estimated through in situ tests and the fatigue life of cable anchorages should also be estimated.

REFERENCES

Ahmadi-Kashani, K. "Vibration of hanging cables". *Computer and Structures*, Vol. **31**, pp.699-715 (1989)

Allemang, R. J. and Brown, D. L. "A correlation coefficient for modal vector analysis". In *Proceedings of the 1st International Modal Analysis Conference*, Florida, U.S.A., pp.110-116 (1982)

Al-Noury, S. I. and Ali, S. A. "Large-amplitude vibrations of parabolic cables". *Journal of Sound and Vibration*, Vol. **101**, pp.451-462 (1985)

Anderson, D. Z. *Linear Programming*. McGraw-Hill, New York (1992)

Baruch, M. "Optimization procedure to correct stiffness and flexibility matrices using vibration tests". *American Institute of Aeronautics and Astronautics Journal*, Vol. **16**, pp.1208-1210 (1978)

Baruch, M. "Correction of stiffness matrix using vibration tests". *American Institute of Aeronautics and Astronautics Journal*, Vol. **20**, pp.441-442 (1982a)

Baruch, M. "Optimal correction of mass and stiffness matrices using measured modes". *American Institute of Aeronautics and Astronautics Journal*, Vol. **20**, pp.1623-1626 (1982b)

Baruch, M. "Methods of reference basis for identification of linear dynamic structures". *American Institute of Aeronautics and Astronautics Journal*, Vol. **22**, pp.561-564 (1984)

Benedettini, F., Rega, G. and Vestroni, F. "Modal coupling in the free nonplanar finite motion of an elastic cable". *Meccanica*, Vol. **21**, pp.38-46 (1986)

Benedettini, F., Rega, G. and Alaggio, R. "Non-linear oscillations of a four-degree-of-freedom model of a suspended cable under multiple internal resonance conditions". *Journal of Sound and Vibration*, Vol. **182**, pp.775-797 (1995)

Benedettini, F. and Rega, G. "Non-linear dynamics of an elastic cable under planar excitation". *International Journal of Non-linear Mechanics*, Vol. **22**, pp.497-509 (1987)

Benedettini, F. and Rega, G. "Planar non-linear oscillations of elastic cables under superharmonic resonance conditions". *Journal of Sound and Vibration*, Vol. **132**, pp.353-366 (1989a)

Benedettini, F. and Rega, G. "Analysis of finite oscillations of elastic cables under internal/external resonance conditions". In *Proceedings of ASME Winter Annual Meeting*, AMD–**192**, pp.39-46 (1989b)

Berman, A. "Mass matrix correction using an incomplete set of measured modes". *American Institute of Aeronautics and Astronautics Journal*, Vol. **17**, pp.1147-1148 (1979)

Berman, A. and Nagy, E. J. "Improved of a large analytical model using test data". *American Institute of Aeronautics and Astronautics Journal*, Vol. **21**, pp.1168-1173 (1983)

Berman, A. and Wei, F. S. "Automated dynamic analytical model improvement". *NASA Contractor Reports No. 3452*, NASA, U.S.A. (1981)

Berman, A., Wei, F. S. and Rao, K. V. "Improvement of analytical dynamic models using modal test data". In *Collection of Technical Papers - AIAA/ASME/ASCE/AHS Structures, Structural Dynamics and Materials Conference*, New York, U.S.A., 12-14 May, 1980, pp.809-814 (1980)

Borowski, E. J. and Borwein, J. M. *Mathematics Dictionary*, HarperCollins, New Youk (1991)

Boyer, C. B. and Merzbach, U. C. *A History of Mathematics*, John Wiley, New York (1989)

Brandon, J. A. "Derivation and significance of second order modal design sensitivities". *American Institute of Aeronautics and Astronautics Journal*, Vol. **22**, pp.723-724 (1984)

Brownjohn, J. M. W., Lee, J. and Cheong, B. "Dynamic Performance of a Curved Cable-Stayed Bridge". *Engineering Structures*, Vol. **21**, pp.1015-1027 (1999)

Brönnimann, R., Nellen, P. M. and Sennhauser, U. "Application and Reliability of a Fiber Optical Surveillance System for a Stay Cable Bridge". *Smart Materials and Structures*, Vol. **7**, pp.229-236 (1998)

Carson, W. W. and Emery, A. F. "Energy method determination of large cable dynamics". *Journal of Applied Mechanics*, ASME, Vol. **43**, pp.330-334 (1976)

Casas, J. R. "A Combined Method for Measuring Cable Forces: the Cable-Stayed Alamillo Bridge, Spain". *Structural Engineering International*, Vol. **4**, pp.235-240 (1994)

Chen, M. J. and Yu, D. J. "A New Method for Measuring Cable Tension in Bridges". *Journal of Vibration, Measurement and Diagnosis*, Vol. **15**, pp.240-242 (1995) (in Chinese)

Chen, J. C. and Garba, J. A. "Analytical model improvement using modal test results". *American Institute of Aeronautics and Astronautics Journal*, Vol. **18**, pp.684-690 (1980)

Cheng, S. -P. and Perkins, N. C. "Free vibration of a sagged cable supporting a discrete mass". *Journal of Acoustical Society of America*, Vol. **91**, pp.2654-2662 (1992a)

Cheng, S. -P. and Perkins, N. C. "Closed-form vibration analysis of sagged cable/mass suspensions". *Journal of Applied Mechanics*, ASME, Vol. **61**, pp.923-928 (1992b)

Cheng, S. -P. and Perkins, N. C. "Theoretical and experimental analysis of the forced response of sagged cable/mass suspensions". *Journal of Applied Mechanics*, ASME, Vol. **61**, pp.944-948 (1994)

Chung, Y. T. and Craig, R. R. "Experimental substructure coupling with rotational coupling coordinate". In *Collection of Technical Papers - AIAA/ASME/ASCE/AHS 26th Structures, Structural Dynamics and Materials Conference*, Orlando, Florida, U.S.A., 1985, pp.484-489 (1985)

Collins, J. D., Young, J. and Kiefling, L. "Methods and applications of system identification in shock and vibration". *System Identification of Vibrating Structures Mathematical Models from Test Data*, New York, pp.45-71 (1972)

Collins, J. D. Hart, G. C., Hasselman, T. K. and Kennedy, B. "Statistical identification of structures". *American Institute of Aeronautics and Astronautics Journal*, Vol. **12**, pp.185-190 (1974)

Crohas, H. and Lepert, P. "Damage detection and monitoring method for offshore plateforms is field-tested". *Oil and Gas Journal*, Vol. **80**, pp.94-103 (1982)

Cunha, A. and Caetano, E. "Dynamic measurements on stay cables of cable-stayed bridges using an interferometry laser system". *Experimental Techniques*, Vol. **23**, pp.38-43 (1999)

Cunha, A., Caetano, E. and Delgado, R. "Dynamic tests on large cable-stayed bridge." *Journal of Bridge Engineering*, ASCE, Vol. 6, pp.54-62 (2001)

Cuthbert, T. R., Jr. *Optimization Using Personal Computers*, John Wiley, New York (1987)

Dailey, R. L. "Eigenvector derivatives with repeated eigenvalues". *American Institute of Aeronautics and Astronautics Journal*, Vol. **27**, pp.486-491 (1989)

Darbre, G. R. "In-plane free vibration of supported/free parabolic cables". *Earthquake Engineering and Structural Dynamics*, Vol. **18**, pp.435-443 (1989)

Dascotte, E. and Vanhonacker, P. "Development of an automatic model updating program". In *Proceedings of the 7th International Modal Analysis Conference*, Nevada, U.S.A., pp.596-602 (1989)

Dascotte, E. "Practical application of finite element tuning using experimental modal data". In *Proceedings of the 8th International Modal Analysis Conference*, Florida, U.S.A., pp.1032-1037 (1990)

Dascotte, E. "Material identification of composite structures from combined use of finite element analysis and experimental modal analysis". In *Proceedings of the 10th International Modal Analysis Conference*, Florida, U.S.A., pp.1274-1280 (1992)

Davis, L. *Handbook of Genetic Algorithms*, Van Nostrand Reinhold, Victoria, Australia (1991)

Davenport, A. G. and Steel, G. N. "Dynamic behavior of massive guy cables". *Journal of the Structural Division*, ASCE, Vol. **91**, pp.43-70 (1965)

Dems, K. and Mróz, Z. "Identification of damage in beam and plate structures using parameter-dependent frequency changes". *Engineering Computations,* Vol. **18**, pp.96-120 (2001)

Downs, B. "Accurate reduction of stiffness and mass matrices for vibration analysis and rationale for selecting master degrees of freedom". *Journal of Mechanical Design*, Vol. **102**, pp.412-416 (1980)

Fabrizio, V. and Capecchi, D. "Damage detection in beam structures based on frequency measurements". *Journal of Engineering Mechanics*, ASCE, Vol. **126**, pp.761-768 (2001)

Fox, R. L. and Kapoor, M. P. "Rates of change of eigenvalues and eigenvectors". *American Institute of Aeronautics and Astronautics Journal*, Vol. **6**, pp.2426-2429. (1968)

Fujino, Y., Pacheco, B. M., Nakamura, S. and Warnitchai, P. "Synchronization of human walking observed during lateral vibration of a congested pedestrian bridge". *Earthquake Engineering and Structural Dynamics*, Vol.**22**, pp.741-758 (1993a)

Fujino, Y. Warnitchai, P. and Pacheco, B. M. "An experimental and analytical study of autoparametic resonance in 3DOF model of cable-stayed beam". *Nonlinear Dynamics*, Vol. **4**, pp.111-138 (1993b)

Gambhir M. L. and Batchelor B. V. "Parametric study of free vibration of sagged cables". *Computers and Structures*, Vol. **8**, pp.641-648 (1978)

Goldenberg, D. E. *Genetic Algorithm Search, Optimization, and Machine Larning*, Addison-Wesley, New York (1989)

Gordis, J. H., Bielawa, R. L. and Flannelly, W. G. "Secant-method adjustment for structural models". *American Institute of Aeronautics and Astronautics Journal*, Vol. **26**, pp.104-112 (1991)

Gudmundson, P. "Eigenfrequency changes of structures due to cracks, notches, or other geometrical changes". *Journal of Mechanics and Physics of Solids*, Vol. **30**, pp.339-353 (1982)

Guyan, R. J. "Reduction of stiffness and mass matrices". *America Institute of Aeronautics and Astronautics Journal*, Vol. **3**, pp.380 (1965)

Hagedorn, P. and Schäfer, B. "On non-linear free vibration of an elastic cable". *International Journal of Non-linear Mechanics*, Vol. **15**, pp.333-340 (1980)

Hart, G. C. and Yao, J. T. P. "System identification in structural dynamics". *Journal of the Engineering Mechanics Division*, ASCE, Vol. **103**, pp.1089-1104 (1977)

Hassiotis, S. and Jeong, G. D. "Identification of stiffness reduction using natural frequencies". *Journal of Engineering Mechanics*, Vol. **121**, pp.1106-1113 (1995)

Haupt, R. L. and Haupt, S. E. *Practical genetic algorithms. A Wiley-Interscience Publication*, John Wiley and Sons, Singapore (1998)

Henghold, W. M. and Russell, J. J. "Equilibrium and natural frequencies of cable structures (A non-linear finite element approach)". *Computer and Structures*, Vol. **6**, pp.267-271 (1976)

Henshell, R. D. and Ong, J. H. "Automatic masters for eigenvalue economization". *Earthquake Engineering and Structural Dynamics*, Vol. **3**, pp.375-383 (1975)

Heylen, W. "Optimization of model matrices by means of experimentally obtained dynamic data". In *Proceedings of the 1st International Modal Analysis Conference*, Florida, U.S.A., pp.32-38 (1982)

Highways Department. *Ting Kau Bridge*. Highways Department, HKSAR, Hong Kong (2000)

Hikami, Y. "Rain vibration of cables in cable stayed bridges". *Journal of Wind Engineering*, Vol. **27**. pp.23-34. (1986)

Hikami, Y. and Shiraishi, N. "Rain-wind induced vibration of cables in cable-stayed bridges". *Journal of Wind Engineering and Industrial Aerodynamics*, Vol. **29**, pp.409-418 (1986)

Hjelmstad, K. D. "On the uniqueness of modal parameter estimation". *Journal of Sound and Vibration*, Vol. **192**, pp.581-598 (1996)

Hoff, C. J., Bernitsas, M. M., Sandstrom, R. E. and Anderson, W. J. "Inverse perturbation method for structural redesign with frequency and mode shape constraints". *American Institute of Aeronautics and Astronautics Journal*, Vol. **22**, pp.1304-1309 (1984)

Holland, J. H. *Adaptation in Natural and Artificial Systems*. The University of Michigan Press, Ann Arbor, Michigan (1975)

Irons, B. "Structural eigenvalue problems: elimination of unwanted variables". *American Institute Aeronautics and Astronautics Journal*, Vol. **3**, pp.961-962 (1965)

Irvine, H. M. and Caughey, T. K. "The linear theory of free vibrations of a suspended cable". In *Proceedings of the Royal Society of London*, Vol. **341**, pp.299-315 (1974)

Irvine, H. M. "Free vibrations of inclined cables". *Journal of the Structural Division*, ASCE, Vol. **104**, pp.343-347 (1978)

Irvine, H. M. and Griffin, J. H. "On the dynamic response of a suspended cable". *Earthquake Engineering and Structural Dynamics*, Vol. **4**, pp.389-402 (1976)

Irvine, H. M. *Cable Structures*. MIT Press, Cambridge (1981)

Kabe, A. M. "Stiffness matrix adjustment using mode data". *American Institute Aeronautics and Astronautics Journal*, Vol. **23**, pp.1431-1436 (1985)

Kajima Corporation, "New Landmark Bridge to Ease Traffic Bottleneck". *Kajima Perspectives*, **15** (1995)

Kammer, D. C. "Test-analysis model development using an exact modal reduction". *The International Journal of Analytical and Experimental Modal Analysis*, pp.174-178 (1987)

Kammer, D. C. "Optimum approximation for residual stiffness in linear system identification". *American Institute of Aeronautics and Astronautics Journal*, Vol. **26**, pp.104-112 (1988)

Kroneberger-Stanton, K. J. and Hartsough, B. R. "A monitor for indirect measurement of cable vibration frequency and tension". *Transactions of the ASAE*, Vol. **35**, pp.341-346 (1992)

Kim, J. and Chang, S. P. "Dynamic stiffness matrix of an inclined cable". *Engineering Structures*, Vol. **23**, pp.1614-1621 (2001)

Kim, K. O. anderson, W. J. and Sandstrom, R. E. "Nonlinear inverse perturbation method in dynamic analysis". *American Institute of Aeronautics and Astronautics Journal*, Vol. **21**, pp.1310-1316 (1983)

Kirkpatrick, S., Gelatt, C. D. Jr, and Vecchi, M. P. "Optimization by simulated annealing". *Science*, Vol. **220**, pp.671-680 (1983)

Koh, C. G., Hong, B. and Liaw, C. –Y. "Parameter Identification of Large Structural Systems in Time Domain" *Journal of Structural Engineering*, ASCE, **126**, pp.953-967 (2000)

Kuo, C. P. and Wada, B. K. "Nonlinear sensitivity coefficients and corrections in system identification". *American Institute of Aeronautics and Astronautics Journal*, Vol. **25**, pp.1463-1468 (1987)

Lallement, G. and Cogan, S. "Reconciliation between measured and calculated dynamic behaviours: enlargement of the knowledge space". In *Proceedings of the 10th International Modal Analysis Conference*, Florida, U.S.A., pp.487-493 (1992)

Lapieere, H. and Ostiguy, G. "Structural model verification with linear quadratic optimization theory". *American Institute of Aeronautics and Astronautics Journal*, Vol. **28**, 1497-1503.

Lee, C. and Perkins, N. C. "Non-linear oscillation of suspended cables containing a two-to-one internal resonance". *Nonlinear Dynamics*, Vol. **3**, pp.365-490 (1992a)

Lee, C. and Perkins, N. C. "Three-dimensional oscillations of suspended cables involving simultaneous internal resonances". In *Proceedings of ASME Winter Annual Meeting AMD*-**144**, pp.59-67 (1992b)

Lee, C. and Perkins, N. C. "Experimental investigation of isolated and simultaneous internal resonances in suspended cables". *Journal of Vibration and Acoustics*, ASME, Vol. **8**, pp.385-391. (1995a)

Lee, C. and Perkins, N. C. "Three-dimensional oscillations of suspended cables involving simultaneous internal resonances", *Nonlinear Dynamics*, Vol. **8**, pp.45-63 (1995b)

Leonard, J. W. and Recker, W. W. "Non-linear dynamics of cables with low initial tension". *Journal of Engineering Mechanics Division*, ASCE, Vol. **98**, pp.293-309 (1972)

Lhermet, N., Claeyssen, F. and Bouchilloux, P. "Electromagnetic stress sensor and its applications: monitoring bridge cables and prestressed concrete structures". In Chase, S. B. and Aktan, A. E., eds., *Health Monitoring and Management of Civil Infrastructure Systems*, *Proceedings of SPIE*, Vol. **3325**, 1998, pp.46-52. (1998)

Lilien, J, L. and Pinto Da Costa, A. "Vibration amplitudes caused by parametric excitation of cable-stayed structures". *Journal of Sound and Vibration*, Vol. **174**, pp.69-90 (1994)

Lin, H. P. and Perkins, N. C. "Free oscillations of a non-linear simple model of a suspended cable". In Petty, M. ed., *Recent Advances in Structural Dynamics*, Vol. **2**, pp.597-609 (1995)

Lin Y.-P. *Cable-Stayed Bridge.* China Communications Press, Beijing (1997) (in Chinese)

Luongo, A. and Piccardo, G. "Non-linear galloping of sagged cables in 1:2 internal resonance". *Journal of Sound and Vibration*, Vol. **214**, pp.915-940 (1998)

Luongo, A., Rega, G. and Vestroni, F. "Monofrequence oscillation of non-linear model of a suspended cable". *Journal of Sound and Vibration*, Vol. **82**, pp.247-269 (1982)

Lungo, A., Rega, G. and Vestronin, F. "Planar non-linear free vibrations of an elastic cable". *International Journal of Non-linear Mechanics*, Vol. **19**, pp.39-52 (1984)

Major Bridge Engineering Bureau. *Collection of Technology for Wuhan 2nd Yangtse River Bridge.* Ministry of Railway. Science Press, Beijing (1998) (in Chinese).

Matsumoto, M., Shiraishi, N., Shiratio, H., Tsuji, M. and Kitazawa, M. Aerodynamic behaviour of cables in cable-stayed bridges". *Journal of Wind Engineering Industrial Aerodynamics*, Vol. **30**, pp.602-609 (1989)

Matta, K. W. "Selecting of degrees of freedom for dynamics analysis". *Journal of Pressure Vessel Technology*, ASME, Vol. **109**, pp.65-69 (1987)

Mehrabi, A. B. and Tabatabai, H. "Unified finite difference formulation for free vibration of cables". *Journal of Structural Engineering*, Vol. **124**, pp.1313-1322 (1998)

Migliore, H. J. and Webster, R. L. "Current methods for analyzing dynamic cable response". *Shock and Vibration Digest*, Vol. **11**, pp.3-16 (1979)

Mills-Curran, W. C. "Calculation of eigenvector derivatives for structures with repeated eigenvectors". *American Institute of Aeronautics and Astronautics Journal*, Vol. **26** pp. (1988)

Mills-Curran, W. C. "Eigenvector derivatives with repeated eigenvalues - comments", *American Institute of Aeronautics and Astronautics Journal*, Vol. **28**, pp.1846-1846 (1990)

Mitchell, M. and Pardoen, G. C. "The estimation of rotational degrees-of-freedom using shape function". In *Proceedings of the 6th International Modal Analysis Conference*, Florida, U.S.A., pp.566-571 (1988)

Miyata, T. "Design consideration for wind effects on long-span cable-stayed bridges". In Ito, M., Fujino, Y., Miyata, T. and Narita, N., eds., *Cable-Stayed Bridges: Recent Developments and Their Future*, Elsevier, Tokyo, Japan, 10-11 December 1991, pp.235-256 (1991)

Morassi, A. and Rovere, N. "Localizing a notch in a steel frame from frequency measurements". *Journal of Engineering Mechanics*, ASCE, Vol. **123**, pp.422-432 (1997)

Mottershead, J. E. and Friswell, M. I. "Model updating in structural dynamics: a survey". *Journal of Sound and Vibration*, Vol. **167**, pp.347-375 (1993)

Nalitolela, N., Penny, J. E. T. and Friswell, M. I. "Updating structural parameters of a finite element model by adding mass or stiffness to the system". In *Proceedings of the 8th International Modal Analysis Conference*, Florida, U.S.A., pp.836-842 (1990)

Narita, N. and Yokoyama K. "A summarized account of damping capacity and measures against wind action in cable-stayed bridges in Japan". In Ito, M., Fujino, Y., Miyata, T. and Narita, N., eds., *Cable-Stayed Bridges: Recent Developments and Their Future*, Elsevier, Tokyo, pp.257-278 (1991)

Nataraja, R. "Structural integrity monitoring in real seas". In *Proceedings of the Fifteenth Annual Offshore Technology* Conference, Houston, Texas, pp.221-228 (1983)

Nayfeh, A. H. N*onlinear Interactions: Analytical, Computational, and Experimental Methods*, John Wiley and Sons, New York (2000)

Nayfeh, A. H. and Balachandran, B. "Modal interactions in dynamical and structural systems". *Applied Mechanics Review*, Vol. **42**, pp.175-21 (1989)

Nayfeh, A. H. and Mook, D. T. *Non-linear Oscillations*. John Wiley and Sons, New York (1995)

Nelson, R. B. "Simplified calculation of eigenvector derivatives". *America Institute of Aeronautics and Astronautics Journal*, Vol. **14**, pp.1201-1205. (1976)

O'Callahan, J. "A procedure for improved reduced system (IRS) model". In *Proceedings of the 7th International Modal Analysis Conference*, Nevada, U.S.A., pp.17-21 (1989)

O'Callahan, J., Lieu, I. W. and Chou, C. M. "Determination of rotational degrees of freedom for transfers in structural modification". In *Proceedings of the 3rd International Modal Analysis Conference*, Florida, U.S.A., pp. 465-470 (1985)

O'Callahan, J., Avitabile, P. and Riemer, R. "System equivalent reduction expansion process (SEREP)". In *Proceedings of the 7th International Modal Analysis Conference*, Nevada, U.S.A., pp.29-37 (1989)

Ogawa, J. and Abe, Y. "Structural damage and stiffness degradation of buildings caused by severe earthquakes". In *Proceedings of 7th World Conference on Earthquake Engineering*, pp.527-534 (1980)

Ojalvo, I. U. "Efficient computation of mode-shape derivatives for large dynamic systems". In *Proceedings of the AIAA 27th structures, structural dynamics, and materials conference*, New York, pp.242-247 (1986)

Ojalvo, I. U. "Efficient computation of mode shape derivatives for large dynamic systems". *American Institute of Aeronautics and Astronautics Journal*, Vol. **25**, pp.1386-1390 (1987)

Ojalvo, I. U. and Pilon, D. "A second order iteration procedure for correlation of analysis frequencies with test data". In *Proceedings of the 9th International Modal Analysis Conference*, Firenze (Florence), Italy, pp.499-502 (1991)

Ojalvo, I. U., Ting, T., Pilon, D. and Twomey, W. "Practical suggestions for modifying math models to correlate with actual modal test results". In *Proceedings of the 7th International Modal Analysis Conference*, Nevada, U.S.A., pp.347-354 (1989)

Ohashi, M. "Cables for cable-stayed bridges". In Ito, M., Fujino, Y., Miyata, T. and Narita, N., eds., *Cable-Stayed Bridges: Recent Developments and Their Future*, Elsevier, Tokyo, Japan, 10-11 December 1991, pp.125-150 (1991)

Ohshima, K. "Aerodynamic stability of the cables of a cable-stayed bridge subject to rain (a case study of the Ajigawa Bridge)". In *Proceedings of the Third U.S.-Japan Bridge Workshop*, Japan, pp.324-336 (1987)

Okamura, H. "Measuring submarine optical cable tension from cable vibration". *Bulletin of JSME*, Vol. **29**, pp.548-555 (1986)

Omegadyne Inc. URL://www.omegadyne.com/pdf/lc1001-lc1011.pdf (2001)

Pakdemirli, M., Nayfeh, S. A. and Nayfeh, A. H. "Analysis of one-to-one autoparametric resonances in cables–discretization vs. direct treatment". *Nonlinear Dynamics*, Vol. **8**, pp.65-83 1995

Perkins, N. C. "Modal interactions in the non-linear response of elastic cables under parametric/external excitation". *International Journal of Non-Linear Mechanics*, Vol. **27**, pp.233-250 (1992)

Persoon, A, J. "The wind induced response of a cable-stayed bridge". In *Bridge Aerodynamics, Proceedings of a Conference*, London, England, pp. 91-95 (1981)

Pierre, D. A. *Optimization*. McGraw-Hill, New Yok, pp.476-482 (1992)

Pinto da Costa, A., Martins, J. A. C., Branco, F. and Lilien, J. L. "Oscillations of bridge stay cable induced by periodic motions of deck and/or towers". *Journal of Engineering Mechanics*, Vol. **122**. pp.613-622 (1996)

Piranda, J., Lallement, G. and Cogan, S. "Parametric correction of finite element models by minimisation of an output residual: improvement of the sensitivity method". In *Proceedings of the 9th International Modal Analysis Conference*, Firenze Incontra, Centro Affari, Firenze (Florence), Italy, pp.363-368 (1991)

Post-Tensioning Institute, *Recommendations for stay cable design, testing and installation*. Post-Tensioning institute, Phoenix, USA (2000)

Prato C. A., Ceballos M. A., Huerta P. J. F., Gerbaudo C. F., Grünbaum C. E. and Hommel D. L. "Diagnosis, construction procedures and design recommendations for replacement of cables in cable-stayed bridges: experience from two current cases in Argentina". In *Recent Advances in Bridge Engineering: Evaluation, Management and Repair*, Dubendorf and Zurich, pp.303-316 (1997)

Press, W. H. *Numerical Recipes*, Cambridge University Press, New York (1992)

Qiu, Y., Ling Y. C. and Hang, Y. L. "Tension measurement of stay cables". In *Proceedings of the 9th Annual Conference of the Associate of Bridge and Structural Engineering, the Associate of China Civil Engineering*, pp.340-352 (1990) (in Chinese).

Ramberg, S.E. and Griffin, O.M. "Free vibrations of taut and slack marine cables". *Journal of the Structural Division*, ASCE, Vol. **103**, pp.2079-2092 (1977)

Rao, G. V. and Iyengar, R. N. "Internal resonance and non-linear response of a cable under periodic excitation". *Journal of Sound and Vibration*, Vol. **149**, pp.25-41 (1991)

Rega, G. and Benedettini, F. "Planar non-linear oscillations of elastic cables under subharmonic resonance conditions". *Journal of Sound and Vibration*, Vol. **132**, pp.367-381 (1989)

Rega, G., Lacarbonara, W., Nayfeh, A. H. and Chin, C. M. "Multiple resonances in suspended cables: direct versus reduced-order models". *International Journal of Non-Linear Mechanics*, Vol. **34**, pp.901-924 (1999)

Rega, G., Vestroni, F. and Benedettini, F. "Parametric analysis of large amplitude free vibrations of a suspended cable". *International Journal of Solides and Structures*, Vol. **20**, pp.95-105 (1984)

Robert, T. L., Bruhat, D. and Gervais, J. P. "Measure de la tension des câbles par méthode vibratoire". *Bulletin de Liaison des Laboratoires des Ponts et Chaussées*, Vol. **173**, pp.109-114 (1991)

Robinson, J. C. "Application of a systematic finite element model modification technique to dynamic analysis of structures". In *Proceedings of the 23rd AIAA/ASME/ASCE/AHS Structures, Structural Dynamics and Material Conference*, **2**, *AIAA* paper (82-0730), pp.489-502 (1982)

Russell, J. C. and Lardner, T. J. "Experimental determination of frequencies and tension for elastic cables". *Journal of Engineering Mechanics*, ASCE, Vol. **124**, pp.1067-1072 (1998)

Salawu, O. S. "Detection of structural damage through changes in frequency: a review." *Engineering Structures*, Vol. **19**, pp.718-723 (1997)

Sandstrom, R. E. and Anderson, W. J. "Modal perturbation methods for marine studies". *Transaction of Society of Naval Architecture and Marine Engineering*, Vol. **90**, pp.41-45 (1982)

SE Corporation, <URL: http://www.se-corp.co.jp/english/Bridge.html>, (1998)

Shan, V. N. and Raymund, M. "Analytical selection of masters for the reduced eigenvalue problem". *International Journal for Numerical Methods in Engineering*, Vol. **18**, pp.89-98 (1982)

Shi, J. J. and Zhang, G. Y. "Cable tension measurement for Rama IX cable-stayed bridge by ambient vibration method". *China Civil Engineering Journal*, Vol. **25**, pp.68-71 (1992) (in Chinese).

Smith, S. W. and Beattie, C. A. "Simultaneous expansion and orthogonalisation of measured modes for structure identification". In *Proceedings of the AIAA/SEM Dynamic Specialists Conference*, Long Beach, California, pp.261-270 (1990)

Smith, S. W. and Johnson, M. "Field test to determine frequencies of bridge stay cables". In *Proceedings of the 17th International Modal Analysis* Conference, Florida, U.S.A., pp.745-751 (1999)

Simpson, A. "The small oscillations of a suspended flexible line". *Journal of Applied Mechanics*, ASME, Vol. **40**, pp.624-626 (1973)

Starossek, U. "Dynamic stiffness of sagging cable". *Journal of Engineering Mechanics*, ASCE, Vol. **117**, pp.2815-2829 (1991)

Starossek, U. "Reduction of dynamic cable stiffness to linear matrix polynomial". *Journal of Engineering Mechanics*, ASCE, Vol. **119**, pp.2132-136 (1993)

Starossek, U. "Cable dynamics – a review". *Structural Engineering International*, Vol. **3**, pp.171-176 (1994)

Stetson, K. A. "Perturbation method of structural design relevant to holographic vibration analysis". *American Institute of Aeronautics and Astronautics Journal*, Vol. **144**, pp.454-460 (1975)

Stetson, K. A. and Palma, G. E. "Inversion of first-order perturbation theory and its application to structural design". *American Institute of Aeronautics and Astronautics Journal*, Vol. **13**, pp.457-459 (1976)

Suarez, L. E. and Singh, M. P. "Dynamic condensation method for structural eigenvalue analysis". *American Institute of Aeronautics and Astronautics Journal*, Vol. **30**, pp.1046-1054 (1992)

Takahashi, K. "An approach to investigate the instability of the multiple-degree-of-freedom parametric dynamic systems". *Journal of Sound and Vibration*, Vol. **78**, pp.519-529 (1981)

Takahashi, M., Tabata, S., Hara, H., Shimada, T. and Ohashi, Y. "Tension measurement by microtremor-induced vibration method and development of tension meter". *IHI Engineering Review*, Vol. **16**, pp.1-6 (1983)

Takahashi, K. and Konishi, Y. "Non-linear vibration of cables in three dimensions: part I: non-linear free vibrations". *Journal of Sound and Vibration*, Vol. **118**, pp.69-84 (1987a)

Takahashi, K. and Konishi, Y. "Non-linear vibration of cables in three dimensions: part II: non-linear forced vibrations". *Journal of Sound and Vibration*, Vol. **118**, pp.69-84 (1987b)

Tadjbakhsh, I. G. and Wang, Y.-M. "Wind-driven nonlinear oscillations of cables". *Nonlinear Dynamics*, Vol. **1**, pp. 265-291 (1990)

Taylor, J. E. "Scaling a discrete structural model to math measured modal frequencies". *American Institute of Aeronautics and Astronautics Journal*, Vol. **15**. pp.1647-1649 (1977)

Thomas, M., Massoud, M. and Beliveau, J. "Identification of system physical parameters from force appropriation technique". In *Proceedings of the 4th International Modal Analysis Conference*, California, U.S.A., pp.1098-1103 (1986)

Tokyo Sokki Kenkyujo Co., Ltd. <URL://www.tokyosokki.co.jp> (2001).

Triantafyllou, M. S. "Dynamics of cables and chains". *Shock and Vibration Digest*, Vol. **16**, pp.9-17 (1984a)

Triantafyllou, M.S. "The dynamics of taut inclined cables". *Quarterly Journal of Mechanics and Applied Mathematics*, Vol. **37**, pp.421-440 (1984b)

Triantafyllou, M. S. "The dynamics of translating cables". *Journal of Sound and Vibration*, Vol. **103**, pp.171-182 (1985)

Triantafyllou, M. S. and Gringfogel, L. "Natural frequency and modes of inclined cables". *Journal of Structural Engineering*, ASCE, Vol. **112**, pp.139-148 (1986)

Udwadia, F. E. and Sharma, D. K. "Some uniqueness results related to building structural identification" *SIAM Journal of Applied Mathematics*. Vol. **34**, pp.104-118 (1978)

Veletsos, A. S. and Darbre, G. R. "Dynamic stiffness of parabolic cables". *Earthquake Engineering and Structural Dynamics*, Vol. **11**, pp.367-401 (1983)

Verwiebe, C. "Exciting mechanisms of rain-wind-induced vibrations". *Structural Engineering International*, Vol. **8**, pp.112-117 (1998)

Wang, D. H., Liu, J. S, Zhou, D. G and Huang, S. L. "Using PVDF piezoelectric film sensors for in situ measurement of stay-cable tension of cable-stayed bridges". *Smart Material and Structures*, Vol. **8**, pp.554-559. (1999)

Wang, M., George, M. L. and Ondrej, H. "Development of a remote coil magnetoelasti stress sensor for steel cable". In Chase, S. B. and Aktan, A. E., eds., *Health Monitoring and Management of Civil Infreqstructure Systems, Proceedings of SPIE*, Vol. **4337**, pp.122-128. (2001a)

Wang, M. L., Chen, Z. L. Koontz, S. S. and Lloyd, G. M. "Magnetoelastic permeability measurement for stress monitoring in steel tendons and cables". In Chase, S. B. and Aktan, A. E., (eds.), *Health Monitoring and Management of Civil Infrastructure Systems, Proceedings of SPIE*, Vol. **3995**, pp.492-500 (2001b)

Wang, W. T. *Cable Replacements in Cable-Stayed Bridges*. China Communications Press, pp.100-146 (1997) (in Chinese).

Wardlaw, R. L. "Cable supported bridges under wind action". In Ito, M., Fujino, Y., Miyata, T. and Narita, N., eds., *Cable-Stayed Bridges: Recent Developments and Their Future*, Elsevier, Tokyo, Japan, 10-11 December 1991, pp.213-234 (1991)

West, H. H., Geschwindner, L. F. and Suhoski, J. E. "Natural vibrations of suspended bridges". *Journal of Structural Division*, ASCE, Vol. **101**, pp.2277-2291 (1975)

Williams, H. P. *Model Solving in Mathematical Programming*, John Wiley, New York (1993)

Witte, R. S., and Witte, J. S. *Statistics* (sixth edition), Harcourt College Publishers, Sydney (2001)

Wolff, T. and Richardson, M. "Fault detection in structures from changes in their modal parameters". In *Proceedings of the 7th International Modal Analysis Conference*, Nevada, U.S.A., pp.87-94. (1989)

Wong, W. M. *15 Most Outstanding Projects in Hong Kong*. China Trend Buildin Press Ltd., Hong Kong (1998)

Woo, H. G. C., Cermak, J. E. and Peterka, J. A. "On vortex locking-on phenomenon for a cable in linear shear flow". *Journal of Wind Engineering and Industrial Aerodynamics*, Vol. **14**, pp.289-300. (1983)

Xiao, X. and Druez, J. "Planar nonlinear forced vibrations of a suspended cable". *Transactions of the Canadian Society for Mechanical Engineering*, Vol. **20**, pp.123-137 (1996)

Xu Y.L., Ko J.M. and Yu Z. "Modal analysis of tower-cable system of Tsing Ma long suspension bridge". *Engineering Structures*, Vol. **19**, pp.857-867 (1997)

Yamaguchi, H. and Fujino, Y. "Stayed cable dynamics and its vibration control," In Larsen, A. and Esdahl, S. eds., *Bridge Aerodynamics*, A. A. Balkema, Rotterdam, pp.235-253. (1998)

Yamaguchi, H., Miyata, T. and Ito, M. "A behaviour on non-linear dynamic response of a cable systems". In *Proceedings of the 24th Symposium of Structural Engineering*, pp.55-61 (1978)

Yang, W. Y. and Xu, B. *Manual for Bridge Construction Engineer*, China Communications Press, Beijing (1995) (In Chinese)

Yen, W. H. P., Mehrabi, A. B. and Tabatabai, H. "Evaluation of stay cable tension using a non-destructive vibration technique". In *ASCE Building to Last: Proceedings of the 15th Structures Congress, Portland, Oregon* Vol. 1, New York. pp.503-507 (1997)

Yoshimura, T. "Aerodynamic stability of four medium span bridges in kyushu district". *Journal of Wind Engineering and Industrial Aerodynamics*, Vol. 41-44, pp.1203-1214 (1992)

Yoshimura, T., Inoue, A., Kaji, K. I. and Savage, M. "A study on the aerodynamic stability of the Aratsu Bridge". In *Proceedings of Canada-Japan Workshop on Bridge Aerodynamics*, Ottawa, Canada, pp.41-50 (1989)

Yu, Z. *Vibration Mitigation of Sag Cables in Cable Supported Bridges Using Only Oil Dampers*. Ph.D Dissertation of Department of Civil and Structural Engineering, The Hong Kong Polytechnic University, Hong Kong (1997)

Zhang, D. W. and Li, S. "Succession-level approximate reduction (SAR) technique for structural dynamic model". In *Proceedings of the 13th International Modal Analysis Conference*, Florida, U.S.A., pp.435-441 (1995)

Zhang, D. W. and Wei, F. S. "Model correction via compatible element method". *Journal of Aerospace Engineering*, ASCE, Vol. 5, pp.337-346 (1992)

Zhang, D. W. and Wei, F. S. "Complete mode-type reduction (CMR) for structural dynamic system". In *Proceedings of the 13th International Modal Analysis Conference*, Florida, U.S.A., pp.616-622 (1995)

Zhang, D. W. and Wei, F. S. "Practical complete modal space and its applications". *American Institute of Aeronautics and Astronautics Journal*, Vol.34, pp.2211-2214 (1996)

Zhang, D. W. and Wei, F. S. "Efficient computation of many eigenvector derivatives using dynamic flexibility method". *American Institute of Aeronautics and Astronautics Journal*, Vol. **35**, pp.712-718 (1997)

Zhang, D. W. and Wei, F., S. *Model Updating and Damage Detection.* Science Press, Beijing (1999) (in Chinese)

Zhang, Q. and Lallement, G. "A complete procedure for the adjustment of a mathematical model from the identified complex modes". In *Proceedings of the 5th International Modal Analysis Conference*, London, England, pp.1183-1189 (1987)

Zheng, G. and Chen, Y. "Modal testing of a cable model". Research Report No. CDT2000-1, Department of Civil and Structural Engineering, The Hong Kong Polytechnic University, Hong Kong (2000)

Zui H., Shinke T. and Namita Y. "Practical formulas for estimation of cable tension by vibration method". *Journal of Structural Engineering, Vol.* **122**, pp.651-656. (1996)